



Nottingham Trent  
University

---

**THE USE OF ARTIFICIAL INTELLIGENCE TO IDENTIFY THOUGHT  
MESSAGES VIA NON-INVASIVE EEG BRAIN SIGNALS**

---

SHARMILA MAJUMDAR

MSc Information Technology, BSc Computer Science and Engineering

A thesis submitted in partial fulfilment of the requirements of Nottingham Trent  
University for the Degree of Doctor of Philosophy

September 12, 2024

## **Copyright Statement**

The copyright in this work is held by the author. You may copy up to 5% of this work for private study, or personal, non-commercial research. Any re-use of the information contained within this document should be fully referenced, quoting the author, title, university, degree level and pagination. Queries or requests for any other use, or if a more substantial copy is required, should be directed to the author.

## Abstract

Brain-Computer Interfaces (BCI) have opened up opportunities by advancing the technology, offering new possibilities in both practical applications and theoretical research. Individuals with Completely Locked-in Syndrome, which can result from conditions such as Motor Neurone Disease and Amyotrophic Lateral Sclerosis, stand to gain significantly from BCIs developments aimed at enhancing communication and overall well-being. This PhD research focuses on developing a system to recognise imagined thoughts through Electroencephalography (EEG) brain signals and Artificial Intelligence (AI), with the goal of implementing a novel methodology to establish a direct communication link between brain functionality and computer interfaces.

Developing effective systems for transforming EEG signals into practical communication outputs for various mental tasks presents significant challenges in the field of signal processing. A novel approach, termed Automated Sensory and Signal Processing System (ASPS), is introduced for feature extraction and selection in EEG signal data. This method enhances the reliability of EEG-based communication by identifying and selecting the most relevant features for classification. The ASPS approach is initially implemented with an elementary model and tested through bespoke analysis. The study is subsequently scaled up by increasing the number of subjects, forming groups, and incorporating various domains analysis in signal processing and statistical functions. Artificial Neural Networks (ANNs) are employed for classification, simultaneously verifying the performance of the ASPS approach. The extracted features, generated as outputs of the ASPS approach, serve as inputs to the ANN. High-quality features that are consistent and distinguishable for each mental task facilitate high accuracy in brain signal classification, demonstrating the effectiveness of the feature extraction technique.

In this study, feature extraction is significantly enhanced by the ASPS approach, leading to more accurate mental imagery recognition. These extracted features are classified using ANN algorithms, specifically Feed Forward Neural Networks (FFNN) and Learning Vector Quantisation, demonstrating high accuracy across bespoke, group-based, and combined analyses. Six different ANN architectures with various combination of neurons and hidden layers are employed. Additionally, Convolutional Neural Network, a widely used image processing technique, is utilised in another experiment to classify signals, demonstrating the capability to recognise imagined thoughts. Based on these architectures, different ANN and

CNN models are trained and tested to identify the most optimised classifier for imagination recognition. The performance of these classifiers is summarised and compared to evaluate the robustness of the classification algorithms. Overall, the single-layered FFNN ensures very consistent and high accuracy in imagination recognition.

Furthermore, EEG sensor optimisation is explored through extensive analysis, followed by a thorough validation of the optimised sensors. These optimised sensors simplify signal processing and enhance the accuracy of imagination recognition. Finally, an experiment with a novel product, the EEG-BCI prototype, introduces an optimised sensor-based interface that enables EEG recording from the scalp and the identification of two distinct thoughts according to the proposed methodology. The system's upward-trending performance indicates potential for future enhancements, paving the way for an affordable and accessible solution that empowers individuals with disabilities to interact with their surroundings and improve their overall well-being.

## **Acknowledgement**

With deep humility, I acknowledge the infinite mercy and guidance of Almighty God. I would like to extend my heartfelt gratitude to Nottingham Trent University for offering the PhD Vice-Chancellor Scholarship, which enabled me to undertake this research. My deepest thanks go to my Director of Study, Professor Amin Al-Habaibeh, for his exceptional support, constant encouragement, insightful guidance, and continuous motivation throughout my PhD journey. His dedicated supports to my academic and personal growth have been truly inspiring and invaluable. I am also profoundly grateful to my second supervisor, Dr Ahmet Omurtag, for providing the commercial EEG system and accessories, valuable guidance, arranging technical training, and offering technical support in EEG data collection and analysis. I also extend my thanks to Dr Luke Siena for his insightful guidance as my independent assessor. Additionally, my sincere thanks go to Dr Ana Souto for providing excellent academic support throughout my PhD journey.

I sincerely appreciate the academic, administrative, and library staff, as well as my colleagues at Nottingham Trent University, for their support and encouragement throughout my studies. I am also grateful to the volunteers who dedicated their time to the experiments. Special thanks to the ADBE technical team, particularly James, for facilitating lab arrangements, and to Susan Allcock for providing essential electronic support. Additionally, I thank Mr. Yusef Al-Habaibeh for recording the instructional voiceovers and Mr. Ahmed Al-Habaibeh for managing the audio editing process.

My deepest gratitude goes to my parents, Entomologist Sanjoy Majumdar and Sumitra Majumdar, for their blessings, love, and unwavering support. I am also immensely thankful to my elder brother, Mr Soumitra Majumdar, and sister-in-law, Tuly Majumdar, whose continuous support allowed me to focus on my PhD by managing my family commitments. My sincere appreciation extends to my parents-in-law, Advocate Devashis Sen and Khushi Sen, for their blessings and good wishes, and to my brother-in-law, Advocate Avijit Sen, and sister-in-law, Antara Sen, for their constant support in handling family responsibilities, enabling me to complete my PhD. Finally, I am profoundly grateful to my husband, Dr Arijit Sen, whose steadfast support and countless sacrifices have been instrumental in this achievement. To my children, Anandi Sen and Aniruddha Sen, I deeply appreciate your patience and understanding, especially when I could not always be present. Your love and support have been invaluable throughout this journey.

## Publication List

### Published papers:

Majumdar, S., Al-Habaibeh, A., Omurtag, A., Shakmak, B. and Asrar, M. (2023) 'A novel approach for communicating with patients suffering from completely locked-in-syndrome (CLIS) via thoughts: Brain computer interface system using EEG signals and artificial intelligence', *Neuroscience Informatics*, 3(2), p. 100126. Available at: <https://doi.org/10.1016/j.neuri.2023.100126>.

### Paper presentation:

Majumdar, S., Al-Habaibeh, A. and Omurtag, A. (2024) 'AI-enhanced low-cost EEG system: bridging accessibility gaps for physically disabled individuals', ADBE Research Conference, Nottingham Trent University. Presentation date: 24 June 2024

### Paper presentation:

Majumdar, S., Al-Habaibeh, A. and Omurtag, A. (2024) 'Empowering the physically disabled through AI-enhanced, low-cost EEG technology', East Midlands Doctoral Network (EMDoc) PGR Conference (online). Hosted by: Universities for Nottingham (UfN). Presentation date: 25 September 2024

### Poster presentation:

Majumdar, S., Al-Habaibeh, A. and Omurtag, A. (2021) 'Advanced Artificial Intelligence system to identify communication messages via Brain signals', ADBE Research Conference, Nottingham Trent University. Presentation date: 9 July 2021

## List of Figures

Figure 1.1: The concept of identifying thoughts for computer interface using the ASPS approach. ....	4
Figure 1.2: The structure of the thesis. ....	9
Figure 2.1: Brain components and functions including limbic system. ....	12
Figure 2.2: Diagrammatic delineation of neurons (Carter <i>et al.</i> , 2019). ....	13
Figure 2.3: Schematic diagram of (A) EEG measurement process (Li <i>et al.</i> , 2022), (B) a typical EEG system. ....	19
Figure 2.4: International 10-20 EEG system (A) 19 electrodes placement, (B) side view of 10%-20% electrode distances, (C) top view of 10%-20% electrode distances (Shriram <i>et al.</i> , 2012). ....	21
Figure 2.5: Schematic representation of different brain imaging techniques. ....	27
Figure 2.6: Sub-band decomposition in DWT (Cvetkovic, Übeyli and Cosic, 2008). ....	34
Figure 2.7: FFNN architecture (Montesinos López Osva Antonio and Montesinos López, 2022). ....	42
Figure 2.8: LVQ architecture (Bhardwaj, 2012). ....	42
Figure 2.9: CNN architecture (Tsinalis <i>et al.</i> , 2016). ....	43
Figure 3.1: The methodology of the research. ....	49
Figure 3.2: Block diagram of the ASPS approach developed by Al-Habaibeh and Gindy (2000). ....	50
Figure 3.3: Volunteers wearing EEG cap and participating in prior signal acquisition. ....	52
Figure 3.4: Signal pre-processing. ....	53
Figure 3.5: The block diagram of the ASPS approach applied to brain signal processing in this research. ....	55
Figure 3.6: Volunteers participating in EEG signal acquisition (second phase). ....	61
Figure 3.7: The cross-tabulation analysis template designed for subject vs sensors. ....	64
Figure 4.1: Selected sensors and their scalp locations for bespoke analysis. ....	66
Figure 4.2: Flowchart of ASPS approach for bespoke analysis. ....	67
Figure 4.3: (A) Raw signals for relax and mental task and (B) copper scale map. ....	68
Figure 4.4: Heatmap of imaginations with selected features for bespoke analysis. ....	70
Figure 4.5: ASM of bespoke experiment for (A) subject 1 and (B) subject 2. ....	72
Figure 4.6: The design of verification steps for bespoke analysis. ....	73
Figure 4.7: Best classification accuracy of four models for all ANN architecture. ....	75

Figure 4.8: Average performance of three datasets for all models. ....	76
Figure 4.9: Average performance comparison for subject-wise training and imaginations for all models.....	77
Figure 5.1: Wavelet decomposition (Cvetkovic, Übeyli and Cosic, 2008). ....	81
Figure 5.2: Flowchart of ASPS approach for group-based analysis. ....	82
Figure 5.3: Illustration of uniqueness of imaginations and mapping between subjects.....	84
Figure 5.4: The design of verification steps for group-based analysis. ....	88
Figure 5.5: Best classification accuracy of group-based analysis for all ANN architecture (A) two imaginations, and (B) three imaginations. ....	89
Figure 5.6: Highest accuracy summary.....	90
Figure 5.7: Best Average performance summary for group-based analysis. ....	92
Figure 6.1: Schematic diagram of combined analysis. ....	98
Figure 6.2: Uniqueness of imaginations in image processing technique (A) imagination 1, (B) imagination 2, (C) imagination 3, (D) imagination 4, (E) imagination 5.....	100
Figure 6.3: The design of verification steps for combined analysis. ....	102
Figure 6.4: Maximum classification accuracy of group-based analysis using ASPS and image processing technique. ....	103
Figure 6.5: Average performance of group-based analysis using ASPS and image processing technique. ....	104
Figure 7.1: Validation process of imagination recognition using optimised sensors. ....	111
Figure 7.2: Performance comparison of bespoke analysis between two phases data. ....	115
Figure 7.3: The performance trend of bespoke analysis between two phases data and methods. ....	116
Figure 7.4: Performance comparison of combined analysis between two phases data. ....	118
Figure 8.1: The schematic diagram of EEG-BCI for signal acquisition.....	125
Figure 8.2: Hardware setup using EEG click board and NI 6009 DAQ for signal acquisition. ....	126
Figure 8.3: Single sensor-based EEG-BCI prototype. ....	127
Figure 8.4: Signal acquisition using prototype. ....	128
Figure 8.5: The accuracy of single sensor-based EEG-BCI prototype (A) Maximum performance and (B) average performance.....	129
Figure 8.6: The application view (A) before recording and (B) after recording.....	130
Figure 8.7: New design of the hardware setup using three sensors-based EEG-BCI prototype for signal acquisition.....	130

Figure 8.8: The connectivity of three EEG Click boards and NI 6009 DAQ. ....	131
Figure 8.9: Sensor cables (A) unshielded cables (B) shielded cables. ....	132
Figure 8.10: Newly developed EEG-BCI prototype (A) top view and (B) side view. ....	132
Figure 8.11: Signal acquisition with newly developed EEG-BCI prototype. ....	133
Figure 8.12: Signal visualisation (A) raw signal recording using EEG-BCI prototype and (B) corresponding FFT plot. ....	133
Figure 8.13: Average classification accuracies of EEG-BCI prototype between various partitions. ....	134
Figure 8.14: Classification performance of EEG-BCI prototype using ASPS using four-part frequency domain generated SCFs. ....	135
Figure 8.15: Classification performance of EEG-BCI prototype using ASPS using five-part frequency domain generated SCFs. ....	135

## List of Tables

Table 2.1: Brainwaves information (Bharti <i>et al.</i> , 2021). .....	14
Table 2.2: Comparison of brain imaging techniques. ....	26
Table 2.3: Commercial EEG devices (Ledwidge, Foust and Ramsey, 2018; Dadebayev, Goh and Tan, 2022).....	28
Table 2.4: Overview of EEG signal pre-processing, feature extraction, and feature selection techniques and their key attributes. ....	30
Table 2.5: Classification algorithms. ....	38
Table 2.6: Utilisation of classifiers and their accuracies in EEG classification studies. ....	40
Table 3.1: Selected imagination list. ....	52
Table 3.2: Hyperparameters of developed FFNN model. ....	58
Table 3.3: Hyperparameters of developed LVQ model. ....	59
Table 3.4: CNN configuration and hyperparameters of developed CNN model. ....	59
Table 3.5: CNN configuration and hyperparameters of developed CNN model (continued from previous page). ....	60
Table 3.6: The summary of participant demographics.....	62
Table 4.1: Definitions and equations of four statistical functions. ....	68
Table 4.2: SCFs calculation for bespoke analysis.....	69
Table 4.3: ANN model architectures for imaginations classification for bespoke analysis.	74
Table 5.1: Features calculation for group-based analysis. ....	83
Table 5.2: Group formation for group-based analysis. ....	87
Table 5.3: ANN model architectures for imaginations classification in group-based analysis.....	88
Table 5.4: Best average performances for two-imagination and three-imagination classification.....	91
Table 6.1: Definitions and equations of fifteen statistical functions for combined experiment.....	97
Table 6.2: Features calculation for all subjects combined experiment. ....	99
Table 7.1: Summarised rating point table. ....	107
Table 7.2: Cross-tabulation between subjects and sensors. ....	109
Table 7.3: Group formation based on sensor optimisation. ....	110
Table 7.4: Performance summary of bespoke result using ASPS through FFT. ....	113
Table 7.5: Performance summary of group-wise result using ASPS through FFT. ....	114

Table 7.6: Performance summary of bespoke result using ASPS through FFT and DWT. .....	115
Table 7.7: Performance summary of group-wise result using ASPS through FFT and DWT. .....	117
Table 7.8: Comparative table of similar studies and this study. ....	120

## Nomenclature

ALS	Amyotrophic Lateral Sclerosis
AI	Artificial Intelligence
ANN	Artificial Neural Networks
ASM	Association Matrix
ASPS	Automated Sensory and Signal Processing Selection System
BCI	Brain-Computer Interfaces
CNN	Convolutional Neural Network
cA	Approximation Component
cD	Details Component
DBN	Deep Belief Networks
DNN	Deep Neural Networks
$\Delta$	Delta
DWT	Discrete Wavelet Transform
EEG	Electroencephalography
FFNN	Feed Forward Neural Network
FFT	Fast Fourier Transform
KNN	K-Nearest Neighbours
LDA	Linear Discriminant Analysis
LVQ	Learning Vector Quantisation
MLP	Multi-Layer Perceptron
MND	Motor Neurone Disease
NN	Neural Network
RF	Random Forest

SAE	Sparse Autoencoder
SCF	Sensory Characteristics Features
SVM	Support Vector Machine
WT	Wavelet Transform

# Table of Contents

Copyright Statement .....	ii
Abstract .....	iii
Acknowledgement.....	v
Publication List .....	vi
List of Figures .....	vii
List of Tables.....	x
Nomenclature .....	xii
Table of Contents .....	xiv
Chapter 1: Introduction .....	1
1.1 Background .....	1
1.2 Research Scope .....	4
1.3 Research Questions .....	5
1.4 Aim.....	6
1.5 Objectives.....	6
1.6 Deliverables and Contributions.....	7
1.7 Thesis Structure.....	7
1.8 Summary .....	9
Chapter 2: Literature Review .....	11
2.1 Introduction .....	11
2.2 Brain Functions and MND .....	11
2.3 Brain Imaging Techniques .....	15
2.3.1 Magnetic Resonance Imaging (MRI) and Functional Magnetic Resonance Imaging (fMRI).....	16
2.3.2 Computed Tomography .....	17
2.3.3 Positron Emission Tomography .....	18

2.3.4 Electroencephalography .....	18
2.3.5 Magnetoencephalography .....	22
2.3.6 Near Infrared Spectroscopy and Functional Near Infrared Spectroscopy .....	23
2.3.7 Hybrid EEG-fNIRS .....	25
2.4 Signal Processing Methods .....	28
2.4.1 Signal Pre-processing.....	29
2.4.2 Feature Extraction and Selection .....	32
<b>2.4.3 ASPS Approach .....</b>	<b>37</b>
2.5 Signal Classification .....	37
<b>2.5.1 Artificial Neural Networks.....</b>	<b>41</b>
<b>2.5.2 Image Processing and CNN .....</b>	<b>43</b>
2.6 BCI Devices for Communication Systems .....	44
2.7 Summary .....	46
Chapter 3: Research Methodology.....	49
3.1 Introduction.....	49
3.2 First Phase: Algorithm Development and Analysis.....	51
3.2.1 Overview of Dataset.....	51
3.2.2 Signal Pre-processing.....	52
3.2.3 Signal Processing and Analysis .....	54
3.2.4 Imagination Recognition Using Classification Algorithm.....	57
3.3 Second Phase: Sensor Optimisation and Algorithm Testing .....	61
3.3.1 Brain Signal Acquisition:.....	61
3.3.2 Signal Processing for Sensor Optimisation:.....	62
3.4 Summary .....	65
Chapter 4: Bespoke Design for an Individual .....	66
4.1 Introduction.....	66
4.2 Workflow for Bespoke Analysis.....	66

4.3 Feature Extraction and Selection for Bespoke Analysis .....	68
4.4 Performance of Classifiers for Bespoke Analysis.....	72
4.5 Summary .....	78
Chapter 5: Imaginations Recognition Through Group-Based Analysis .....	80
5.1 Introduction .....	80
5.2 Workflow for Group-based Analysis .....	80
5.3 Feature Extraction and Selection for Group-based Analysis .....	82
5.4 Performance of Classifiers for Group-based Experiment .....	87
5.5 Summary: .....	94
Chapter 6: Imaginations Recognition Through Image Processing .....	96
6.1 Introduction .....	96
6.2 Workflow for Combined Analysis .....	96
6.3 Feature Extraction and Selection with a Combined Method .....	99
6.4 Performance of Classifier for Combined Analysis .....	102
6.5 Summary: .....	105
Chapter 7: Sensor Optimisation and Validation.....	107
7.1 Introduction .....	107
7.2 Analysis of Sensor Optimisation.....	107
7.3 Cross-tabulation Analysis .....	108
7.4 Group Creation.....	110
7.5 Validation.....	111
7.6 Result and Discussion .....	112
7.6.1 ASPS through FFT .....	113
7.6.2 ASPS through FFT and DWT .....	114
7.7 Assessment of Achieved Accuracy and Comparison with Existing Studies .....	119
7.8 Summary .....	122
Chapter 8: Design and Development of EEG-BCI Prototype.....	124

8.1 Introduction .....	124
8.2 Design and Development .....	125
8.3 Product Implementation .....	127
8.4 Signal Acquisition .....	128
8.5 Signal Processing .....	128
8.6 Classification .....	129
8.7 GUI-based Application Development .....	129
8.8 Summary .....	136
Chapter 9: Discussion and Conclusion .....	138
9.1 Introduction .....	138
9.2 Addressing Research Questions and Accomplishing Objectives .....	138
9.3 Contribution to The Knowledge .....	140
9.4 Key Findings .....	141
9.5 Limitations and Future Work .....	145
9.6 Summary .....	146
References .....	148
Appendix .....	170

# Chapter 1: Introduction

## 1.1 Background

The transmission of information directly from the brain, achieved through the use of brain signals, is made possible by Brain Computer Interaction. People with physical disability and Motor Neuron Disease (MND) frequently experience impairments in body movement due to the disrupted communication between lower and upper motor neurons. Despite these physical limitations, cognitive abilities such as imagining and memorising usually remain intact. For those affected by Completely Locked-in Syndrome, often resulting from MND conditions such as Amyotrophic Lateral Sclerosis (ALS), Brain-Computer Interfaces (BCIs) offer significant potential to improve communication and overall quality of life (Lazarou *et al.*, 2018). Much like individuals without disabilities, those experiencing physical impairments or MND are mostly capable of producing spontaneous electrical signals with their thought process. The psychological theories suggest that emotions can be more effectively detected through internal physiological signals, for instance, brain electrical activity since there is a strong connection between human's emotional states and cognitive processes. Various applications have emerged by processing brain signals to recognise emotions (Wijeratne and Perera, 2012; Jirayucharoensak, Pan-Ngum and Israsena, 2014; Wan Ismail *et al.*, 2016; Li, Chao and Zhang, 2019; Dadebayev, Goh and Tan, 2022; Dar *et al.*, 2022), mental tasks (Lin and Hsieh, 2009; Agarwal, Shah and Kumar, 2015; Gupta *et al.*, 2020), biometric pattern (Maiorana, 2020), imagined character (Ullah and Halim, 2021), shapes (Llorella *et al.*, 2021), imagined words (Datta and Boulgouris, 2021), imagined colour (Yu and Sim, 2016) and more.

Heraz and Frasson (2011) reveal that individuals with physical disabilities experience emotions and feelings that can be detected through brain signals. Tan and Nijholt (2010) listed some potential techniques used as brain imaging technologies, for example, Electroencephalography (EEG), Magnetoencephalography (MEG), Functional Magnetic Resonance Imaging (fMRI), Functional Near Infrared Spectroscopy (fNIRS) and so on. Among these, EEG is noted for its continuous recording of brain wave patterns and is considered superior due to its high temporal resolution, non-invasiveness, portability, and cost-effectiveness. EEG significantly contributes to both medical diagnosis and biomedical engineering research field (Blinowska and Durka, 2006) and therefore, greatly advancing

BCI technology. For individuals with ALS, communication options are limited, with eye activity-based systems (such as eye gaze) and cognitive activity-based systems (like P300 BCI) being commonly used. A comparative study by García et al. (2017) found that BCIs offer greater control and comfort compared to eye-tracking systems. Some patients experience stress with eye-tracking systems because of the constant eye movements, prolonged focus on a single direction, and the requirement of wearing a head-mounted device. Moreover, eye-tracking systems are not suitable for use in a lying position. In comparison, BCIs involve fewer limitations and require less time commitment.

Following the acquisition of brain signals, they are processed and analysed using various methods to advance BCI applications (Naseer and Hong, 2015; Niha and Banu, 2016; Aggarwal and Chugh, 2019). Signal processing in BCI is broad, involving the processing, classification, and conversion of brain signals into control commands through numerous techniques (Huang and Wang, 2021). Raw signals can be analysed using mathematical and/or statistical functions. To achieve higher performance brain signals are typically analysed across multiple domains, including time, frequency, and time-frequency. Time domain analysis reflects temporal characteristics of the signal (Bashashati *et al.*, 2007).

Among the various signal processing techniques, the Fast Fourier Transform (FFT), which extracts the characteristics features from the frequency domain, is widely utilised (Ishino and Hagiwara, 2003; Akrami *et al.*, 2005; Murugappan and Murugappan, 2013; Sałabun, 2014). Wavelet Transform (WT), another effective technique operates in time-frequency domain and employs variable window size with certain wavelet function. WT has been exemplified in many research work (Ishino and Hagiwara, 2003; Cvetkovic, Übeyli and Cosic, 2008; Kousarrizi *et al.*, 2009; Nguyen *et al.*, 2015; al-Qerem *et al.*, 2020). Overall, feature extraction and selection are very challenging tasks for signal processing, which is being addressed by many researchers considering factors such as stationary and nonstationary signals, data size, reduction of feature dimension, artefacts or noise sensitivity, computation time, and method complexity (Lakshmi, Prasad and Chandra Prakash, 2014; Vaid, Singh and Kaur, 2015; Niha and Banu, 2016; Aggarwal and Chugh, 2019). Effective extraction and selection of relevant features enable improved classification performance. Significant research has successfully employed either FFT or Discrete Wavelet Transform (DWT) techniques to extract valuable features. In some cases, studies use both methods to determine the most effective approach; however, selecting the most appropriate signal

processing method based on the sensory signals and objectives remains a complex task in BCI development.

Researchers often face the challenge of selecting distinct techniques for feature extraction and optimisation, which can be both time-consuming and resource intensive. To address this issue, Al-Habaibeh and Gindy (2000) introduced a novel concept known as Automated Sensory and Signal Processing System (ASPS), designed to automate the process of feature extraction and selection based on sensory signals. This approach, grounded in Taguchi's orthogonal arrays, was initially applied to condition monitoring in milling processes. This research aims to investigate the application and effectiveness of the ASPS approach within the field of EEG-based sensor signals. While the ASPS method has been previously applied across various machinery domains, this research seeks to extend its application to brain signal processing, with the objective of extracting pertinent features for the recognition of imagined activities.

The subsequent stage in brain signal analysis involves classification based on the extracted features, which enables brain signals to be interpreted as control commands for various applications (Bashashati *et al.*, 2007; Aggarwal and Chugh, 2019). Artificial Intelligence (AI) based classification models can be used for this purpose; however, selecting an appropriate classifier from a wide array of classification and regression algorithms presents a significant challenge, as it depends on the characteristics of the sensory signals and the classifiers themselves. Machine learning (ML), a branch of AI, comprises various classification algorithms and statistical models that enable computers to learn and execute tasks independently. Commonly used classifiers include Support Vector Machines (SVM), Linear Discriminant Analysis (LDA), Naïve Bayes, K-Nearest Neighbours (KNN), and Artificial Neural Networks (ANNs), all of which have demonstrated adequate performance in brain signal classification (Niha and Banu, 2016). Among these, ANNs such as Feed Forward Neural Network (FFNN) (Sarić *et al.*, 2020; Majoros, Oniga and Xie, 2021) as well as Learning Vector Quantisation (LVQ) (Pfurtscheller and Pregenzer, 1999; Mizuno *et al.*, 2010), have proven effective for specific tasks. Additionally, numerous researchers have applied other deep learning techniques to brain signal classification. Convolutional Neural Network (CNN), which are widely used for image processing and classification, feature multiple convolutional layers combined with activation functions to facilitate feature learning (Tsinalis *et al.*, 2016; Wang *et al.*, 2016; Acharya *et al.*, 2018; Llorella *et al.*, 2021).

Therefore, integrating the ASPS approach with AI would present a novel method for classifying EEG signals and advancing BCI applications. The concept of identifying thoughts to produce communication outputs (for example, cursor movement) using ASPS approach is demonstrated in Figure 1.1. This innovative approach aims to resolve the challenges associated with signal processing techniques in brain signal analysis by automatically extracting relevant features with less complex mathematical and computational methods.

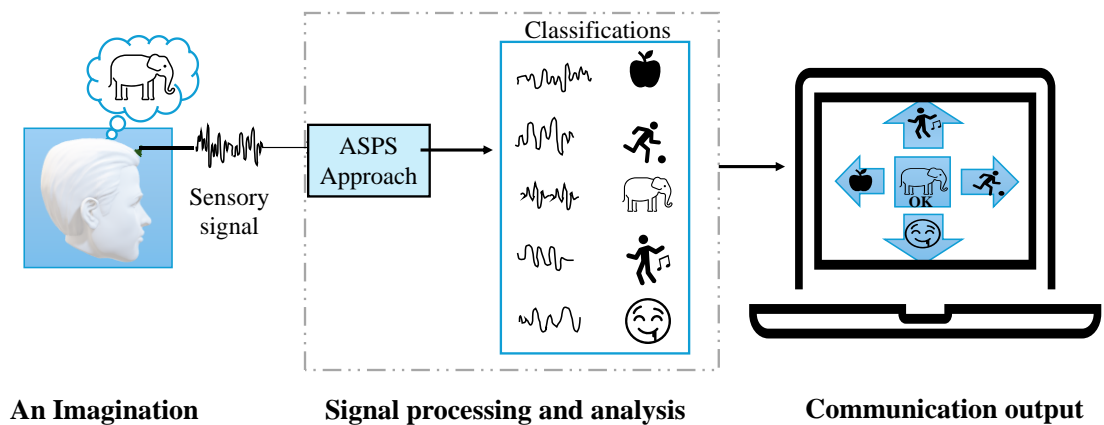


Figure 1.1: The concept of identifying thoughts for computer interface using the ASPS approach.

Additionally, combining hardware with the developed signal processing and classification model could introduce a groundbreaking communication method within the BCI domain. This integration promises to enhance the efficiency and effectiveness of BCIs, making them more accessible and practical for users with severe physical impairments.

## 1.2 Research Scope

The scope of research in brain signal processing begins with the crucial phase of signal acquisition. This involves the deployment of EEG technology to capture brain signals. The quality and fidelity of EEG data are paramount; thus, research must focus on optimising electrode placement to ensure comprehensive coverage of the scalp and specific brain regions of interest. Moreover, the development and refinement of advanced techniques for minimising noise and artifacts, such as those caused by muscle movements and eye blinks, are essential. Investigating both real-time and offline acquisition methods allows for a thorough understanding of the advantages and limitations inherent in each approach, ensuring the most effective data collection strategy for subsequent analysis.

Once signals are acquired, the next important step is signal processing and analysis. This phase involves transforming raw EEG data into a format suitable for further examination. Preprocessing steps, such as noise reduction, filtering, and normalisation, are vital to enhance the quality of the data. Feature extraction techniques, which identifies essential characteristics from the EEG signals, are a focal point of research, with frequency and/or time-frequency analysis methods like FFT, WT being particularly promising. There are many other signal processing techniques being applied towards specific BCI applications.

The integration of machine learning, ANNs, and Deep Neural Networks (DNNs) represents a frontier in brain signal processing research. Machine learning algorithms, encompassing both supervised and unsupervised learning paradigms, are employed to classify and interpret EEG signals. The adaptability and learning capabilities of ANNs and DNNs make them particularly suited for this task. These models can uncover intricate patterns and relationships within the data, facilitating more accurate predictions and interpretations of brain activities. Research in this area focuses on enhancing the architecture of neural networks by adjusting parameters such as the number of hidden layers and neurons, as well as refining train-test methodologies to improve their performance and reliability.

Exploring network models, architecture, and performance is another pivotal aspect of brain signal processing research. Developing robust and efficient network models that can handle the complexity and variability of EEG data is essential. This involves experimenting with different network architectures to identify those that offer optimal performance in terms of accuracy, speed, and computational efficiency.

In summary, the research scope in brain signal processing is vast and multifaceted, encompassing signal acquisition, signal processing and analysis, ANNs and optimal network model development. Each of these areas offers significant opportunities for innovation and advancement, driving forward our understanding and utilisation of brain signals in various applications.

### **1.3 Research Questions**

This study investigates the development of a communication system that utilises EEG and AI to interpret thought messages through non-invasive brain signals. To explore this possibility, the primary question to be addressed is: Can a communication system be developed using non-invasive EEG and AI to interpret thought messages through brain

signals? This primary question leads to several specific research questions that must be answered:

1. How do existing neuroscience principles, brain imaging technologies, and signal processing methodologies contribute to the development of an effective EEG-based BCI system?
2. What and how can a brain signal processing algorithm be optimised to accurately extract and validate robust brain features using ANNs?
3. How can EEG signals be systematically collected using a commercial EEG device, considering the number of subjects, trials, and mental tasks, to ensure the development and evaluation of the brain communication system?
4. What optimisation strategies can be employed to enhance ANN performance in brain signal classification, and which architecture is best suited for this research?
5. How can an EEG-BCI prototype be designed and developed to facilitate effective signal acquisition, processing, and communication, and how can its performance be systematically evaluated?

#### **1.4 Aim**

The project aims to develop an advanced artificial intelligence system capable of identifying and interpreting thought messages from EEG brain signals, thereby enabling a novel communication approach.

#### **1.5 Objectives**

1. To conduct a comprehensive literature review on fundamental neuroscience concepts, brain imaging systems, signal processing methods, classification algorithms, and relevant commercial products.
2. To develop an EEG-based brain signal processing algorithm and analyse the captured signals using the algorithm, validating the results with appropriate ANNs.
3. To conduct experiments to collect brain signals using a commercial EEG device.
4. To optimise the parameters of neural network model and identify the most suitable ANN for this research.
5. To design, develop an EEG based BCI prototype for recording EEG signals and a software interface and evaluate its effectiveness in creating a communication system.

## **1.6 Deliverables and Contributions**

Guided by the research questions, aim, and objectives, this study outlines key deliverables and contributions. These represent significant advancements in the field of BCIs, realised through innovative methodologies and meticulous analysis.

1. Novel Implementation of ASPS Approach: A novel implementation of the ASPS approach for brain signal processing, contributing towards the advancement of BCI development.
2. Distinguishable features for imagination: A unique combination of Sensory Characteristics Features SCFs that effectively capture the distinctiveness of recognising specific imaginations and highlight similarities across subjects.
3. Optimised Sensor configuration: Identification of the optimal number and placement of sensors on the scalp to facilitate the recognition of thought messages from brain signals.
4. Imagination Recognition Method: A robust methodology for recognising specific imaginations through the ASPS-based feature extraction approach, integrated with ANN for effective signal classification.
5. Identification of Suitable ANN Model: Determination of the most suitable ANN model and layer architecture for different sets of imagination recognition.
7. EEG based BCI Prototype: The novel communication product prototype capable of identifying thought messages through brain signals.

## **1.7 Thesis Structure**

The thesis is organised into nine chapters, each addressing a specific aspect of the research. These chapters include the introduction, literature review, methodology, imagination recognition through bespoke analysis, imagination recognition through group-based analysis, imagination recognition through image processing, sensor optimization and validation, the development of a novel EEG-BCI prototype, and the conclusion.

The structure of each chapter is outlined below:

Chapter One: This chapter provides the background of the current research on the development of BCIs. It discusses the research scope, aligning it with the research questions, aim, objectives, deliverables and contributions.

Chapter Two: A comprehensive literature review covers fundamental neuroscience concepts, brain imaging systems, signal processing methods, classification algorithms, and relevant BCI products. The chapter concludes by identifying the research gap after evaluating other relevant studies.

Chapter Three: The research methodology employed in this PhD study is presented in this chapter. It includes an explanation of the various stages of methodology, supported by graphical representations and flow charts.

Chapter Four: This chapter presents a bespoke design for an individual analysis and development, employing an elementary signal processing model to identify and verify different sets of imagined tasks. It utilises data from three EEG sensors, along with time-domain and frequency-domain analyses and employs FFNN and LVQ classification algorithms to measure the performance of various imagination recognition tasks.

Chapter Five: This chapter addresses the design, development, and assessment of group-wise analysis for recognising various sets of imagined tasks, utilising an advanced brain signal processing model. The study utilises data from three EEG sensors, incorporating time-domain, frequency-domain, and time-frequency domain analyses, as well as group-wise analyses. It employs FFNN and LVQ classifiers to evaluate the performance in recognising various imagination tasks.

Chapter Six: The chapter investigates the performance of imagination recognition by integrating the ASPS approach with image processing techniques. This study uses data from 19 EEG sensors, applying frequency-domain and group-based analyses. The chapter examines the performance of imaginations recognition across different groups using CNN as the classifier.

Chapter Seven: This chapter focuses on sensor optimisation and evaluates the proposed model using a new EEG dataset. It also compares the performance of the models discussed in Chapters Three through Six with the newly obtained results. The factors contributing to achieving high accuracy are discussed, along with a comparison between other relevant work and this study.

Chapter Eight: This chapter outlines the design and development of a novel EEG-BCI prototype using the proposed methodology, including real-time data testing. This chapter outlines the steps involved in the development and integration of hardware and software for identifying communication messages.

Chapter Nine: The conclusion summarises the thesis, emphasising the achievement of objectives, key findings, and the research's contributions to knowledge. It concludes with recommendations for future research.

The names of all the aforementioned chapters and their key features are illustrated in Figure 1.2. This figure highlights the main aspects and structure of the chapters discussed.

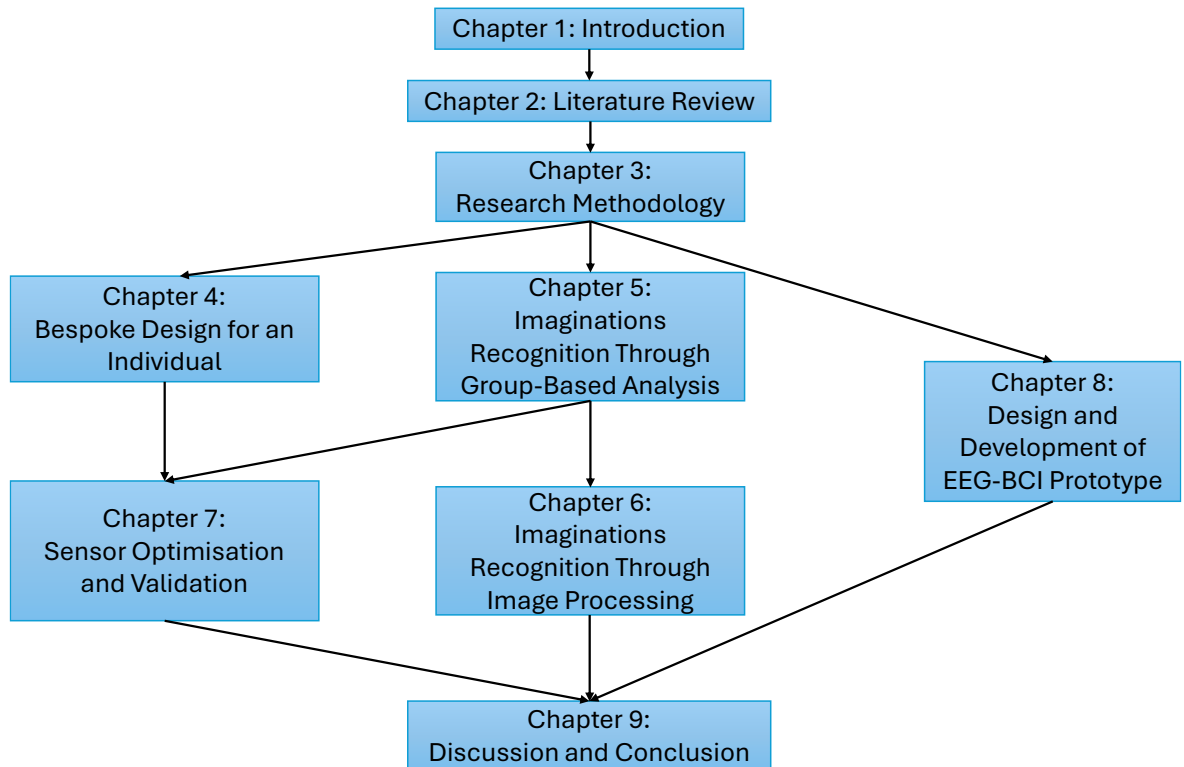


Figure 1.2: The structure of the thesis.

## 1.8 Summary

This chapter starts by outlining the necessity and potential of BCI technologies. In the context of various signal processing methods and classification algorithms applicable to BCI systems, this research seeks to develop an innovative communication approach capable of interpreting thought messages through brain signals. To address the challenge of selecting appropriate methodologies, a novel strategy that integrates ASPS in brain signals and ANN model is proposed. Subsequent sections presented the research scope, aim, objectives of the thesis, and the research questions to be addressed. The chapter concludes with an overview of the thesis structure.

The next chapter provides an in-depth review of brain signal analysis and the scope of BCI development. It explores fundamental neuroscience concepts and their relevance to MND,

brain imaging systems, signal processing methods, signal classification algorithms, and commercial BCI products.

## Chapter 2: Literature Review

### 2.1 Introduction

This chapter includes a comprehensive review of the brain signal analysis and BCI development extents. To ensure thorough coverage that all relevant areas are divided into the following sections: Section 2.2 covers Brain functions and MND which briefly reflects fundamental neuroscience concepts and their role in MND; Section 2.3 discusses Brain imaging systems, Section 2.4 focuses on brain signal processing methods, Section 2.5 explores Classification algorithms and Section 2.6 reviews relevant commercial BCI products.

### 2.2 Brain Functions and MND

The human brain is an indispensable organ composed of billions of neurons with a highly complex structure. It comprises three main parts: the cerebrum, cerebellum, and brainstem. The cerebrum, the largest section, accounts for two-thirds of the brain's volume and is divided into left and right hemispheres, connected by over 200 million nerve fibres forming the corpus callosum. It governs higher cognitive functions, including sensory processing and emotions. The outer layer, the cerebral cortex, features numerous folds and ridges, consisting of grey matter, while the inner structure comprises white matter. Each hemisphere of the cerebrum is divided into four lobes: frontal, temporal, parietal, and occipital, each associated with specific functions (DeSesso, 2009).

The frontal lobe, the largest brain region, comprises one-third of the hemisphere and governs abstract thinking, creativity, problem-solving, reasoning, movement, and speech. Adjacent to it, the parietal lobe handles object recognition, spatial orientation, and sensory discrimination. The temporal lobe, located behind the ears, processes auditory information, language comprehension, and long-term memory. The occipital lobe, at the back of the head, manages visual processing. Beneath the cerebrum, the cerebellum, the second-largest brain region, coordinates motor and cognitive functions, including posture and balance. The brainstem links the cerebrum, cerebellum, and spinal cord, regulating vital functions such as breathing, digestion, heart rate, and body temperature (Carter *et al.*, 2019).

The limbic system comprises several adjacent components, divided into cortical and subcortical types, each with specific tasks. Phylogenetically, the subcortical parts are older

than the cerebral cortex (Tan and Nijholt, 2010). For instance, the hippocampus is crucial for forming permanent memories, while the amygdala regulates emotions, fear, and anxiety. The thalamus acts as a relay between sense organs and the brain, and the hypothalamus connects the nervous system to the endocrine system via the pituitary gland, controlling body temperature and behaviours. Another interconnecting part, the mammillary bodies, links the amygdala, thalamus, and hippocampus.

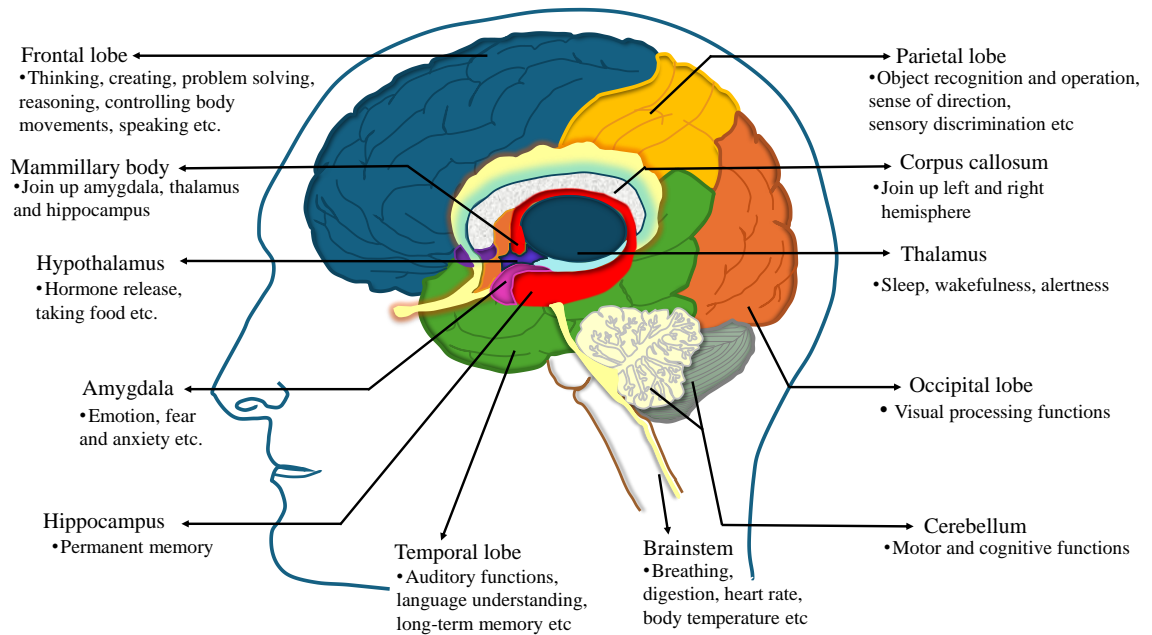


Figure 2.1: Brain components and functions including limbic system.

Figure 2.1 illustrates a medial view of the brain, highlighting the components of the limbic system. Information transmission from different organs to the brain, and from the brain to other organs, is facilitated by a series of activated nerve cells, or neurons. During excitation, a neuron transmits an electrical impulse that propagates through a network of neurons to reach various body organs. These processes are co-ordinated by the nervous system, one of the most complex systems in the human body, with the neuron or nerve cell being its fundamental building block.

Figure 2.2 is a diagrammatic representation of neurons, showing the main internal parts of a middle neuron. This neuron receives and sends information from the previous neuron and the next neuron, known as the presynaptic and postsynaptic neurons, respectively. The neuronal junction, or synapse, is the common point between two neurons. The synaptic cleft, a nanometric gap, is where the axon terminal of the presynaptic neuron communicates with the dendrite of the postsynaptic neuron. Communication occurs via synaptic transmission, a

mechanism for forwarding electrochemical signals facilitated by a rapid voltage change known as the action potential.

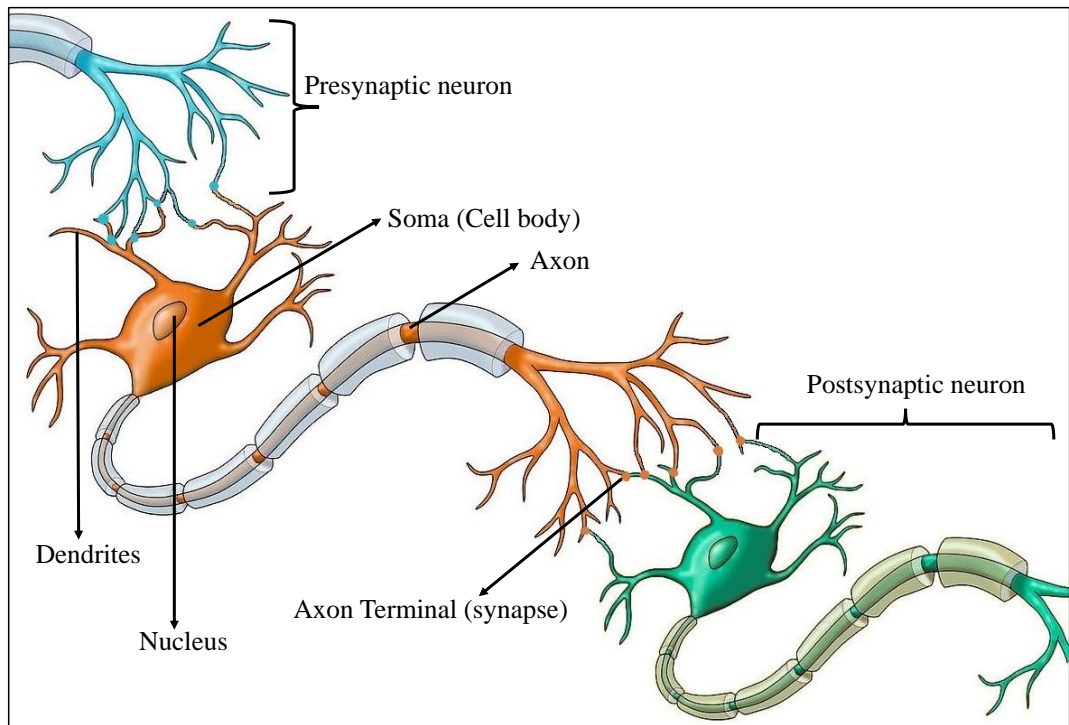
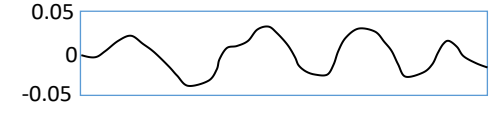
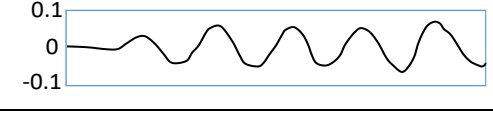
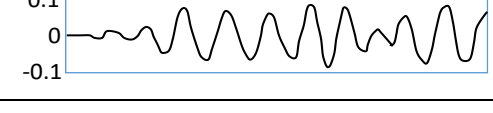
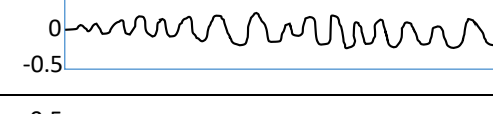


Figure 2.2: Diagrammatic delineation of neurons (Carter *et al.*, 2019).

This action potential, generated by each neuron, travels down the axon to the axon terminal of the previously excited neuron and reaches the receptor of the next neuron. The action potential is a key component of the brain's electrical signalling, formed by the charge differences inside and outside the neuron, known as the electrochemical gradient. Neuron codes, both electrical and chemical, are generated from the activities of dendrites, neuron cells, axons, and axon terminals (Smythies, 1995). Consequently, the excitation of consecutive brain neurons produces electrical potential or voltage, referred to as brain waves.

Human brain waves, based on frequency levels, are broadly divided into five categories: delta ( $\delta$ ), theta ( $\theta$ ), alpha ( $\alpha$ ), beta ( $\beta$ ), and gamma ( $\gamma$ ). Each category of brain waves has a distinct frequency range and is associated with various brain states depending on the subject's posture, organ movements, thoughts, emotions, and other factors. Table 2.1 lists the general characteristics of brain waves, classifying individual frequency ranges, brain states, and visual representations in ascending order according to their band names. These brain waves can be measured using brain imaging technologies, which are discussed in Section 2.2.3.

Table 2.1: Brainwaves information (Bharti *et al.*, 2021).

Frequency band	Frequency ranges	Brain states	Visual representation
<b>Delta (<math>\delta</math>)</b>	0.5 – 4 Hz	Sleep, unconscious	
<b>Theta (<math>\theta</math>)</b>	4 – 8 Hz	Drowsiness, deeply relaxed	
<b>Alpha (<math>\alpha</math>)</b>	8 – 12 Hz	Restful, meditative	
<b>Beta (<math>\beta</math>)</b>	12 – 35 Hz	Active, busy	
<b>Gamma (<math>\gamma</math>)</b>	> 35 Hz	Heightened activity, anger, anxious etc.	

Psychological theories suggest that various emotions can be more accurately detected through internal physiological signals, such as brain electrical activity, due to the strong connection between human feelings and cognitive processes (Wijeratne and Perera, 2012). Emotions, being intrinsic to every individual, form the basic foundation of human interaction. Typically, people express their emotions through facial expressions, speech, and body language, influenced by their environment, mental state, relationships, and inherent nature.

Research indicates that individuals with physical disabilities also experience emotions that can be detected through brain signals (Yuen *et al.*, 2009; Heraz and Frasson, 2011; Jirayucharoensak, Pan-Ngum and Israsena, 2014). This capability offers significant potential for assisting individuals with physical disabilities and speech disorders by providing a more accurate means of recognising and interpreting their emotions.

Dysfunction or degeneration of motor neurons can impair body movements and progressively lead to partial or complete disability. This condition is collectively referred to as MND. This encompasses a range of disorders that can be classified based on genetic or sporadic causes. Disabilities arising from MND can be further classified according to whether they affect upper motor neurons, lower motor neurons, or both. Some conditions may result from the degeneration of both upper and lower motor neurons. Several terms are

used internationally to describe MND, including neurodegenerative neuromuscular disease (in the UK and Australia), ALS, and Lou Gehrig's disease (in Canada and the US) (Talbot, 2002). Although these terms may vary slightly based on specific syndromes and the areas of the brain or other organs affected, they generally refer to similar conditions. Among MND cases, a small percentage of patients may have disorders affecting only lower motor neurons or only upper motor neurons, depending on the aetiology. Progressive muscular atrophy (PMA) specifically refers to cases involving only lower motor neuron disease, whereas Primary lateral sclerosis (PLS) is used to describe cases involving only upper motor neuron disease.

Although motor neurons are impaired, the brain continues to generate signals associated with positive thoughts and emotions. These brain signals, which reflect effective thoughts and emotions, can be processed and analysed for emotion detection, and emerging technologies are increasingly capable of decoding these signals into speech and written text (Herff *et al.*, 2015; Akbari *et al.*, 2019).

In the context of individuals with MND, the establishment of an effective communication system is vital for preserving autonomy. The research rationale emphasises the necessity of developing such communication systems, as they are integral to enabling patients to articulate their needs and preferences, thereby significantly enhancing their quality of life. Additionally, these systems play a crucial role in reducing the emotional and physical strain on carers, facilitating a more supportive and collaborative caregiving environment. This dual benefit highlights the importance of communication systems in promoting the well-being of both MND patients and their carers.

### **2.3 Brain Imaging Techniques**

Brain waves are inevitably and consistently generated by each part of the brain in all states of mind. The five primary categories of brain waves mentioned in Section 2.1 are broadly classified based on various brain states. With advancements in technology, internal brain images can now be acquired using sophisticated devices, allowing for the visual representation of brain waves. These technologies are collectively referred to as brain imaging or neuroimaging (Cvetkovic, Übeyli and Cosic, 2008; Al-Fahoum and Al-Fraihat, 2014). Neuroimaging encompasses a range of techniques used to obtain detailed images of the structure and function of the nervous system and brain. These technologies enable the precise capture, storage, and analysis of cognitive activities, facilitating comprehensive

diagnosis and monitoring of neurological issues such as brain injury, brain tumour, Alzheimer's disease, epilepsy, multiple sclerosis, and more (Pandarinathan *et al.*, 2018). Consequently, the treatment process has become more effective.

Brain imaging techniques vary in their degree of specialisation and invasiveness. They are recognised globally and are robust methods employed across various fields, including biomedical research, neuroscience, neurology, and neurocognition. There are two main types of imaging characteristics: structural imaging and functional imaging. Structural imaging allows for the visualisation of the brain's anatomical arrangement, assisting in the diagnosis of brain injuries, tumours, and congenital abnormalities (Wahlund, 2020). Functional imaging, on the other hand, captures the brain's functional activities through metabolic changes and neural activity, and is applied in the research and diagnosis of neurodegenerative diseases, cognitive psychology, and mental disorders (Lewine, 1995).

Several brain imaging methods have been developed and commercialised, including Magnetic Resonance Imaging (MRI), Computed Tomography (CT) scan, Positron Emission Tomography (PET) scan, EEG, and Magnetoencephalography (MEG). A discussion of these technologies follows.

### 2.3.1 *Magnetic Resonance Imaging (MRI) and Functional Magnetic Resonance Imaging (fMRI)*

MRI technology employs a combination of magnets, radio waves, gradient coils, and a computer system. Superconducting magnets generate a powerful external magnetic field that influences the spinning nuclei of atoms in the body, such as Hydrogen (H) and Phosphorus (P). When exposed to short pulses of radiofrequency waves within this magnetic field, the nuclei become excited. Gradient coils, typically arranged in three sets for three-dimensional imaging, create variations in the magnetic field intensity, allowing for the localisation of different body parts (Agnihotri, Fazel-Rezai and Kaabouch, 2010).

The external magnetic field aligns all water molecules in the body to oscillate at the same frequency due to the natural attraction between the magnetic field and the molecules. However, low-energy molecules, which do not move in sync with high-energy molecules, absorb the energy required for excitation. The radiofrequency waves help identify resonant and non-resonant molecules. The computer system then constructs images based on these energy signals, enabling detailed examination of soft tissues within specific organs. Diffusion-Weighted Imaging (DWI) is an MRI technique that utilises the principles of

Brownian motion to assess water molecule diffusion and is particularly useful for studying brain connectivity issues (Grover *et al.*, 2015). Another prominent variant of MRI is Functional MRI (fMRI), which detects regional brain activity triggered by sensory stimuli. While MRI provides detailed anatomical structure, fMRI offers insights into metabolic functional activities in addition to anatomical information. The human brain, muscles, and organs require glucose, fat, and oxygen. The brain, in particular, consumes a high volume of oxygen and blood, relying on a nearby and adaptable blood supply. During neuronal activation, there is an increase in oxygenated blood flow to specific areas.

Oxyhaemoglobin, which is a combination of ferro haemoglobin and oxygen, lacks unpaired electrons and is called diamagnetic (non-magnetic). Conversely, deoxyhaemoglobin, which lacks oxygen and contains unpaired electrons, is paramagnetic (magnetic). fMRI measures changes in oxyhaemoglobin and deoxyhaemoglobin levels through Blood Oxygenation Level-Dependent imaging (BOLD), a technique widely used in fMRI studies (XUE *et al.*, 2010). This process maps activated brain networks in response to external stimuli, revealing corresponding activities in body parts.

Despite its advantages, fMRI has limitations, including low temporal resolution due to the slow metabolic changes associated with hemodynamic activity and potential signal attenuation. Additionally, there may be spatial distortions in the frontal and parietal lobes due to magnetic susceptibility differences between brain tissue and air. Nonetheless, fMRI offers high spatial resolution, high-quality outputs, and is widely available in both medical and research settings (Glover, 2011). Both MRI and fMRI, although susceptible to noise from the magnetic field, are non-invasive methods that do not involve radiation exposure to the subject.

### 2.3.2 *Computed Tomography*

CT scan, is a structural brain imaging technique that involves a series of X-ray images taken from multiple angles. These images are then processed to generate detailed cross-sectional, and often Three-Dimensional (3D), images of internal structures. The CT technique utilises an X-ray tube, a radiation detector, and a computer. The X-ray tube, housed within a gantry, rotates around the patient, emitting a powerful X-ray beam. Detectors measure the amount of X-ray absorption by the body and send these measurements to a computer, which compiles them into detailed images.

CT scans are particularly effective at visualising bones and soft tissues, and can diagnose conditions such as blood clots, fractures, tumours, and internal bleeding or injuries (Mishra *et al.*, 2022). Although CT scans are generally faster than MRI and fMRI, they involve higher doses of ionising radiation, which increases the risk of cancer (Power *et al.*, 2016). According to authors' study, the use of large doses of radiation can elevate the risk of developing cancer in certain organs. Efforts are being made by physicians to optimise radiation exposure to mitigate these potential risks.

### 2.3.3 *Positron Emission Tomography*

PET is a functional imaging modality that constructs precise 3D images using radiotracers and radio detectors. This technique is particularly valuable in diagnosing cardiovascular and neurological conditions and in detecting various stages of cancer. Radiotracers are radioactive compounds, often referred to as radioisotopes, that are injected into the bloodstream. Fluorodeoxyglucose (FDG), a type of sugar tagged with fluorine-18 (F-18), is commonly used to measure glucose absorption by active neurons (Hartshorne, 1995).

The injected radioactive isotope emits positrons, which interact with electrons in the body. This interaction results in the annihilation of both particles, producing two photons that travel in opposite directions. Detectors measure these photons, and images are reconstructed based on the density of positron-electron annihilation, indicating areas of metabolic activity where glucose is absorbed. Advanced analytical and iterative algorithms are employed to enhance image quality.

PET scans can be combined with CT or MRI scans to create multimodal imaging techniques, such as PET-CT and PET-MRI, which provide more comprehensive physiological and morphological views (Vaquero and Kinahan, 2015). Although these multimodal imaging setups are expensive to maintain and operate, they offer lower radiation doses compared to CT scans and are effective in diagnosing neurological diseases, such as Alzheimer's disease and epilepsy (Hartshorne, 1995).

### 2.3.4 *Electroencephalography*

EEG is a specialised brain imaging technique used to record the electrical activity of the brain, capturing brain waves associated with various mental states and cognitive functions. In contrast to the previously discussed imaging techniques, EEG measures electrical activity directly from the cerebral cortex through a series of electrodes placed on the subject's scalp. The core principle of EEG involves detecting the electrical activity generated by neural

circuits. When neurons in the brain become active, they produce minute voltage fluctuations as a result of synaptic transmission. These voltage fluctuations, typically in the microvolt range, are recorded by the EEG system. The precise arrangement of electrodes can vary depending on the specific research requirements, with common setups including 64 to 256 electrodes (XUE *et al.*, 2010) . The internationally recognised 10-20 system (Klem *et al.*, 1999) is frequently employed to standardise the placement of these electrodes, ensuring consistent and reproducible data collection.

Pyramidal neurons, which are abundant in the brain cortex and limbic system, create electrical potential differences due to the summation of postsynaptic graded potentials, as discussed in Section 2.2. The EEG device captures these potential differences by placing electrodes on the scalp. During brain activation, thousands of pyramid-shaped neurons fire synchronously. These neurons are aligned in a specific orientation, running parallel to each other and perpendicular to the cortical surface. This alignment allows the electrical signals generated by the neurons to sum up effectively and propagate to the scalp surface, where they are detected by the EEG (Niedermeyer, Schomer and Lopes da Silva, 2017). Figure 2.3 (A) provides the schematic diagram how the EEG measurement takes place and Figure 2.3 (B) shows a visual representation of EEG system.

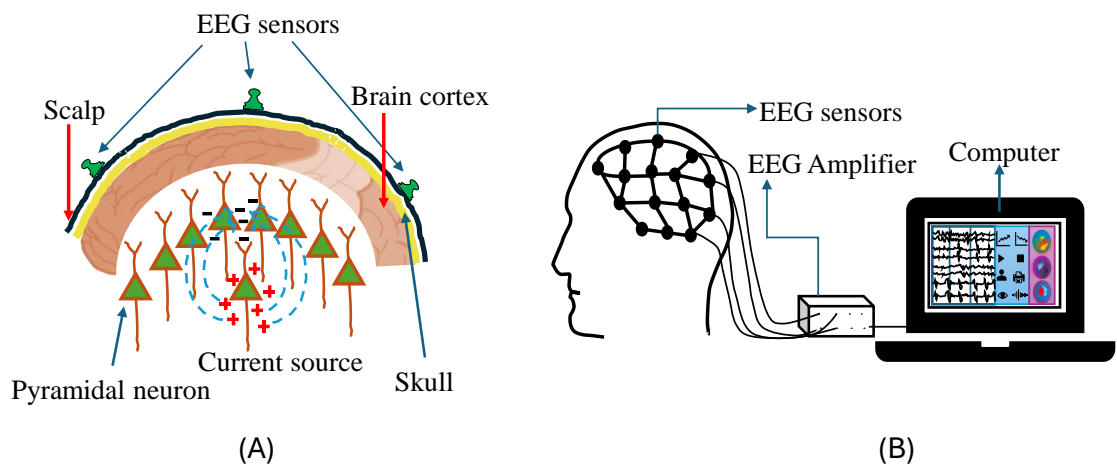


Figure 2.3: Schematic diagram of (A) EEG measurement process (Li *et al.*, 2022), (B) a typical EEG system.

EEG signal acquisition is typically performed with a sampling rate ranging from 250 to 2000 Hz. However, modern EEG systems can achieve sampling rates of up to 20,000 Hz, providing higher resolution data. The amplitude of EEG brain signals in adults generally falls within the range of 10 to 50  $\mu\text{V}$  (Xu and Xu, 2019). Because the initial voltage signals

detected by EEG are relatively faint, they require amplification to enhance their clarity. The amplified signals are then digitised and stored in a computer for further analysis.

EEG is particularly valued for its high temporal resolution, allowing researchers to track rapid changes in brain activity. However, the spatial resolution is relatively lower compared to other imaging modalities. Despite this, EEG remains a powerful tool for studying brain function, diagnosing neurological disorders, and exploring cognitive processes.

EEG is a completely safe and widely used instrument for individuals of all ages. It is employed across a diverse range of diagnostic and research domains, including the assessment of physical damage, cognitive and neurocognitive functions, neurological diseases and disorders, brain development, and the evaluation of drug effects (Gevins *et al.*, 1999). The advancement of digital technology has enhanced the capabilities of EEG systems, which are now available with various features, performance levels, and costs. Both wired and wireless EEG systems offer ease of use, though each comes with its own set of advantages and disadvantages.

An EEG system comprises four main components: electrodes with conductive media, amplifiers with filters, an analogue-to-digital (A/D) converter, and a recording device. The electrodes are placed on the scalp according to the internationally recognised 10-20 system, which specifies the placement of electrodes to maintain a distance of either 10% or 20% of the head's circumference from one another. This system ensures consistent and reproducible electrode placement, covering key brain regions such as the frontal, central, parietal, and temporal areas. Electrode locations are referenced to anatomical landmarks including the nasion, inion, and preauricular points (Abhang, Gawali and Mehrotra, 2016).

Various types of electrodes are utilised, including disposable, reusable discs, headbands, electrode caps, saline-based electrodes, and needle electrodes. Each type has specific applications and benefits depending on the requirements of the study or clinical evaluation. The amplifiers in the EEG system are responsible for boosting the initially weak electrical signals generated by the brain to a level suitable for digitalisation. The A/D converter then transforms these analogue signals into digital form, allowing for accurate and efficient data processing. Finally, the recording device stores the digitised data for subsequent analysis. EEG systems, with their ability to provide detailed information about brain activity, play a crucial role in both research and clinical settings, enabling the investigation of brain function and the diagnosis of neurological conditions.

The design of a typical EEG cap and the positioning of its sensors are illustrated in Figure 2.4. This figure clearly demonstrates that each channel or sensor in the EEG system is assigned a specific name corresponding to a particular region on the surface of the head. The fundamental reference points include: 1) Nasion, 2) Inion, and 3) Preauricular Point.

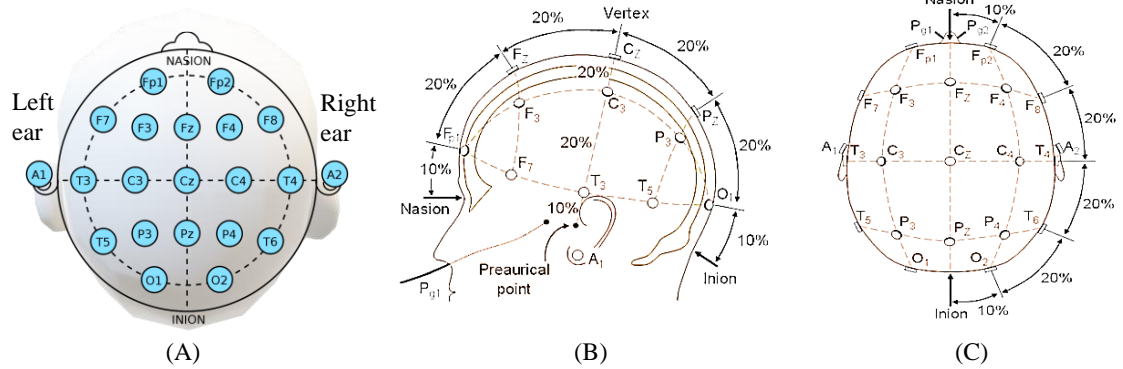


Figure 2.4: International 10-20 EEG system (A) 19 electrodes placement, (B) side view of 10%-20% electrode distances, (C) top view of 10%-20% electrode distances (Shriram *et al.*, 2012).

Three key reference points are illustrated in Figure 2.4 (A): the nasion, which is the lowest point between the forehead and the nose; the inion, located at the lowest point at the back of the head; and the left and right preauricular points, positioned just in front of the ears. Channels are named as follows: Fp refers to frontopolar, F denotes frontal regions, C denotes central regions, P denotes parietal regions, and T denotes temporal regions. The designation Z refers to electrodes placed along the midline, while A represents the auricular regions (MacDonald, 2015).

Each channel is strategically located to acquire signals corresponding to specific brain functions. For instance, F7 is positioned near areas responsible for rational activities, F8 is close to sources of emotional impulses, the cortex around C3, C4, and Cz is associated with sensory and motor functions, and T3 and T4 are near emotional processors (Abhang, Gawali and Mehrotra, 2016).

EEG signals are inherently non-linear, non-Gaussian, random, and non-correlated and these signals also exhibit variability influenced by factors such as the subject's age, mental state, and other conditions (Vaid, Singh, and Kaur, 2015). To understand the variability and interpret the EEG signals, various signal analysis techniques are employed. The widely used signal analysis techniques include:

- i. Spectral Analysis: This technique measures significant frequencies within the EEG data.
- ii. Temporal Analysis: This analysis determines both normal and abnormal brain wave characteristics and assesses the presence or absence of specific rhythms.
- iii. Spatial Analysis: This method is used to map the distribution of rhythms across various brain regions.

Normal EEG signals exhibit numerous characteristics influenced by parameters such as age, disease type, sleep states, and muscle movements (e.g., eye movements). Frequency levels can vary depending on these parameters and brain locations, as discussed in detail by Marcuse, Fields and Yoo (2016). For instance, maximal beta frequencies are often observed in the frontocentral region, and the presence of open eyes does not significantly affect beta characteristics.

EEG signals are significantly impacted by various events such as sleep, epileptic seizures, reflexology, anaesthesia, and meditation (Subha *et al.*, 2010). The presence of different frequency bands in brain waves plays a crucial role in determining signal characteristics. Sleep modes are analysed to diagnose sleep disorders, such as sleep apnoea. Additionally, EEG is effective in measuring abnormal neuronal activity associated with epilepsy. Other disorders, including dementia, Alzheimer's disease, cognitive impairment, and autism, can be diagnosed through specific feature extraction and selection processes. Different meditative states (Hebert *et al.*, 2005) and various types of music (Huisheng, Mingshi and Hongqiang, 2005) are also distinguishable within EEG signals.

The EEG system has gained widespread global acceptance due to its significant features. However, a notable limitation arises in accurately identifying the source of electrical activity on the scalp. This difficulty is attributed to variations in skull conductivity, which can be influenced by factors such as skull size and asymmetrical, non-homogeneous conductivity of the skull (Pohlmeier *et al.*, 1997).

### 2.3.5 Magnetoencephalography

MEG is a functional neuroimaging technique that directly measures the magnetic activity resulting from the electrical activity of brain neurons. Both chemical and electrical processes in the brain are stimulated by the movement of ions and electrolytes, which generates a magnetic field within the brain tissues. This technology specifically detects tangential dipoles corresponding to the locations of functional activity in the brain. The weak magnetic

fields produced by neural activity are recorded using highly sensitive magnetometers, most commonly Super-Conducting Quantum Interference Devices (SQUIDS). To minimise external magnetic interference, including that from the Earth's magnetic field, MEG systems are housed in magnetically shielded rooms. This imaging technique is particularly effective in brain mapping and guiding epilepsy surgery (Singh, 2014). MEG offers several advantages: it provides high spatial and temporal resolution, operates without inducing noise, and does not interfere with patient movement. Moreover, it is a non-contact recording method. However, MEG remains more expensive than EEG (Williamson *et al.*, 1991) and is not suitable for individuals with metal implants or other metallic objects in their bodies.

EEG and MEG share similarities, as both utilise neuronal activity as their primary source of data. To identify neuronal oscillations using either EEG or MEG, it is necessary to demonstrate a spectral peak within a specific frequency band. The characteristics of these oscillations—such as peak frequency, bandwidth, and amplitude—define the specific brainwave patterns. Lopes da Silva (2013) explores the relevance of EEG and MEG in neuroscience, examining the acquisition of brain electric and magnetic fields from the perspectives of biophysics and neurophysiology. The study also highlights common signal properties and interactions, such as oscillation frequency, and discusses the significance of EEG and MEG oscillations in various cognitive processes. The research identifies six types of neuronal oscillations: ultra-slow, theta, alpha, beta, gamma, and high-frequency oscillations (HFOs). Three fundamental functions of brain oscillations are discovered: coding specific information, regulating and modulating brain attentional states, and facilitating communication between neuronal populations.

### *2.3.6 Near Infrared Spectroscopy and Functional Near Infrared Spectroscopy*

NIRS is a non-invasive spectroscopic technique that has garnered significant attention in the field of brain imaging. Similar to MRI, NIRS tracks the real-time oxygenation of brain tissue. During cognitive or physical tasks, the brain regions involved consume more oxygen, which can be monitored using near-infrared light. Near-infrared (NIR) light, with wavelengths between 700 and 900 nm, penetrates biological tissue. This light is scattered minimally, and certain biological molecules, such as haemoglobin and myoglobin, absorb it. These molecules have distinct absorption spectra depending on their oxygenation states. By applying this optical technique, changes in blood flow and oxygenation can be measured. NIRS instruments generally fall into three categories: continuous wave (CW) measurement, time domain measurement, and frequency domain measurement. Among these, the CW

measurement is commonly used to monitor dynamic blood flow in the cerebral region by measuring changes in cerebral haemoglobin concentration. However, CW measurement is limited in its ability to quantify these concentration changes accurately (Hoshi, 2009).

Functional NIRS (fNIRS) employs source and detector probes placed on the scalp. Typically, a few centimetres of separation are maintained between the source and detector. fNIRS acquisition involves recording data both during and outside of tasks to establish baseline brain functions. By comparing haemoglobin measurements during resting and task states, brain activation can be assessed. However, data processing and analysis can vary widely. While fNIRS shares similarities with the fMRI BOLD measurement technique, it is more cost-effective and suitable for mobility and dual-task studies, making it frequently used in various pathological investigations. Nevertheless, fNIRS has some limitations, such as limited probe penetration depth, which restricts measurements to superficial layers of the brain cortex. This limitation can result in low spatial resolution and an inability to provide whole-brain outputs. Additionally, external contamination from superficial tissues and motion artifacts are challenges associated with fNIRS (Udina *et al.*, 2020).

NIRS is widely used in diverse fields such as agriculture, particle measurement, material science, astronomical spectroscopy, and medicine. In the realm of functional neuroimaging, it is referred to as functional NIRS (fNIRS). Udina *et al.* (2020) discuss hemodynamic activity in the brain during both movement and cognitive functions in adults. fNIRS allows for the monitoring of neuroimaging outputs through the measurement of oxygenated and deoxygenated haemoglobin during tasks such as walking. The authors reviewed numerous studies tracking hemodynamic functioning of the frontal lobe during motor tasks, cognitive activities, and combined actions. Their findings indicated that individuals with various neurological conditions exhibited higher cognitive activation compared to healthy individuals, suggesting that functional impairments in neurological conditions might be characterised by such activation patterns.

Gallegos-Ayala *et al.* (2014) successfully developed a brain communication system for fully locked-in patients using fNIRS. The system was designed for an individual with ALS, who had been in a fully locked-in state for approximately four years and was unable to communicate verbally or through body movements, including eye movements. The patient's bodily functions were maintained through artificial ventilation and a percutaneous endoscopic gastrostomy tube. The study ultimately developed an effective method using

hemodynamic brain activity detected by fNIRS. The communication system was used to assess correct or incorrect responses processed through the auditory system, resulting from functional activation in the brain cortex. Fixed sets of sentences were presented, with intervals of 25 seconds to align with hemodynamic activity. Responses were classified into 'yes' or 'no' using SVM for feature extraction and classification. The accuracy of known answers improved with successive sessions, reaching 76.30% in the final period, and achieving 100% accuracy in some sessions. This indicated that the system was effective for communication with locked-in patients, suggesting that metabolic BCI could be a promising and stable solution for individuals with severe physical disabilities. A similar study by Chaudhary *et al.* (2017) developed an online fNIRS classification system for four advanced ALS patients, where responses were represented as 'yes' or 'no'.

fNIRS has certain limitations that merit careful consideration in research contexts. Pinti *et al.* (2023) discuss several challenges associated with current fNIRS systems, particularly the reliance on approximate measurements of blood flow, which can impede the accuracy of direct neural activity assessments. Additionally, the presence of melanin in individuals with darker or thicker hair may further complicate measurements, as melanin is a strong absorber of near-infrared light and can interfere with signal acquisition. Moreover, fNIRS measures neural activation based on the timing of the hemodynamic response, which operates on the order of seconds. This temporal resolution is notably slower than that of EEG system, which can detect electrical neural responses within milliseconds (Su *et al.*, 2023). Therefore, while fNIRS offers valuable insights into brain activity, its limitations in temporal resolution and susceptibility to signal interference must be considered when selecting appropriate neuroimaging techniques for research.

### 2.3.7 Hybrid EEG-fNIRS

Both EEG and fNIRS are functional neuroimaging methods that, while differing in their measurement techniques, offer complementary benefits in terms of spatial and temporal resolution. These methods are cost-effective and portable, making them a holistic approach for neuroimaging. Consequently, the hybrid EEG-fNIRS technique has emerged as a promising method in the research field of BCI (Almajidy *et al.*, 2023).

Buccino, Keles and Omurtag (2016) conducted an experiment integrating EEG and fNIRS to assess multiple motor tasks. The study involved four types of movements: right-arm, left-arm, right-hand, and left-hand functions, executed by 15 subjects. Each subject performed

these four movements, which included arm rising and hand gripping, a total of 25 times per movement, organised into blocks. In total, five blocks were completed. Data acquisition for both EEG and fNIRS was conducted simultaneously throughout the experiment. The fNIRS system utilised a combination of 12 sources and 12 detectors, with 34 channels in total. An extended EEG cap was employed to mount both EEG electrodes and fNIRS optodes. The performance of the hybrid EEG-fNIRS technique was evaluated in real-time and was found to surpass that of single imaging techniques. The accuracy of the combined EEG-fNIRS approach demonstrated a significant improvement over the individual modalities. This enhanced performance underscores the potential of hybrid neuroimaging as a valuable alternative for investigating central nervous system functions. Ahn and Jun (2017) review a range of studies that explore the use of hybrid EEG-fNIRS systems. Their analysis highlights the potential benefits of multi-modal integration in enhancing system performance. However, they also identify significant challenges associated with this approach. The distinct characteristics of blood-based signals and electrical activity present inherent difficulties, and the integration of these modalities involves complex and time-consuming experimental setups and sensor configurations. These limitations underscore the need for careful consideration when designing and implementing multi-modal systems in research. A summary of the discussed brain imaging technologies is presented in Table 2.2.

Table 2.2: Comparison of brain imaging techniques.

<b>Imaging methods</b>	<b>MRI</b>	<b>fMRI</b>	<b>CT scan</b>	<b>PET scan</b>	<b>EEG</b>	<b>MEG</b>	<b>fNIRS</b>
<b>Imaging type</b>	Structural	Functional	Structural	Molecular	Functional	Functional	Functional
<b>Physical structure</b>	Blood flow	Blood flow	Soft tissue, blood vessels and bones	Blood flow	Electrical field	Magnetic field	Blood flow
<b>Signal measured</b>	Anatomic information of grey and white matter	Indirect metabolic	Anatomic information of brain	Indirect metabolic	Direct electrical	Direct magnetic	Indirect metabolic
<b>Concept</b>	Detecting resonant and non-resonant molecules	Measuring hemodynamic activity	Create 3D image from multiple cross-sectional X-ray images	Detecting chemical activity by injecting radiotracer	Measuring electrical activity in the form of brain signal	Measuring magnetic field resulting from electrical activity	Measuring hemodynamic activity

Table 2.2: Comparison of brain imaging techniques. (continued from previous page)

Imaging methods	MRI	fMRI	CT scan	PET scan	EEG	MEG	fNIRS
Used approach	Magnet and radio waves	Magnet and radio waves	Electromagnetic Radiation	Electromagnetic Radiation	Electrodes, amplifier, AC/DC Converter	Probes, Strong magnet	Probes, near infrared light
Risk	Low	Low	High	High	No	No	No
Spatial resolution	Very high (3-6mm)	Very high (3-6mm)	Very high (1mm)	Very high (5mm)	Low (1-2cm)	Low (1-2cm)	High (<1cm)
Temporal resolution	Low (~30s)	Low (~30)	Medium (10s)	Low (30-40s)	Very high (~0.05s)	Very high (~0.05s)	Low (5-8s)
Moving flexibility	No	No	No	No	Yes	No	Yes
Cost*	(\$2-3M) (Sarracani <i>et al.</i> , 2015)	(\$2 M) (Lystad and Pollard, 2009)	(<\$2M) (Rehana <i>et al.</i> , 2013)	\$8M (Lystad and Pollard, 2009)	\$100K (Lystad and Pollard, 2009)	\$2M (Lystad and Pollard, 2009)	\$350K (Lystad and Pollard, 2009)
Popular products	Siemens, GE, Philips, Toshiba, Hitachi	Siemens, GE, Philips, Toshiba, Hitachi, Resonance Tech etc.	Siemens, GE, Philips, Shimadzu, Toshiba, Hitachi	Siemens, GE, Philips, Shimadzu	NeuroScan, Greentek, Brain Products, BioSemi, Emotiv etc.	Brain Products	Greentek, NIRx, Hitachi, Artinis

\*Approximate cost

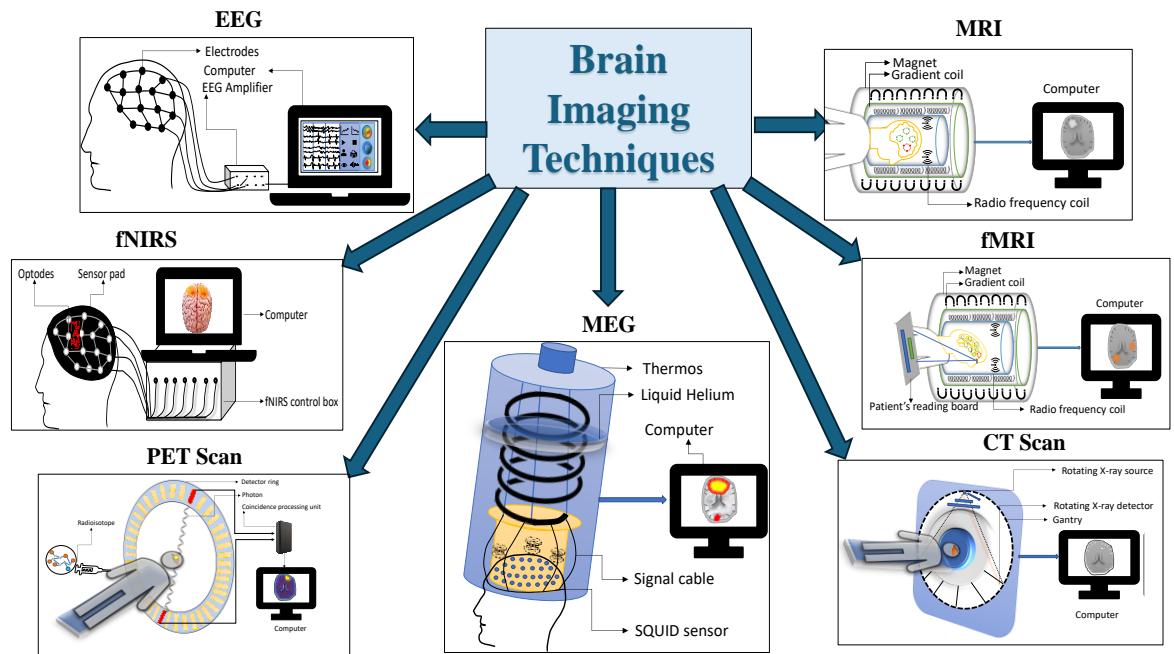


Figure 2.5: Schematic representation of different brain imaging techniques.

In addition, these technologies are schematically illustrated in Figure 2.5. Both table and figure have collected information from multiple online resources (*Top 10 Diagnostic*

*Imaging Device Manufacturers & Leading Way, 2012; Top 5 Vendors in the Global Brain Monitoring Devices Market From 2017 to 2021: Technavio | Business Wire, 2017; Neuroimaging Market - Share, Size and Industry Analysis, 2023*). Commercial EEG devices have been manufactured with varying numbers of sensors, sampling rates, prices, and purposes (Ledwidge, Foust and Ramsey, 2018). Most common manufacturers are Emotiv, openBCI, NeuroSky, NeuroScan, Brain Products, Artinis Medical system, g.tech, Neuroelectronics, EGI, BioSemi etc. Emotiv released multiple production with different configurations (Dadebayev, Goh and Tan, 2022). Table 2.3 provides some of the models, their intended purposes, and key specifications.

Table 2.3: Commercial EEG devices (Ledwidge, Foust and Ramsey, 2018; Dadebayev, Goh and Tan, 2022).

Commercial EEG Manufacturer	Device name	Year of Release	Number of sensors	Sampling rate (Hz)	Price* (USD)	Purpose
Emotiv	EPOC+	2013	14	128/256	699	Academic
Emotiv	INSIGHT	2015	5	128	299	Everyday use
Emotiv	EPOC FLEX	2018	Maximum 32	128	1699	Research-grade
Emotiv	EPOC X	2020	14	128/256	799	Neuroscience research with broader scope
BioSemi	Active Two	2016	32 256	≥2048 Hz (subjective to the version and bandwidth)	20K 87K	EEG lab at Undergraduate institution
Brain Products	actiCHamp	2011 (first)	32 160	Up to 100kHz (latest version)	43K 80K	EEG lab

\*Approximate price

A variety of brain imaging techniques are available, each offering distinct advantages and limitations. Among these, EEG is recognised as the most suitable and widely employed method. This research opts to utilise EEG system, and the following sections provide a detailed discussion of the EEG signal processing methods and algorithms used in the development of BCIs.

## 2.4 Signal Processing Methods

EEG brain signals undergo a series of processing and analysis steps, which are crucial for the development of BCIs. Some review articles offer an extensive exploration of potential

techniques for each stage of EEG signal processing in BCI applications. They also provide insights into the various application domains that require sophisticated brain signal processing and analysis (Nicolas-Alonso and Gomez-Gil, 2012; Al-Fahoum and Al-Fraihat, 2014; Vaid, Singh and Kaur, 2015; Niha and Banu, 2016; Aggarwal and Chugh, 2019; Huang and Wang, 2021; Stancin, Cifrek and Jovic, 2021). Developing algorithms for EEG signal processing is a complex task, given that there are approximately fifty algorithms designed to measure brain activity through Event-Related Potentials (ERP). This section provides a comprehensive literature review of well-established techniques in signal processing, focusing on the basic steps: preprocessing, feature extraction, and feature selection. While some research integrates feature extraction and selection concurrently, other studies apply these techniques sequentially. Below, we discuss various techniques employed in preprocessing, feature extraction, and feature selection:

#### *2.4.1 Signal Pre-processing*

Once EEG signals are captured, they require processing to enhance their quality, as initial signals are often contaminated with noise, power line interference, artefacts, eye or muscular movements, and cardiac activity. To address these disruptions, several methods can be employed, including Adaptive Filtering, Common Spatial Patterns (CSP), Surface Laplacian (SL), Principal Component Analysis (PCA), Common Average Referencing (CAR), and Independent Component Analysis (ICA).

Garcés and Orosco (2008) explore EEG signal processing within the context of BCIs, where human thoughts are translated into actionable commands for devices. High-pass and low-pass filters can be used to remove low-frequency interruptions ( $<0.5$  Hz) and mitigate high-frequency noise (50-70 Hz), respectively. Additionally, biological signals such as electrocardiogram (ECG), eye-blinking (EOG) and artifacts of movements (EMG) often contaminate EEG recordings, however techniques like PCA, ICA, or Adaptive Filtering (AF) can effectively eliminate these unwanted noises. Signal enhancement can also be achieved through Common Average Referencing (CAR) technique, which involves calculating the difference between the mean value of all EEG channels and each individual channel, thus reducing undesired influences within the channels. A summary of popular techniques for preprocessing, feature extraction, and feature selection is presented in Table 2.4, with information collected from various sources (Garcés and Orosco, 2008; Lotte, 2012; Nicolas-Alonso and Gomez-Gil, 2012; Gupta *et al.*, 2014; Sankar *et al.*, 2015; Albuquerque *et al.*, 2016; Sankar *et al.*, 2019).

Table 2.4: Overview of EEG signal pre-processing, feature extraction, and feature selection techniques and their key attributes.

Techniques	Type	Attribute
<b>Adaptive filter</b>	Signal pre-processing	<ul style="list-style-type: none"> <li>- Removing noise from acquired signal.</li> <li>- Effective for signals with overlapped spectra.</li> </ul>
<b>High-pass filter</b>	Signal pre-processing	<ul style="list-style-type: none"> <li>- Removing low frequency interruptions (e.g. breathing).</li> <li>- Cut-off frequency is <math>&lt;0.5</math> Hz.</li> </ul>
<b>Low-pass filter</b>	Signal pre-processing	<ul style="list-style-type: none"> <li>- Mitigating high-frequency (50-70Hz) noise.</li> <li>- Cut-off frequency between 50 and 70 Hz.</li> </ul>
<b>Common spatial pattern (CSP)</b>	Signal pre-processing, feature extraction	<ul style="list-style-type: none"> <li>- Measuring random activity of signal and converting into matrix.</li> <li>- No prerequisite skill for patients' frequency band.</li> </ul>
<b>Surface Laplacian (SL)</b>	Signal pre-processing	<ul style="list-style-type: none"> <li>- Estimating the existing density and eliminating ocular movements from signal.</li> <li>- Effective for the artefacts from uncovered head area of sensors.</li> </ul>
<b>Common average referencing (CAR)</b>	Signal pre-processing	<ul style="list-style-type: none"> <li>- Reducing noise through placing the electrodes and enhancing the signals for better classification.</li> <li>- Inadequate result from the area which is not covered by sensors as well as with certain sample density.</li> </ul>
<b>Principal component analysis (PCA)</b>	Signal pre-processing, Feature extraction, Feature selection	<ul style="list-style-type: none"> <li>- Extracting basic components from decomposition of multi-channel sensor observations to separate estimated noise.</li> <li>- Feature extraction from the domain of space-time frequency.</li> <li>- Higher classification accuracy</li> <li>- Detecting the most relevant features from multiple attributes.</li> </ul>
<b>Independent component analysis (ICA)</b>	Signal pre-processing, Feature extraction, Feature selection	<ul style="list-style-type: none"> <li>- Segregating the required artefact according to data characteristics and decomposing the multiple signal channels to time based independent and fixed spatial component.</li> <li>- More computation oriented.</li> <li>- Adequate decomposition for big data.</li> <li>- Good number of features can be extracted.</li> <li>- Detecting the most relevant features from multiple attributes.</li> </ul>

Table 2.4: Overview of EEG signal pre-processing, feature extraction, and feature selection techniques and their key attributes. (continued from previous page)

Techniques	Type	Attribute
<b>Auto regressive</b>	Feature extraction	<ul style="list-style-type: none"> <li>- Extracting features based on frequency domain.</li> <li>- Efficient for non-stationary signals.</li> <li>- Different subcategories are available and useful for the data with short duration.</li> </ul>
<b>Wavelet transform (WT)</b>	Feature extraction	<ul style="list-style-type: none"> <li>- Extracting features by B-spline parameters for time- frequency domain, and filtering for multi-resolution analysis.</li> <li>- Different window sized signals can be analysed.</li> </ul>
<b>Wavelet packet decomposition (WPD)</b>	Feature extraction	<ul style="list-style-type: none"> <li>- Extracting features for both time and frequency domain.</li> <li>- Efficient for non-stationary signals.</li> <li>- Useful for decomposition of low-frequency wavelets.</li> <li>-Time-intensive procedure.</li> </ul>
<b>Fast Fourier transform (FFT)</b>	Feature extraction	<ul style="list-style-type: none"> <li>- Extracting features in frequency domain.</li> <li>- Effective for stationary signal to produce successful outcome in linear random process.</li> </ul>
<b>Entropy</b>	Feature extraction	<ul style="list-style-type: none"> <li>- Extracting features by analysing chaos and dynamic characteristics.</li> <li>- Provides qualitative estimation of chaos from brain signals.</li> <li>- Effective subcategories are available.</li> </ul>
<b>Wavelength optimal spatial filter (WOSF)</b>	Feature extraction	<ul style="list-style-type: none"> <li>- Extracting waveform length features.</li> <li>- Signal complexity can be measured.</li> <li>- Successfully implemented for both motor imagery and mental rotation tasks.</li> <li>- Higher accuracy towards classification.</li> </ul>
<b>Genetic algorithm</b>	Feature selection	<ul style="list-style-type: none"> <li>- Optimisation procedure to select potential features.</li> <li>- Implement as an automated feature extraction in certain applications.</li> </ul>
<b>Sequential selection</b>	Feature selection	<ul style="list-style-type: none"> <li>- Selecting optimised features.</li> <li>- A subcategory named sequential forward floating search (SFFS) is effective in dimensional reduction.</li> </ul>

Table 2.4: Overview of EEG signal pre-processing, feature extraction, and feature selection techniques and their key attributes. (continued from previous page)

Techniques	Type	Attribute
<b>Distinctive Sensitive Learning Vector Quantisation (DSL VQ)</b>	Feature selection, Classifier	- Detecting unique features towards the accurate classification. - Applicable for the features within frequency domain.

#### 2.4.2 Feature Extraction and Selection

Visual representation of signals is commonly subjective and not easy to shape for statistical analysis or equivalent standardisation. Therefore, intermediate techniques are required to quantify the information contained within the signals. In the frequency and time-frequency domains, various methods are employed for the feature extraction of EEG signals. Feature extraction modalities generally fall into two categories: statistical characteristics and syntactic descriptions (Cvetkovic, Übeyli and Cosic, 2008; Al-Fahoum and Al-Fraihat, 2014).

Several approaches can be used for extracting features from EEG signals, including time-domain analysis, spectral analysis, time-frequency analysis (such as wavelet transform), chaos and dynamic analysis (including entropy), and others (Garcés and Orosco, 2008). Prominent techniques for feature extraction include ICA, PCA, LDA (Atangana *et al.*, 2020), Autoregressive models, WT, Wavelet Packet Decomposition (WPD), FFT etc (Sankar *et al.*, 2019).

EEG signals are processed and analysed through both feature extraction and feature selection stages. This process allows for the extraction of significant characteristics from a set of brain signals, and the selection of the most relevant features from these extracted characteristics. It is crucial to identify intrinsic characteristics from sensor-generated signals using feature extraction techniques that align with the desired objectives. For example, some key frequency properties of EEG signals include amplitude value, Band Power, Power Spectral Density, Autoregressive parameters, adaptive autoregressive parameters, time-frequency features (T-F), and features derived from inverse models (Niha and Banu, 2016). The power spectral density, which is computed via the Fourier transform of the estimated autocorrelation sequence, is a fundamental method for determining signal characteristics.

This sequence is obtained using nonparametric methods, providing insights into the signal's frequency content (Stancin, Cifrek and Jovic, 2021).

To characterise and analyse brain activity, various properties of EEG signals play a crucial role. These properties are essential in the subsequent classification phase, which is pivotal for developing effective BCI applications. The choice of feature properties depends on the classifier used, making it critical to select the most relevant characteristics for accurate signal interpretation. For example, Stancin, Cifrek and Jovic (2021) reviews a range of EEG brain signal features for various domains in terms of driver drowsiness detection system. The features are not limited to certain domain, advanced techniques within both the time-frequency and space-time-frequency domains are employed to extract a combination of features from the time and frequency domains (Vaid, Singh and Kaur, 2015). For instance, linear analysis methods such as FFT and DWT are widely used for feature extraction from EEG signals (Al-Fahoum and Al-Fraihat, 2014).

#### 2.4.2.1 Frequency Domain Analysis Using FFT

In the field of signal processing, the FFT is extensively utilised as a technique for frequency domain analysis. The EEG spectrum is traditionally divided into four primary frequency bands: delta (<4 Hz), theta (4–8 Hz), alpha (8–12 Hz), and beta (12–35 Hz). The raw EEG data, initially presented as a time-domain signal, is transformed into the frequency domain using FFT, which decomposes the signal into its constituent frequency components. The resulting FFT output quantifies the relative strengths (i.e., magnitudes) of these frequency components.

The FFT output is computed by converting the time-domain signal  $x(n)$  into the frequency domain  $X(k)$ . This transformation is mathematically represented by the following Equations (2.1) and (2.2) (Akin, 2002).

$$X(k) = \sum_{n=0}^{N-1} x(n) \cdot e^{-\frac{j2\pi kn}{N}} \quad (2.1)$$

$$x(n) = \frac{1}{N} \sum_{k=0}^{N-1} X(k) \cdot e^{\frac{j2\pi kn}{N}} \quad (2.2)$$

where,  $j = \sqrt{-1}$ ,  $N =$  length of  $x(n)$ .

FFT operates solely in the frequency domain, which contrasts with the DWT, a technique capable of analysing both time and frequency domains. Each method has its respective advantages and limitations. FFT is particularly effective for identifying and quantifying periodic components within the signal, making it a valuable tool for feature extraction in various studies (Hadjiyannakis *et al.*, 1997; Uchida *et al.*, 1999; Subasi *et al.*, 2005; Polat and Güneş, 2008; Murugappan and Murugappan, 2013; Sařabun, 2014; Jaswal, 2016; Delimayanti *et al.*, 2020; Li and Chen, 2021).

#### 2.4.2.2 Time-frequency Domain Analysis Using DWT

In contrast to frequency domain analysis, the DWT provides a time-frequency domain analysis, capturing both temporal and spectral information through varying window sizes. This flexibility allows for the analysis of high-frequency components with shorter windows and low-frequency components with longer windows, thus offering a more detailed and comprehensive analysis of the signal (Aggarwal and Chugh, 2019). The DWT decomposes the original signal into two primary components: the Approximate Component (cA) and the Detail Component (cD). This decomposition is achieved using low-pass and high-pass filters, respectively.

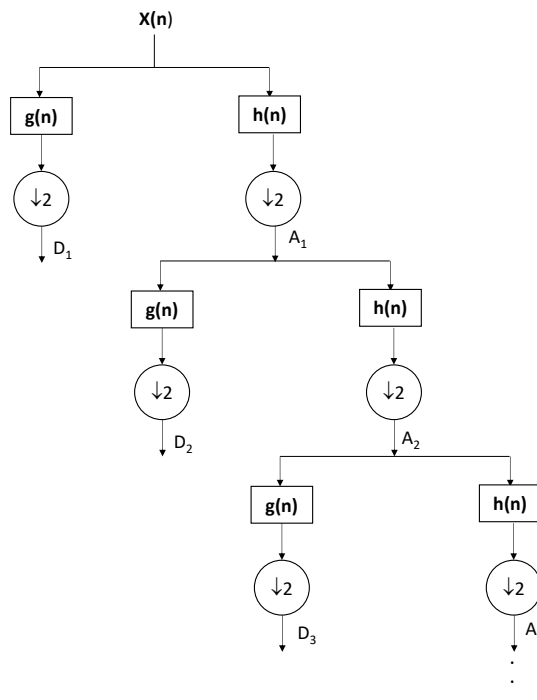


Figure 2.6: Sub-band decomposition in DWT (Cvetkovic, Übeyli and Cosic, 2008).

The process of decomposition can be recursively applied to the cA in subsequent stages, thereby enabling a multi-resolution analysis of the signal (Cvetkovic, Übeyli and Cosic,

2008). The mathematical basis of the DWT is rooted in the Wavelet Transform, where the scaling function  $\varphi(x)$  is defined in Equation (2.3) (Alkhadafe, Al-Habaibeh and Lotfi, 2016)

$$\varphi(x) = \sum_{k=0}^{l-1} c(k)\varphi(2x - k) \quad (2.3)$$

where,  $c(k)$ = wavelet coefficient,  $k$ =index,  $l$ =decomposition level.

One of the significant advantages of DWT is its efficiency in data compression and rapid computation (Usha Kumari *et al.*, 2020). The breakdown diagram in Figure 2.6 shows the procedure of multiresolution decomposition for a signal  $x(n)$ . This process consists of repeated stages and each stage has 2 digital filters [discrete mother wavelet high pass filter  $g(n)$  and mirror version low pass filter  $h(n)$ ] and 2 down samplers by 2. Two filters produce down-sampled outputs called D1 as detail and A1 as approximation. The process is iteratively repeated, with each stage performing down-sampling by a factor of 2, allowing for a progressive refinement of the signal's time-frequency representation.

The standard quadrature mirror filter condition ensures that the low-pass filter used in the DWT is appropriate for wavelet transforms, maintaining the integrity of the frequency components across different scales. DWT offers a robust framework for time-frequency analysis, facilitating the examination of both transient and periodic features within EEG signals. Its capability for multiresolution decomposition makes it particularly useful for applications requiring detailed time-frequency information.

For signal analysis, selecting the appropriate wavelet and the number of decomposition levels is both crucial and challenging. The outcome of the wavelet transform is highly dependent on the choice of wavelet because the basic waveforms differ among wavelet types. No single wavelet is universally optimal for all types of input signals; rather, specific wavelets may be more suitable for particular situations. Consequently, the choice of wavelet affects the quality of the wavelet coefficients, which are used as input features for classification tasks. Proper wavelet selection can therefore significantly influence the accuracy of classification (Glassman, 2005).

Various wavelets (Bajaj, 2021) have been employed as mother wavelets in brain signal processing, including variations of Daubechies (Shaker, 2007; Cvetkovic, Übeyli and Cosic, 2008; Murugappan, Ramachandran and Sazali, 2010; Usha Kumari *et al.*, 2020; Jacob *et al.*, 2021; Rajashekhar, Neelappa and Rajesh, 2022), Haar (Kousarrizi *et al.*, 2009; El Bahy *et*

*al.*, 2017; Abed *et al.*, 2018), Sym9 (Graumann *et al.*, 2004), Meyer (Samar *et al.*, 1999; Glassman, 2005), and Rbio (Sairamya, Subathra and Thomas George, 2022) among others. Each wavelet has unique properties that make it effective depending on the characteristics of the signal being analysed. To determine the most suitable wavelet for a given application, researchers sometimes test various wavelets with different numbers of decomposition levels and select the one that demonstrates the highest efficiency for the specific application (al-Qerem *et al.*, 2020). The selection of the appropriate mother wavelet is often based on the characteristics of the input signals and a comparative analysis of the outputs produced by different wavelets (Glassman, 2005).

The number of decomposition levels in wavelet analysis is determined by the signal's dominant frequency components. The levels of decomposition must be sufficient to ensure that the signal's parts are adequately correlated with the desired frequency bands for effective classification. For instance, Cvetkovic, Übeyli and Cosic (2008) and Ji *et al.* (2019) employed a four-level decomposition for EEG signals, yielding four cDs (termed as D1 through D4) and one final cA (termed as A4). On the other hand, Rajashekhar, Neelappa and Rajesh (2022) decomposed EEG signals into 7 levels (D1 to D7). The decomposition is highly dependent on some parameters such as wavelet function, wavelet order, sampling rate of the signal, the characteristic of required frequency bands of interest, such as alpha and/or beta waves etc. Thus, the choice of wavelet and the number of decomposition levels are fundamental considerations in wavelet-based signal processing, with significant implications for the accuracy and effectiveness of the analysis.

Shaker (2007) conducted a comparative study of both FFT and WT for analysing EEG brain signals. The study found that WT outperformed FFT in detecting brain diseases. Despite this, the author utilised DWT as a classifier for filtered EEG frequencies. The observation about the higher performance of DWT over FFT is consistent in the studies of Akin (2002) and Kit *et al.* (2023), who compared FFT and DWT for feature extraction. Although DWT was proposed as a solution, the performance of FFT was found to be comparable. The effectiveness of these techniques depends on several factors, including the length of the data, wavelet selection, scaling, and shifting properties (Akin, 2002).

In the realm of feature extraction and selection Bashashati *et al.* (2007), and Lakshmi, Prasad and Chandra Prakash (2014) emphasised that selecting the most appropriate techniques remains a significant challenge. It is important to note that no single technique is universally

superior for all problems. The efficacy of a particular method can vary widely depending on the specific problem being addressed. Therefore, while multiple techniques may offer valuable insights, the optimal choice often depends on the unique characteristics of the data and the goals of the analysis.

### **2.4.3 ASPS Approach**

In the field of brain signal processing and analysis, selecting the most appropriate method from a range of feature extractors, selectors, and classifiers presents a significant challenge. Researchers often choose separate techniques for feature extraction and optimisation, which can be time-consuming and labour-intensive. To tackle this challenge, a groundbreaking approach called the ASPS approach has been introduced (Al-Habaibeh and Gindy, 2000; Al-Habaibeh, 2000). This approach was originally developed based on Taguchi's orthogonal arrays and was initially applied to condition monitoring in milling processes.

The ASPS approach utilises multiple sensors to acquire signals and processes them to extract the most informative SCFs. It offers a straightforward and efficient method for extracting useful information from a variety of signals. The process involves collecting data from standard sensors, which is then subjected to a systematic processing method to identify the most significant features. After basic pre-processing, signals undergo advanced processing techniques such as FFT and/or DWT. Following data collection and processing, the ASPS approach identifies the most sensitive SCFs necessary for developing the desired system.

The ASPS approach addresses the challenge of selecting appropriate signal processing techniques for specific purposes. It reduces experimental effort, time, and cost by streamlining the feature extraction and selection process. The ASPS approach is noted for its theoretical simplicity and practical applicability in extracting valuable information from multiple sensory signals. Subsequent research has expanded on the ASPS approach, with notable contributions by Abbas, Al-Habaibeh and Su (2011), Al-Habaibeh, Zorriassatine and Gindy (2002), Alkhadafe (2015), Alkhadafe, Al-Habaibeh and Lotfi (2016), Shakmak (2016), and Al-Azmi, Al-Habaibeh and Abbas (2023). These studies demonstrated the effectiveness of the ASPS approach in various applications, including condition monitoring of gearboxes, tools, and water leakage detection systems.

## **2.5 Signal Classification**

For further use of brain signals based application development an inevitable step is signal classification which enables brain signals to be operated as control commands. This process

allows brain signals to be translated into control commands (Bashashati *et al.*, 2007; Aggarwal and Chugh, 2019). The choice of the most suitable classification algorithm is determined by the existing feature properties. The importance of selecting appropriate feature characteristics is discussed in Section 2.4. Examples of such feature properties may include noise and outliers, high dimensionality, temporal information, non-stationarity, and the presence of small training datasets. These factors must be carefully considered during the feature extraction process to ensure the optimal performance of the BCIs system.

At this stage, brain signals are referred to as BCI control signals. These signals possess certain features related to signal type, training, information transfer rate, and the specific BCIs type. The classification method applied at this point further refines the BCIs control signals for practical use. Choosing an appropriate classification or regression algorithm is critical (Nicolas-Alonso and Gomez-Gil, 2012).

Classification methods can be evaluated based on themes such as generative versus discriminative, dynamic versus static, stable versus unstable, and linear versus non-linear. Among the numerous classifiers available, common choices in BCIs development include LDA (Trammel *et al.*, 2023), ANNs (Hramov *et al.*, 2017), Hidden Markov Models (HMM) (Akrami *et al.*, 2005), KNN (Narayan, 2021), fuzzy logic (Nguyen *et al.*, 2015), and SVM (Subasi and Gursoy, 2010). Table 2.5 outlines the major attributes of various classification techniques, demonstrating that ANNs and other non-linear classifiers generally outperform linear, generative, and static classifiers in terms of effectiveness.

Table 2.5: Classification algorithms.

Techniques	Type	Attribute
LDA	Linear classifier	<ul style="list-style-type: none"> <li>- Easy to implement.</li> <li>- Computationally cost effective.</li> </ul>
SVM	linear classifier	<ul style="list-style-type: none"> <li>- Produce well generalisation through complexity reduction.</li> <li>- High performance as well as computational complexity.</li> </ul>
Naïve Bayes classifier	Generative-model classifier	<ul style="list-style-type: none"> <li>- Generates non-linear decision boundary.</li> <li>- Inadequate to estimate the exact class probability.</li> <li>- Works for small training dataset.</li> </ul>
KNN	Non-linear	<ul style="list-style-type: none"> <li>- Easy implementation and debugging.</li> <li>- Higher performance in terms of complex classification tasks.</li> <li>- Not good for large dataset, irrelevant as well as redundant features.</li> </ul>

Table 2.5: Classification algorithms (continued from previous page)

Techniques	Type	Attribute
ANNs	Non-linear classifier	<ul style="list-style-type: none"> <li>- Multilayer perceptron neural network.</li> <li>- Supports neurons for bunch of layers.</li> <li>- Deep learning techniques are used (e.g. DNN, CNN etc.).</li> <li>- Works effectively with dataset of varying size, contingent upon the choice of classifier.</li> <li>- Easy implementation, very efficient and widely used</li> </ul>

ML techniques, a subset of AI, involves a range of algorithms and statistical models designed to train computers to perform tasks autonomously (Abiodun *et al.*, 2018). ML is primarily classified into two categories based on learning techniques: supervised and unsupervised learning. Supervised machine learning further divides into classification and regression. Classification involves predicting discrete labelled outcomes, while regression generates continuous output without labelled data (Soofi and Awan, 2017). Prediction tasks can be approached as either classification or regression problems depending on the specific requirements and availability of data. Similarly, signal features can be learned through either supervised or unsupervised methods. In recent years, ML techniques have been increasingly applied to brain signal classification. (Fabietti, Mahmud and Lotfi, 2021) provide a comprehensive review of 40 articles in portable EEG system, focusing on various ML techniques employed in EEG-based BCI applications. Among the diverse array of methods explored, including SVM, LDA, Logistic Regression (LR), Markov-ChainMonte-Carlo (MCMC), Passive-Aggressive Algorithm type-I, Extreme Gradient Boosting (XGBoost), Neural Networks (NN) and Decision Trees (DT), the authors highlight that SVM (37%) and NN (42%) have been the most extensively utilised in recent research. Within the category of NN algorithms, FFNN and CNN dominate, accounting for 88% of the neural network approaches investigated in the literature. This survey underscores a pronounced preference for these methods in the development of EEG-based BCI systems. Numerous research studies have focused on comparing various classifiers to identify the most effective algorithm for specific tasks. For instance, Trammel *et al.* (2023) conducted a study on EEG classification to decode semantic relatedness, in which they compared three machine learning classifiers: SVM, RF, and LDA. Among these, the SVM outperformed the others, achieving the highest decoding accuracy along with the greatest sensitivity. Notably, even with a limited number of training trials, the SVM model was capable of accurately

classifying EEG signals, demonstrating its suitability as a robust method in cognitive science research. Table 2.6 provides a summary of several such studies, listing the classifiers employed and their corresponding accuracies. This table highlights the widespread utilisation of SVM and ANN in various EEG classification tasks.

Table 2.6: Utilisation of classifiers and their accuracies in EEG classification studies.

Authors	Classifiers	Best accuracy	Study
(Bilucaglia <i>et al.</i> , 2020)	SVM KNN LDA	63.8% 63.7% 63.68%	EEG classification in emotion-related brain anticipatory activity
(Xu and Xu, 2019)	Proposed Armiti model CNN SVM K-means	96.4% 80.1% 74.7% 65.6%	EEG classification with few channels
(El Bahy <i>et al.</i> , 2017)	SVM NN (Multi-Layer Perceptron [MLP]) trained with backpropagation NN	84% 82.6%	Mental tasks classification from EEG signals
(Jacob <i>et al.</i> , 2021)	SVM Random Forest (RF) MLP	93.17% 97.67% 94.67%	EEG classification for the diagnosis of encephalopathy
(Rajashekhar, Neelappa and Rajesh, 2022)	KNN Naïve Bayes Euclidean distance SVM ANN	92.77% 85.8% 78.80% 98.37% 94.75%	EEG signals classification for detecting left and right-hand movements
(al-Qerem <i>et al.</i> , 2020)	SVM DT Naïve Bayes KNN AdaBoost ANN	95.5-100% 94-99.6% 86.33-100% 97-100% 97-100% 97-100%	EEG classification for proposed feature extraction model using wavelet family
(Sharma, Kim and Gupta, 2022)	SVM KNN RF Gaussian Naïve Bayes Bernoulli Naïve Bayes Logistic regression MLP	72% 76% 85% 75% 59% 66% 85%	EEG classification for different motor imagery tasks

Most of the studies listed in Table 2.6 involve performance comparisons across various parameters, such as differences between subjects, feature sets, or methods. However, only the highest accuracies of the ML techniques are presented here to provide a comparative overview of the algorithms' performances. It is important to note that no single algorithm consistently outperforms all others across all scenarios. An algorithm such as SVM may produce varying results across different research contexts.

### 2.5.1 Artificial Neural Networks

ANNs, particularly those employing deep learning algorithms, are extensively utilised classifiers that deliver remarkable results in pattern recognition, image recognition, natural language processing, and emotion recognition. They have found successful applications across various fields, including neuroscience, neuro engineering, and biomedical engineering. A comprehensive survey on deep learning methods for EEG analysis by (Li *et al.*, 2020) reveals that several architectures, such as Deep Belief Networks (DBN), Sparse Auto Encoders (SAE), DNN, and semi-supervised DBNs, have been explored by researchers. These methods have been applied to classify EEG raw data and frequency spectra in diverse contexts, including motor imagery tasks, emotion detection, seizure detection, and Alzheimer's disease detection.

For motor imagery tasks involving left and right-hand movements, An *et al.* (2014) demonstrated that the DBN model, with eight hidden layers, achieved superior performance compared to SVM. Notably, the number of neurons in the network did not significantly impact accuracy. In addition to supervised techniques, unsupervised methods have also been explored in ongoing state-of-the-art research on EEG classification. Unsupervised learning techniques, including various clustering algorithms and association rules, are instrumental in analysing unlabelled data. These techniques are prevalent in bioscience research and often yield results comparable to those produced by supervised models (Långkvist, Karlsson and Loutfi, 2012). Clustering algorithms, for instance, facilitate the partitioning of data into distinct classes or clusters based on similarity, thus aiding in the organisation and interpretation of complex datasets.

In the realm of intracranial EEG (iEEG), which provides detailed insights into brain functions, Saboo *et al.* (2019) employed an unsupervised learning technique to identify active electrodes. Their study involved data collection from 115 patients performing a verbal memory task. By applying Gaussian Mixture Models (GMM) to multiple matrices, both separately and in combination, the authors achieved 97% sensitivity and 92.9% specificity for the most efficient matrix.

Pfurtscheller and Pregenzer (1999) investigated the classification of 17-channel EEG signals corresponding to four types of body movement tasks using LVQ based on single-trial data. They examined both time and frequency components before and after the reaction stimulus for each task. Their model achieved a classification accuracy of 70% for the four distinct

movements. Mizuno *et al.* (2010) also utilised LVQ for clustering EEG signals, focusing on five mental tasks performed by three subjects. Their approach attained an accuracy of 81%. In their study, they employed the maximum entropy method in conjunction with frequency analysis to evaluate feature availability within the alpha and beta frequency bands. Figure 2.7 and Figure 2.8 schematically represent the architecture of FFNN and LVQ, respectively.

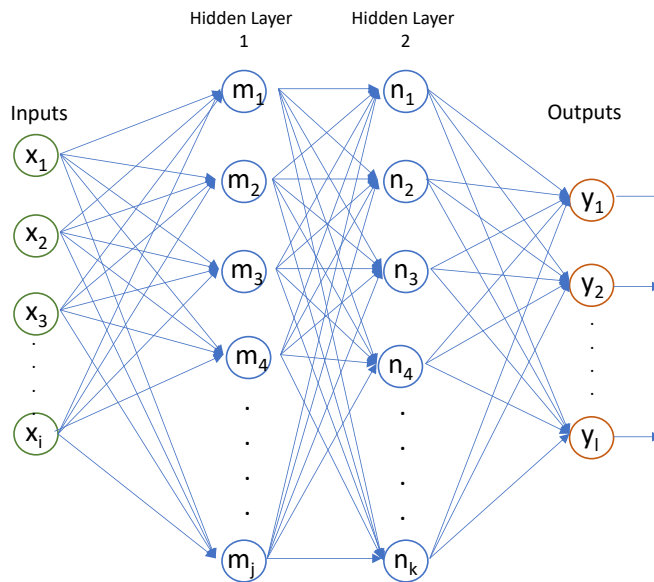


Figure 2.7: FFNN architecture (Montesinos López Osval Antonio and Montesinos López, 2022).

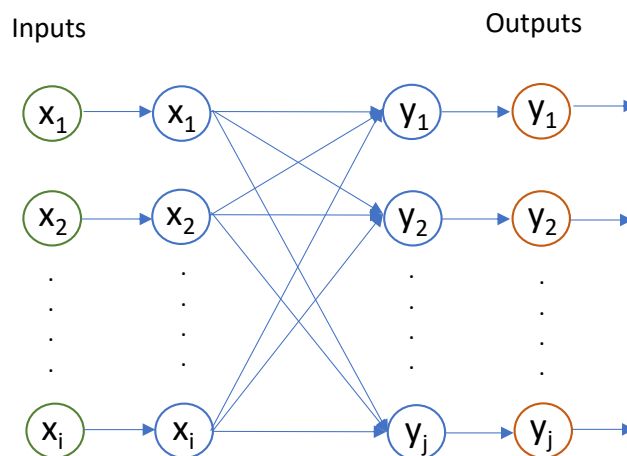


Figure 2.8: LVQ architecture (Bhardwaj, 2012).

Comparing MLP and LVQ, (Barna and Kaski, 1990) and (Rögnvaldsson, 1992) found that LVQ and MLP perform well for high dimensional and lower dimensional inputs respectively. However, both techniques have comparable sensitivity in terms of smaller size of training

data and MLP is a faster training process. MLP usually follows the form of FFNN (Kotsiopoulos *et al.*, 2021) where data progresses in one direction. However, it can be trained by backpropagation NN as well (El Bahy *et al.*, 2017). MLP algorithm is commonly employed for pattern classification tasks (Atangana *et al.*, 2020).

### 2.5.2 Image Processing and CNN

In recent years, several deep learning algorithms with the capacity to learn discriminative features have been successfully applied to EEG classification. These algorithms are employed to classify EEG signals based on various cognitive activities, including emotion recognition, motor imagery, and mental workload. Among the deep neural networks, CNN have demonstrated superior performance compared to other algorithms such as SAE, MLP, Recurrent Neural Networks, and DBN (Craik, He and Contreras-Vidal, 2019).

CNN are typically used with inputs that are either raw signal values or processed images, such as spectrograms. CNN consist of multiple convolutional layers with activation functions for feature learning, followed by fully connected layers with activation functions for output classification. Figure 2.9 shows the schematic representation of a typical CNN's architecture.

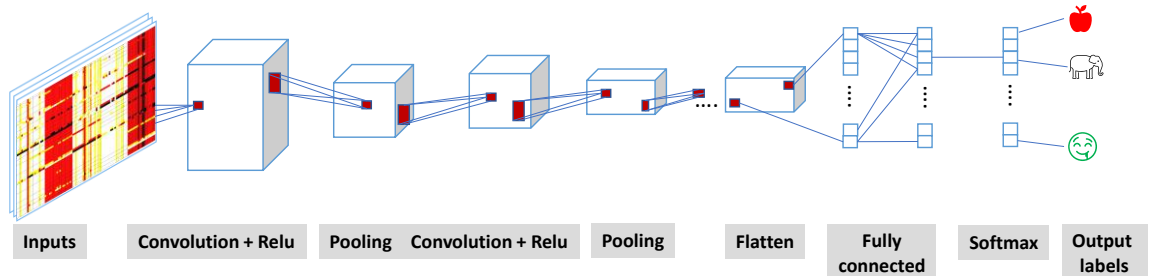


Figure 2.9: CNN architecture (Tsinalis *et al.*, 2016).

The convolutional layers, or lower network layers, perform the majority of the image recognition computations. Pooling layers, which down-sample the input image features, reduce the computational burden. The fully connected layers, or higher network layers, are responsible for classifying images based on the features extracted from the previous layers (Sainath *et al.*, 2015). CNN have proven effective in various research areas, including automatic sleep stage scoring, anomaly detection, seizure detection, and the imagination of geometric shapes (Tsinalis *et al.*, 2016; Wang *et al.*, 2016; Sakhavi and Guan, 2017; Acharya *et al.*, 2018; Llorella *et al.*, 2021).

## 2.6 BCI Devices for Communication Systems

EEG is valued for its simplicity and cost-effective equipment, contributing to its extensive use in modern BCI systems. These systems depend on different types of electrical brain activity, including the slow cortical potentials, event-related P300, sensorimotor rhythm like mu ( $\mu$ ) rhythm, and steady-state visual evoked potentials, to facilitate communication (Aggarwal and Chugh, 2019). Of these, only mu ( $\mu$ ) rhythm which is found at routine motor activities (Rihana, Damien and Moujaess, 2012) is specifically related to motor tasks. Motor imagery based BCI applications encompass a range of technologies, such as wheelchair control, virtual reality, and neurorehabilitation.

Nicolas-Alonso and Gomez-Gil (2012) and Niha and Banu (2016) review various applications and devices activated by BCIs. Key categories include medical applications (e.g., diagnosis, monitoring, and health forecasting), communication aids, environmental control (e.g., managing domestic devices), motor restoration (e.g., functional electrical stimulation), entertainment (e.g., games), and locomotion (e.g., wheelchair control). Notable EEG-based communication devices include thought translation systems (Hinterberger *et al.*, 2004), spelling devices (Birbaumer *et al.*, 1999), spelling applications utilising the P300 component (Farwell and Donchin, 1988) as well as systems that enable spelling through the control of intact eye movements (Treder and Blankertz, 2010).

Bansal and Mahajan (2019) discuss various BCI applications developed using the MATLAB programming environment. These include in-house systems for eyeblink-based BCIs, external device control applications, Arduino Uno hardware interfacing, prosthetic hand control, intelligent stress relief systems, cursor movement control based on imagined limb movement, musical brain caps, and mini-drones. Target-oriented computer mouse control using brain signals can be achieved through both invasive and non-invasive EEG techniques (McFarland *et al.*, 2008). Although invasive methods generally offer superior performance due to better signal-to-noise ratios, non-invasive EEG methods are evolving in terms of signal acquisition, processing, and analysis for specific applications. The study compared BCI systems across healthy and physically disabled individuals, revealing varied accuracies in target selection. Correlation values between control signals and target selection reached a maximum of 0.38 for horizontal cursor movement and 0.44 for vertical cursor movement.

EEG-based control applications are particularly beneficial for individuals with physical disabilities. For instance, an in-house developed eyeblink-based BCI system can activate

specific device control applications. The "Emotiv" neuroheadset, featuring 14 EEG channels and an Arduino Uno board, serves as an interface between brain signals and control applications. The Emotiv headset operates at a sampling rate of 128 Hz, with data wirelessly transmitted to a computer. Control activation occurs when a certain threshold ERP value is reached (Subha *et al.*, 2010). Additionally, g.BCIsys have been employed to control cursor movement based on EEG signals. Using the g.STIMunit setup, the imagination of limb movements can move the cursor horizontally. Brain signals collected from the C3 sensor (left hemisphere) during right-hand movement imagination and from the C4 sensor (right hemisphere) during left-hand movement imagination facilitate horizontal cursor movement (Bansal and Mahajan, 2019).

Ramadan and Vasilakos (2017) provide a comprehensive review of various mental control signals, BCI hardware and software technologies, highlighting the distinct focus of the BCI market across different continents. In North America, there is a significant emphasis on the development and investment in invasive BCI technologies. In contrast, European and Asian markets are prioritising the advancement of non-invasive EEG-based devices, with particular attention to minimising costs. This reflects that these regions are prioritising cost-effectiveness and accessibility in their approach to BCI technology, likely to make these devices more widely available and to cater to a broader audience, including those in healthcare or consumer markets where budget constraints might be a significant consideration. After reviewing, the authors observe that the BCI community struggles with a lack of standardisation, leading to tedious and often complex EEG procedures, as well as widespread incompatibility among the various BCI devices.

A few studies have been attempting to translate brain activity into text. For example, Yang *et al.* (2023) developed a thought-based EEG-to-text system, where the methodology incorporates the Eurasian Oystercatcher Wild Geese Migration Optimisation (EOWGMO) algorithm for signal processing, the Multiscale Dilated Adaptive DenseNet with Attention Mechanism (MDADenseNet-AM) technique for text conversion, and the Morse code technique for interpreting alphanumeric letters. The study achieved an accuracy of 96.41% using a publicly available dataset based on 14 motor movement or imagery tasks. However, the optimisation technique does not guarantee a globally optimal solution, as its performance is influenced by problem characteristics and parameter settings. Additionally, the Morse code technique requires fast typing, which may pose challenges in practical applications (Bhuvaneshwari *et al.*, 2021).

Bhuvaneshwari et al. (2021) conducted a review on EEG-based assistive brain-computer interface (BCI) systems designed for individuals with neurodegenerative diseases. The study categorises these systems into four types: wheelchair control, communication tools (such as organ movement decoders), speller-based systems, and eye-tracker systems. However, none of the reviewed research focuses on developing an EEG-based communication system capable of directly interpreting various thoughts.

Imran et al. (2024) developed a brain-controlled computer task system for individuals with disabilities, enabling cursor movement using thought-based EEG signals. Four cursor directions (left, right, up, and down) were generated based on distinct brain states, such as alpha, beta, and gamma rhythms, using data from a single sensor. The study compared various machine learning techniques including SVM, RF, and NN classifiers, with an updated model architecture, achieving an accuracy of 52%. However, employing a CNN improved accuracy to 80% (Imran *et al.*, 2024). The authors utilised a private dataset in their experiments and recommended future studies to incorporate real data collected from a group of participants for further validation.

Recently, numerous EEG-based emotion recognition systems have been developed for brain-computer interface (BCI) applications, achieving high accuracy. However, in practice, the establishment of a unified and comprehensive methodological framework is essential (Hamzah and Abdalla, 2024). The use of fewer EEG sensors is also recommended to minimise setup time, memory requirements, computational load, and overall system complexity.

Current challenges include the reliability of deep learning models in BCI applications across diverse participants and the consistency of signal quality in EEG acquisition systems for groups of subjects. The authors provide a comprehensive analysis of BCI development trends, highlighting user-based and technology-based challenges, as well as potential research advancements. Their findings indicate that ongoing studies focus on optimising computational techniques and facilitating seamless interaction between individuals and automated systems.

## **2.7 Summary**

This chapter presents a comprehensive review of brain signal analysis and the development of BCIs. To ensure thorough coverage of the relevant areas, the review is divided into five sections: biological components of the brain and MND patients which are discussed in

Section 2.2, brain imaging systems, detailed in Section 2.3; brain signal processing methods, investigated in Section 2.4; classification algorithms, explored in Section 2.5; and relevant BCI developments, reviewed in Section 2.6. Each subsection delves into the essential aspects and current advancements in its respective area, providing a thorough understanding of the state-of-the-art in BCI technology, its applications and developments.

The development of thought interpretation for communication remains a relatively unexplored area, particularly in assistive and non-invasive technologies for individuals with severe motor impairments. While a few studies have genuinely attempted to interpret brain signals from specific thoughts to facilitate communication with the surroundings, such systems remain largely limited to device-based implementations, such as computers, rather than directly interpreting thoughts in a natural, device-independent manner. To develop an intelligent communication system, the methodology for brain signal interpretation is a crucial area where numerous opportunities remain unexamined.

One of the primary challenges is achieving accurate interpretation of thoughts or imaginations, followed by the development of an effective method that can function reliably across both individuals and larger groups. Such a method must be computationally efficient, minimally complex, cost-effective, and robust in performance. However, existing state-of-the-art methodologies predominantly focus on specific mental tasks, such as motor imagery, and brain signal processing is typically restricted to task-based signals.

A critical limitation in current research is the lack of exploration beyond conventional task-based approaches, particularly in the context of communication using brain-computer in BCI systems. This research aims to evaluate the applicability and efficacy of the ASPS approach for processing EEG-based sensor signals to extract relevant features for recognising mental imagery. The ASPS approach introduces delta ( $\Delta$ ) value analysis, which has not yet been considered in brain signal processing. According to theoretical principles, brain signals should exhibit a deviation when transitioning from a relaxed state to a state of specific imagination. If brain signal characteristics can be analysed through  $\Delta$  value assessment to identify these deviations, and the uniqueness of imaginations can be detected using a computationally efficient and low-complexity approach, this would represent a significant advancement in brain signal analysis. Therefore, further investigation into  $\Delta$  value-based methodologies has the potential to address existing limitations and contribute to the

development of more reliable and generalisable EEG-based communication systems capable of directly interpreting thoughts in a natural, device-independent manner.

To the best of the author's knowledge, no existing studies have genuinely attempted to explore this approach. Therefore, this research aims to bridge this gap by investigating the potential of  $\Delta$  value analysis, using the ASPS approach, to interpret brain signals associated with specific thoughts. This offers a new direction for developing more intuitive and accessible communication systems. By focusing on reducing computational complexity and enhancing the reliability of the ANN model, this study seeks to contribute to the development of EEG-based communication systems that can operate seamlessly across individuals, ultimately fostering a more direct and natural interaction between users and their environment.

The methodology of this research is outlined in the next chapter. It discusses the three stages of BCI development in this study: signal acquisition, signal processing and analysis, and classification. The chapter provides insights into the algorithms used in the methodology, as well as the design of signal acquisition, processing, analysis, classification, sensor optimisation, and evaluation.

# Chapter 3: Research Methodology

## 3.1 Introduction

This chapter presents the research methodology employed in this PhD study. As established in the state-of-the-art review in Chapter 2:, the development of a BCI necessitates three fundamental stages: brain signal acquisition, signal processing and analysis, and classification. The stages of methodology are depicted in Figure 3.1. These stages are initially undertaken to develop an algorithm aligned with the proposed methodology.

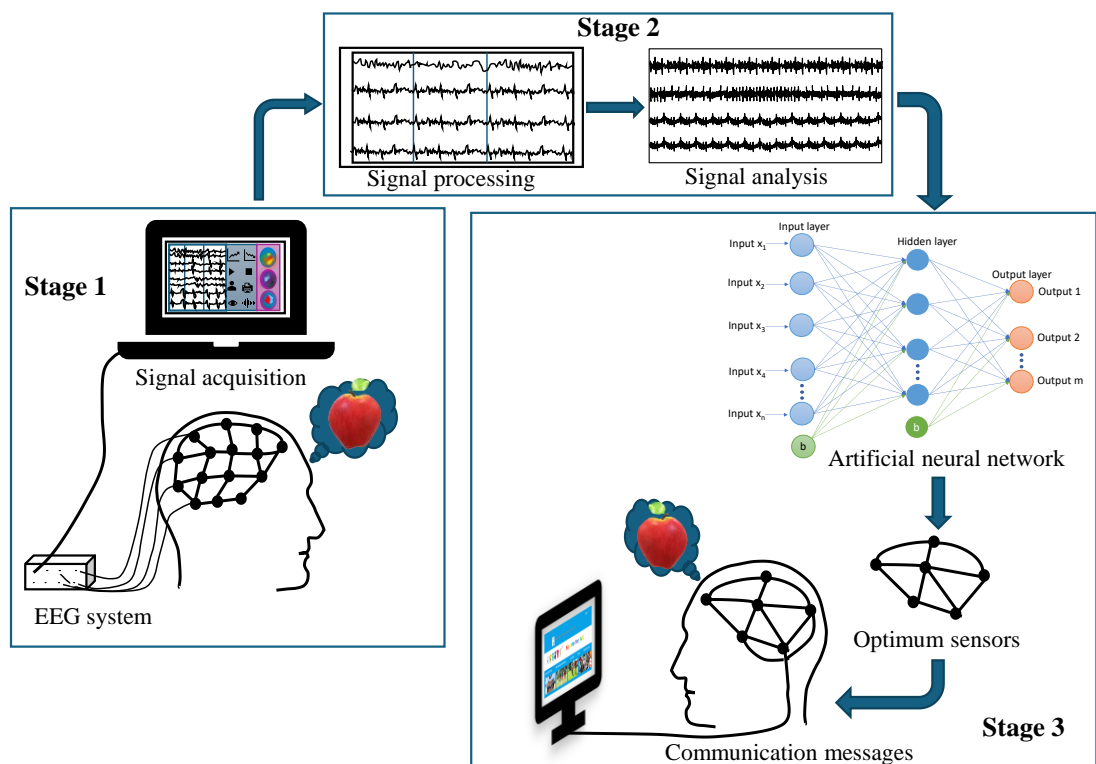


Figure 3.1: The methodology of the research.

Section 3.2 offers an in-depth discussion on the development of this algorithm, utilising the necessary stages identified for this research. Section 3.3 elaborates on the sensor optimisation process and the subsequent testing of the algorithm with the optimal number of sensors. The organisation of the following chapters is briefly outlined in Section 3.4.

The state-of-the-art review presented in Chapter 2 explores traditional signal processing techniques used in BCI development, highlighting the challenge of selecting appropriate

techniques. To address this challenge, the ASPS approach, as introduced by (Al-Habaibeh, 2000) and (Al-Habaibeh and Gindy (2000)), is proposed as a solution for technique selection. Figure 3.2 presents the block diagram of the ASPS approach, which has been successfully applied to machinery condition monitoring. This approach is designed to process a set of sensory signals in an innovative manner by amalgamating multiple conventional signal processing techniques and applying various statistical functions to their outputs.

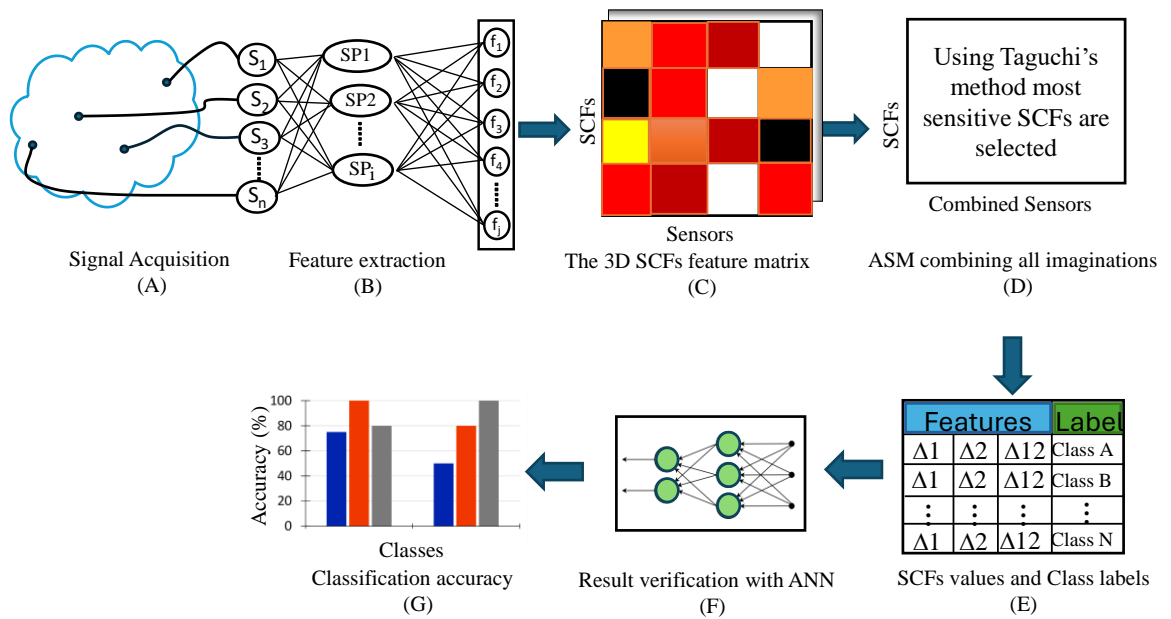


Figure 3.2: Block diagram of the ASPS approach developed by Al-Habaibeh and Gindy (2000).

In the figure, step (A) illustrates the signal acquisition process, where sensors ( $s_1, s_2 \dots s_n$ ) capture data from the region of interest. The acquired signals undergo different signal processing techniques ( $sp_1, sp_2 \dots sp_i$ ), followed by the application of various statistical functions ( $f_1, f_2 \dots f_j$ ), as depicted in step (B). The resulting function values are compiled into an SCF feature matrix in step (C). Using Taguchi's method, this matrix is organised by dependency coefficients in step (D), forming the Association Matrix (ASM). The next step (E) computes the  $\Delta$  values by determining the difference between two states of the machinery components under monitoring. The necessary values are then grouped and labelled according to the objective of the analysis. Step (F) evaluates the performance of the selected features using an ANN to predict the machinery condition, and finally, step (G) summarises the classification accuracy of the prediction.

The ASPS approach presents a promising paradigm for application in brain signal processing. Similar to machinery condition monitoring, brain signals are also sensory in nature and

require signal processing techniques and statistical functions for meaningful feature extraction. Since existing literature indicates that each signal processing technique has its own advantages and limitations, identifying the most suitable technique through individual experimentation is both time-consuming and computationally expensive. The ASPS approach offers a more efficient alternative by integrating multiple techniques, thereby reducing the overall experimental workload and processing time.

A key strength of the ASPS approach is its use of  $\Delta$  values to identify the most significant features. This PhD study assumes that computing  $\Delta$  values from the difference between the relaxed state and a specific mental task state could yield valuable insights. Thus, this research aims to implement the ASPS approach in brain signal processing and analysis, with the objective of investigating its effectiveness in feature extraction and selection for BCI development.

The methodology is presented in two phases. Section 3.2 details the development of the algorithm, incorporating the essential stages identified for this research. Section 3.3 focuses on sensor optimisation and the evaluation of the algorithm using the optimal sensor configuration.

### **3.2 First Phase: Algorithm Development and Analysis**

This section outlines the information of acquired brain signal data, the initial development of the algorithm for the proposed methodology, and its implementation plan. Given the complexity of the overall model, this phase begins with the creation of an elementary model—a basic framework designed to scale up gradually in terms of data size and various analysis parameters. Different classifiers with diverse architectures will be investigated to assess their performance. All performances will be compared to evaluate the different models and determine the optimal classifier configuration. The following sections address the first phase of data collection, signal processing and analysis, and classification.

#### *3.2.1 Overview of Dataset*

The development of the algorithm and foundational model in this study leveraged prior data available within the university. This data, stored in a dedicated repository, was originally acquired using the international 10-20 EEG system (Klem *et al.*, 1999), involved 19 scalp sensors to capture brain signals. The TMSi system, developed by Twente Medical Systems International, was utilised for EEG recording at a sampling frequency of 2 Hz. TMSi produces high-quality EEG acquisition systems for both research and clinical applications,

incorporating various amplifiers designed for high-resolution electrophysiological recordings. Gel-based electrodes were employed to ensure high-quality signal acquisition. Data acquisition, visualisation, and basic analysis were conducted using Polybench, TMSi’s proprietary software. As depicted in Figure 3.3, signal acquisition occurred during a previous project, collecting data from 19 NTU staff and students. Participants completed 22 mental tasks or imagination commands under a consistent recording protocol across two trials: Experiment A (trial 1) and Experiment B (trial 2). Trials included alternating relaxation and imagination periods within an audio stream.



Figure 3.3: Volunteers wearing EEG cap and participating in prior signal acquisition.

### 3.2.2 Signal Pre-processing

All recorded signals were organised and stored in anonymised, subject-specific folders. The 22 imaginations encompass a diverse range of mental tasks, including imagining objects, motor imagery tasks, experiencing emotions, performing mental calculations, and more. From these, five imaginations are selected, taking into account the complexity of the model and representing five distinct mental tasks. The objective is to determine whether the characteristics of these tasks are distinguishable from one another. To explore thought-based communication, five distinguishable imaginations are considered for analysis. Table 3.1 lists all five selected imaginations and enumerates a series of consecutive cognitive tasks.

Table 3.1: Selected imagination list.

Number	Description	imagination
1	Imagine an African Elephant	

Table 3.1: Selected imagination list. (continued from previous page)

Number	Description	imagination
2	Imagine kicking a football with left foot	
3	Calculate of 2x2 in your mind	
4	Imagine smelling a rotten egg	
5	Imagine walking on a warm sandy beach	

Two identical experiments, named Experiment A (trial 1) and Experiment B (trial 2), were carried out on all participants to detect any potential discrepancies between them. Participants were prompted with different mental simulations successively, each comprising two segments: an initial relaxation phase followed by a specific cognitive task. The selection of mental simulations was based on a range of tasks, including motor imagery, mental arithmetic, visualising objects, thinking about smells, and visualising moving around coupled with environmental awareness. The recorded raw brain signals are appropriately trimmed for each trial, as illustrated in Figure 3.4.

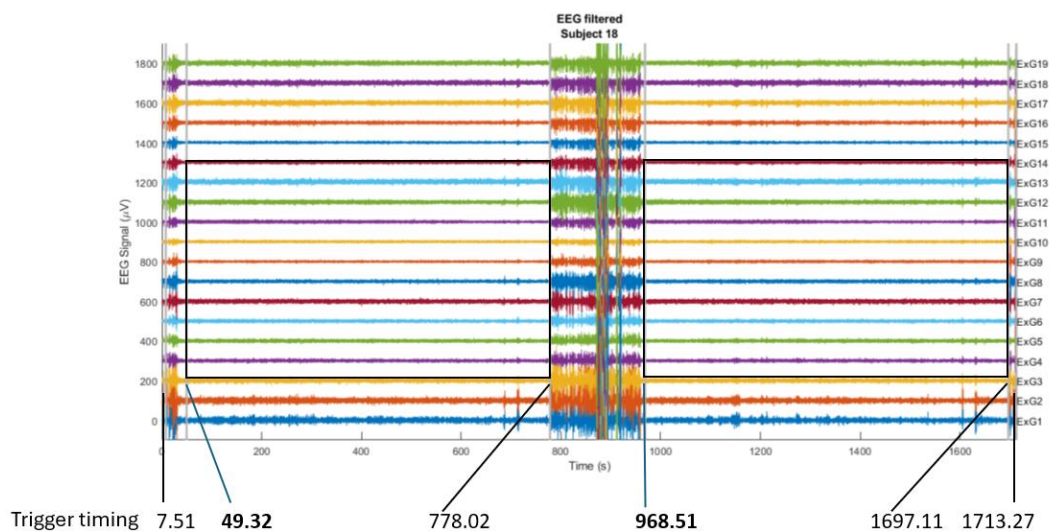


Figure 3.4: Signal pre-processing.

Subsequently, data matrices are created based on each imagination task and the preceding relaxation periods. In this stage, no additional preprocessing techniques are employed to ensure the preservation of all naturally occurring features. Furthermore, this research aims to apply the signal processing technique (ASPS approach) based solely on raw data, thereby simplifying the analysis process while maintaining the integrity of these natural features.

### *3.2.3 Signal Processing and Analysis*

This stage is carefully designed, taking into account a wide range of parameters. The pre-processed dataset is characterised by 19 sensors, 19 subjects, and 5 distinct imaginations. One of the most challenging tasks is selecting the most suitable signal processing method to extract appropriate features that address the project's objectives, as highlighted by the review of current advancements presented in Chapter 2. This research aims to investigate the ASPS approach in brain signal processing, given its theoretical simplicity and practical utility for extracting valuable information from multiple signals.

The ASPS approach is a 'black-box' concept (Al-Habaibeh, 2000; Al-Habaibeh, Zorriassatine and Gindy, 2002), in which the transformation between input and output parameters is analysed to determine the condition of the monitored entity. This approach is considered applicable to specific problems within particular applications and can be generalised to various types of processes, provided they share common specific parameters. In the development of BCIs, the selection of the optimal number of features significantly influences the accuracy of emotion recognition from brain signals (Murugappan *et al.*, 2008). Therefore, this research will apply the ASPS approach for feature extraction and optimisation of brain signals and investigate the performance of imagination recognition.

The ASPS approach can employ multiple sensors to acquire and process signals, extracting the most useful SCFs. These SCFs are crucial for identifying changes in the collected signals as the condition of the monitored entity evolves. Detecting and processing these changes enables a precise assessment of the entity's condition. For instance, sensitive features can be derived from differences between two distinct states of the monitored entity. A higher differential indicates greater sensitivity concerning a specific sensor, allowing the construction of a sensitivity matrix, referred to as the ASM. Taguchi's orthogonal array is potentially used to determine feature sensitivity and reduce the number of experimental trials. In the ASPS approach, the SCFs calculated for various sensors form a 3D matrix called the Sensory Feature Matrix, where Taguchi's method can be applied to assess the sensitivity of

each feature. Features with high sensitivity and their corresponding sensors are then selected as part of the optimisation process.

In the domain of brain signal processing, sensitive features are derived from the differences observed between relaxed and active phases (e.g., during mental tasks) of brain signal recordings. Due to the brain's complexity, where multiple regions may influence specific mental processes, the analysis of the ASM differs significantly from that used in mechanical processes. The unique nature of brain activity necessitates a more detailed approach to ASM analysis to accurately capture the intricate relationships between brain regions and their corresponding signal variations. By applying various statistical functions to these parameters and combining their results, a substantial matrix can be generated. Figure 3.5 illustrates the block diagram of ASPS approach within the context of this research.

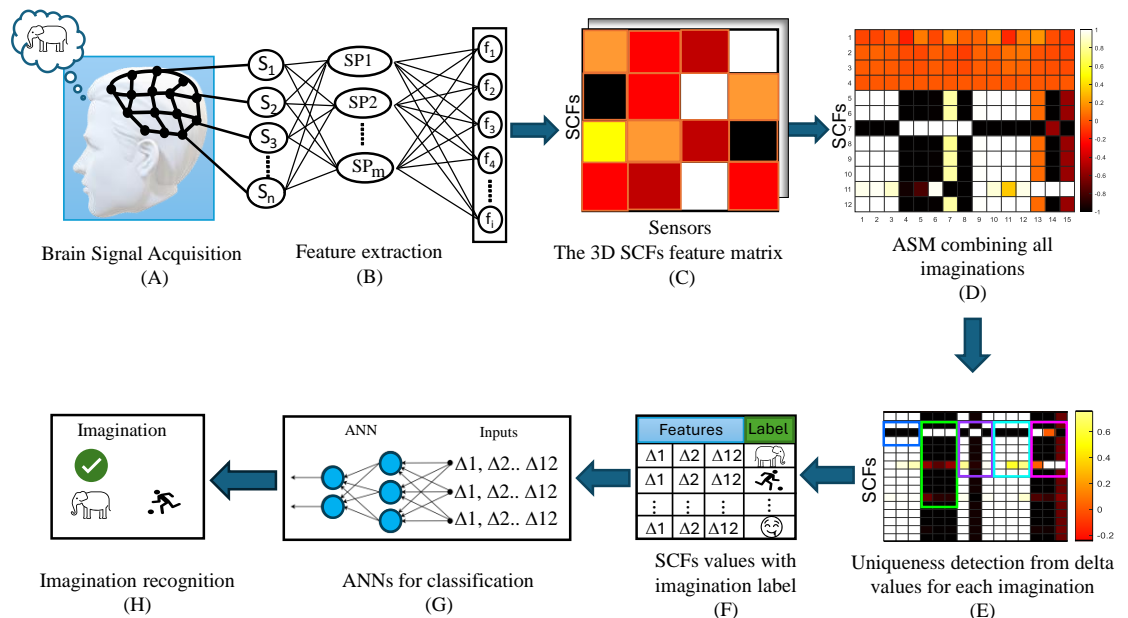


Figure 3.5: The block diagram of the ASPS approach applied to brain signal processing in this research.

To evaluate the effectiveness of a new signal processing method and to develop the algorithm for this research methodology, it is essential to start with a simplified model that has reduced dimensionality. This research aims to explore both an elementary model and the subsequent expansion in dimensionality.

Signal acquisition involves the use of multiple sensors placed on the scalp to capture brain wave activity during periods of relaxation as well as during the performance of mental tasks. The acquired signals are subsequently processed using various signal processing techniques,

including those based on the time domain, frequency domain, and time-frequency domain, among others. These methods facilitate the analysis and interpretation of the brain's electrical activity, allowing for a deeper understanding of the neural processes underlying different cognitive states.

A range of statistical functions, such as mean, standard deviation, and variance, are applied to these domains during both relaxation and mental tasks. Statistics are essential in human neuroscience for examining the variability in brain structure and functions (Chén, 2019). Investigating this variability is useful for identifying individual differences and group-wise patterns, which significantly enhance the understanding of cognitive and neural processes. Applying the same statistical functions to signals recorded during relaxation and mental tasks should yield distinct significance, as relaxation and mental tasks represent conceptually different mental states. These states exhibit variations in amplitude and frequency, necessitating differential interpretation of the statistical outcomes. In this study,  $\Delta$  values are computed by subtracting the features of the relaxation state from those of the subsequent mental task, allowing for a direct comparison of the changes in brain activity between these two distinct states. After extraction, the resultant features, termed SCFs, are organized into a matrix structure to form the ASM. For  $n$  number of EEG sensors and  $m$  number of signal processing techniques (including FFT and/or DWT as well as raw signals), the ASM can be expressed in Equation (3.1) (Al-Habaibeh and Gindy, 2000).

$$ASM = \begin{bmatrix} d_{11} & d_{12} & d_{13} & \dots & d_{1m} \\ d_{21} & d_{21} & d_{21} & \dots & d_{2m} \\ \dots & \dots & \dots & \dots & \dots \\ d_{n1} & d_{n2} & d_{n3} & \dots & d_{nm} \end{bmatrix} = d_{xy} \text{ where } 1 \leq x \leq n \text{ and } 1 \leq y \leq m \quad (3.1)$$

As a result, the ASM can be constructed, where each element of  $d_{xy}$  denotes the dependency coefficient between features. By analysing these ASMs, a set of SCFs is selected that sufficiently distinguishes the uniqueness of each imagination. The ASPS approach has the capacity to incorporate additional signal processing techniques for constructing the ASM. To assess the effectiveness of the extracted features from the ASM in recognising different imaginations, their performance needs to be evaluated. This evaluation is carried out using an appropriate classification algorithm.

Considering all parameters, the signal processing, analysis, and classification in this research are designed to be executed in three distinct approaches. The rationale is to use the ASPS approach to determine how well imagination can be recognised across varying numbers of

subjects, sensory signals, and SCFs. Subsequently, the performance of recognition is evaluated through various ANN architectures. These three approaches are termed Bespoke analysis, Group-based analysis, and Combined analysis. The purpose of each analysis is outlined below:

- a) Bespoke analysis: This process entails the design and experimentation with an elementary signal processing model using the ASPS approach for recognising imagination, initially focusing on two subjects. In this analysis, EEG signals from three sensors are processed, the ASPS approach is applied to both the time-domain (raw signals) and frequency-domain components of the EEG data. The analysis employs a limited set of SCFs to assess whether the ASPS approach can adequately extract the necessary features to distinguish between five imaginations. Chapter 4 provides a detailed account of the design, development, and evaluation of this bespoke analysis.
- b) Group-based analysis: This approach expands upon the bespoke analysis by scaling up to three groups, with group-wise analysis conducted to further investigate the performance of recognising five imaginations. This analysis extends to additional domains, including the time domain, frequency domain, and time-frequency domain, to enhance feature extraction from three sensor signals and consequently generate a greater number of SCFs in the ASMs. Chapter 5 elaborates on the design, development, and assessment of imagination recognition using a group-based analysis methodology.
- c) Combined analysis: This experiment involves using all 19 sensory signals from all 19 subjects to explore the performance in recognising the five imaginations. It employs the ASPS approach for feature extraction and image processing techniques for classification. The design and implementation of this comprehensive experimental work are described in Chapter 6.

#### *3.2.4 Imagination Recognition Using Classification Algorithm*

This research has designed three distinct analyses using ASPS approach in which ANN models are employed to classify signals for the recognition of different imaginations. It is crucial to consider the project goals, data size and complexity, and the potential of the ANN models in this context. The selected SCFs using the ASPS approach serve as inputs for the classification model. In supervised ANN models, inputs are divided into two groups: training and testing inputs. The model is trained and tested with the training and testing datasets,

respectively. The train-test split ratio typically ranges between 70-30 and 80-20, depending on the available data size and number of classes (Gholamy, Kreinovich and Kosheleva, 2018; Rácz, Bajusz and Héberger, 2021). Proper training of the ANN models is essential for achieving high accuracy, making it a flexible and powerful classifier (Abiodun *et al.*, 2018). However, due to the limited number of trials, this phase of analysis and verification employs a single trial for training and uses the remaining trial for testing.

Considering the state-of-the-art in classifier selection and the specific aspects of this research, three ANN models are explored to evaluate classification performance. FFNN and LVQ are applied as classifiers in both bespoke and group-based analyses and are compared across different architectures to assess performance variations. The combined analysis employs image processing techniques and CNN for the classification of mental imagery. In this approach, an extensive ASM is generated, comprising data from 19 sensors and a larger set of statistical functions applied to these data. To explore the broad spectrum of SCFs within these ASMs, image processing techniques are employed. CNNs, widely used in deep learning for brain signal processing, are selected for classifying mental imagery. The ASMs, processed as images, serve as the input to the CNN. Chapter 6 presents the application of CNN for classifying different types of mental imagery. Verification is conducted across three distinct groups, with performance comparisons made between them.

The architecture of ANN models allows for significant flexibility, such as varying the number of layers and neurons, which can impact the performance of the classification model (Montesinos López Osva Antonio and Montesinos López, 2022). Therefore, this research investigates various architectural performances for ANN models, as exemplified in Chapters 4 and 5. Tables 3.2 and 3.3 present the hyperparameters' values of developed FFNN and LVQ model respectively.

Table 3.2: Hyperparameters of developed FFNN model.

Hyperparameters of FFNN model	Value
net	Patternnet
Training function	Traincgb
Activation function	Tansig for hidden layers, softmax for output layer
Maximum epochs	1000
Performance function	Crossentropy (default)

Table 3.3: Hyperparameters of developed LVQ model.

Hyperparameters of LVQ model	Value
net	Lvqnet
learning function	Learnlv1
Learning rate	0.01
Maximum epochs	25
Performance function	performFcn (default)

Pattern recognition networks are a type of feedforward network designed to classify inputs into target classes. The target data for these networks should be represented as vectors. The function ‘traincgb’ is employed for network training, where it updates weight and bias values through conjugate gradient backpropagation with Powell-Beale restarts (Powell, 1977). The cross-entropy operation computes the loss between the network's predictions and the target values and is applicable to both single-label and multi-label classification problems.

LVQ neural networks are structured in two layers. In the first layer, input vectors are mapped into clusters identified by the network during the training process. The second layer then aggregates these clusters into classes as defined by the target data. The number of clusters in the first layer is dictated by the number of hidden neurons. A larger hidden layer facilitates the learning of more clusters by the first layer, thereby allowing for a more nuanced mapping from inputs to target classes. The allocation of clusters to the target classes is determined based on the distribution of target classes at the time of network initialisation.

CNN model implementation includes a number of consecutive layers and hyperparameters, which are presented in the Table 3.4.

Table 3.4: CNN configuration and hyperparameters of developed CNN model.

CNN configuration and hyperparameters	Value
Layer 1: image input	256x256x3 images
Layer 2: 2-D convolution	8, 3x3 convolutions with stride [1 1] and padding [0 0 0 0]
Layer 3: ReLU	ReLU
Layer 4: 2-D Max Pooling	2x2 max pooling with stride [2 2] and padding [0 0 0 0]
Layer 5: 2-D convolution	16, 3x3 convolutions with stride [1 1] and padding [0 0 0 0]
Layer 6: ReLU	ReLU
Layer 7: 2-D Max Pooling	2x2 max pooling with stride [2 2] and padding [0 0 0 0]
Layer 8: Fully connected	5 (Number of class labels)
Layer 9: Softmax	Softmax
Layer 10: Classification Output	Crossentropyex
Training function	trainNetwork
Epoch	50

Table 3.5: CNN configuration and hyperparameters of developed CNN model (continued from previous page).

CNN configuration and hyperparameters	Value
Learning rate	0.01
Validation frequency	30
Maximum epoch	20

The trainedNet function is designed to train and return a network tailored for classification tasks, using an image datastore with categorical labels. In the image datastore, 2D images are stored with dimensions of 256x256 pixels and 3 colour channels. The dimensions specify the height and width of the input images, with each image being 256 pixels in both height and width. The three colour channels indicate that the images are in RGB format, representing the red, green, and blue channels. The image input layer allows these 2D images to be used as inputs to the CNN model and facilitates data normalisation. Central to a CNN is the convolutional layer, which comprises a set of filters whose parameters are optimised during training. This layer is essential for feature extraction from given images. Padding is a technique employed in CNNs where extra pixels are added around the input image or feature map. This approach preserves spatial dimensions throughout the convolution process. The Rectified Linear Unit (ReLU) activation function, commonly used in CNN, outputs 0 for any negative input and returns the positive input value unchanged.

Max pooling is another fundamental component of CNN architecture. It reduces the spatial dimensions of the data while emphasising significant features. The fully connected layer, by connecting every neuron from the previous layer to each neuron in the fully connected layer, captures global patterns and relationships within the data. Finally, the softmax layer, located at the end of the CNN, transforms raw output scores into a probability distribution, facilitating classification tasks.

All LVQ, FFNN, and CNN models are developed using MATLAB 2022a. The system specifications utilised include an Intel Core i7 10th Gen Processor and 16 GB of RAM. The performance of all experiments is calculated by calculating the average percentage accuracy, determined by the proportion of predicted values that match the actual values, as defined in Equation 3.2.

$$\text{Classification accuracy} = \frac{\text{Number of correct predictions}}{\text{Number of total predictions}} \times 100\% \quad (3.2)$$

Each model architecture is executed 100 times to evaluate both the optimal and average performance, with the results summarised in the following chapters.

### 3.3 Second Phase: Sensor Optimisation and Algorithm Testing

The methodology outlined in Section 3.2 is centred on the initial phase of collected brain signal data. The second phase of data collection and analysis is specifically designed to address the challenges identified earlier. This section provides a comprehensive overview of the second phase, encompassing brain signal acquisition, signal processing aimed at sensor optimisation, and the final evaluation. The evaluation is conducted using a new dataset and optimised sensors, applied across various groups of subjects.

#### 3.3.1 Brain Signal Acquisition:

The second phase of brain signal recording has been conducted with an expanded scope. The focus has been to increase the number of trials to facilitate a more robust analysis of sensor performance. Recognising that the two trials from the first phase were insufficient for comprehensive analysis, this phase aims to record a minimum of five trials from each of ten subjects to evaluate the consistency of sensor performance. Figure 3.6 demonstrates subjects participating in data collection.



Figure 3.6: Volunteers participating in EEG signal acquisition (second phase).

This phase serves two main purposes. Firstly, the increased number of trials allows for a more thorough assessment of sensor performance, which aids in developing effective sensor optimisation strategies. Secondly, the algorithm developed in Section 3.2 would be evaluated

using the newly collected data, incorporating insights gained from the sensor optimisation process.

The brain signal acquisition for the second phase mirrors that outlined in Section 3.2.1. The International 10-20 EEG recording system (Klem *et al.*, 1999), which includes 19 sensors, is used to collect brain signal data from ten subjects. Participants are given the same set of instructions through audio stimuli to imagine a sequence of mental tasks. Each subject completes at least five trials under the same conditions. One of the volunteers contributed 12 trials, which were collected to provide deeper insights into the comparison of different set of trials. The study involves ten healthy volunteers from NTU staff and students, all are above 18 years old. The details of the participants are written in Table 3.5

Table 3.6: The summary of participant demographics.

Participant ID	Age (years)	Gender	Ethnicity
S1	29	Female	Asian/ Asian British -Indian
S2	28	Male	Asian/ Asian British -Indian
S3	43	Male	Asian/ Asian British -Bangladeshi
S4	23	Male	Black/Black British - African
S5	32	Male	Asian/ Asian British -Pakistani
S6	34	Male	Asian/ Asian British-Indian
S7	56	Male	Arab
S8	60	Male	Arab
S9	41	Female	Asian/ Asian British -Bangladesh
S10	58	Male	White-British

### 3.3.2 Signal Processing for Sensor Optimisation:

The signal processing procedures adhere to the ASPS approach outlined in Section 3.2.3. Specifically, within the analysis categories, bespoke analysis has been designed to develop an elementary analysis model for individual aimed at simplifying the feature extraction and selection process. Second phase involves applying the bespoke signal processing method across 10 subjects, each undergoing 5 trials. A key objective of this phase is to evaluate the performance of 19 sensors to determine the optimal number of sensors required. Identifying optimised sensors and their corresponding brain locations can highlight the areas responsible for the selected mental tasks in this research. In line with current advancements, EEG system source imaging plays a crucial role in providing insights into cerebral neural activities. It

considers factors such as spatial sampling, signal quality, practical considerations, and computational complexity (Michel *et al.*, 2004). Concurrently, efforts to improve system feasibility include reducing setup time, managing computational complexity, minimising costs, enhancing portability, and ensuring participant comfort (Tacke *et al.*, 2022).

Sensor performance variation depends on the distribution of cognitive sources and the level of cognitive activity within specific brain regions, which is inherently subjective relative to anatomical structures. Additionally, overlapping waveforms can occur in experimental settings due to brief intervals between stimuli (Tian and Huber, 2008). This study focuses on sensor selection based on the performance of ASPS-generated features from specific mental tasks. It involves analysing data from five, four, three, and two imagined tasks for each of the 19 sensors across all subjects. The primary aim is to conduct a comparative analysis to evaluate the effectiveness of imagination recognition for each sensor across all subjects. These efforts may aid in grouping subjects based on similarities in source imaging and potentially generalise sensor selection, contributing to the development of a subject-independent BCI system.

The proposed methodology is designed to support various communication outputs, such as cursor movement, with a target range of 2 to 5 control commands. These commands correspond to the number of distinct mental imaginations performed by the user. The relationship between the number of mental tasks and the resulting control commands is established to ensure that interaction with the BCIs is both intuitive and efficient.

To determine the optimal sensor configuration for the BCI system, the number and placement of sensors are guided by the 5, 4, 3, and 2 mental imaginations used in the experimental paradigm. The selected mental tasks are chosen for their ability to activate specific brain regions, thereby influencing sensor placement. To assess the reliability of sensor performance, data from a total of 5 trials are collected and designed to analyse.

In this experiment, only single layered FFNN architecture is employed as the classification model since single layered FFNN is found most suitable in first phase analysis. For each subject and sensor combination, the FFNN model is trained and evaluated using data from the 5, 4, 3, and 2 mental imaginations. To assess the stability of the FFNN architecture, each model is trained and tested 25 times, varying the number of neurons in the single hidden layer from  $i$  to  $3i$ , where  $i$  represents the number of neurons tailored to the dataset's sample size.

Among the five trials, three are allocated for training, while the remaining two are used to test the efficacy of the selected sensor configurations. The classification accuracy of each FFNN model is evaluated, recording both the highest and average accuracy achieved. The primary aim of this experiment is to achieve higher classification accuracy while minimising the number of electrodes utilised in the BCI system. This objective aligns with the goal of developing an efficient and user-friendly interface that can reliably translate imaginative states into control actions with minimal hardware requirements.

Initially, a ranking is designed based on the tentative five sensors with the highest accuracy for each subject, considering 5, 4, 3, and 2 imaginations separately. These top five sensors are assigned rating points of 40, 30, 15, 10, and 5 for the highest to lowest ranks, respectively. Determining the optimal number of sensors for different numbers of imaginations at this stage would be challenging. However, analysing the tentative top five sensors would provide an initial indication of the minimum number of sensors required for various imaginations. The performance of top five sensors was considered for rating. The average value of all subjects' rating points is then calculated for each number of imaginations. Based on these values, the top six performing sensors among the 19 sensors are selected. Cross tables are created for the top six sensors (rows) versus subjects 1 to 10 (columns), where the frequent relationships between selected sensors and subjects are marked. A cumulative comparison is designed for the cross-tabulations, as demonstrated in Figure 3.7. In the figure, each row represents the sensor performance for a particular subject, while each column represents the performance of a particular sensor across all subjects. Subgroups are formed based on subjects with the best three sensors.

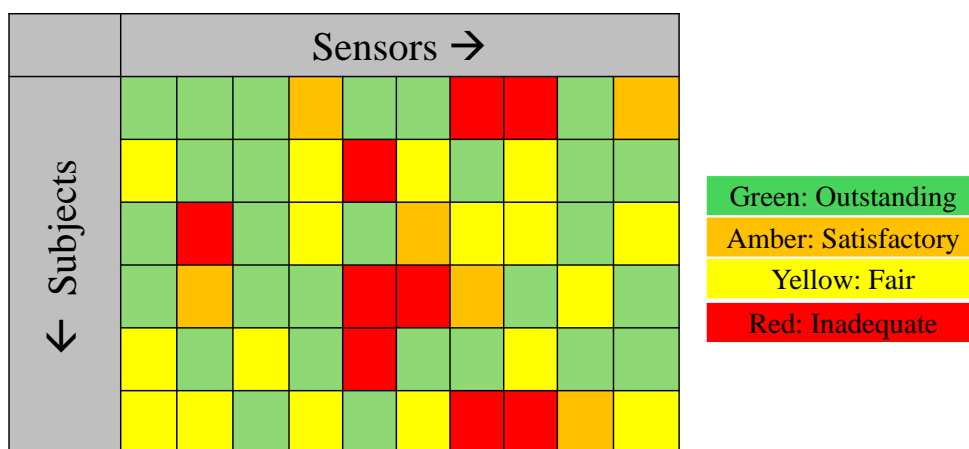


Figure 3.7: The cross-tabulation analysis template designed for subject vs sensors.

This analysis provides a detailed understanding of sensor performance for each subject and the created groups. To evaluate the effectiveness of imagination recognition using optimised sensors, a verification step has been designed, incorporating many of the approaches outlined in Section 3.2.3. This rigorous validation process utilises the selected sensors and includes most of the previously discussed analytical approaches. Chapter 7 provides a detailed analysis, results, and discussion of sensor optimisation and verification. The evaluation encompasses bespoke analysis, sensor-specific group analysis, and combined analysis using the new dataset for two approaches derived in Chapter 4 and 5, with all possible combinations considered for validation. A single-layer FFNN model is employed to classify all sets of imaginations. Each FFNN model is executed 25 times, and all performance metrics are recorded. This comprehensive analysis ultimately identifies the best and average performances by comparing the ASPS analysis approaches (as detailed in Chapter 4 and 5) across bespoke analysis, various subject groups, and the entire cohort of subjects.

### **3.4 Summary**

This chapter outlines the steps of the methodology undertaken in this research. In the first phase of the study, three experiments are designed, focusing on feature extraction and selection, analytical approaches, subject participation, verification steps, and classification algorithms. The study employs the ASPS approach, integrating techniques such as FFT, DWT, and classification methods including FFNN, LVQ, and CNN. The second phase centres on the design of sensor optimisation and classification with additional trials. The detail designs, analyses and results from these phases are described in Chapters 4 through 7. During the analysis of the data collected in the first phase, limitations related to data size are identified. To address these issues, a second phase of data collection is conducted. The proposed methodology is then evaluated using this expanded dataset, and the performance outcomes are summarised.

The following chapter presents a bespoke approach for individual analysis and development, utilising a fundamental signal processing model to identify and classify different sets of imagined tasks. It aims to assess the effectiveness of the ASPS approach in processing individual brain signals for the recognition of imagined tasks.

# Chapter 4: Bespoke Design for an Individual

## 4.1 Introduction

This chapter presents a bespoke design focused on individual analysis, verification of results, and a discussion pertaining to the elementary signal processing model briefly introduced in Chapter 3, Section 3.2.3. The methodology aims to evaluate the efficacy of the ASPS approach in processing brain signals for the recognition of imagined tasks. In Section 4.2, the detailed procedure is discussed, in Section 4.3, an in-depth analysis is provided, and in Section 4.4, the classifier performance within this customised framework is described.

## 4.2 Workflow for Bespoke Analysis

As an initial exploration of the ASPS approach for brain signal feature extraction, this section presents a basic model where three sensors are randomly chosen from a set of 19, with each sensor positioned at a different location on the brain, as illustrated in Figure 4.1. The sensors include  $Fp_2$  and  $Cz$  from the frontal lobe and  $O_1$  from the occipital lobe.

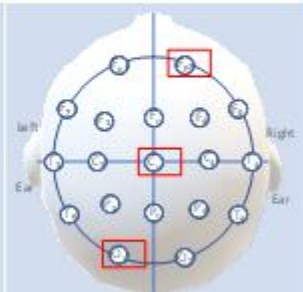
Selected Sensor	Locations from side view	Locations from top view
1. $Fp_2$ (2)		
2. $Cz$ (10)		
3. $O_1$ (18)		

Figure 4.1: Selected sensors and their scalp locations for bespoke analysis.

The figure shows the side and top views of the sensor locations on the scalp. The rationale for choosing three distinct brain locations is to examine the varying effects of signals from electrodes that are spaced apart, as they capture the activities of brain regions associated with different functions (Kumar and Bhuvaneshwari, 2012; Abhang, Gawali and Mehrotra, 2016).

This study builds on the basic ASPS approach discussed in Chapter 3, investigating a novel method to extract and select brain signal features from both the time and frequency domains. The fundamental flowchart of the feature extraction and selection process using the ASPS

approach is depicted in Figure 4.2. The algorithm processes EEG data as input, which then undergoes feature extraction. Time-domain and frequency-domain features are extracted for both relaxed and mental task states.

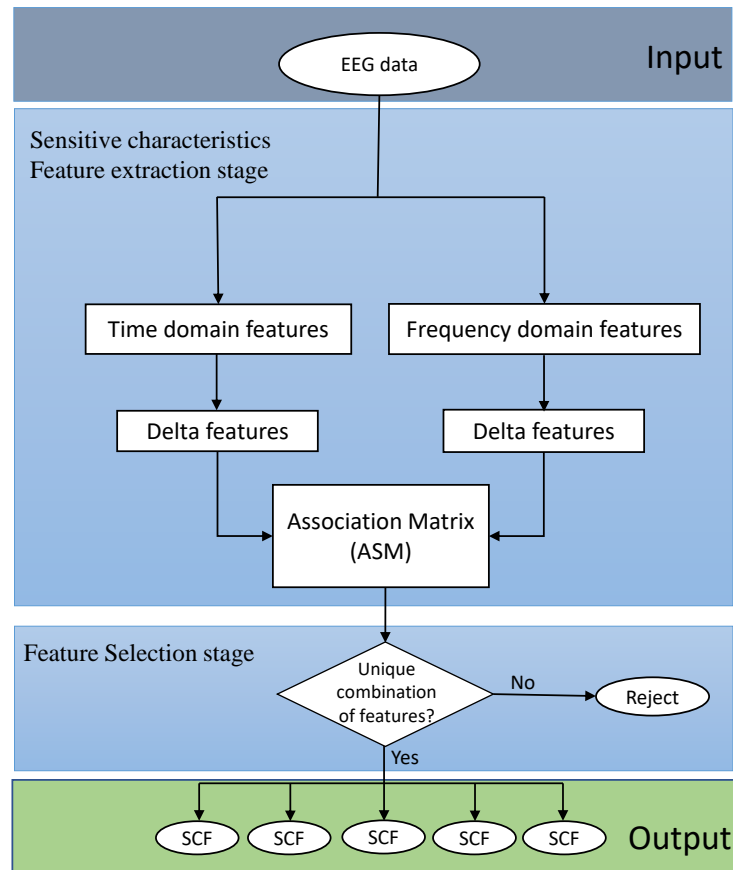


Figure 4.2: Flowchart of ASPS approach for bespoke analysis.

An ASM is constructed using  $\Delta$  feature values from both domains. In the feature selection stage, unique feature combinations within the ASM are identified. Relevant SCFs are selected, while non-contributory SCFs are discarded.

This experiment is designed to assess the performance of customised applications using two individual subjects. In this study, four statistical functions are employed as features in Table 4.1 for both the time and frequency domains. The time domain analysis focuses on raw signals, while the frequency domain analysis utilises FFT technique. It is crucial to emphasise that there is no universally prescribed number of features; instead, the selection is based on the number that most effectively characterises the signal.

Table 4.1: Definitions and equations of four statistical functions.

Index	Definition	Equation
1	Mean	$E_1 = \frac{1}{n} \sum_{i=1}^n x_i$
2	STD	$E_2 = \sqrt{\frac{\sum_{i=1}^n (x_i - E_1)^2}{N}}$
3	Variance	$E_3 = \frac{\sum_{i=1}^n (x_i - E_1)^2}{N}$
4	Max	$E_4 = \max(x_i)$

For example, Kousarrizi *et al.* (2009) used three features that achieved an accuracy of 88.75% in classifying cursor movements. Usha Kumari *et al.* (2020) employed four features for detecting obstructive sleep apnoea from EEG signals, achieving a success rate of 98% with an SVM classifier. Yuen *et al.* (2009) applied six statistical functions to classify five categories of emotion, obtaining an accuracy of 95% with a backpropagation neural network. In this experiment, four statistical functions namely, Mean, STD, Variance and Maximum are chosen to minimise the costs associated with the microprocessor board and to enhance the system's affordability for patients.

### 4.3 Feature Extraction and Selection for Bespoke Analysis

It is observed during the signal acquisition phase that each imagination consists of two segments: an initial relaxation phase and a specific mental task, as shown in Figure 4.3.

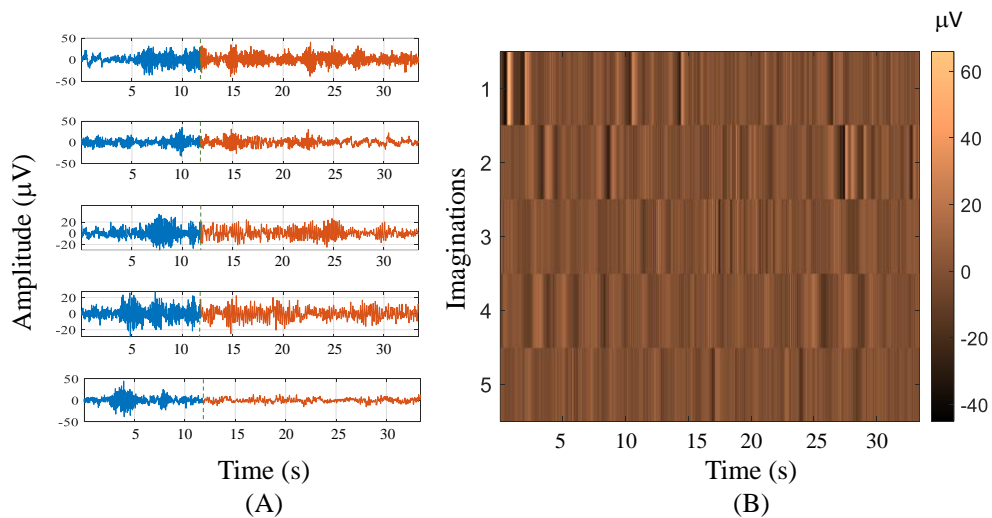


Figure 4.3: (A) Raw signals for relax and mental task and (B) copper scale map.

Figure 4.3 (A) illustrates the raw signals for relaxation (blue) and mental tasks (orange) across five different imaginations, which are further represented in Figure 4.3 (B) using a copper scale map. The imaginations are categorised based on the types of mental tasks, including motor imagery, mental calculation, object imagination, olfactory imagination, and environmental motion sensing. This approach aims to recognise imaginations based on bespoke analysis. In this study, normalised features are extracted from successive signals during both relaxation and mental tasks for each imagined task. The raw data, consisting of time-domain signals, is processed by applying the statistical functions listed in Table 4.1. To derive frequency-domain features, the FFT is performed on the individual raw signal data. The significant portion of the FFT output is then divided into two equal segments, with statistical functions calculated for each segment. This process generates eight frequency-domain features, while an additional four features are derived directly from the time-domain signal, yielding a total of 12 features as detailed in Table 4.2.

Table 4.2: SCFs calculation for bespoke analysis.

Signal pattern	Number of input statistical functions	Number of extracted and selected features (SCFs)/sensor
Raw signal	4	4
FFT signal	4	4 X 2=8
Total features=		12

The ASPS approach produces 12 SCFs using four statistical functions applied to both the time and frequency domains, calculating the difference between relaxation and imagination features. According to brain wave theory, a relaxed state is most commonly represented by alpha waves, whereas various mental tasks are associated with beta and gamma waves (Ishino and Hagiwara, 2003). The amplitude and frequency of each wave category possess distinct characteristics, allowing differentiation between a relaxed mind state and one engaged in specific imaginations. The features of imagined and relaxed brain signals are expected to differ and analysing  $\Delta$  values can reveal the most sensitive features. The ASMs, constructed from the obtained SCFs as outlined in Chapter 3 (Equation 3.1), serve as inputs for classifiers. ANNs such as FFNN and LVQ are employed to evaluate the performance of imagination recognition.

A precise analysis is performed to assess the sensitivity of SCFs with individual sensors for each type of imagination. The influential characteristics of  $\Delta$  SCFs are depicted in a heatmap in Figure 4.4, with colour representation indicating sensitivity.

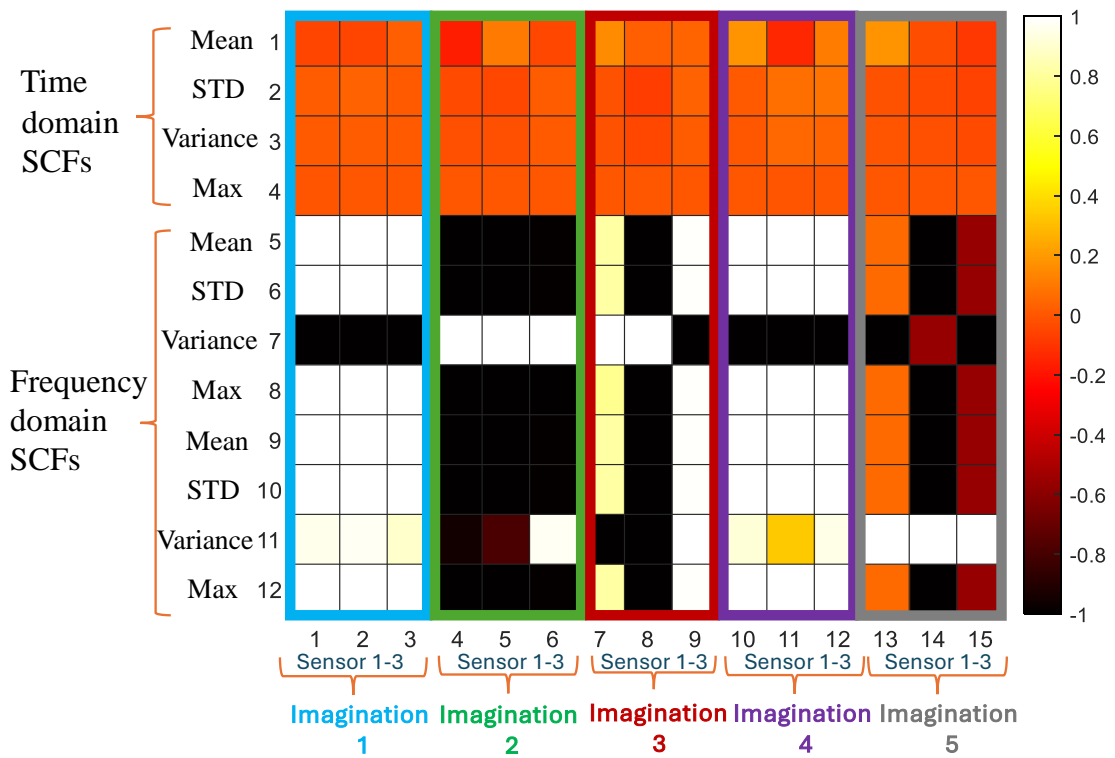


Figure 4.4: Heatmap of imaginations with selected features for bespoke analysis.

The analysis steps are:

- a) Observing the combination of SCFs values for individual imaginations.
- b) Comparing different imaginations with each other.
- c) Analysing ASMs between two subjects.

The first step involves identifying the deflection of SCFs values and recognising a unique combination of SCFs within an imagination. The analysis indicates that the uniqueness of SCF combinations results in varying levels of sensitivity. This is an important step because each mental task or imagination is expected to generate distinct patterns in brain signals. By examining the deflection, or variation, in SCFs values, it can be determined how a group of SCFs responds to an imagination. The second step is crucial for evaluating the ability of SCFs to differentiate individual imaginations. Identifying a unique combination of SCFs is essential for several reasons, including imagination differentiation, sensitivity analysis of various SCFs, improved classification, and model generalisation. To accurately distinguish between different imaginations, each must possess a unique signature or combination of SCFs. The sensitivity analysis indicates that the uniqueness of SCFs combinations results in varying levels of sensitivity. By identifying unique combinations of SCFs, it becomes

apparent which SCFs are most sensitive and informative for distinguishing between different imaginations.

Unique SCFs combinations ultimately enhance the performance of classification models. When each imagination has a distinct set of SCFs, the classifier can more easily learn and recognise the patterns associated with each mental task, leading to more accurate and reliable classification results. Furthermore, unique SCFs combinations contribute to the robustness and generalisation of the model. When the model learns from distinct and non-overlapping SCF sets, it can better generalise to new data, making it more effective in real-world applications where variability in brain signals is common.

Figure 4.4 presents two significant findings: the variance in the statistical function of the FFT's first part (SCF 7) and second part (SCF 11) exhibits substantial alterations compared to other SCFs, and individual sensors demonstrate distinct behaviours for each type of imagination. For instance, there is a notable difference between sensors for imaginations 3 and 5. Imagination 1 and 4 are distinguished by SCF 11, whereas imagination 2 contrasts with imaginations 1 and 4. These differences result in unique SCF combinations for each imagination, although some resemblances are evident between imaginations 1 and 4. Partial similarities are also observed between imaginations 3 and 5.

To evaluate the classification performance across different imaginations, distinct datasets are constructed based on the preceding discussion. One dataset comprises imaginations 2, 3, 4, and 5, while another includes imaginations 2, 4, and 5. A dataset containing all five imaginations is considered essential for analysing performance variations across sets with five, four, and three imaginations. This approach aims to investigate the performance deviation with the inclusion and exclusion of partly similar SCFs sensitivities. All 12  $\Delta$  SCFs are selected because relying solely on extreme SCFs (both positive and negative) is insufficient to recognise an imagination among the five. Moreover, the likelihood of similar patterns in certain SCFs for any two or three imaginations increases, thereby reducing the distinctiveness of each imagination's characteristics. Unique SCFs combinations contribute to the robustness and generalisation of the model. When the model learns from distinct and non-overlapping SCF sets, it can better generalise to new data, making it more effective in real-world applications where variability in brain signals is common.

To assess the robustness and generalisation of the selected SCFs, it is crucial to examine the consistency of brain wave patterns across different subjects. Consistent patterns indicate that

the SCFs can reliably capture essential features of brain signals, ensuring the model's applicability to a broader population. Figure 4.5 illustrates the third analysis step, which involves mapping all five imaginations (first trial) between two subjects.

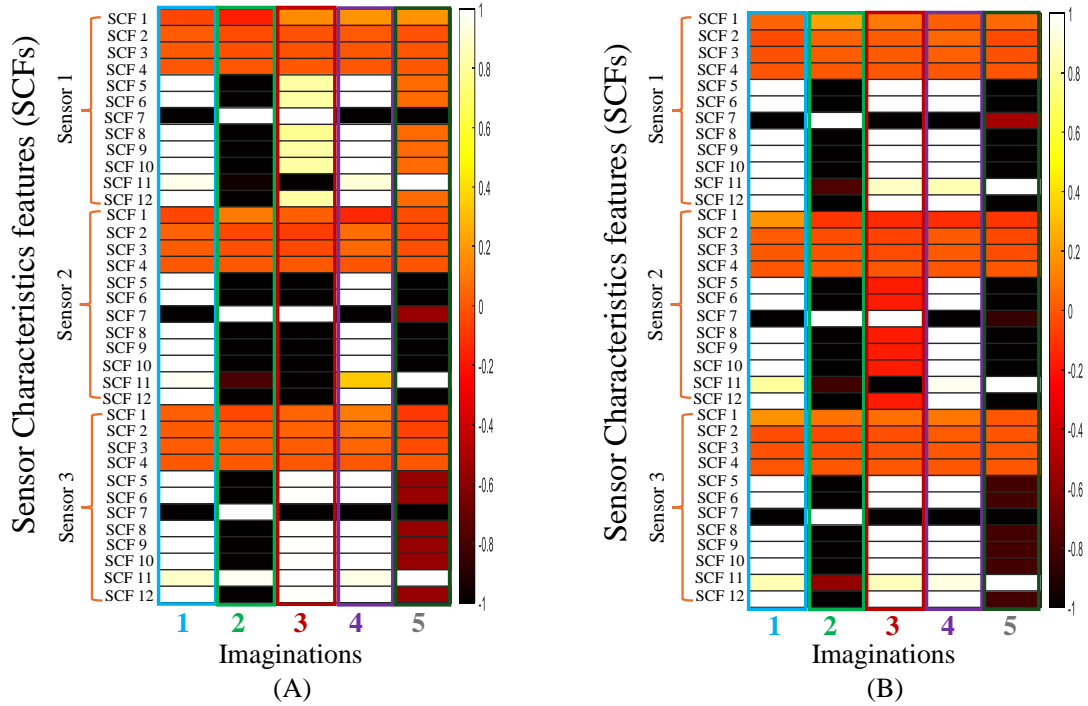


Figure 4.5: ASM of bespoke experiment for (A) subject 1 and (B) subject 2.

The figure shows that imaginations 1, 2, and 4 exhibit consistent SCF combinations for both subjects. For imagination 3, sensors 2 and 3 display similar sensitivity patterns; however, sensor 2 differs by  $\pm 0.5$  on the heatmap colour scale between subjects and has lower sensitivity than sensor 1 in both cases. For imagination 5, both subjects show identical patterns between sensors 2 and 3. For sensor 1 in imaginations 3 and 5, SCFs 7 and 11 exhibit opposite combinations between subjects, though both SCFs demonstrate differences in either case. Therefore, most SCFs are commonly found, effectively characterising imaginations 3 and 5. Additionally, imaginations 1 and 2, or imaginations 2 and 4, are quite different, which helps create a distinctive nature between the imaginations.

#### 4.4 Performance of Classifiers for Bespoke Analysis

The verification step is designed to evaluate the capability of the ASPS approach in recognising different imaginations. For bespoke analysis, considering the purpose and input data size, two types of ANNs, namely FFNN and LVQ, are utilised as classifiers to verify the  $\Delta$  values extracted and selected using the ASPS approach. To study the performance

across different numbers of imaginations for two subjects, three imagination datasets are used, and four train-test models are designed in Figure 4.6.

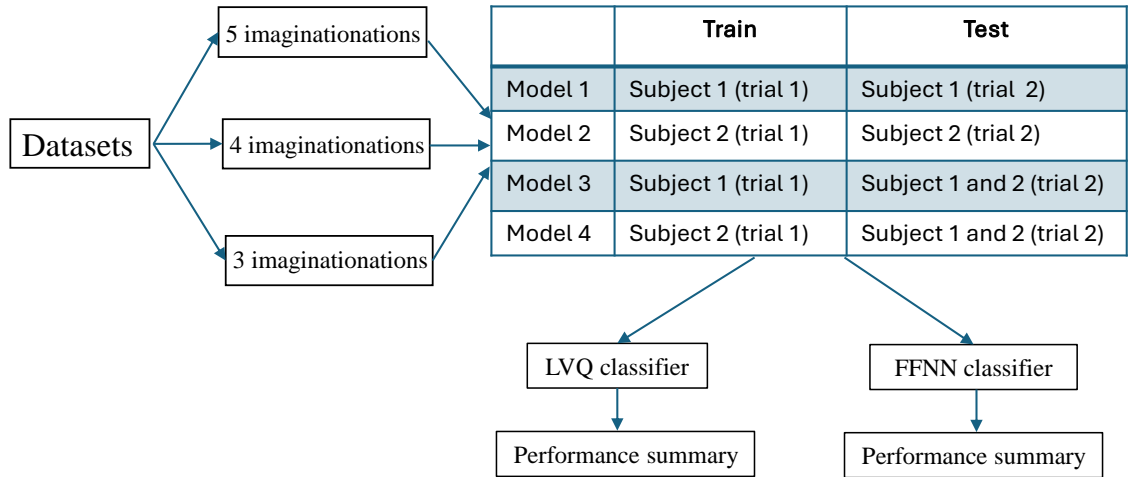


Figure 4.6: The design of verification steps for bespoke analysis.

Based on the analysis of extracted features, the dataset is divided into three subsets: five, four, and a dataset of three imaginations. Given the small data size from the two trials conducted during signal acquisition, the train-test splitting ratio is adjusted to meet the minimum requirements. Four models are utilised for verification. Model 1 is trained using data from subject 1's trial 1 and tested on subject 1's trial 2. Model 2 is trained on subject 2's trial 1 and tested on subject 2's trial 2. Model 3 is trained on subject 1's trial 1 and tested on trial 2 data from both subjects 1 and 2. Model 4 follows the same structure as Model 3 but is trained on subject 2's trial 1. Each model is evaluated using both LVQ and FFNN classifiers. Various ANN model architectures are designed for imagination classification, with their performances meticulously recorded.

In both FFNN and LVQ, various ANN architectures are tested, considering the following factors:

- i. The number of hidden layers and the number of neurons in each layer.
- ii. Different combinations of training and test data from two subjects.
- iii. Three different combinations of imagination datasets.

Six architectures are explored for ANNs as mentioned in Table 4.3. For the LVQ model, a single-layer architecture is employed, with the number of neurons ranging from 1 to 100 to determine the configuration that yields the best performance.

Table 4.3: ANN model architectures for imaginations classification for bespoke analysis.

Architecture index	ANN type	Number of imaginations for classification	Number of neurons in layer 1	Number of neurons in layer 2	Number of models run
1	LVQ	5, 4, 3	N, N=1,2, ...100	N/A	100
2	FFNN	5, 4, 3	N, N=1,2, ...100	N/A	100
3	FFNN	5, 4, 3	$i$	$i$	100
4	FFNN	5, 4, 3	$i$	$2i$	100
5	FFNN	5, 4, 3	$2i$	$i$	100
6	FFNN	5, 4, 3	$2i$	$2i$	100

\* $i$  = number of neurons in each layer = number of samples

Similarly, the single-layered FFNN architecture is designed following the same concept. Additionally, FFNN architectures with two layers are investigated, featuring four combinations of neuron numbers:  $(i, i)$ ,  $(i, 2i)$ ,  $(2i, i)$ , and  $(2i, 2i)$ , where  $i$  represents the number of neurons in each layer and corresponds to the number of samples used in the ANNs. All ANN architectures are executed 100 times to assess the stability of performance and to measure the average classification accuracy. The classification accuracy, as defined in Chapter 3 (Equation 3.2) of, is used to measure both the best and average performances. Each model shown in Figure 4.6 is executed using the aforementioned six ANN architectures, resulting in 24 different combinations. Each combination is experimented with datasets containing 5, 4, and 3 imaginations, respectively, and all ANNs are executed 100 times to observe both the best and average performances.

The experiments involved four models (Model 1, Model 2, Model 3, and Model 4) and are conducted across three scenarios involving five, four, and three imaginations. The classifiers employed, LVQ and FFNN, are configured with varying numbers of hidden layers and neurons to determine the optimal architecture. The highest performances for all models are summarised in Figure 4.7.

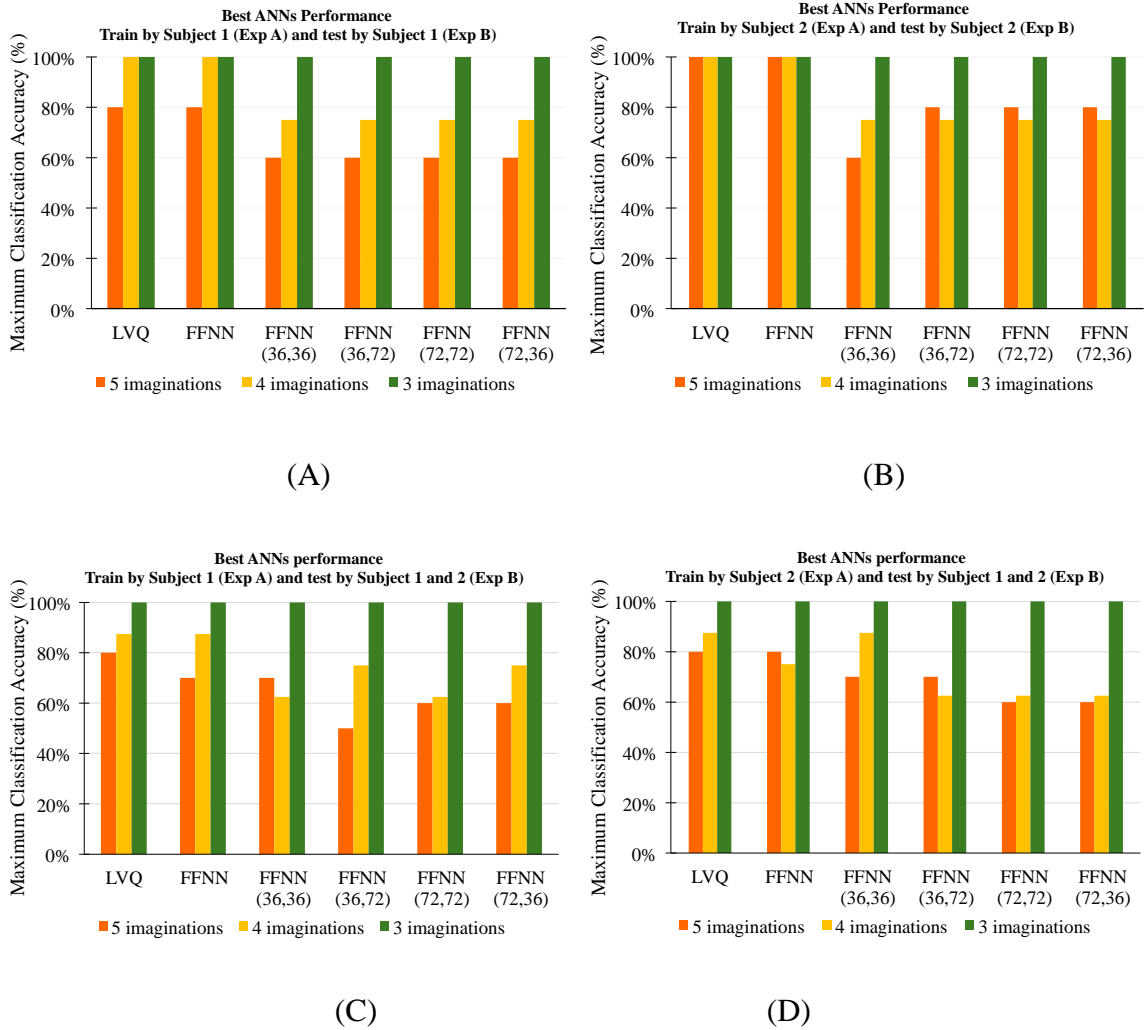


Figure 4.7: Best classification accuracy of four models for all ANN architecture.

The scenario with three imaginations demonstrated uniformly high performance across all models and classifiers. Both LVQ and FFNN classifiers, including all FFNN configurations, consistently achieved 100% accuracy in Models 1, 2, 3, and 4. This uniformity indicates that the classifiers can robustly distinguish among a smaller set of imaginations, irrespective of the model or network configuration. When the number of imaginations is four, both LVQ and single layered FFNN classifiers achieved 100% accuracy in Models 1 and 2. However, a notable decline in performance is observed in Models 3 and 4. LVQ achieved 87.5% accuracy in Model 3 and 75% in Model 4. FFNN matched the LVQ performance in Model 3 with 87.5% and outperformed it slightly in Model 4 with 87.5%. The various FFNN configurations showed a general trend of lower accuracy in Models 3 and 4, with the best configurations (two layers with (36, 72) and (72, 36) neurons) achieving 75% accuracy in Model 3 but only 62.5% in Model 4. This suggests that while Models 1 and 2 maintain high

performance, Models 3 and 4 exhibit reduced capability in accurately distinguishing between four imaginations.

In the scenario involving five imaginations, the best performance of the LVQ classifier varied significantly across the models. LVQ achieved an accuracy of 80% in Models 1, 3, and 4, whereas it attained 100% accuracy in Model 2. The single layer based FFNN classifier also demonstrated variability, with the standard configuration achieving 80% accuracy in Models 1 and 3, 70% in Model 4, and 100% in Model 2. When considering the different two layers-based FFNN configurations: FFNN (36, 36) architecture achieved 60% accuracy in Model 1 and 70% in Models 3 and 4. FFNN (36,72) architecture showed improved performance in Model 2 with 80% accuracy, while its performance ranged from 50% to 70% in other models. FFNN (72, 72) and FFNN (72, 36) both architectures attained a consistent 60% accuracy in Model 1 but showed higher variability across other models. The overall analysis indicates that Model 2 consistently outperforms the other models, particularly with LVQ and FFNN achieving perfect accuracy, suggesting subject 2 has superior ability to distinguish among the five imaginations.

Average performance of every architecture is calculated for 100 times each model runs. All models' average performances for subjects 1 and 2 are summarised in Figure 4.8.

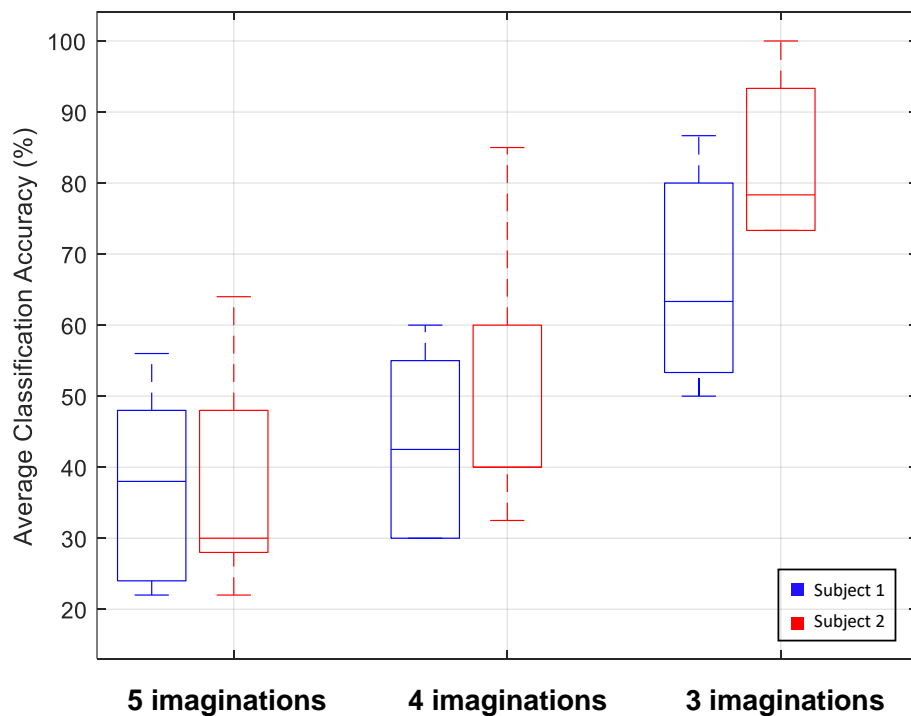


Figure 4.8: Average performance of three datasets for all models.

The box and whisker plot indicates greater median values for subject 2 across all imaginations' scenarios and wider interquartile ranges for subject 2, indicating more variability but consistently higher performance. The higher averages for subject 2 across all configurations and number of imaginations indicate a more consistent and robust performance. LVQ might be more suitable for applications requiring higher accuracy and consistency, particularly when the number of imaginations decreases. However, LVQ is performing slightly better due to smaller size of input data. These insights suggest refining ANN architectures, improving the generalisation capabilities of models and explore the ANN model performances for larger dataset in this research.

Combining both subject's performances, 3-imagination datasets achieve an average accuracy between 72-100%, while 4-imagination and 5-imagination datasets attain average accuracies up to 77% and 67.40%, respectively. An investigation into the average performance deviation between the four train-test models is illustrated in Figure 4.9, suggesting that the methodology can potentially work in a subject-independent manner.

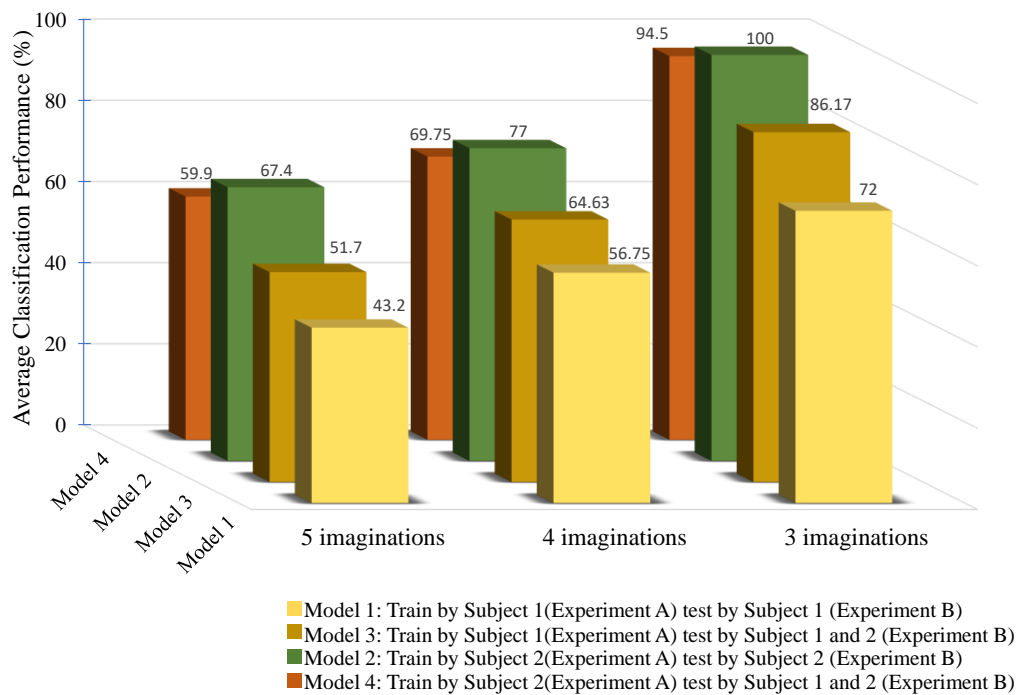


Figure 4.9: Average performance comparison for subject-wise training and imaginations for all models.

The quality of imaginations produced by subjects significantly influences the outcomes. For instance, overall performance is better when ANNs are trained with data from subject 2. This

consistency across different models and datasets further indicates that the ASPS approach is capable of extracting necessary brain signal features for BCIs development.

In line with similar studies on classifiers' performance in brain signal processing, research has demonstrated a range of outcomes. For instance, Mizuno *et al.* (2010) reported highest accuracy between 31% and 86% and average performance between 54.8% and 65% for classifying five different mental tasks using LVQ. In a comparable experiment employing MLP trained with backpropagation neural networks and SVM, El Bahy *et al.* (2017) achieved accuracy rates ranging from 64% to 84%. These variations in performance are primarily influenced by the scope of the experiment, the datasets used, and the classifiers applied. In the present study, our bespoke experiments yielded overall best performances with accuracy rates between 80% and 100% for recognising five imaginations using both FFNN and LVQ classifiers.

#### **4.5 Summary**

This chapter elaborates on the design, analysis, verification results, and discussion for the bespoke experimental setup. The study implemented the ASPS approach with a range of SCFs, extracting features from raw time domain signals and frequency domain analyses with different partitions. The detail of the bespoke design has been presented in Section 4.2. Section 4.3 of this chapter thoroughly discusses the analysis of identifying the uniqueness of imaginations and similarities between subjects. These obtained SCFs are verified using FFNN and LVQ classification algorithms. The results of various ANN architectures for different groups of imaginations are summarised in Section 4.4.

Both LVQ and FFNN are adequate in imaginations recognition. LVQ performed better in most cases, as the size of the dataset favoured this classifier. However, FFNN is faster than LVQ in all classifications of imagination recognition. The FFNN classifier demonstrated flexibility with different hidden layer configurations, although the standard FFNN configuration often performed as well or better than the more complex configurations. This suggests that while complexity in network architecture can enhance performance, it is not always necessary for achieving high accuracy.

The analysis found that both subjects achieved good results in recognising three and four imaginations. However, this indicates that the bespoke experiment is influenced by the quality of each individual's thoughts. Different individuals exhibit varying qualities of imagination, which affects the recognition accuracy. This variance in performance

underscores the importance of considering individual differences in cognitive processes. In terms of methodology, the ASPS approach, including two-part FFT features, can recognise the five imaginations for the bespoke method. Among the two ANN models (LVQ and FFNN), a single hidden layer FFNN is a suitable in terms of accuracy, architectural complexity, and computational time.

The next chapter explores the design, implementation, and assessment of a group-based analysis framework for identifying various imagined tasks, employing an advanced brain signal processing model. It intends to assess the effectiveness of the ASPS approach in analysing brain signals from multiple individuals for the recognition of imagined tasks.

# **Chapter 5: Imaginations Recognition Through Group-Based Analysis**

## **5.1 Introduction**

This chapter provides a comprehensive design and development of group-based analysis, along with a discussion of the results obtained. The primary focus is to evaluate and validate the performance of the ASPS approach in recognising mental imagery across an expanding number of participants. Section 5.2 offers a detailed design of the group-based analysis. Section 5.3 outlines the analysis of feature extraction and selection, following the framework established in the previous section. This analysis aims to assess the efficacy of the ASPS approach across different groups of subjects. Subsequently, in Section 5.4, the performance of the classifier is examined, providing insights into the verification of group-based performance outcomes. Two types of ANNs, namely FFNN and LVQ, are utilised individually as classifiers for verification purposes.

## **5.2 Workflow for Group-based Analysis**

The ASPS approach enables the integration of multiple signal domain features into the ASMs (Al-Habaibeh, Zorriassatine and Gindy, 2002). To explore this capability, the experiment incorporates time-domain raw features, frequency-domain features obtained through FFT, and time-frequency domain features derived from DWT. The analysis extends to additional divisions of FFT to extract more nuanced and detailed characteristics. By incorporating a range of signal processing techniques through the ASPS approach, the study aims to evaluate the distinctiveness of different mental imaginations concerning signal characteristics and their inherent properties. While the range of signal processing domains is expanded, the number of statistical functions is maintained at four to ensure that dimensionality remains manageable.

The signals from three spatially distanced EEG sensors, as shown in Chapter 4, Figure 4.1, are consistently maintained throughout this study and are processed for all participants involved. All four statistical functions listed in Chapter 4, Table 4.1 are applied to raw signals, FFT output signals divided into four segments, and DWT output signals with three cDs. The decomposition process of this study is illustrated in Figure 5.1 where LPF and HPF denote low pass filter and high pass filter respectively.

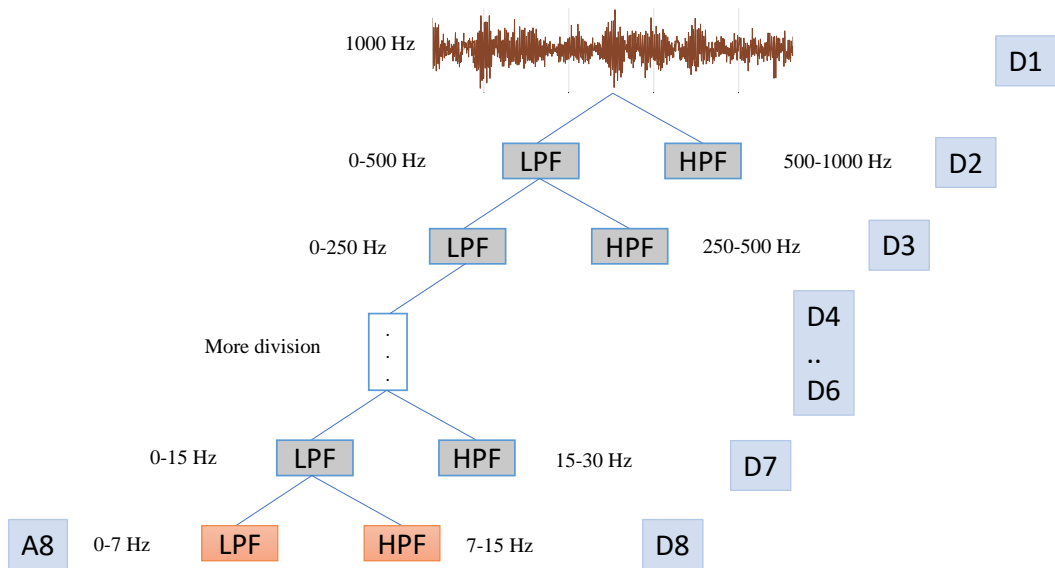


Figure 5.1: Wavelet decomposition (Cvetkovic, Übeyli and Cosic, 2008).

The decomposition level of the EEG signal is influenced by the sampling rate and the targeted frequency bands, such as alpha and/or beta. In this experiment, the signal is decomposed up to eight levels (cD8) to capture both beta and alpha frequencies, given the sampling rate of 2000 Hz. The analysis revealed that cD8, cD7, and cD6 exhibit significant values, covering frequencies between 7 Hz and 62 Hz.

The selection of wavelet functions is a critical and complex task, as highlighted by the literature. Given the varied characteristics of wavelet outputs, this research tested several wavelet functions. The study determined that the wavelet functions 'db4' wavelet provides the most relevant features compared to other wavelet functions, such as, db2, db10, coif4, coif5, and sym9 wavelets. In this context, db4, db2, and db10 correspond to the 4th, 2nd, and 10th orders of Daubechies wavelet functions, respectively. Similarly, Coif4 and Coif5 denote the 4th and 5th coefficients of the Coiflet wavelet function, while Sym9 represents the 9th order of the Symlet wavelet function.

Figures 5.2 illustrates the flowchart for the group-based analysis. The raw data, which comprises time-domain signals, is subjected to various statistical functions. To derive frequency-domain features, the experiment applies FFT to the raw signal data. The resulting FFT output is then divided into four equal segments, with the aforementioned statistical functions calculated for each segment.

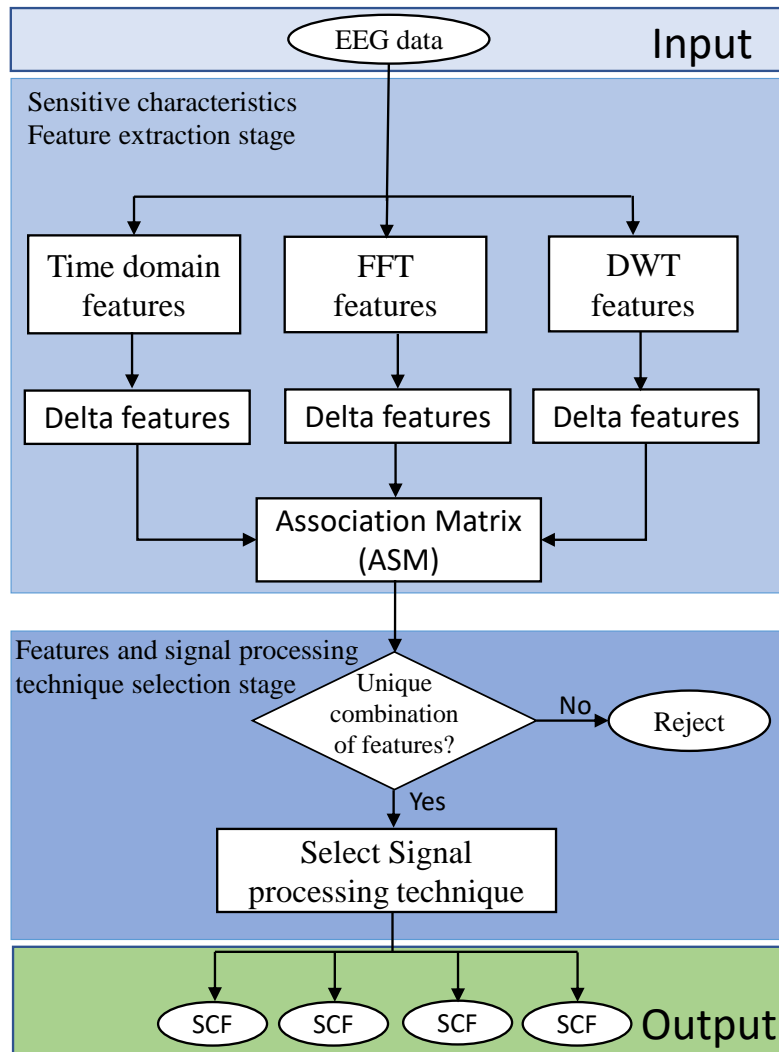


Figure 5.2: Flowchart of ASPS approach for group-based analysis.

For obtaining time-frequency domain features, the analysis employs DWT with ‘db4’ wavelet function and applies the same statistical functions to three components: cD8, cD7, and cD6. ASMs are produced as per ASPS approach, analysed, and the SCFs are prepared for classification input, specifically for ANNs.

### 5.3 Feature Extraction and Selection for Group-based Analysis

From the design of the previous section, ASPS approach employs time domain, frequency domain and time-frequency domain analysis. 4 statistical functions are applied over raw signal, FFT output and DWT output resulting greater number of SCFs from all mentioned domains. All domains and their subdivision values calculate  $\Delta$  values by subtracting relax from subsequent mental task, aiming to recognise imaginations based on group-based experiments.

The SCFs are derived according to the calculations outlined in Table 5.1.

Table 5.1: Features calculation for group-based analysis.

Signal processing technique	Number of statistical functions	Number of divisions	Number of extracted SCFs	Imagination selected for specific technique	Number of selected features (SCF)
Time domain	4	0	4	N/A	N/A
Frequency domain	4	4	4 X 4=16	Imagination# 2,4,5	12
Time-frequency domain	4	3	4 X 3=12	Imagination# 1,3	12
Total extracted features=			32	Total selected features per imagination	12

The SCFs are given as inputs of FFNN and LVQ models to investigate the performance of imaginations recognition. Feature extraction is performed using the ASPS approach methodology. Time-domain features are extracted from raw signals by calculating four statistical functions, as detailed in Table 3.4. Consequently, each raw signal generates four SCFs for each sensor. In the frequency domain, features are extracted from the FFT outputs. The FFT is divided into four parts, and four statistical functions are applied to each part, resulting in a total of 16 SCFs from this domain. For the DWT analysis using the 'db4' wavelet function, three components (cD8, cD7, and cD6) are considered, and features are extracted from each.

A total of 12 SCFs are derived after applying four statistical functions to these components. After calculating all 32  $\Delta$  SCFs, an ASM is produced for each individual and each imagination. Similarly, ASMs are generated for other subjects and mapped between them. Three key observations emerge at this stage:

- a) Observing the combination of  $\Delta$  SCFs for individual imaginations across domains.
- b) Comparing domains and five imaginations to identify the uniqueness of each imagination within a specific domain.
- c) Analysing ASMs across multiple subjects to form groups.

Figure 5.3 illustrates the ASM heatmaps of four subjects, facilitating the discussion of these observations.

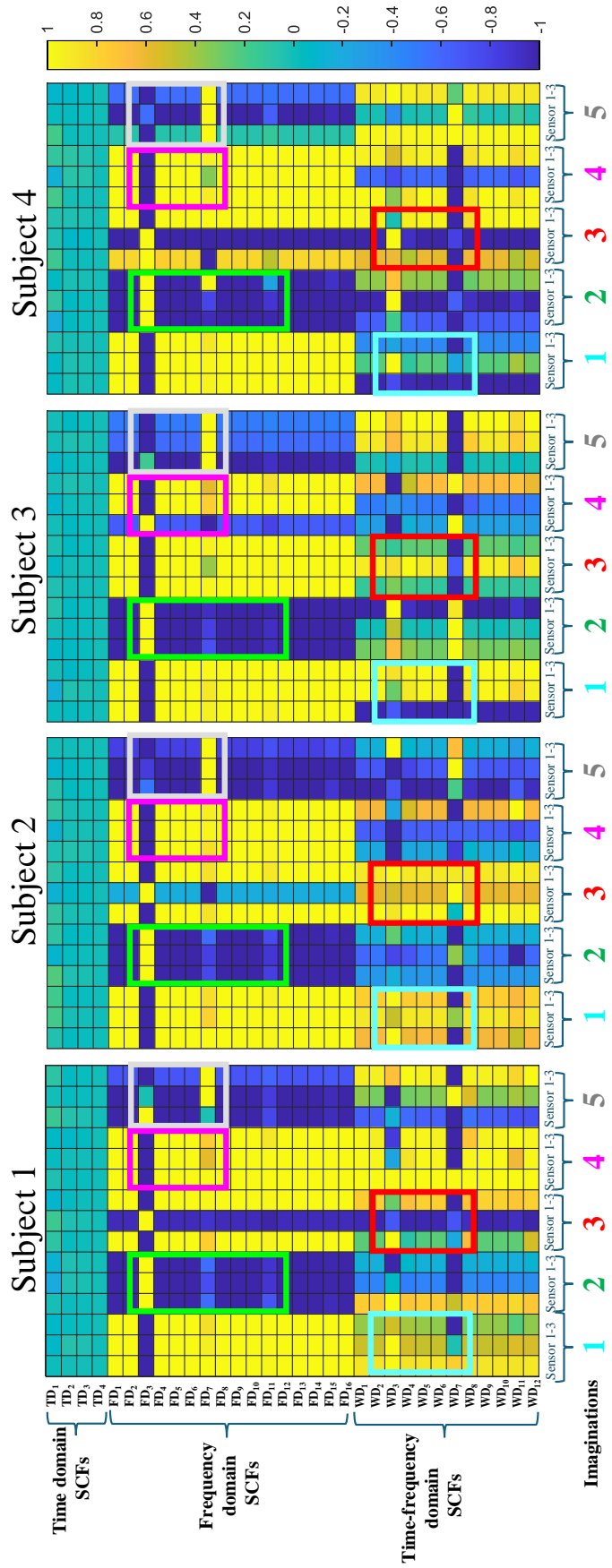


Figure 5.3: Illustration of uniqueness of imaginations and mapping between subjects.

Firstly, time-domain SCFs are insufficient to distinguish characteristics between imaginations. In the frequency domain, for imagination 1,  $FD_3$  creates a substantial characteristic, while  $FD_7$  adds a subtle one alongside other SCFs. Conversely, the time-frequency domain presents a slightly better set of SCFs, including  $WD_3$  and  $WD_7$ . For the second imagination,  $FD_3$ ,  $FD_7$ , and  $FD_{12}$  from the frequency domain show clear significance compared to time-frequency domain SCFs.

Imaginations 1 and 3 in the frequency domain exhibit similarities, except for sensor 2's characteristics, which differ from those of sensors 1 and 3. Despite minor differences in  $FD_7$ , it suggests a consistency check between subjects. On the other hand, imaginations 1 and 3 in the time-frequency domain show distinct differences. Imagination 4 closely resembles the first imagination, with better  $FD_7$  characteristics in the frequency domain. The time-frequency domain for imagination 4 has a notable combination of SCFs, suggesting a consistency check between subjects. Imagination 5 exhibits unique SCF combinations in  $FD_3$  and  $FD_7$  within the frequency domain, while the time-frequency domain shows variable sensor characteristics, with  $WD_3$  and  $WD_7$  differing from other SCFs.

Secondly, examining the frequency domain and five imaginations reveals those imaginations 1, 3, and 5 share similarities in  $FD_3$  and  $FD_7$  attributes. Sensor 2 for imagination 3 might not be a strong indicator since sensors are chosen randomly, and sensor optimisation analysis might select a different sensor. In such a case, frequency domain SCFs for imagination 3 can only be chosen if other subjects exhibit the same characteristics, necessitating its inclusion in the sensor optimisation. In contrast, imaginations 2 and 5 show distinct uniqueness with the sensitivity of  $FD_3$  and  $FD_7$ . The time-frequency domain offers better distinguishable SCFs for imaginations 1, 3, and 4 compared to frequency domain SCFs. Both FFT and DWT-generated SCFs show more consistent sensor sensitivity for imaginations 1 and 4, suggesting these imaginations might not be significant from either domain.

Comparing  $FD_3$ - $FD_7$  and  $WD_3$ - $WD_7$ , imagination 1 is better represented in the time domain, while imagination 4 has a stable representation in the frequency domain. However, these can be selected only if all subjects exhibit similar characteristics. The third imagination shows consistent characteristics for sensor 2 in both frequency and time-frequency domains. Comparing  $FD_3$ - $FD_7$  and  $WD_3$ - $WD_7$ , imagination 3 demonstrates better uniqueness in the time-frequency domain. Nonetheless, characteristics between subjects need to be examined to finalise the domain for each imagination and select the SCFs.

Thirdly, these observations are analysed across subjects. Despite showing stable  $FD_3$  attributes between subjects in the frequency domain, imagination 1 may be confused with imagination 4 in the frequency domain. In contrast,  $WD_3$ - $WD_7$  characteristics in the time-frequency domain show consistency between subjects for imagination 1. Among imaginations 1, 3, and 4, the FFT-generated SCFs show similarities, but only the fourth imagination is better represented in the frequency domain. The third imagination shows unstable characteristics for sensor 2 in both domains and might have FFT domain similarities with either imagination 1 or 4 across subjects. DWT-generated SCFs are more consistent than FFT in terms of sensor and subject consistency. Therefore, among imaginations 1, 3, and 4, the first and third imaginations have finer SCFs in the time-frequency domain, while the second imagination has superior SCFs in the frequency domain. All subjects consistently show unique characteristics in the frequency domain for imaginations 2 and 5. Figure 5.3 illustrates these differences between domains and the resemblance between subjects, with various colours highlighting distinct areas of significant SCFs for each imagination.

The mapping displays data from four randomly selected subjects, leading to the formation of groups based on their resemblance. Subjects demonstrating strong similarity are placed into group one, while five other subjects exhibiting considerable uniformity form another group. The remaining subjects exhibit anomalous characteristics either in sensor readings or imagination. The criteria for group formation are not fixed, and different analytical perspectives may result in varying cohort sizes. This analysis supports the classification of five imaginations. Chapter 4 also successfully identified five imaginations with at least 80% accuracy. However, bespoke analysis and the limited number of trials (only two) may bias the classifiers. Generalisation should be considered to ensure applicability to a broader population. When ASMs for only four subjects are mapped, multiple imaginations may produce identical situations within a single domain, as depicted in Figure 5.3. This could reduce classification accuracy. The ASPS approach's advantage of integrating multiple domains into one matrix suggests that this analysis is optimal for classifying a larger number of imaginations across a broader population.

SCFs are selected based on the preceding analysis. time-domain SCFs (raw signals) are excluded due to their lack of substantial intrinsic characteristics. SCFs  $FD_1$  to  $FD_{12}$  are selected from the first three segments of the frequency domain, and  $WD_1$  to  $WD_{12}$  are chosen from the time-frequency domain. This outcome supports the classification of imaginations 2, 3, and 5, demonstrating the capability of the selected SCFs from two different domains.

Increasing the number of cohorts leads to the creation of groups based on the resemblance of different imaginations between subjects. Three groups are formed: group 1 consists of four subjects, group 2 includes nine subjects, and group 3 comprises nineteen subjects.

#### 5.4 Performance of Classifiers for Group-based Experiment

For the group-based experiment, feature extraction and selection are conducted differently. The study distinguishes the selected features from the total extracted features. Based on signal processing techniques, features for three imaginations are derived from FFT, and features for two imaginations are derived from DWT. First two groups of subjects are identified based on the order of similarity. Third group combines all 19 subjects. The study analyses the performance differentiating factors and summarises the results for bespoke and group-based experiments in this section. Table 5.2 presents information on the formation of groups.

Table 5.2: Group formation for group-based analysis.

	Subjects	Train	Test
Group 1	4	Experiment A	Experiment B
Group 2	9	Experiment A	Experiment B
Group 3	19	Experiment A	Experiment B

Group 1 is created based on the strong resemblance of the SCF characteristics between subjects. Group 2 includes the subjects from Group 1 and adds five more subjects, selected based on a considerable resemblance of the SCF characteristics. Group 3 is a combined group, consisting of all 19 subjects. Since the dataset contains two trials, one trial is used for training and the other for testing the ANN models.

Various ANN model architectures are explored for group-based analysis, which follows a bespoke analysis approach. However, the number of imaginations datasets differs; two imaginations' SCFs are derived from DWT, while three imaginations' SCFs are derived from FFT. To evaluate the performance of individual techniques, this verification step prepares the datasets for two imaginations, three imaginations, and one combined dataset for a total of five imaginations. Table 5.3 presents the ANN model architectures used for classifying imaginations in group-based analysis.

Table 5.3: ANN model architectures for imaginations classification in group-based analysis.

Layer architecture index	ANN type	Number of imaginations set	Number of neurons in layer 1	Number of neurons in layer 2	Number of models run
1	LVQ	2,3,5	$N, N=1, 2, \dots, 100$	N/A	100
2	FFNN	2,3,5	$N, N=1, 2, \dots, 100$	N/A	100
3	FFNN	2,3,5	$i$	$i$	100
4	FFNN	2,3,5	$i$	$2i$	100
5	FFNN	2,3,5	$2i$	$i$	100
6	FFNN	2,3,5	$2i$	$2i$	100

\* $i$  = number of neurons in each layer = number of samples

Figure 5.4 illustrates the overall design of the verification for group-based analysis, clearly demonstrating the dataset preparation using three different groups and various imaginations derived from FFT, DWT, and a combination of both. The classification algorithms are employed with six architectures, and all the performances are summarised.

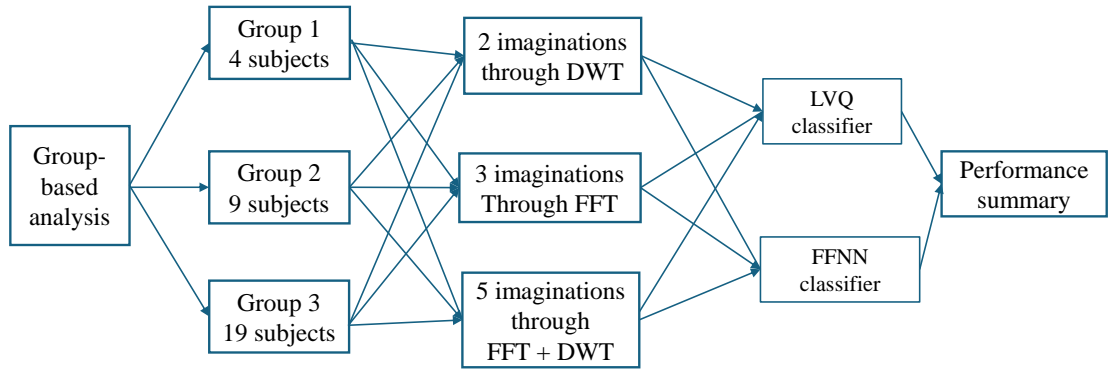


Figure 5.4: The design of verification steps for group-based analysis.

FFNN and LVQ, two ANNs are employed to evaluate classification performance. As discussed in the beginning of the section, three groups of subjects are selected based on the resemblance of their unique features to examine the variability in classification accuracy. These groups, named Group 1, Group 2, and Group 3, comprise 4, 9, and 19 subjects, respectively. Group 1 is the smallest and includes the subjects of Group 2. Group 3 encompasses all subjects who participated in the data collection process. This section presents the results for recognising 2, 3, and 5 imaginations using classification algorithms.

Each model architecture is run 100 times, and the best average performance is determined from these iterations. The optimal and mean performances are assessed based on classification accuracy, as outlined in Equation (3.2) of Chapter 3. The performance metrics for classifying two imaginations using DWT-generated SCFs, three imaginations using FFT-generated SCFs, and five imaginations using both are detailed in Appendix where each table includes the information of layer architecture, highest accuracy, and best average performance. All models are executed 100 times, and the best average performance is calculated from these runs. For each architecture, a single hidden layer for both LVQ and FFNN is tested with 1 to 100 neurons, with each size running 100 times. The neuron counts at which the highest accuracy is achieved is indicated in the single-layer models. The best accuracies are illustrated in Figure 5.5 (A) and (B) for the recognition of 2 and 3 imaginations, respectively, providing a convenient visualisation of the highest results.

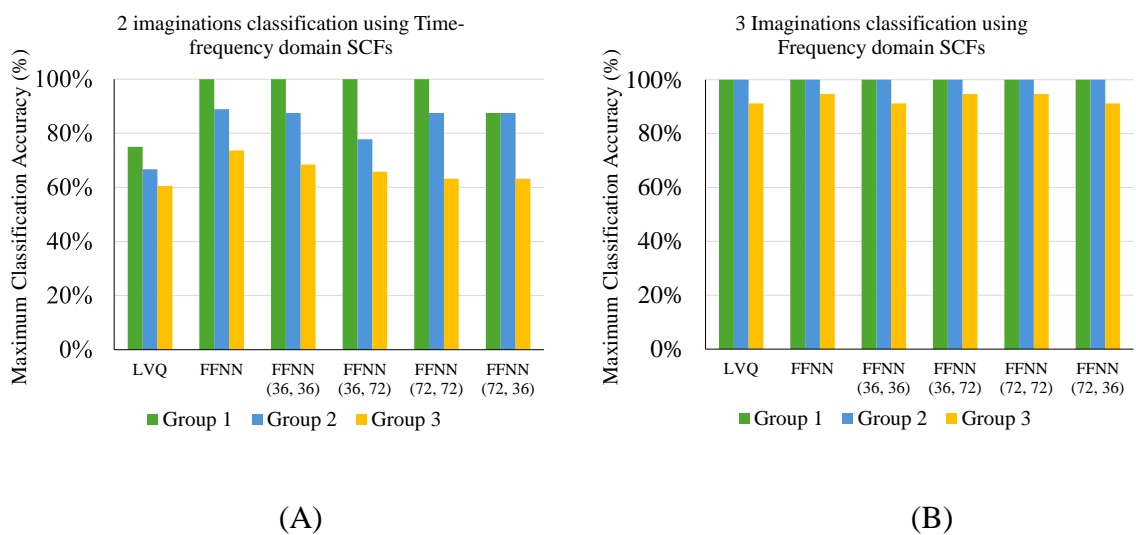


Figure 5.5: Best classification accuracy of group-based analysis for all ANN architecture (A) two imaginations, and (B) three imaginations.

Two classifications of imaginations used DWT-generated  $\Delta$  SCFs, while three classifications used FFT-generated  $\Delta$  SCFs. From these bar charts, it is evident that the FFNN model consistently outperforms the LVQ model across all three groups. In the scenario of 2 imaginations recognition for Group 1, the FFNN achieves a perfect classification accuracy of 100%, significantly surpassing the LVQ model, which achieves an accuracy of 75%. The FFNN also excels in Group 2 with an accuracy of 88.89%, compared to the LVQ's 66.67%. The performance of the FFNN drops slightly in the group of 19 subjects (Group 3), with an accuracy of 73.68%, though it remains superior to the

LVQ's 60.52%. Two-layer configurations of the FFNN are tested, including variations in the number of neurons in the hidden layers. The analysis indicates that the FFNN model configurations of (36, 36) and (72, 72) are generally more consistent, achieving high accuracies across Groups 1 and 2. The configuration with a size of (72, 36) slightly underperforms, particularly in Group 1, where it achieves only 87.50%, while others achieve 100%. However, no configuration of the 2-layered FFNN performs exceptionally well across all groups, highlighting the complexity and variability in EEG signal classification tasks.

In the case of three imaginations, all models show improved performance when using FFT features compared to DWT features. For Group 1 and Group 2, all models achieve perfect classification accuracy of 100% across these two groups, indicating that the FFT features are highly effective in distinguishing between the three different mental imaginations. In Group 3 the single layered FFNN and two double layered configurations (size with FFNN (36, 72), and FFNN (72, 72)) again demonstrate superior performance, achieving the highest accuracy of 94.74%. The LVQ model follows closely with an accuracy of 91.22%. The configurations FFNN (36, 36) and FFNN (72, 36) have slightly lower accuracies, both achieving 91.23%. Figure 5.6 summarises the highest accuracies achieved for 2, 3, and 5 imaginations across all groups.

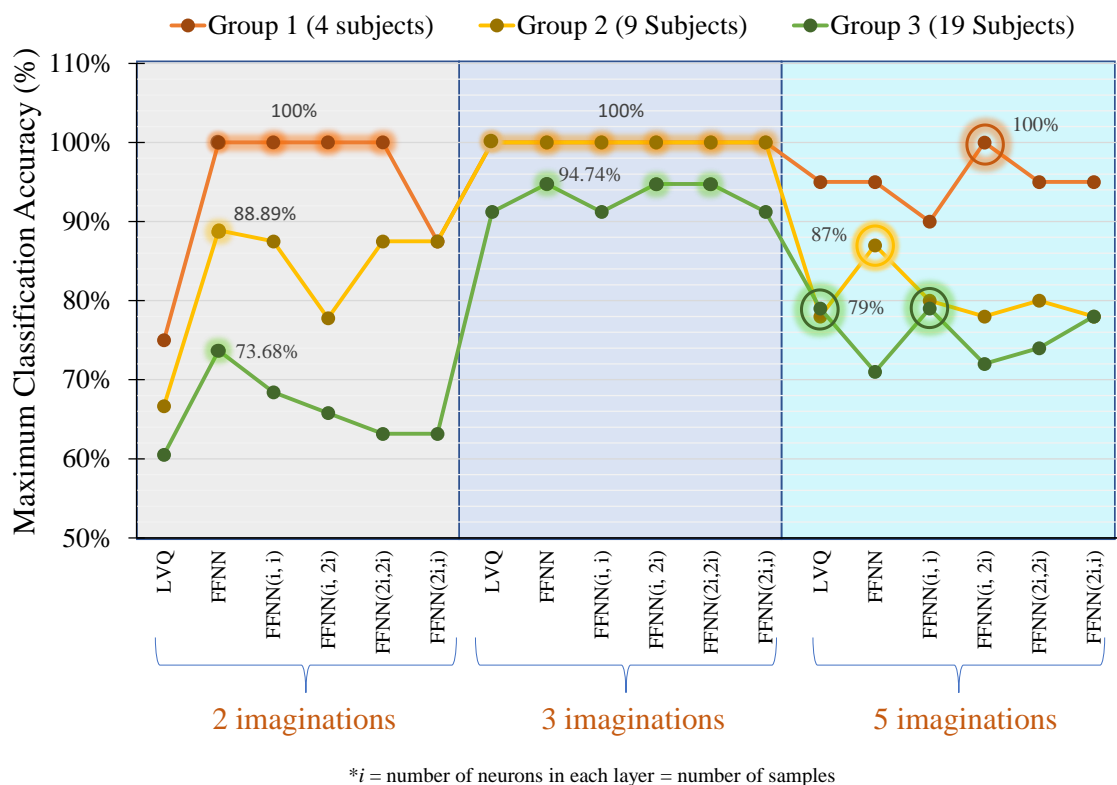


Figure 5.6: Highest accuracy summary.

Classifying five imaginations using a combination of FFT and DWT SCFs proves to be particularly challenging across the models evaluated. The LVQ model exhibits moderate performance in this context, with accuracy rates of 95.00% in Group 1, 77.78% in Group 2, and 78.95% in Group 3. The standard FFNN model maintains high accuracy in Group 1 (95.00%) and Group 2 (86.67%), but its performance significantly decreases to 70.53% in Group 3. The FFNN (36, 72) model emerges as the most reliable model for the five-imaginations classification task, particularly in Group 1, where it achieves 100% accuracy. In contrast, the FFNN (36, 36) and FFNN (72, 72) models demonstrate consistent performance across all groups, with accuracy rates ranging from 77.78% to 80.00% in Groups 2 and 3. This consistency, while at a slightly lower performance level, reflects a stable classification capability in more complex scenarios.

The analysis reveals that the FFNN models generally outperform the LVQ model across most tasks, particularly in scenarios with fewer imaginations. The FFNN models show excellent classification performance, especially in the two-imaginations task with DWT generated  $\Delta$  SCFs and the three-imaginations task with FFT generated  $\Delta$  SCFs. However, as the number of imaginations increases to five, the complexity of the classification task becomes more apparent, with performance varying significantly across models and groups. The combination of FFT and DWT features provides a robust foundation for effective classification, and the selection of the neural network model along with the specific group of subjects plays a crucial role in determining the maximum accuracy. Moreover, investigating the average accuracy across all groups can offer valuable insights into optimising model architecture.

While ANN models are repeated for 100 times of training and testing, allowing for the calculation of the average accuracy performance for each model in relation to different subject groups. The aggregated results of the best average classification accuracies for two and three imaginations are presented in Table 5.4.

Table 5.4: Best average performances for two-imagination and three-imagination classification.

Layer Architecture index	Model	2 imaginations classification with DWT SCFs			3 imaginations classification with FFT SCFs		
		Group 1	Group 2	Group 3	Group 1	Group 2	Group 3
1	LVQ	61.25%	53.33%	50.52%	98.30%	97.04%	84.03%
2	FFNN	71.25%	59.44%	55.52%	100.00%	97.04%	88.60%
3	FFNN ( $i, i$ )	56.25%	55.25%	51.34%	99.50%	94.81%	84.56%

Table 5.4: Best average performances for two-imagination and three-imagination classification (continued from previous page).

Layer Architecture index	Model	2 imaginations classification with DWT SCFs			3 imaginations classification with FFT SCFs		
		Group 1	Group 2	Group 3	Group 1	Group 2	Group 3
4	FFNN ( $i, 2i$ )	56.00%	48.33%	51.26%	100.00%	94.59%	85.72%
5	FFNN ( $2i, 2i$ )	53.50%	57.50%	50.11%	100.00%	95.41%	84.70%
6	FFNN ( $2i, i$ )	53.75%	57.50%	50.13%	99.17%	95.11%	85.19%

Overall average results for 2, 3 and 5 imaginations recognition are plotted in Figure 5.7 along with a demonstration of average trend of the results. In the task of classifying two imaginations using DWT generated  $\Delta$  SCFs, the average accuracies across the models reveal distinct patterns in performance.

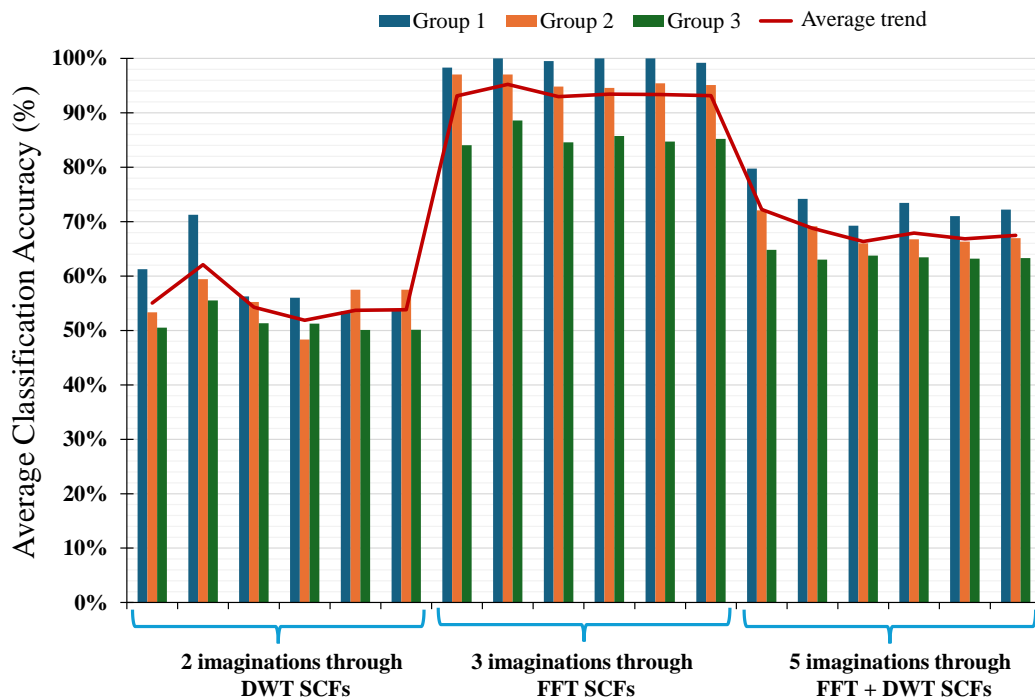


Figure 5.7: Best Average performance summary for group-based analysis.

The FFNN model consistently outperforms the other models, achieving an average accuracy of 71.25% in Group 1, 59.44% in Group 2, and 55.52% in Group 3. This indicates that FFNN is particularly effective in Group 1, although its performance diminishes slightly in subsequent groups. The LVQ model shows lower performance in two imaginations recognition across all groups, with an average accuracy of 61.25% in Group 1, 53.33% in

Group 2, and 50.52% in Group 3. These results suggest that while LVQ can provide moderate classification accuracy, it does not match the effectiveness of FFNN, particularly in more complex scenarios involving a more diverse subject pool.

The FFNN variants exhibit varying levels of performance in recognising two imaginations, with the FFNN (36, 36) and FFNN (36, 72) models achieving slightly higher accuracy compared to other configurations, particularly in Group 1 and Group 3, where they reached at least 56% and 51%, respectively. Group 2, however, performed better with the FFNN (72, 72) and FFNN (72, 36) models for recognising two imaginations.

When considering the classification of three imaginations using FFT features, all models exhibit significantly improved performance. The FFNN model achieves perfect accuracy in Group 1 (100%) and maintains high performance in Group 2 (97.04%) and Group 3 (88.60%). This highlights FFNN's robustness and superior ability to generalise across different subject groups when handling more mental tasks. LVQ also demonstrates strong performance in this context, particularly in Group 1 (98.30%) and Group 2 (97.04%). However, its accuracy drops to 84.03% in Group 3, indicating a slightly lower generalisability compared to FFNN. The FFNN (36, 72) and FFNN (72, 72) models both reach 100% accuracy in Group 1, matching the standard FFNN model. Their performance in Group 2 and Group 3 is slightly lower, ranging from 94.59% to 85.72%. This suggests that while these variants can achieve high accuracy in certain groups, they may not consistently outperform the single layered FFNN model across all groups.

The analysis of the five-imaginations recognition task using FFT and DWT features reveals distinct performance trends across different model architectures and groups. The LVQ model outperforms the other configurations, achieving the highest accuracy in Group 1 (79.75%) and showing relatively better performance in Group 2 (72.06%) and Group 3 (64.83%). Among the FFNN variants, the single-layer FFNN achieves the highest accuracy in Group 1 (74.20%) while exhibiting a decline in performance across Groups 2 (69.13%) and 3 (63.02%). The multi-layer FFNN models, including the FFNN (36, 36), FFNN (36, 72), FFNN (72, 72), and FFNN (72, 36) configurations, demonstrate consistent yet slightly lower accuracies, particularly in Group 1, where the highest accuracy reached 73.45% (FFNN 36, 72). These models also show a steady decline in performance across Groups 2 and 3, with accuracies clustering around 66-67% and 63-64%, respectively. Overall, the results indicate that while LVQ shows a stronger performance, the FFNN models, despite being multi-

layered, do not significantly surpass the single-layer FFNN, suggesting potential challenges in leveraging deeper architectures for this specific task.

The experimental findings presented in Chapter 4 demonstrated impressive accuracy levels ranging from 80% to 100% in recognising 5 imaginations. When comparing these results to the outcomes of the current study, it is observed that the same imaginations can be recognised with up to 100% accuracy for a group of 4 subjects. The classification accuracies achieved for the groups of 9 and 19 subjects are between 78.95% and 86%, respectively. Increasing the number of subjects provides a larger dataset for training the ANN models, leading to more stable and high-quality performance during testing. However, ensuring the uniformity of imaginations across multiple subjects poses a challenge, especially with groups of varying sizes. Among the classifiers employed, the FFNN mostly outperformed the LVQ, and the overall performance of single-layered FFNN is satisfactory for all subject groups and imagination sets. This research follows the ASPS approach investigated in Chapter 4, incorporating wavelet analysis as an additional signal processing technique. The meticulous selection process of signal processing techniques and features through the ASPS approach reveals that recognising 5 imaginations is possible with accuracies ranging from 78.95% to 100% across groups consisting of 4 to 19 subjects.

The analysis results reveal that the performance metrics for classifying 2, 3, and 5 imaginations vary across the groups. Group 1, being the smallest, serves as a baseline, while Group 3's results reflect the broader population's variability. The findings suggest that employing multiple domains within a single matrix enhances classification accuracy for a larger number of imaginations. This approach is particularly beneficial for generalising the model to a wider population.

### **5.5 Summary:**

In this chapter, the design, analysis, verification results, and discussion of the group-based experimental setup are elaborately presented based on advanced signal processing methodologies. The experiment conducted aimed to implement the ASPS approach with a range of SCFs for various groups of subjects. Features are extracted from raw time-domain signals, frequency domain analysis with different partitions, and time-frequency domain analysis. Feature selection has been carried out in two ways: identifying significant combinations of SCFs that ensure the uniqueness of each imagination and selecting features from specific signal processing techniques, such as FFT or DWT-generated SCFs.

Furthermore, group-based verifications highlight the potential for generalising the methodology to a wider population. The extracted and selected SCFs through the ASPS approach are verified using classification algorithms, namely FFNN and LVQ. The results of various ANN architectures for different groups of imaginations are summarised in Section 5.4. Their performance varies depending on the size of input data and the complexity of model architectures. In the discussion, the optimised ANN architecture is nearly identified. The findings of these experiments will be helpful in finalising the developed algorithm. The ASPS approach, including FFT and DWT SCFs, has the capability to recognise five imaginations. Group-based, 100% accuracy can be achieved for three imaginations, and 78.95% accuracy is achievable for the largest group of subjects in recognising five imaginations. Among the two ANN models (LVQ and FFNN), a single hidden layered FFNN is found to be the most feasible model in terms of accuracy, architectural complexity, and computational time. The FFNN, in bespoke analysis, is faster at achieving the best results. However, increasing the number of subjects in this analysis slows down the overall ANN process. The use of a greater number of statistical functions and trials will be reviewed in subsequent experiments to help determine the analytical properties of signal processing and finalise the proposed model.

The following chapter investigates the effectiveness of imagination recognition by combining the ASPS approach with image processing technique. It includes an analysis of performance across the same groups as in this chapter, with CNN employed as the classification method.

# Chapter 6: Imaginations Recognition Through Image Processing

## 6.1 Introduction

This chapter presents the design, analysis, verification results, and discussion for the third experiment, briefly introduced in Chapter 3. It includes a combined analysis where all 19 sensor signals are processed, incorporating a broader range of statistical functions and an increasing number of subjects. The methodology explores the effectiveness of integrating the ASPS approach with image processing techniques to enhance the recognition of imagined tasks across a larger subject pool. The design is detailed in Section 6.2, outlining the workflow steps. Section 6.3 provides an in-depth analysis based on the outlined design, while in Section 6.4, the performance of the CNN classifier is evaluated across different subject groups.

## 6.2 Workflow for Combined Analysis

This experiment employs the ASPS approach for feature extraction and selection, along with image processing methods, to classify five mental tasks using data from 19 sensors and 15 statistical functions. Previous analyses were limited to three randomly selected sensors and four statistical functions, which were not optimised. Consequently, this study evaluates the performance differences between these selected sensors and a full array of sensors and investigates whether a broader range of statistical functions can enhance performance and effectiveness in brain signal processing.

Drawing on the performance of the methodologies in Chapters 4 and 5, this analysis focuses exclusively on frequency domain features within the ASPS approach. The FFT output is segmented into 10 parts, with all 15 statistical functions applied across these segments. This approach aims to investigate group-based performance by incorporating all 19 sensors and using multiple partitions and statistical functions. The rationale for this analysis is outlined as follows:

I. Sensor Comparison: Previous chapters examined imagination recognition using only three randomly selected sensors. This chapter assesses the performance of all 19 sensors, comparing it to the previously used subset.

II. Statistical Function Analysis: Earlier analyses utilised only four statistical functions. This chapter explores the effectiveness of a broader range of fifteen statistical functions in brain signal processing.

III. Domain Performance: Previous studies explored the time, frequency, and time-frequency domains, finding that frequency domain analysis improved with increased FFT partitions. This chapter further investigates the frequency domain with more detailed partitions and additional statistical functions, raising questions about the sufficiency of frequency domain features alone for distinguishing between five imagined tasks.

IV. Image Processing Integration: Earlier investigations used specific SCFs to analyse task uniqueness and subject similarity. This analysis incorporates image processing techniques, such as CNNs, which enhance data mapping. This integration offers three benefits: (a) it simplifies ASM image creation by incorporating more sensors and statistical functions, (b) it tests the adaptability of established techniques with the ASPS approach, and (c) it evaluates performance in terms of efficiency, time, and complexity.

All 15 statistical functions are detailed in Table 6.1, these functions are calculated in this analysis. Function names and corresponding equations are mentioned in the table.

Table 6.1: Definitions and equations of fifteen statistical functions for combined experiment.

Definition	Equation	Definition	Equation
<b>Mean</b>	$E_1 = \frac{1}{n} \sum_{i=1}^n x_i$	<b>Crest factor</b>	$E_9 = \frac{\max  x_i }{E_{13}}$
<b>STD</b>	$E_2 = \sqrt{\frac{\sum_{i=1}^n (x_i - E_1)^2}{N}}$	<b>Clearance factor</b>	$E_{10} = \frac{\max  x_i }{E_{11}}$
<b>Variance</b>	$E_3 = \frac{\sum_{i=1}^n (x_i - E_1)^2}{N}$	<b>Absolute Mean</b>	$E_{11} = \left( \frac{1}{n} \sum_{i=1}^n \sqrt{ x_i } \right)^2$
<b>Max</b>	$E_4 = \max (x_i)$	<b>Power</b>	$E_{12} = \left( \frac{1}{n} \sum_{i=1}^n  x_i  \right)^2$
<b>Min</b>	$E_5 = \min (x_i)$	<b>RMS</b>	$E_{13} = \sqrt{\frac{\sum_{i=1}^n (x_i)^2}{n}}$

Table 6.1: Definitions and equations of fifteen statistical functions for combined experiment (continued from previous page).

Definition	Equation	Definition	Equation
<b>Median</b>	$E_6 = \frac{n + 1}{2} \text{ th term,}$ <p style="text-align: center;"><i>when n is even</i></p> $E_6 = \frac{n}{2} \text{ th term}$ $+ \frac{n + 1}{2} \text{ th term,}$ <p style="text-align: center;"><i>when n is even</i></p>	<b>IQR (interquartile range of time)</b>	$E_{14} = Q_3 - Q_1$
<b>Skewness</b>	$E_7 = \frac{\sum_{i=1}^n (x_i - E_1)^3}{(n - 1)E_2^3}$	<b>Range (Range of radio wave propagation)</b>	$E_{15} = E_4 - E_5$
<b>Kurtosis</b>	$E_8 = \frac{\sum_{i=1}^n (x_i -  x )^4}{(n - 1)E_5^4}$		

To address the aforementioned rationales, the methodology is designed to employ only the frequency domain within the ASPS approach. The schematic diagram illustrating the combined analysis is presented in Figure 6.1.

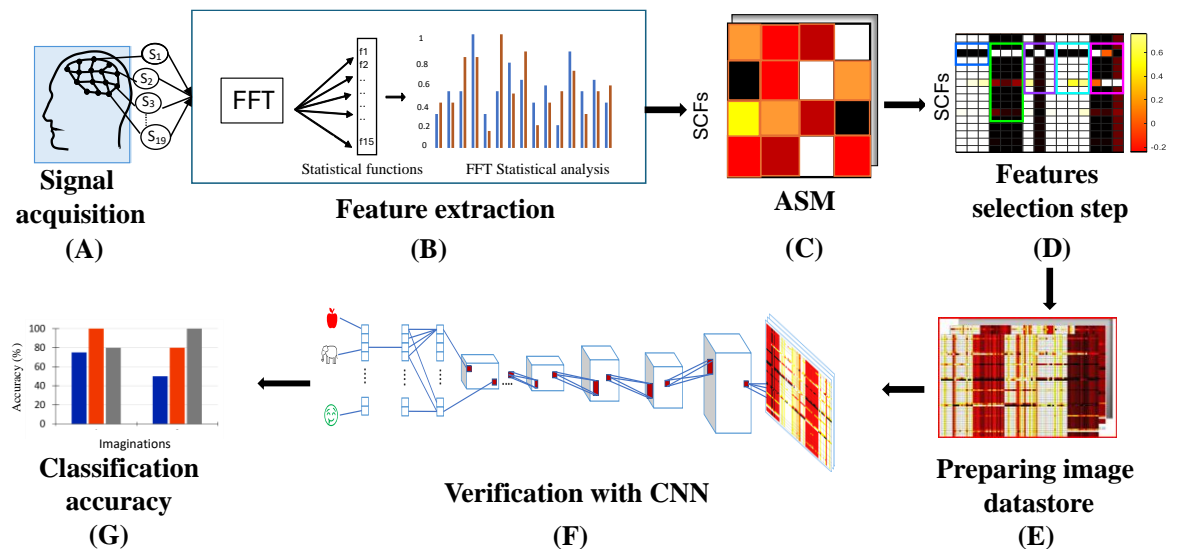


Figure 6.1: Schematic diagram of combined analysis.

The figure illustrates the collected signals undergoing frequency-domain analysis using various statistical functions. An ASM is generated from FFT-derived SCFs, and a selection

process is performed based on the analysis. The selected SCFs are then used to prepare an image data store as input for the CNN. Finally, the CNN classifies the signals, and performance is evaluated.

### 6.3 Feature Extraction and Selection with a Combined Method

Fifteen statistical functions are applied to ten segments of the FFT in both relaxed and mental task signals. These functions names and equations are applied in Table 6.1. This process results in 150  $\Delta$  SCFs for each type of imagination. After producing the ASM, it was found that the first 60 rows contain the most significant components for identifying an imagination. The remaining components are considered trivial and are excluded in the feature selection step to reduce the input size. This analysis step focuses only on the selected 60 SCFs, aiming to recognise imaginations based on group-based experiments. Feature calculations for extraction and selection are shown in Table 6.2.

Table 6.2: Features calculation for all subjects combined experiment.

Signal pattern	Number of input statistical functions	Number of extracted features (SCF)/sensor	Number of selected features (SCF)/sensor
FFT signal	15	10 X 15=150	60

These matrices are converted into heatmap images for further image processing. The heatmap images of constructed ASMs for 3, 4, and 5 imaginations are used as inputs to a CNN model to investigate the performance of imagination recognition across three groups.

Figure 6.2 (A – E) illustrates the heatmaps of five imaginations for one subject. The X-axis represents 19 sensors, and the Y-axis represents the selected 60 SCFs generated from ten segments of the frequency domain. The observations are discussed as follows:

Imagination 1: The heatmap shows that SCFs numbered 3, 12, 18, 27, 33, and 42 form distinct combinations compared to other SCFs. However, these SCFs are not equally significant across all 19 sensors. For example, SCFs such as 3, 12 are mostly prominent in the frontal, central, and partly temporal areas, while the occipital and partly parietal areas show less significance. Since sensor optimisation analysis has not been conducted yet, this study focuses on SCFs that show significant differences across all 19 sensors.

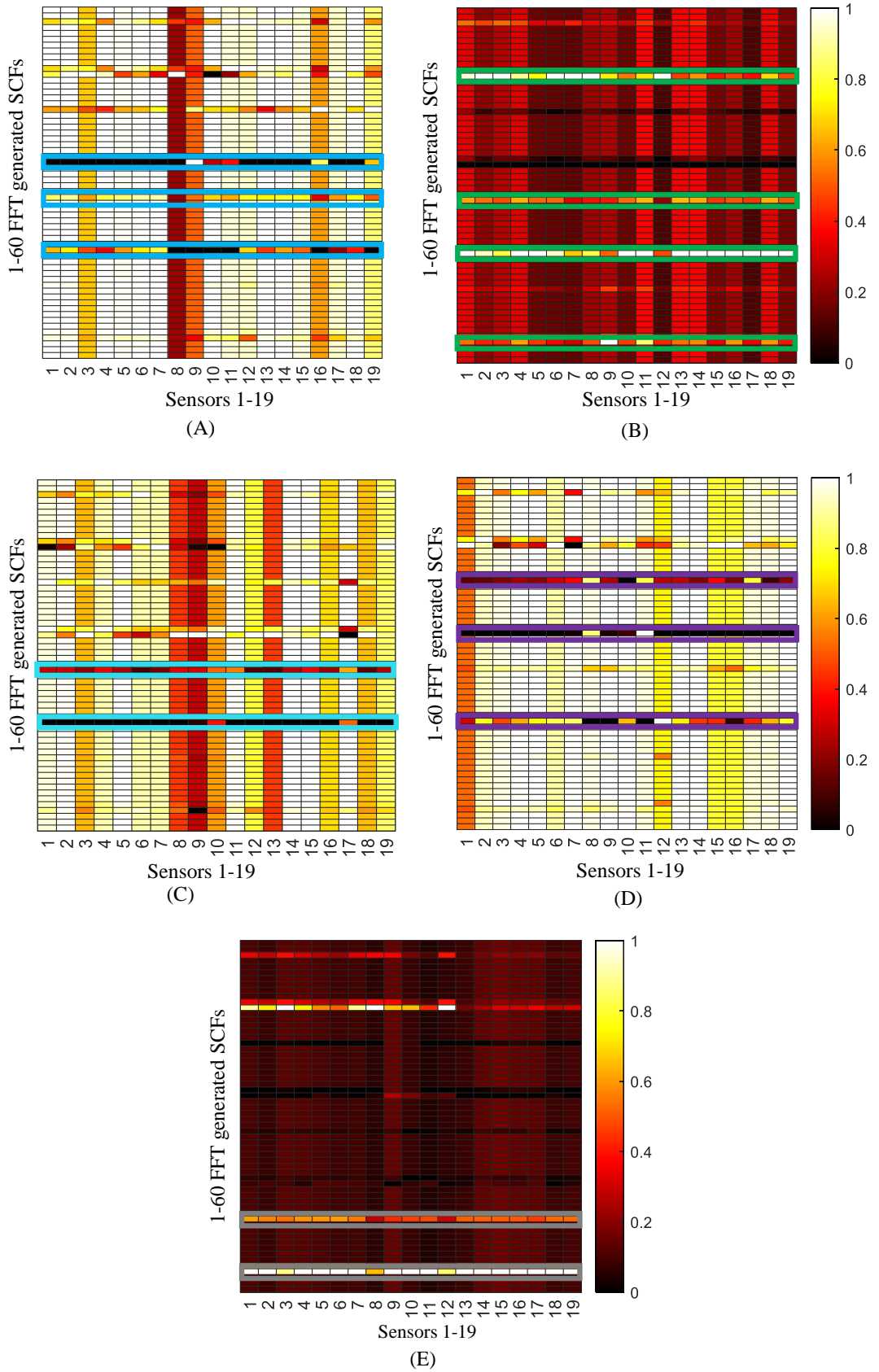


Figure 6.2: Uniqueness of imaginations in image processing technique (A) imagination 1, (B) imagination 2, (C) imagination 3, (D) imagination 4, (E) imagination 5.

SCFs numbered 27, 33, and 42, representing part 2 power, and part 3 variance and power of the FFT respectively, are found to be the most consistent and significant for imagination 1.

Imagination 2: The heatmap shows that SCFs numbered 3, 12, 18, 27, 33, 42, and 57 form distinct combinations compared to other SCFs. Although not all are very significant, their effect is consistent across all 19 sensors, impacting the entire head. SCFs numbered 12, 33, 42, and 57 are strongly visible in the heatmap. These SCFs correspond to FFT part 1 power, part 3 variance, power, and FFT part 4 power. This combination differs from imagination 1.

Imagination 3: The heatmap shows that SCFs numbered 3, 12, 18, 27, 33, 42, and 57 form distinct combinations compared to other SCFs. In this case, most SCFs have less significance except for 33 and 42, which represent frequency domain part 3 variance and power. Thus, the uniqueness of this imagination is mostly present in part 3 of the FFT output.

Imagination 4: The heatmap shows that SCFs numbered 3, 12, 18, 27, 33, and 42 form distinct combinations compared to other SCFs. As in previous imaginations, all SCFs exhibit different levels of sensitivity variation. SCFs numbered 18, 27, and 42 are emphasised for identifying the uniqueness of this imagination. These SCFs correspond to variance, and power from FFT part 2 and power from FFT part 3.

Imagination 5: The heatmap shows that SCFs numbered 3, 12, 18, 27, 33, 42, 48, and 57 form distinct combinations compared to other SCFs. Few SCFs such as 3, 12 etc are almost significant between sensors 1 and 12, suggesting that the frontal and central areas are valuable. Among them, power (SCF 12) has better representation across sensors. However, SCFs numbered 48 and 57 significantly influence the entire heatmap. These values are extracted from FFT part 4 with function variance, and power, differing notably from the previous imaginations.

The above observations clearly indicate that each imagination possesses distinct attributes across the 19 sensors. Previous analyses identified slight similarities between imaginations 1, 3, and 4 in the frequency domain. Employing the DWT technique introduced variations in the uniqueness of these imaginations. The variances in different parts of the FFT and DWT created distinctions between them. From all the functional characteristics, the analysis reveals that both variance and power are crucial for the uniqueness of imaginations. Furthermore, using more partitions of the FFT demonstrates that increased partitioning influences the characterisation of imaginations. This suggests that previous similarities between imaginations 1, 3, and 4 can be more distinguishable using additional partitions

and/or statistical functions. Another finding is that some statistical functions have minimal impact on imagination characteristics, implying that they can be ignored or removed from the ASMs. However, certain functions should be retained to support the creation of various sensitivity combinations that contribute to the uniqueness of the imagination.

#### 6.4 Performance of Classifier for Combined Analysis

In this study, CNN is employed to explore all possible combinations of three subject groups and three sets of imaginations. Figure 6.3 depicts the verification design, which incorporates the groups as outlined in the group-based analysis and divides the dataset into three sets based on imaginations.

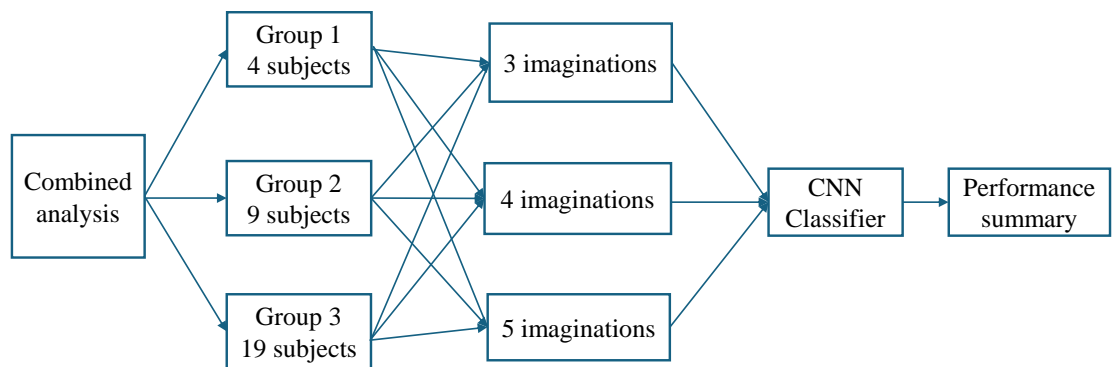


Figure 6.3: The design of verification steps for combined analysis.

This analysis focuses exclusively on frequency domain SCFs derived from FFT, applying 15 statistical functions over 10 divisions. Consequently, the dataset is segmented according to the bespoke analysis approach. Heatmap images of the produced ASMs are fed into the CNN to classify imaginations across all aspects of the groups and imaginations. For verification using ASPs and image processing technique is unable to execute bespoke analysis, since 2 trials are not sufficient to run CNN. Thus, groups are evaluated as per previous design in Table 5.2, where 3 increasing number of groups are created based on the resemblance of the imaginations between groups. So, Group 1, 2 and 3 consist of 4 subjects, 9 subjects and all 19 subjects. ASMs with selected features which are illustrated with heatmaps in previous section, these heatmap images are produced for all subjects to feed into deep learning method, CNN. The hyperparameters are presented in Chapter 3, Table 3.4. All images are used with 256x256 pixel format including RGB format. For better representation the colour code sensitivity is set between 0 and 1. Three sets of imaginations are prepared for classification, they are 3, 4 and 5 imaginations. Classification of two imaginations is

excluded from this experiment, as the analysis employed only one frequency domain method, and three imaginations have already been recognised with 100% accuracy using FFT-generated SCFs, as studied in Chapter 4. The performance logically ensures that 2 imaginations through frequency domain SCFs will be recognised with high accuracy.

Previous ANN models, such as FFNN and LVQ, were executed 100 times in Chapter 4 and 5 to assess the stability of their performance. However, due to the significant computational demands associated with image processing, the CNN model could not be repeated 100 times. The system permits a maximum of 60 runs; therefore, in this study, CNN model is run for 60 times for each combination and average accuracy is measured along with best result. The optimal and average performances are evaluated based on classification accuracy, as specified in Equation (3.2) of Chapter 3. Figure 6.4 presents the maximum accuracy achievable for group-based analysis using ASPS and image processing technique.

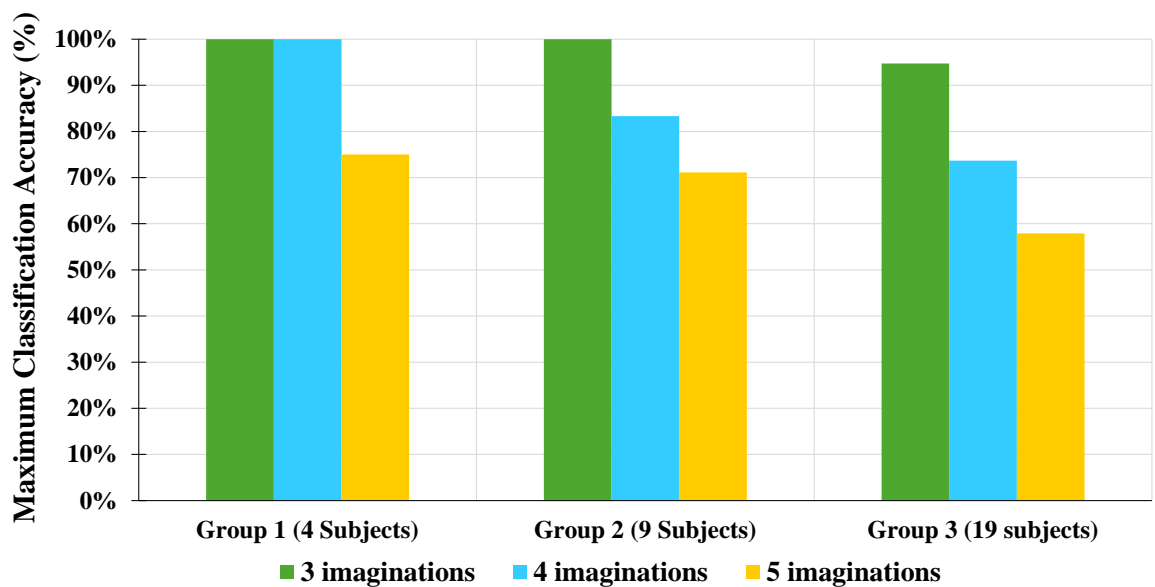


Figure 6.4: Maximum classification accuracy of group-based analysis using ASPS and image processing technique.

The results of the imagination recognition experiment across three groups of subjects demonstrate varying levels of accuracy depending on the number of imaginations and the group size. For Group 1, consisting of 4 subjects, the recognition accuracy is 100% for both 3 and 4 imaginations, while it decreased to 75% for 5 imaginations. This indicates a high level of consistency and reliability in recognising three and four imaginations although a noticeable drop in performance is observed as the complexity increases to five imaginations. In Group 2, which included 9 subjects, the recognition accuracy is maintained at 100% for

3 imaginations. However, there is a decline to 83.33% accuracy when recognising 4 imaginations, and a further reduction to 71.11% accuracy for 5 imaginations. This suggests that as the number of imaginations increases, the model's ability to accurately distinguish between them diminishes. Group 3, the largest group with 19 subjects, showed a recognition accuracy of 94.73% for 3 imaginations. The accuracy decreased to 73.68% for 4 imaginations and further to 57.89% for 5 imaginations. This trend highlights a significant challenge in maintaining high accuracy levels as the number of imaginations and the cohort size increase.

The CNN effectively achieved recognition of 3 imaginations across all three groups, similar to the performance of the FFNN in previous experiments. Notably, the recognition of 4 imaginations for Group 1 also achieved 100% accuracy, which is highly promising. Furthermore, Groups 2 and 3 demonstrated accuracy in a comparable range (73-83%) for the classification of 4 imaginations. The classification of 5 imaginations for 9 subjects is accomplished with over 70% accuracy. Overall, the CNN performs adequately, especially for scenarios with up to 4 imaginations, although there is room for improvement in 5 imaginations. The training time of the CNN model is comparatively faster than that of LVQ and FFNN. However, preparing images in the appropriate format requires slightly more time and storage space compared to ANNs. The average performances of 60 runs for different groups and numbers of imaginations are summarised in Figure 6.5.

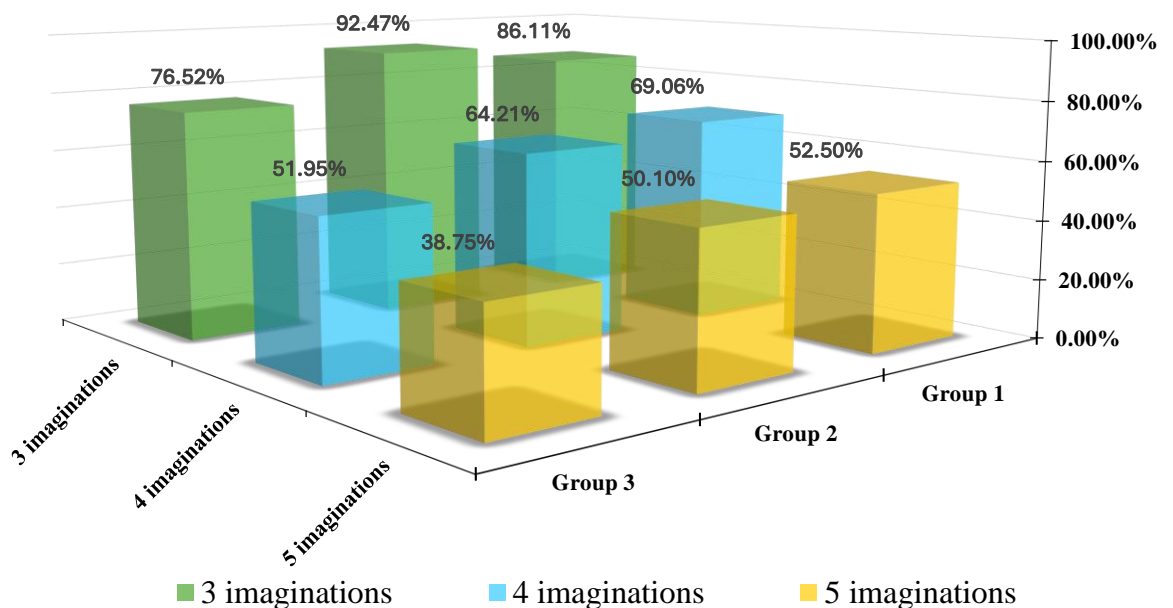


Figure 6.5: Average performance of group-based analysis using ASPs and image processing technique.

The figure indicates that the classification of 3 imaginations across all three groups is comparatively consistent. Conversely, the classification of 5 imaginations for 19 subjects demonstrates the lowest performance throughout.

Finally, although the performance of the CNN model for the three group sizes is lower than that reported in Chapter 5, the results of this study remain significant. The observed decline in performance may be attributed to the model's configuration, particularly the use of FFT with a relatively high number of 10 partitions. It is likely that reducing the number of partitions and incorporating DWT could lead to improved performance. Additionally, while using a greater number of statistical functions (15) does not appear to enhance performance, incorporating the power feature—due to its significant contribution to the uniqueness in imaginations—could improve results. Therefore, adding the power feature to the set of features used in previous chapters would be beneficial. Further research into these adjustments is recommended, as they may address the performance decline and enhance the model's overall efficacy. Moreover, additional experimentation with the CNN, including modifications to the number of layers and other specifications, is advised to explore potential enhancements in performance.

### **6.5 Summary:**

The design, analysis, verification results, and discussion of the group-wise image processing experimental setup are comprehensively detailed in this chapter. The experiment is conducted to implement the ASPS approach with a diverse range of SCFs across various groups of subjects. Features are extracted from frequency domain analysis using 10 partitions. The extracted and selected features, identified through the ASPS approach, are verified using a deep learning algorithm, specifically CNN. This image processing technique employs supervised learning to understand feature characteristics from images and classify the imaginations accordingly. Two trials of imagination data are used in the CNN: one for training and the other for testing. Three cohort sizes are tested.

For the deep learning model, hardware specifications sometimes limit the number of runs possible. For instance, the proposed CNN model could not be run more than 60 times due to the high computational demand of image processing. The results of various CNN architectures for different groups of imaginations are summarised in Section 6.4. The ASPS approach, incorporating only FFT-generated SCFs, has the capability to recognise 5 imaginations through image processing, achieving more than 70% accuracy for up to 9

subjects. For bespoke experiments, the FFNN is sufficient to achieve the best results. However, increasing the number of subjects in this experiment slows down the ANN process. Nonetheless, the CNN is also an adequate classifier for the specified imaginations. In the group-based experiment, the CNN is generally faster than the LVQ and FFNN. Further research and experimentation would focus on reducing the number of partitions and incorporating DWT, as well as exploring modifications to the number of CNN layers and other model specifications.

The ASPS approach has proven successful in brain signal processing; however, the analysis was conducted using 19 sensors and two trials of data. The focus of the next chapter is on sensor optimisation and the evaluation of the proposed model using a new and larger EEG signal dataset. Additionally, it compares the performance of the models discussed in Chapters Four to Six with the newly obtained results.

## Chapter 7: Sensor Optimisation and Validation

### 7.1 Introduction

This chapter delves into the optimisation and validation of sensors, focusing on brain signals collected during the second phase of signal acquisition. In Section 7.2 and in Section 7.3, detailed analyses of sensor optimisation and cross-tabulation analysis are provided, respectively. Drawing from these analyses, in Section 7.4, various groupings are formulated to further refine the approach. In Section 7.5, the validation of these groupings is conducted, while in Section 7.6, a comprehensive summary of the results obtained is presented. The chapter presents these results through a variety of analytical approaches, including bespoke, group-wise, and combined analyses. Additionally, the findings are compared with those reported in Chapters 4 and 5 to assess the relative effectiveness of the methods employed.

### 7.2 Analysis of Sensor Optimisation

Based on the methodology design outlined in Section 3.3.2 of Chapter 3, the ranking and assignment of rating points across 19 sensors are carried out for each of the 10 subjects, taking into account various imagination datasets. The ranking of 19 sensors based on average rating points for all subjects with 5, 4, 3 and 2 imaginations is listed down in Table 7.1.

Table 7.1: Summarised rating point table.

Sensor# (Ch)	Sensor name	5 imaginations	4 imaginations	3 imaginations	2 imaginations	Sensor rank
1	Fp1	17	18	16	2	17
2	Fp2	7	14	13	7	9
3	F7	6	19	18	17	19
4	F3	14	14	5	1	7
5	Fz	2	1	2	6	2
6	F4	12	7	8	4	5
7	F8	17	11	18	12	18
8	T3	12	8	11	9	8
9	C3	9	16	16	9	14
10	Cz	5	3	6	4	4
11	C4	17	6	9	19	15

Table 7.1: Summarised rating point table (continued from previous page).

Sensor# (Ch)	Sensor name	5 imaginings	4 imaginings	3 imaginings	2 imaginings	Sensor rank
12	T4	7	13	6	18	11
13	T5	9	16	3	15	10
14	P3	1	1	1	7	1
15	Pz	3	4	11	14	6
16	P4	9	12	15	15	15
17	T6	16	10	10	9	12
18	O1	4	4	4	3	3
19	O2	14	9	13	12	13

The sensor performance with frequent top 5 rating is highlighted with yellow. Considering the frequency of 1-5 and overall rating point of rest of the columns six sensors are selected which are highlighted with green.

The methodology outlined in Chapter 3 includes the selection of the tentative top 5 sensors. However, during the selection process detailed in Table 7.1, the top 4 sensors (Fz, Cz, P3, and O1) are readily identified. The selection of the 5th sensor presents a tie between F3 and Pz, as both sensors exhibit similar frequency characteristics. Specifically, F3 performs well for recognising 2 and 3 imaginings, while Pz is more effective for recognising 4 and 5 imaginings. Consequently, both F3 and Pz are included in the analysis, resulting in a total of 6 sensors being ranked among the top.

It is also notable in Table 7.1 that sensor 6 has been ignored in this selection though its overall ranking is 5. The reason is that the individual performance of 5, 4, 3 and 2 imaginings for sensor 6 has less significance. Rather sensor 15 and sensor 4 have better ranking frequency for different number of imaginings performance.

### 7.3 Cross-tabulation Analysis

In Table 7.1, it is found that selected 6 sensors are 14 (P3), 5 (Fz), 18(O1), 10 (Cz), 15 (Pz) and 4 (F3). Sensors are selected based on the frequency of obtaining top ranked from 5, 4, 3 and 2 imaginings performance. To investigate more details various number of imaginings and selected sensors' performances for each subject's is gathered in Table 7.2.

Table 7.2: Cross-tabulation between subjects and sensors.

Green: Outstanding  
 Amber: Satisfactory  
 Yellow: Fair  
 Red: Inadequate

		Sensor number					
Imaginations	Subject	14	5	18	10	4	15
5 imaginations	S1	Green	Green	Amber	Amber	Amber	Green
	S2	Yellow	Green	Red	Green	Amber	Green
	S3	Amber	Green	Amber	Green	Amber	Amber
	S4	Yellow	Green	Yellow	Yellow	Green	Green
	S5	Green	Red	Yellow	Red	Red	Green
	S6	Green	Yellow	Green	Red	Green	Yellow
	S7	Red	Green	Yellow	Yellow	Amber	Red
	S8	Red	Green	Amber	Green	Green	Red
	S9	Yellow	Amber	Green	Green	Yellow	Green
	S10	Green	Amber	Yellow	Red	Yellow	Green
4 imaginations	S1	Green	Amber	Green	Amber	Amber	Green
	S2	Yellow	Green	Red	Green	Amber	Green
	S3	Green	Amber	Amber	Amber	Amber	Red
	S4	Yellow	Green	Yellow	Green	Yellow	Green
	S5	Green	Red	Green	Red	Red	Green
	S6	Green	Green	Green	Red	Green	Yellow
	S7	Red	Green	Yellow	Green	Amber	Red
	S8	Red	Yellow	Green	Green	Yellow	Red
	S9	Green	Green	Green	Yellow	Green	Green
	S10	Amber	Green	Yellow	Red	Yellow	Yellow
3 imaginations	S1	Green	Yellow	Green	Green	Yellow	Yellow
	S2	Green	Green	Red	Amber	Green	Yellow
	S3	Green	Green	Green	Green	Yellow	Green
	S4	Amber	Yellow	Yellow	Green	Green	Yellow
	S5	Green	Red	Green	Red	Red	Green
	S6	Green	Yellow	Amber	Red	Green	Yellow
	S7	Red	Green	Yellow	Amber	Green	Red
	S8	Red	Yellow	Yellow	Green	Yellow	Red
	S9	Green	Green	Green	Yellow	Green	Amber
	S10	Amber	Green	Yellow	Green	Green	Yellow
2 imaginations	S1	Green	Green	Green	Green	Green	Yellow
	S2	Yellow	Yellow	Red	Green	Green	Yellow
	S3	Green	Green	Green	Green	Green	Yellow
	S4	Yellow	Green	Green	Yellow	Green	Yellow
	S5	Green	Green	Green	Red	Green	Yellow
	S6	Yellow	Yellow	Yellow	Red	Green	Green
	S7	Green	Amber	Yellow	Yellow	Yellow	Green
	S8	Red	Green	Green	Green	Green	Red
	S9	Yellow	Amber	Amber	Green	Amber	Green
	S10	Yellow	Amber	Green	Yellow	Amber	Amber

Four colours are used: green, amber, yellow and red to indicate the performance category as outstanding, satisfactory, fair and inadequate respectively. To obtain the top-ranking sensors, the rating has been done through a comparative study. Therefore, there is no such threshold value taken to measure the performance of the sensor. Rather for certain number of imaginations the performance of 19 sensors is categorised which are found differently for different subjects. The green colour (outstanding) is applied to the top 5 performances. The satisfactory (ember colour) is taken above -average, often demonstrates significant competence closer to top 5 performances. The yellow cells are around average value in the performance range. Inadequate or red colour is found very poor functioning in imagination recognition. Sensor 4 (F3), 5 (Fz) and 10 (Cz) are located in brain frontal lobe. The brain cortex around Cz (sensor 10) covers sensory and motor functions. Frontal lobe overall operates higher cognitive functions such as attention, planning, emotionality, mental processes and so on (Di Ieva, 2011). Sensor 14 (P3) and 15 (Pz) are located in parietal lobe, they deal the human activities of perception and differentiation (Abhang, Gawali and Mehrotra, 2016). Sensor 18 (O1) is in occipital lobe which primarily works in visual related functions. However, functional activity increases in sensory thalamus and somatosensory areas which covers motor activity, sensory motor association functions, emotions, memory etc (Wei *et al.*, 2018).

#### 7.4 Group Creation

In this study, for any subject at least three sensors are found well performing to recognise different set of imaginations. The performance deviation of the sensor's vs subject in the table for 5, 4, 3, and 2 imaginations shows moderate consistency in many cases though it is reasonable to relate with the localisation of the brain function for different set of imaginations and it may vary subject to subject (McFarland *et al.*, 2008) . Based on the consistency of stable sensor performance there are three groups are made as Group G1, G2 and G3. Table 7.3 is the summary of the groups for the number of subject's vs sensor with similar characteristics.

Table 7.3: Group formation based on sensor optimisation.

Group name	Subject number	Sensor#	Sensor name
G1	S1, S3, S4, S6, S9, S10	Ch 5, 14, 18	Fz, P3, O1
G2	S2, S7, S8	Ch 4, 5, 10	F3, Fz, Cz
G3	S5	Ch 14, 15, 18	P3, Pz, O1

Corresponding sensor names are included in the table. This grouping is done by taking three sensors which are found either outstanding (green) or satisfactory (Amber) for certain subjects in most of the imagination’s recognition. In some cases, fair (yellow) performances are taken into account while the same sensor is found outstanding for a subject in other set of imaginations recognition. However, inadequate (red) sensors are carefully removed from the group where subjects have consistent poor performances. To select or reject the sensors the performance of individual sensor in terms of 5 and 4 imaginations are prioritised since this project aims to convert the signals into control commands. Therefore, higher number of imaginations would be transformed into that number of control commands. Total 6 subjects fall in group ‘G1’ where selected sensors are Cz, P3 and O1. 3 subjects are categorised into group ‘G2’ where selected sensors are F3, Fz and Cz. Only one subject has a different sensor performance report where P4, Pz and O1 are functioning adequately. Therefore, this is named as group ‘G3’.

### 7.5 Validation

To assess the collective performance of the selected sensors, evaluations are designed based on the framework outlined in Table 7.3. The validation steps are illustrated in Figure 7.1.

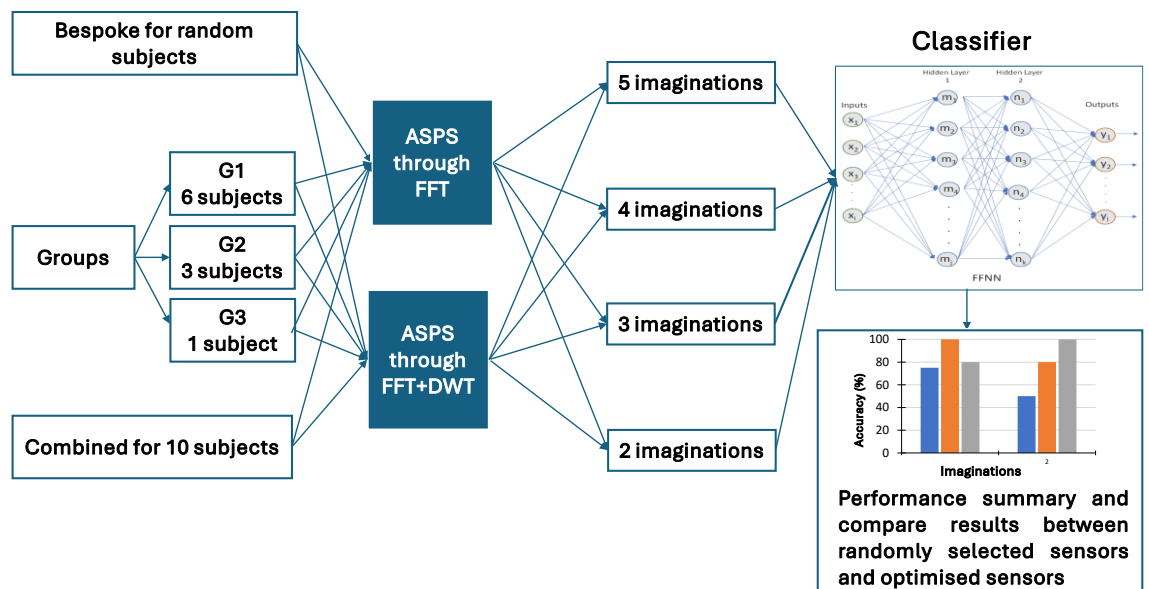


Figure 7.1: Validation process of imagination recognition using optimised sensors.

The method developed for recognising imaginations, using the ASPS feature extraction and selection approach detailed in Chapter 3, is applied with the optimised sensors to evaluate performance. This comprehensive validation process incorporates the selected sensors and integrates the majority of previously discussed analytical methods. A single-layer FFNN

model is utilised to classify all sets of imaginations, with each model being executed 25 times. Performance metrics are recorded and presented in subsequent sections. The performance of the optimised sensors is then compared to the results obtained from randomly selected sensors in Chapters 4 and 5, which were based on the initial phase of collected data. Figure 7.1 shows all possible combinations for verification in terms of subjects (bespoke, groups, combined), ASPS approaches (using only FFT or both FFT and DWT generated  $\Delta$  SCFs), and imaginations (ranging from 2 to 5). These combinations are applied based on the second phase of collected brain signal data.

## **7.6 Result and Discussion**

This discussion is primarily divided into two ASPS analyses that have described in Chapter 4 and 5. The methodology in Chapter 4 has been applied on bespoke experiment for random subjects and random 3 sensors from 1<sup>st</sup> phase of EEG signal data. In Chapter 5, both the frequency domain and time-frequency domain are incorporated in the ASPS approach to improve accuracy with an increasing number of imaginations, and group-based evaluations have been recorded. Both studies are to apply in 2<sup>nd</sup> phase data to investigate the overall performances. The first study is ASPS feature extraction through only frequency domain and the result of 2<sup>nd</sup> phase data is discussed in the Section 7.6.1. The second part experimental result and discussion covers features extraction using both FFT and DWT in ASPS approach. A thorough verification of bespoke, group-wise, and combined performances is presented in Section 7.6.2.

The optimised sensors data are used for 5, 4, 3 and 2 imaginations recognition. 75% data are used for training and 25% for testing in all cases, FFNN single layer is employed as classifier since single layer-based FFNN was obtained adequate classifier in imagination recognition. The performance is measure with highest classification accuracy as per in Equation (3.2) of Chapter 3. The ANN is run for 25 times and average classification accuracy is recorded. In previous chapters the average classification was recorded for 100 runs which consumed huge time. To optimise time, it is investigated that how many times the model need to be run that does not significantly affect the highest and average accuracy comparing 100 runs. It is found that at least 25 runs attain comparable result in terms of maximum, average and standard deviation of 100 times model run.

### 7.6.1 ASPS through FFT

The methodology in Chapter 4 involves implementing bespoke experiment on the 2<sup>nd</sup> phase data. The ASPS feature extraction emphasises 4-part FFT generated  $\Delta$  SCFs in the ASM. The following two subsections include the result and discussion for bespoke, group-wise and combined experiment respectively.

#### 7.6.1.1 Bespoke performance for random subjects using ASPS through FFT

Three subjects are chosen in this step. 2<sup>nd</sup> phase data was collected for 10 subjects. Among them this research collects 12 trials from only one subject to verify the performance of bespoke design analysis with more trials. Rest of the subjects are participated for 5 trials. The subject with 12 trials is taken intentionally and other two subjects are randomly selected. Following the methodology in Chapter 4, Subject number 3, 5 and 9 are evaluated. In Table 7.4 the bespoke results using ASPS with only FFT and compare the bespoke results between 1<sup>st</sup> and 2<sup>nd</sup> phase data are demonstrated.

Table 7.4: Performance summary of bespoke result using ASPS through FFT.

No. of imaginations Recognition	Bespoke result									
	2nd phase data						1st phase data			
	S3: 12 Trials		S9: 5 trials		S5: 5 trials		S1: 2 trials		S2: 2 trials	
	Maximum	Average	Maximum	Average	Maximum	Average	Maximum	Average	Maximum	Average
5 imaginations	86.7%	61.6%	90.0%	54.0%	80.0%	52.8%	80.0%	43.2%	80.0%	39.2%
4 imaginations	83.3%	70.3%	100.0%	74.0%	100.0%	74.5%	100.0%	56.8%	100.0%	46.0%
3 imaginations	100.0%	96.0%	100.0%	100.0%	100.0%	94.0%	100.0%	72.0%	100.0%	81.3%
2 imaginations	100.0%	100.0%	100.0%	100.0%	100.0%	100.0%	100.0%	100.0%	100.0%	100.0%

It is noticeable that 2<sup>nd</sup> phase results with selected optimised sensors obtained higher accuracy than 1<sup>st</sup> phase result with randomly selected sensors. The performance of various set of imaginations are subject to the participant, however, highest accuracy is more than 80% in all cases. Table shows that both 2 and 3 imaginations are all through recognised with 100% for all subjects. Except one subject, 4 imaginations are recognisable with 100% accuracy. In the 1<sup>st</sup> phase of data analysis, 5 imaginations with 2 trials achieved 80% accuracy. However, in the 2<sup>nd</sup> phase, where at least 5 trials are considered, the accuracy improved to 90%. Average performance values are overall much higher than 1<sup>st</sup> phase data analysis. Same methodology applied in both phase data, the difference is subject and the number of trials. More trials would be able to increase the performance level since more data are used to train the ANN model; nevertheless, two subjects with 5 trials have higher (90%) and lower performance (80%) than the subject with 12 trials (86.7%). Average classification performances are observed increasing for 5, 4 and 3 imaginations.

### 7.6.1.2 Group-wise results and combined performance using ASPS through FFT

In Section 7.4 and Table 7.3, three group-wise evaluations have been conducted for G1, G2 and G3. Additionally, a combined performance assessment has been measured for all 10 subjects. All best and average accuracies are listed down in Table 7.5.

Table 7.5: Performance summary of group-wise result using ASPS through FFT.

No. of imaginations Recognition	Group-wise result						Combined 2nd phase data	
	2nd phase data							
	G1: S1,S3,S4,S6,S9,S10		G2: S2,S7,S8		G3: S5			
	Maximum	Average	Maximum	Average	Maximum	Average	Maximum	Average
5 imaginations	66.2%	57.7%	53.3%	41.1%	80.0%	52.8%	60.9%	53.8%
4 imaginations	82.7%	71.2%	70.8%	50.8%	100.0%	74.5%	75.0%	67.0%
3 imaginations	100.0%	92.8%	88.9%	67.6%	100.0%	94.0%	95.2%	87.3%
2 imaginations	96.2%	94.0%	91.7%	86.7%	100.0%	100.0%	97.5%	94.8%

The feature extraction and selection are carried out by ASPS approach in Chapter 4. This overall result is comparatively lower than bespoke performance in Section 7.6.1.1. It is also reflected in Table 7.5 where group 3 (G3) has one subject while G1 and G2 have six and three subjects respectively. Group-wise and combined performances are obtained reasonably for 4, 3 and 2 imaginations. Improving overall performances of 5 and 4 imaginations yet to be investigated with modified methodology.

### 7.6.2 ASPS through FFT and DWT

The analysis applied in Chapter 5 has been conducted on 2<sup>nd</sup> phase data. The result of 5 imaginations recognition of the analysis attained promising result (group results in Chapter 5) comparing the bespoke design analysis (bespoke result in Chapter 4). In this part of research, the newly created groups based on the selected optimised sensor from 2<sup>nd</sup> phase of recorded EEG signal data. All 5, 4, 3 and 2 imaginations recognition for bespoke performances are discussed in Section 7.6.2.1 and group-wise (G1, G2 and G3) and combined in Section 7.6.2.2.

#### 7.6.2.1 Bespoke performance for random subjects using ASPS through FFT and DWT

Same three subjects (S3, S5 and S9) are considered to investigate the performance variation of using ASPS through FFT and DWT. Table 7.6 summarises all the bespoke performances with highest and average accuracy. All sets of imaginations are recognisable with 100% accuracy in this manner.

Table 7.6: Performance summary of bespoke result using ASPS through FFT and DWT.

No. of imaginations Recognition	Bespoke result					
	2nd phase data					
	S3: 12 Trials		S9: 5 trials		S5: 5 trials	
	Maximum	Average	Maximum	Average	Maximum	Average
5 imaginations	100.0%	82.4%	100.0%	85.2%	100.0%	84.4%
4 imaginations	100.0%	96.7%	100.0%	98.0%	100.0%	89.5%
3 imaginations	100.0%	96.0%	100.0%	100.0%	100.0%	94.0%
2 imaginations	100.0%	100.0%	100.0%	100.0%	100.0%	100.0%

The best correctness between subject with multiple trials vs any number of imaginations have converged eventually. The average performance values are also greater than previous all average performances. The dispersion of the average performance of three different subjects as well as set of imaginations is relatively very close which indicates tightly clustered accomplishment. The average performance of 1<sup>st</sup> phase Bespoke analysis (discussed in Chapter 4), 2<sup>nd</sup> phase bespoke analysis with only FFT in Section 7.6.1.1 and 2<sup>nd</sup> phase bespoke analysis with both FFT and DWT are illustrated in Figure 7.2.

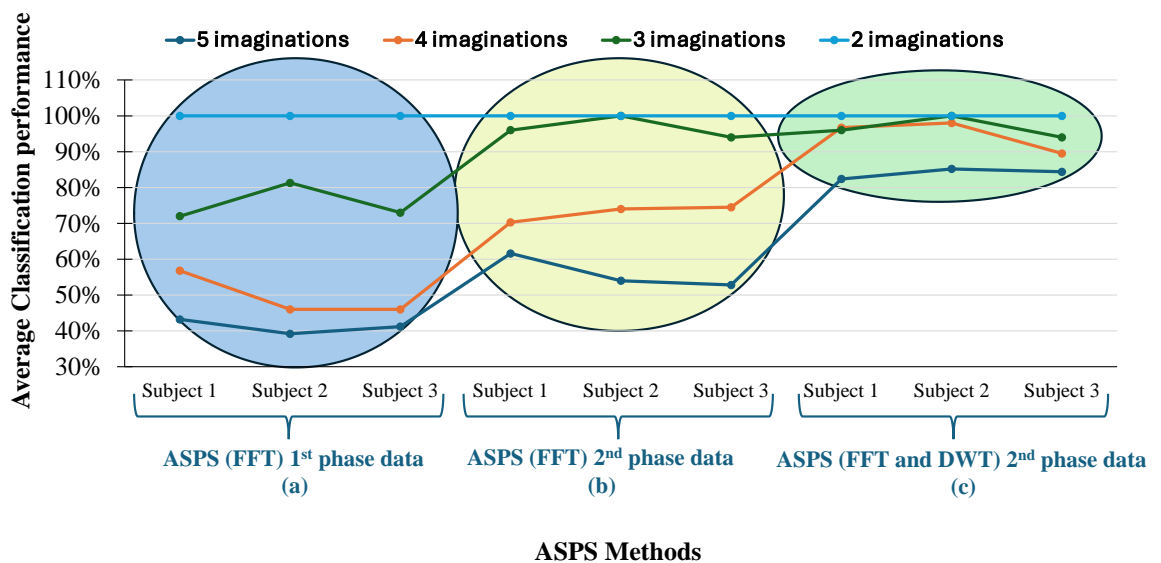


Figure 7.2: Performance comparison of bespoke analysis between two phases data.

The plot delineates the improvement in performance while adding the number of trials and/or domains such as FFT, DWT. In terms of 4 and 5 imaginations recognition the overall achievement is significant. For example, subject 2 from 2<sup>nd</sup> phase data attained up to 85.2% which has an increase of 31.2 percentage points in 5 imaginations recognition and 24 percentage points increment in 4 imaginations. The achievement rates are nearly doubling

or more for subjects when compared to initial success rate. Overall, the improvement of all subjects shows a remarkable increase in achievement rates in changing some aspect of methodology. The main properties of the analysis for these three cases as below:

- a) The 1<sup>st</sup> phase of collected EEG data and the initial analysis had two trials from the subject. 3 random sensors location (Fp2, Cz, O1) were selected for EEG signal analysis. ASPS approach employed time-domain (raw) and frequency domain (FFT) generated SCFs.
- b) The 2<sup>nd</sup> phase data of EEG data and the analysis carried out based on minimum 5 trials and maximum 12 trials. Three optimised sensors are selected subject to the participant. ASPS approach employed time-domain and frequency domain generated SCFs.
- c) Same EEG data as (b). ASPS approach included both FFT and DWT. Among 5 imaginations, three imaginations are taken by FFT, and two imaginations are taken by DWT technique.

Figure 7.3 illustrates the performance trend of bespoke analysis across the data and methods of the two phases.

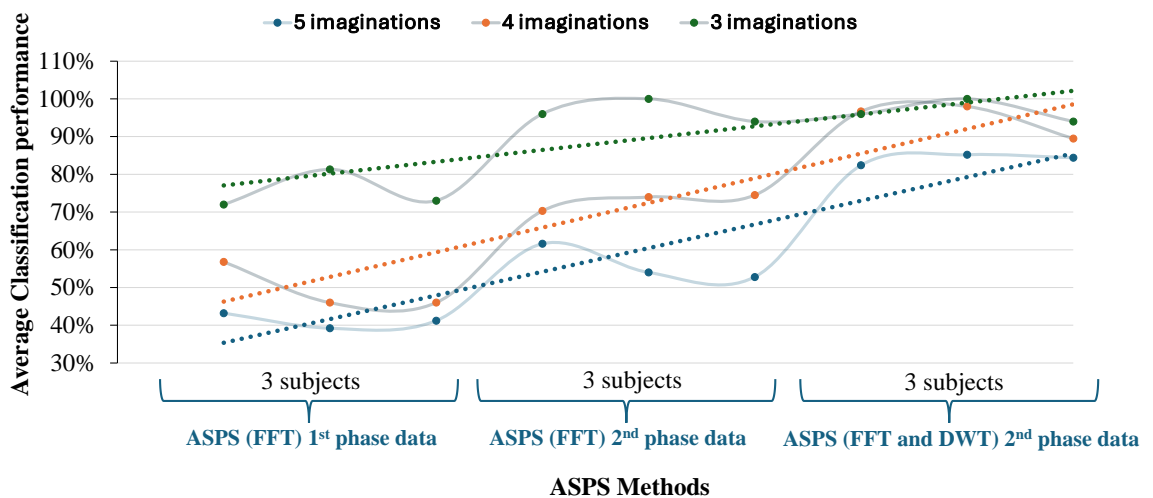


Figure 7.3: The performance trend of bespoke analysis between two phases data and methods.

It is noteworthy that, there is an upward trend in Figure 7.3 while changing some aspect of the methodology and size of data. The indication clearly imply that the approach (c) is more capable in producing consistent performance in order to recognise higher number of imaginations (3, 4 or 5).

7.6.2.2 Group-wise results and combined performance using ASPS through FFT and DWT:

In Section 7.4, groups have been created into three categories of subjects with selected sensors. ASPS approach including frequency and time-frequency domain generated  $\Delta$  SCFs are applied into three individual groups and combining 10 subjects together to see the performance deviation. Table 7.7 summarises the group-wise performance using ASPS through FFT and DWT, presenting both the highest and average accuracy.

Table 7.7: Performance summary of group-wise result using ASPS through FFT and DWT.

No. of imaginations Recognition	Group-wise result						Combined 2nd phase data	
	2nd phase data							
	G1: S1,S3,S4,S6,S9,S10		G2: S2, S7, S8		G3: S5			
	Maximum	Average	Maximum	Average	Maximum	Average	Maximum	Average
5 imaginations	81.5%	70.8%	73.3%	60.7%	100.0%	84.4%	78.1%	69.1%
4 imaginations	98.1%	93.3%	91.7%	78.3%	100.0%	89.5%	95.2%	89.1%
3 imagination	100.0%	92.8%	88.9%	67.6%	100.0%	94.0%	95.2%	87.3%
2 imaginations	100.0%	100.0%	100.0%	100.0%	100.0%	100.0%	100.0%	100.0%

The performance of Group G1 shows excellent and steady performance for different number of imaginations. Starting at 81.5% for five imaginations, Group G1 reaches a perfect performance score of 100% when the tasks are reduced to three and two. The average performances for 5, 4, 3 and 2 imaginations are pretty good and has similar trend as best performances. In four imaginations recognition, the performance gap narrows, with Group G1 outperforming Group G2 by 6.4%. Both groups show improvement, but Group G1 demonstrates a more substantial increase. The performance of 3 imaginations recognition between G1 and G2 is closer and show high accuracy. Group G3, represented by a single subject, shows consistently very high performance across all sets of imaginations.

The combined performance of 10 subjects EEG data indicates a clear trend of improvement as the number of imaginations decreases. With five imaginations, the highest performance recorded is 78.1%, and the average performance is 69.1%. There is a substantial increase in both highest and average performance scores in 4 imagination recognition, with the highest at 95.2% and the average at 89.1%. Further reduction to three imaginations shows a slight decrease in the highest performance score to 86.9%, but the average performance increases to 93.7%. This suggests that while individual peak performance may vary, overall group performance stabilizes and improves. Finally, with two imaginations, both the highest and average performance scores reach 100%, indicating perfect performance across all subjects.

This group analysis clearly outperforms the group analysis presented in Section 7.6.2.2 and Table 7.5. Same subjects and same size of dataset are used in both analyses, only adding DWT along with FFT in ASPS approach gives a sharp increase in performance. This comparison absolutely helps to distinguish the analysis approach. Same approach was followed in Chapter 5 where the result shows combined performance of 19 subjects attained 78.95% accuracy. It is notable that 2 trials were processed for 19 subjects which gathers in total 38 trials from 1<sup>st</sup> phase of collected data. In second phase this combined performance has carried out on 10 subjects, 9 subjects with 5 trials and 1 subject with 12 trials that incorporates total 57 trials. The 2<sup>nd</sup> phase data achieves 78.1% best accuracy for 57 trials that apparently looks comparable to the 1<sup>st</sup> phase 38 trials. Moreover, considering the total number of trials, the average classification performance has been increased in 2<sup>nd</sup> phase combined experiment.

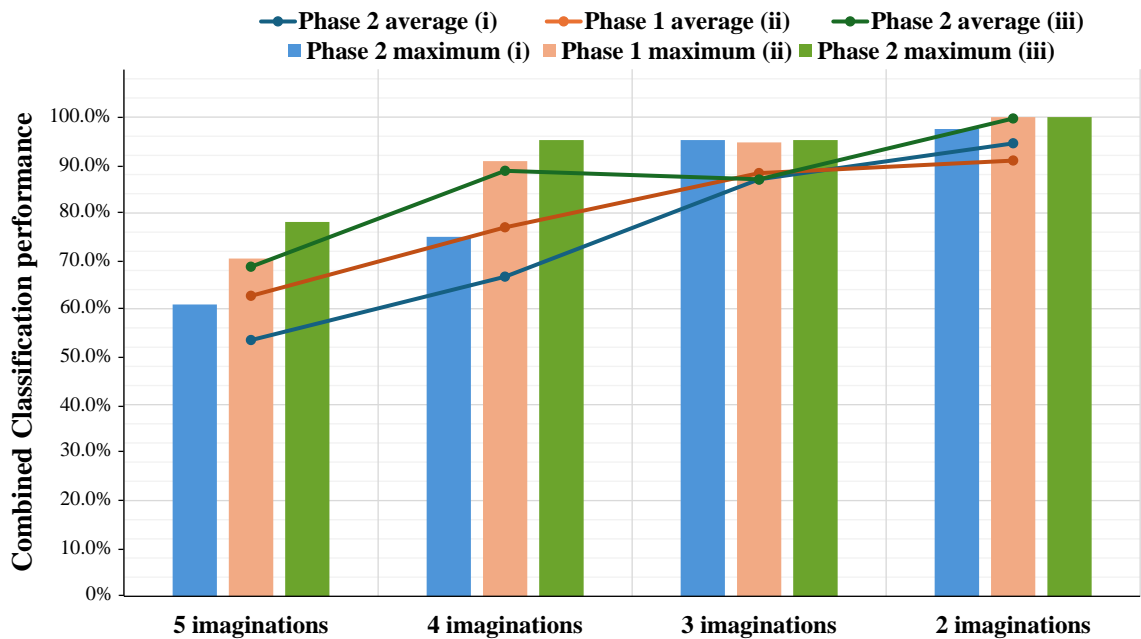


Figure 7.4: Performance comparison of combined analysis between two phases data.

Figure 7.4 illustrates a comparative result analysis of combined imagination recognition performance in terms of using only frequency domain and time-frequency domain in ASPS approach. Three categories:

- i. ASPS using only FFT on the 2<sup>nd</sup> phase combined data:

Properties: 10 subjects, 57 trials and 3 sensors

In the first result set, where only FFT generated  $\Delta$  SCFs are utilised, the performance metrics show a notable progression as the number of imaginations decreases. The best accuracy

improves from 60.9% with 5 imaginations to 97.5% with 2 imaginations. Similarly, the average accuracy rises from 53.8% to 94.8%. This suggests that FFT generated  $\Delta$  SCFs alone can yield high accuracy, especially with fewer imaginations.

ii. ASPS using both FFT and DWT on the 1<sup>st</sup> phase combined data:

Properties: 19 subjects, 2 trials and 3 sensors

The second result set combines FFT and DWT generated  $\Delta$  SCFs and includes a larger subject group. The highest accuracies range from 70.5% with 5 imaginations to 100.0% with 2 imaginations, while the average accuracies improve from 63.0% to 91.2%. Incorporating DWT generated  $\Delta$  SCFs alongside FFT improves the system's signal processing accuracy, demonstrating the robustness of the combined  $\Delta$  SCFs even with a larger number of subjects.

iii. ASPS using both FFT and DWT on 2<sup>nd</sup> phase combined data:

Properties: 10 subjects, 57 trials and 3 sensors

The third result set also uses combined FFT and DWT generated  $\Delta$  SCFs, though with the same number of subjects as the first dataset. Here, the highest accuracies range from 78.1% with 5 imaginations to 100.0% with 2 imaginations. The average accuracies improve from 69.1% to a perfect 100.0%. This dataset demonstrates the highest performance levels, indicating the combined feature set's effectiveness in improving recognition accuracy, especially in the 2<sup>nd</sup> phase of data collection.

The analysis highlights a positive correlation between reducing the number of imagination tasks and improving performance. As the cognitive load decreases, subjects achieve higher and more consistent performance levels, culminating in perfect scores when the tasks are reduced to two imaginations. The overall classification performance demonstrates impressive results when using SCFs generated by both FFT and DWT, compared to using SCFs generated by FFT alone.

### **7.7 Assessment of Achieved Accuracy and Comparison with Existing Studies**

Validation involves evaluating different methodological approaches (using either FFT alone or both FFT and DWT) within the ASPS model for recorded data obtained with optimised sensors. As demonstrated in the previous section, superior performance in recognising imaginations is achieved when the ASPS approach incorporates SCFs generated by both FFT and DWT. Recognition of two imaginations for the largest cohort and five imaginations for individuals achieved up to 100% accuracy. The following factors contributing to the

achievement of 100% accuracy were identified through the assessment of the achieved results.

Feature extraction with FFT and DWT in ASPS: The combination of FFT and DWT within ASPS captures both time and frequency domain characteristics, enhancing SCF separability, minimising class overlap, and ensuring high classification performance.

Uniqueness of feature combination in ASM: The ASPS approach arranges the extracted features in a unique combination of values within the ASM, allowing each imagination to be distinctly represented. This enhances the ANN's ability to classify effectively when the SCFs and corresponding labels are clearly differentiated for each imagination.

Impact of a small number of imaginations: Fewer imagination classes simplify classification, leading to more distinct separations between classes. 100% accuracy is achieved for two imaginations in the largest cohort and five imaginations for individual subjects, highlighting that fewer decision boundaries improve classification outcomes.

Consistency in signal nature for individual participants: The recognition of five imaginations per individual with 100% accuracy is due to the stability of their neural signals. Unlike multi-subject studies, where inter-subject variability complicates classification, individual patterns remain consistent, supporting perfect classification. Table 7.8 presents a comparison of the key aspects of the most relevant studies and the current research. The table highlights the study objectives, methodologies, accuracy rates, and other relevant factors that influence performance. The methodology includes the feature extraction techniques, number of tasks, and number of subjects, providing a comparison of the experimental dimensions and corresponding results.

Table 7.8: Comparative table of similar studies and this study.

Criteria	(Hinterberger <i>et al.</i> , 2004)	(Yang <i>et al.</i> , 2023)	(Imran <i>et al.</i> , 2024)	This research
Goals/objectives	Development of thought translation device using self-regulation of slow cortical potentials.	conversion of thoughts into text using EEG signals.	Brain-controlled computer task enabling cursor movement based on thought-driven EEG signals	Communication system to identify thought messages via EEG signals

Table 7.8: Comparative table of similar studies and this study (continued from previous page).

Criteria	(Hinterberger <i>et al.</i> , 2004)	(Yang <i>et al.</i> , 2023)	(Imran <i>et al.</i> , 2024)	This research
Methodology	EEG signals are processed during eye movements for two tasks, and the classified signals are converted into spelling. Number of subjects: 20	Eurasian Oystercatcher Wild Geese Migration Optimisation (EOWGMO) algorithm is used for signal processing and adaptive deep learning for classification. -14 motor movement/ imagery tasks -Publicly available dataset of 109 volunteers.	EEG brain signals are collected using the BrainLink device for eight brain states (delta, theta, alpha, etc.), processed, and classified for four cursor movements using a CNN-based approach. Privately labelled dataset is used.	EEG signals are processed and analysed across 2 to 5 different mental tasks. The ASPS approach is applied for signal processing, and ANN is used for classification. - 1st dataset: 19 volunteers with two trials. - 2nd dataset: 10 volunteers with five trials.
Accuracy	Overall: 70%	Overall: 96.41%	Overall: 80%	Individual: 100% for any number of imaginations Biggest cohort 2 imaginations: 100% 5 imaginations: 78.1%
Strength	Demonstrates significant voluntary brain control. Performance improves through adaptive methods.	Implements a powerful optimisation technique. Compares various features, including spectral, temporal,	Enables control of a cursor in four directions (up, down, left, right). Utilises a low-cost, single-channel EEG device.	Supports up to five distinct communication outputs. Selects three optimal sensors for signal acquisition.

Table 7.8: Comparative table of similar studies and this study (continued from previous page).

Criteria	(Hinterberger <i>et al.</i> , 2004)	(Yang <i>et al.</i> , 2023)	(Imran <i>et al.</i> , 2024)	This research
	Utilises multichannel EEG recordings. Employs an innovative methodology.	statistical, and spatial aspects. Evaluated with multiple classification algorithms.		Identifies unique imagination patterns from delta wave values using feature sensitivity analysis. Evaluated with various cohort sizes and three classification algorithms.
Limitation	-High intersubject variability reduces generalisability. - Sequential trial-to-trial interactions may hinder user consistency.	-No guarantee of finding the global optimum. - Performance is influenced by problem complexity and parameter settings.	Accuracy depends on proper preprocessing (noise reduction, artefact removal, signal normalisation, and feature extraction). Variability in volunteer data may limit scalability.	Performance is affected by the number of imagined tasks and cohort size.

## 7.8 Summary

This chapter presents the results and discussion of sensor optimisation for the second phase of data analysis and overall algorithm validation. The discussion encompasses sensor ratings, rankings, and cross-table analyses between sensors and subjects, as well as group formations based on the second phase of collected data. Validation involves assessing various methodological approaches (using only FFT or both FFT and DWT) using the ASPS model

for recorded data with optimised sensors. These approaches examine the effectiveness of incorporating frequency domain and/or time-frequency domain in the ASPS model. The chapter includes several comparisons between the data from the two phases and the different ASPS methods. The comparison results demonstrate higher performance in recognising imaginations when the ASPS approach is utilised with both FFT and DWT-generated SCFs. Ultimately, the discussion of these comparisons highlights the most suitable approach for this research.

The next chapter details the design and development of a novel EEG-BCI prototype, created in accordance with the proposed methodology. It includes the hardware components and the integration of hardware and software, as well as the testing of real-time data to validate the functionality of the prototype.

## Chapter 8: Design and Development of EEG-BCI Prototype

### 8.1 Introduction

The integration of brain imaging technologies, notably EEG and ANNs, has introduced a new dimension in communication between the human brain and computers. Previous analyses reveal that recognising imaginations is achievable using commercial EEG systems. However, a typical commercial EEG system consists of numerous sensors, such as 19, which can be time-consuming to set up and are often unaffordable for many individuals. The cost of these systems varies based on hardware and software requirements (Ledwidge, Foust and Ramsey, 2018), with a direct correlation between product quality, performance, and cost. Comprehensive EEG packages with multiple configurations can exceed \$100K (Lystad and Pollard, 2009). Although more economical options are available, they often suffer from limitations such as lower sampling rates, fewer channels, and reduced functionality (Dadebayev, Goh and Tan, 2022). Consequently, these less expensive systems would not meet our research needs, which require sensors targeting specific brain locations and compatibility with the developed brain signal processing model.

This research, as established in Chapter 7, demonstrates that three sensors can effectively recognise mental imagery. However, to evaluate the efficiency of optimised sensors in practical scenarios, a customised system is necessary. Integrating hardware and software for specific BCI applications would represent a significant advancement in communication systems. Moreover, this system will enhance portability, reduce complexity, and improve affordability.

In response, this research introduces the design and implementation of a cost-optimised EEG-BCI prototype as an innovative communication system. The objectives of this study are as follows:

- i. Designing a basic prototype where EEG sensors can record signal data from the scalp.
- ii. Developing the prototype using reliable and cost-effective equipment as per the design specifications.
- iii. Acquiring signals using the prototype.

- iv. Processing and analysing the signals according to the developed ASPS approach model.
- v. Developing a Graphical User Interface (GUI) application to manage signal acquisition, processing, and communication output.
- vi. Evaluating the performance of the system.

This approach aims to advance the current state of BCI technology by providing a more accessible and efficient solution for practical applications.

## 8.2 Design and Development

The design and development of the system have been executed in two distinct phases. The first phase focuses on creating a prototype of an EEG-based BCI utilising a single sensor for signal acquisition. Initially employing a single sensor simplifies the design, development, and evaluation processes of the system. Figure 8.1 presents the schematic diagram of the EEG-BCI utilised for signal acquisition. In the initial phase, the emphasis is placed on the creation of a prototype EEG-based BCI that incorporates a single sensor for signal acquisition. This approach simplifies the system's design, development, and evaluation processes. Figure 8.1 illustrates the schematic diagram of the EEG-BCI used for signal acquisition.

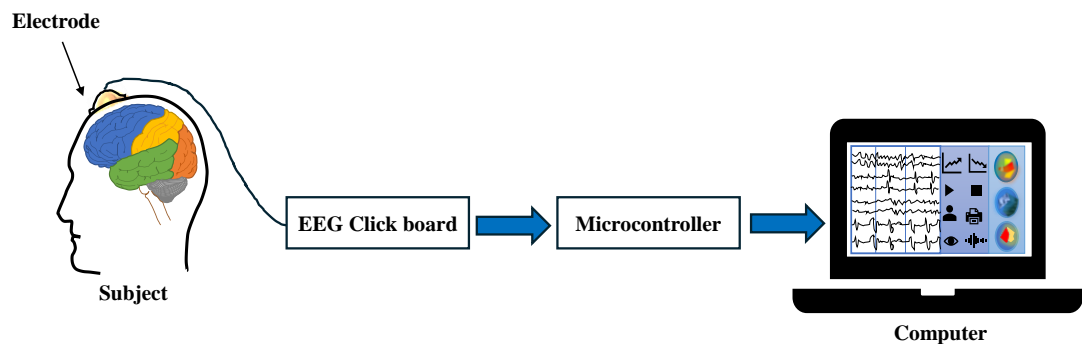


Figure 8.1: The schematic diagram of EEG-BCI for signal acquisition.

The EEG Click board interfaces with EEG sensors to capture brainwave signals. It is equipped with components for signal conditioning, filtering, and amplification, ensuring that the EEG signals are both reliable and usable. The board typically connects to development platforms via standard communication protocols such as Inter-Integrated Circuit (I2C) or Serial Peripheral Interface (SPI). Designed for compatibility with various Mikroelektronika development boards and microcontrollers, the EEG Click board is versatile and adaptable to

different applications. The Microcontroller Unit (MCU) plays a crucial role in this setup by processing inputs from the EEG sensors, executing programmed instructions, and managing outputs. As the central component of any embedded system, the microcontroller enables the correct combination and connection of the EEG Click board, facilitating accurate recording of EEG signal data within the system.

The design of the EEG-BCI prototype in this study utilises the NI 6009 as the MCU. The NI 6009, a multifunction DAQ device manufactured by National Instruments (NI), is designed for low-cost portable data acquisition applications and is widely used in education, research, prototyping, development, and industrial monitoring. The EEG Click Board and the NI 6009 DAQ are integrated into the data acquisition system, as shown in Figure 8.2.

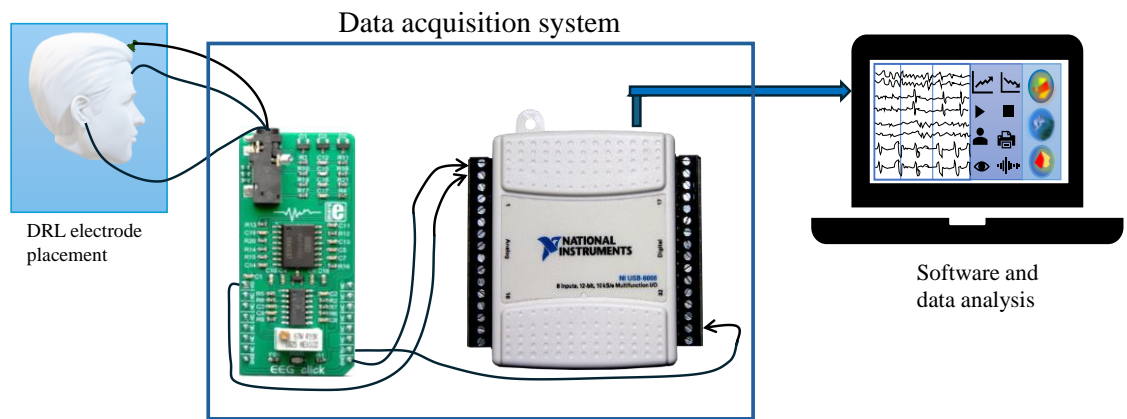


Figure 8.2: Hardware setup using EEG click board and NI 6009 DAQ for signal acquisition.

The NI 6009 DAQ supports high sampling rates, meeting the requirements of this research. Additionally, it offers direct compatibility with the MATLAB programming environment via the NI-DAQmx driver, enabling seamless connectivity through the MATLAB Data Acquisition Toolbox. Given these advantages, this research adopts the NI 6009 DAQ for further development.

Compared to alternative data acquisition cards such as Arduino and LabJack, the NI 6009 demonstrates superior feasibility for EEG-BCI applications. While a rate of 512 Hz is sufficient, a higher sampling rate can provide even greater precision and reduce the risk of aliasing, resulting in more reliable data (Halford *et al.*, 2016). The Arduino Uno R3 is unsuitable due to its low sampling rate, which fails to meet the necessary frequency requirements for brain signal acquisition. Although the LabJack U6 offers a high sampling

rate, its incompatibility with MATLAB and the need for additional software integration introduce potential reliability and compatibility issues. In contrast, the NI 6009 provides both high sampling rates and direct MATLAB integration, ensuring a more robust and efficient data acquisition system. The subsequent sections will discuss the implementation and evaluation of the prototype in detail.

### 8.3 Product Implementation

This section details the practical application of the developed prototype. The implementation process for the EEG-BCI prototype is as follows:

- a) **Verification of Connections:** Using an AVO meter, all connections between the EEG Click Board and the NI 6009 DAQ are verified.
- b) **Calibration:** Calibration is performed using an oscilloscope, NI MAX software, and the MATLAB Data Acquisition Toolbox. The necessary gain adjustments are made.
- c) **Health and Safety:** Ensuring the main power source adheres to health and safety standards.
- d) **Signal Monitoring:** The sensor is attached to the hand, and signals are monitored under both stable and moving conditions.
- e) **MATLAB Configuration:** Necessary settings in the MATLAB Data Acquisition Toolbox are configured.



Figure 8.3: Single sensor-based EEG-BCI prototype.

Upon completion of these checks, the system is ready for signal acquisition. Figure 8.3 illustrates the prototype, showing the complete connection between components, all housed in a suitable enclosed box. The box is equipped with a high-speed USB cable port and a 3.5 mm jack port for sensor connectivity and signal acquisition.

## 8.4 Signal Acquisition

Signal acquisition is conducted using a single EEG sensor, as illustrated in Figure 8.6. The sensor cable consists of three components: one for brain location and two for neutralising the EEG signals.



Figure 8.4: Signal acquisition using prototype.

The signal acquisition uses a sampling rate of 1 kHz. To simplify both signal recording and processing, this study examines two mental tasks: imagining kicking a football with the left foot and imagining walking on a warm sandy beach. These tasks correspond to imaginations 2 and 5 from the list detailed in Chapter 3, Table 3.1. Following verbal instructions, the subject performs each imagination task for 5 seconds. The instructions consist of two phases: first, a relaxation period, followed by the specific mental task.

## 8.5 Signal Processing

The captured data are stored directly in the MATLAB workspace, with a total of 40 trials recorded from one subject. The signals are processed according to the initially developed signal processing model. This model, based on the ASPS approach, focuses exclusively on the frequency domain. Given that the experiment involves only two imagination tasks—while experiments in Chapters 4 and 5 demonstrate successful recognition for three different imaginations—the recorded signals are processed using a five-part FFT and four statistical functions within the ASPS model, resulting in 20  $\Delta$  SCFs for each imagination. The ASM is generated from the extracted SCFs, and the normalised SCF values are input into a FFNN model for classification of the imaginations.

## 8.6 Classification

A single-layered FFNN is employed for the classification of mental imaginations. The SCFs generated by the FFT for the two mental tasks are used as inputs for the FFNN model. Train-test datasets are prepared with a 70:30 ratio. Various neuron configurations, ranging from  $N$  to  $3N$  (where  $N$  represents the number of samples), are tested. For each neuron configuration, the model is executed 25 times, and the average performance is calculated. The best and average performances are measured using classification accuracy, as defined in Equation (3.2) of Chapter 3. Figure 8.5 presents the best and average performances of the single-sensor EEG-BCI prototype.

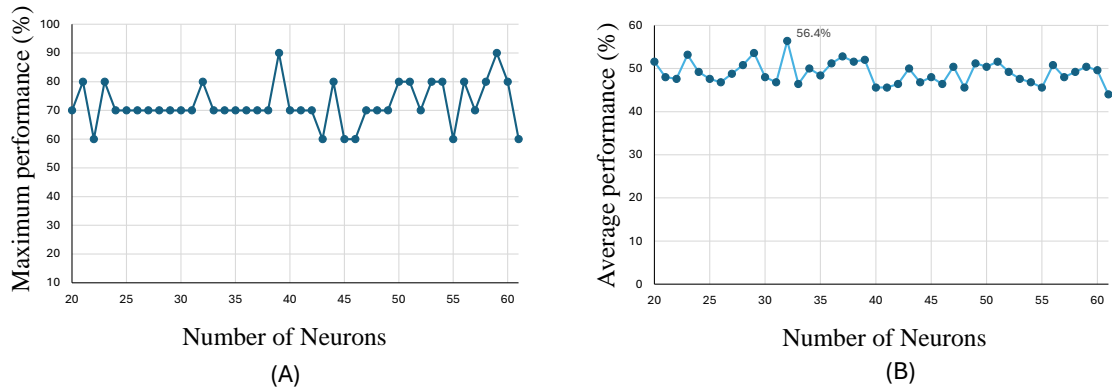


Figure 8.5: The accuracy of single sensor-based EEG-BCI prototype (A) Maximum performance and (B) average performance.

The results indicate that the highest performance across various neuron configurations ranges from 60% to 90%, with 70% being achievable in many cases. The hidden layer size of 32 neurons yields the overall best results, achieving a maximum accuracy of 80% and an average accuracy of 56.4%. This performance is challenging compared to industry benchmarks, as there are no existing systems with the same target orientation. Based on previous analysis, this research sets a performance goal of at least 70% average accuracy to ensure the communication system's quality. Potential factors contributing to the performance limitations may include the use of a single sensor and the unshielded sensor cable, which can introduce noise.

## 8.7 GUI-based Application Development

A GUI-based application has been developed using MATLAB R2022a. This application provides a user-friendly platform for controlling signal recording and processing, as well as generating communication outputs for the user. The software leverages various GUI

components, such as buttons, labels, and signal plots, to enhance user interaction. The application features two buttons designed for recording signals during relaxation and mental task periods. Clicking a button initiates a session that connects to the NI 6009 DAQ for data acquisition related to the selected task—either relaxation or mental task. Data are collected for 5 seconds, and the visualisation panel displays the recorded signals.

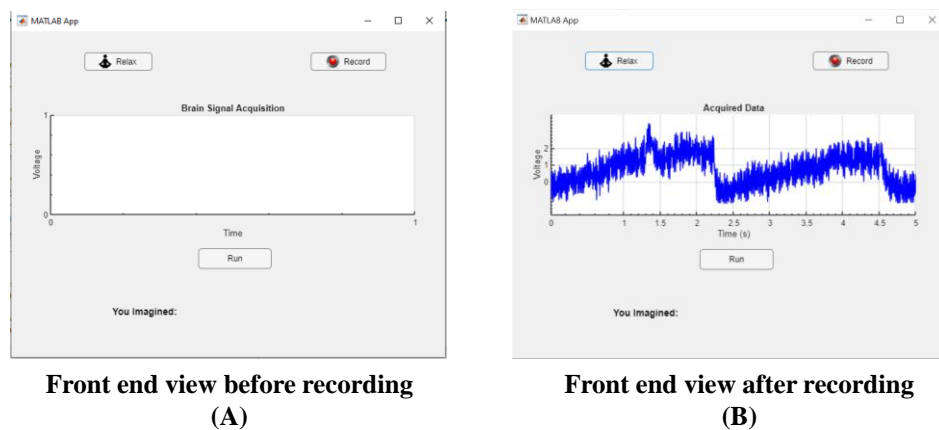


Figure 8.6: The application view (A) before recording and (B) after recording.

Figure 8.6 illustrates the application's interface: (A) before recording and (B) after recording. The "Run" button activates the signal processing method in the background, classifies the signals, and displays the communication output on a label. This application is designed with bespoke manner, where the internal FFNN model is trained offline for individual subjects. The system processes real-time data from the subject and generates the corresponding communication output based on the trained model.

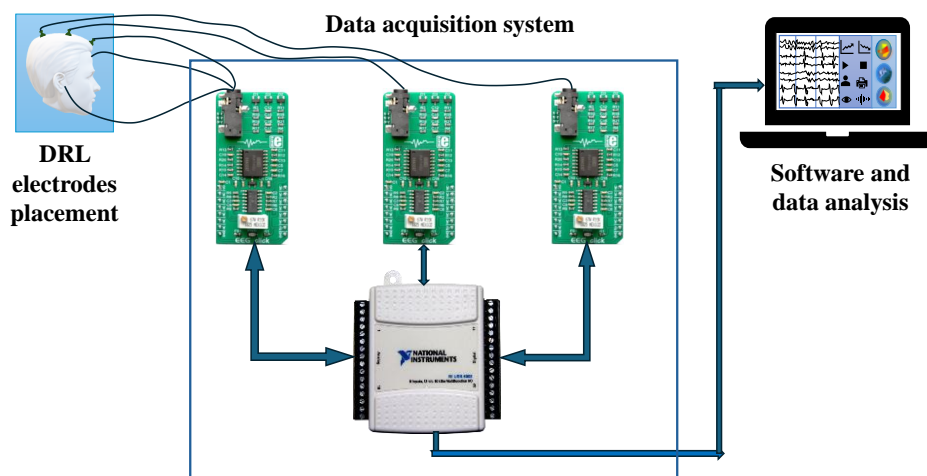


Figure 8.7: New design of the hardware setup using three sensors-based EEG-BCI prototype for signal acquisition.

Figure 8.7 depicts the updated design of the EEG-BCI prototype. To enhance the performance of the EEG-BCI prototype, this study explores the incorporation of additional sensors, based on the analysis presented in Chapter 7. The sensor optimisation analysis has determined that three sensors placed at specific brain locations are sufficient for accurate imagination recognition. Consequently, this study revisits the initial design phase and integrates a three-sensor configuration into the EEG-BCI prototype. Three unit of MIKROE EEG Click Boards are utilised to support the three sets of EEG sensors. Given that the NI 6009 DAQ includes multiple input and output channels, it readily accommodates the three EEG Click Boards.

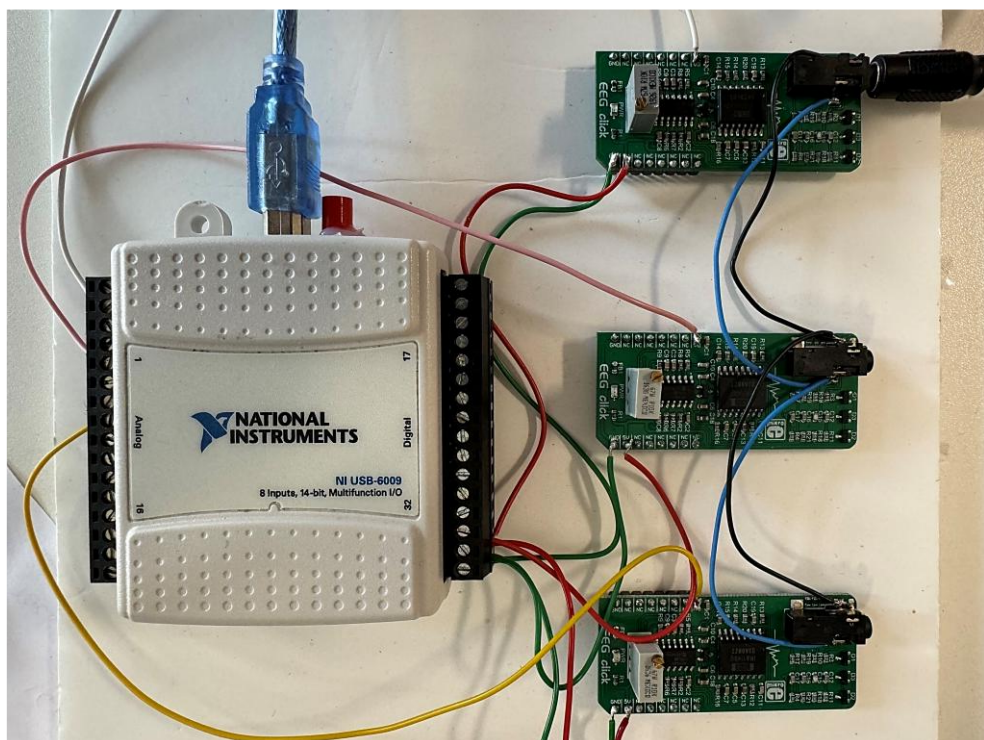


Figure 8.8: The connectivity of three EEG Click boards and NI 6009 DAQ.

Figure 8.8 illustrates the hardware setup, showing all input and output connections for the three EEG Click Boards and the NI 6009 DAQ, all housed within a single enclosure. The product implementation process replicates the entire procedure outlined in Section 8.3, but with the newly configured hardware setup. To enhance the Signal-to-Noise Ratio (SNR), all EEG sensor cables have been shielded. Figure 8.9 highlights the distinction between the previous unshielded cables and the new shielded cables.



Old look  
Unshielded sensor cable  
(A)

New look  
Shielded sensor cable  
(B)

Figure 8.9: Sensor cables (A) unshielded cables (B) shielded cables.

Following this updated development, the EEG-BCI prototype is reconfigured for signal acquisition. Figure 8.10 displays the updated prototype, with (A) showing the top view and (B) presenting the side view of the newly designed EEG-BCI prototype.



Top view of the EEG-BCI prototype  
(A)

Side view of the EEG-BCI prototype  
(B)

Figure 8.10: Newly developed EEG-BCI prototype (A) top view and (B) side view.

Signal acquisition is conducted using a newly developed prototype. Three sensors are employed to record simultaneous signals from three specific brain locations: Fp1, Fp2, and Fz. These locations are selected based on the findings from the sensor optimisation analysis detailed in Chapter 7, which is reviewed in light of this prototype study, currently limited to two types of mental imagery. The accuracy ratings for individual sensors corresponding to these two mental imaginations are examined, revealing that Fp1, Fp2, and Fz achieve

consistently high accuracy. Additionally, these brain locations are chosen for their convenience in attaching sensors to the scalp for data recording. Figure 8.11 shows the signal acquisition with three sensors using newly developed EEG-BCI prototype.



Figure 8.11: Signal acquisition with newly developed EEG-BCI prototype.

The signals from the three sensors are processed using the ASPS approach, which focuses solely on frequency domain characteristics. The signal processing model explores two different partitions of the FFT within the ASPS approach: a four-part and a five-part FFT, each associated with four statistical functions—mean, standard deviation, variance, and maximum. The equations for these functions are provided in Chapter 3, Table 3.2.

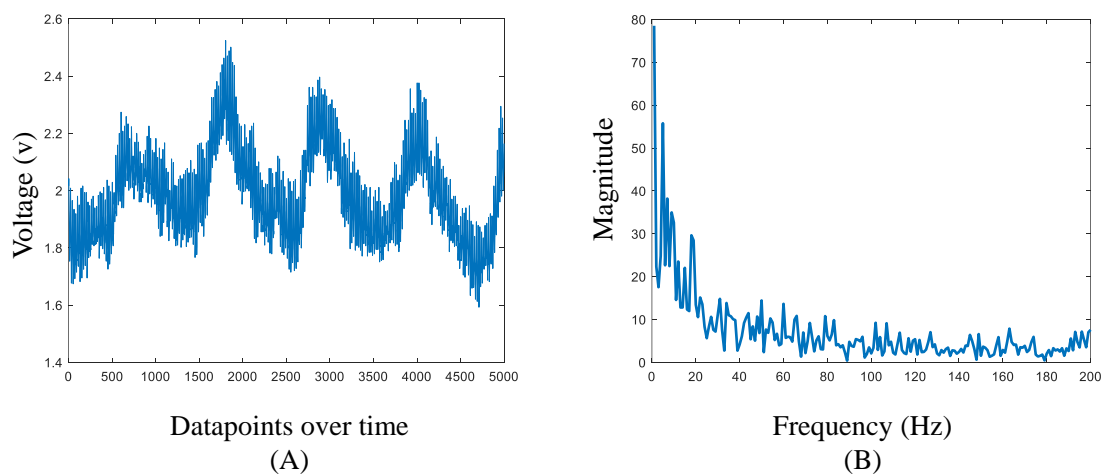


Figure 8.12: Signal visualisation (A) raw signal recording using EEG-BCI prototype and (B) corresponding FFT plot.

The FFT partitions are determined by considering the FFT outcomes of the raw signals, as illustrated in Figure 8.12, which displays (A) the raw signal and (B) the corresponding FFT outcome. Environmental noise creates high frequency at 250Hz which is visible in full length of FFT outcomes. Signal analysis considers the range of the frequency with a realistic manner to process appropriate features in this step.  $\Delta$  values of SCFs help to minimise the line noise and motion noise. The four-part and five-part frequency domain partitions generate ASMs with 16 and 20  $\Delta$  SCFs, respectively. These SCFs serve as inputs to a single-layered FFNN, the classification algorithm used to identify the mental imaginations. To assess the performance of the FFNN, hidden layer sizes ranging from 1 to 120 neurons are applied, and the model is executed 50 times for each layer size. The highest and average performances are recorded. Figure 8.13 presents the average performance of the FFNN model for both the four-part and five-part FFTs.

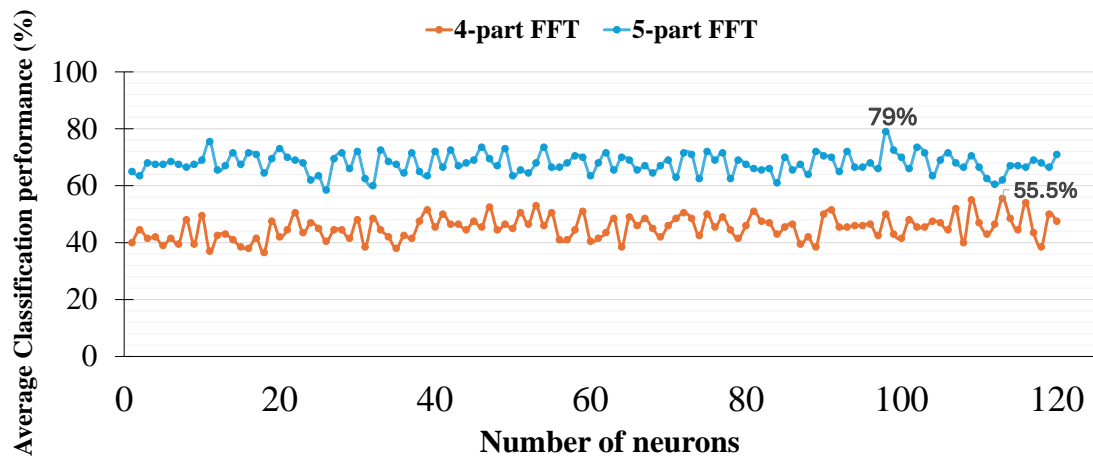


Figure 8.13: Average classification accuracies of EEG-BCI prototype between various partitions.

The variation in classification outcomes is evident, with the four-part FFT-generated SCFs achieving an average classification accuracy of 55.5%, while the five-part FFT-generated SCFs reach an average accuracy of 79%. In 50 runs with any number of neurons, the model achieves 100% accuracy at least once, highlighting the effectiveness of the extracted SCFs. This variation underscores the significance of FFT partitioning, as it aligns with the performance differences observed in Chapters 4, 5, and 6, which explore 2, 4, and 10 partitions, respectively. In this study, the partitions within the alpha, beta, and gamma frequency bands demonstrate a distinct characteristic between relaxation state and the corresponding mental task. Figure 8.14 depicts the classification performance of ASPs using a four-part frequency domain SCFs.

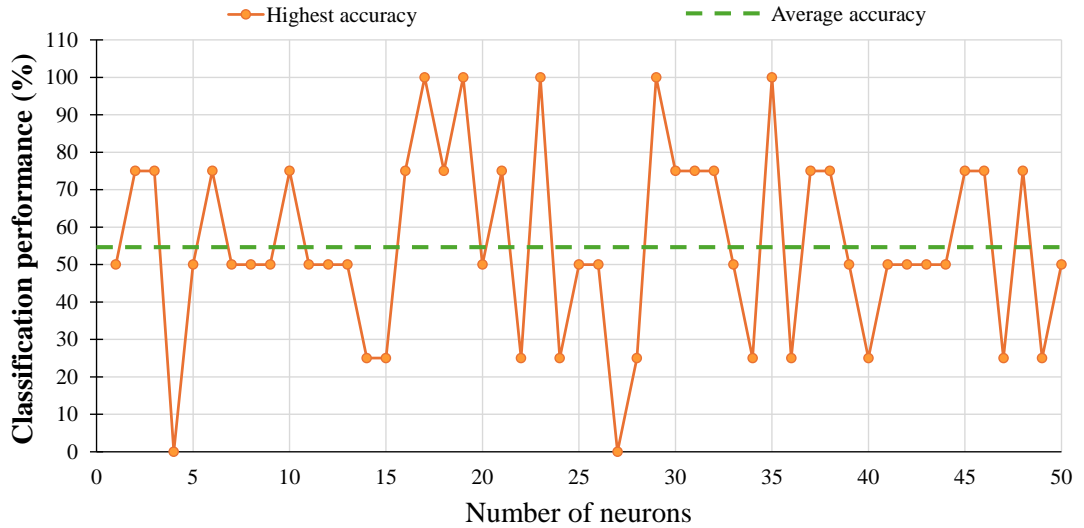


Figure 8.14: Classification performance of EEG-BCI prototype using ASPS using four-part frequency domain generated SCFs.

The chart illustrates the highest performance recorded over 50 runs, with a dotted line representing the mean performance across these runs. The values generally fall between 50% and 75%, with occasional peaks reaching 100%. Some values decrease to 25%, and 0% appears rarely, reflecting instances of minimal output. Figure 8.15 showcases the classification performance of ASPS when employing a five-part frequency domain SCFs.

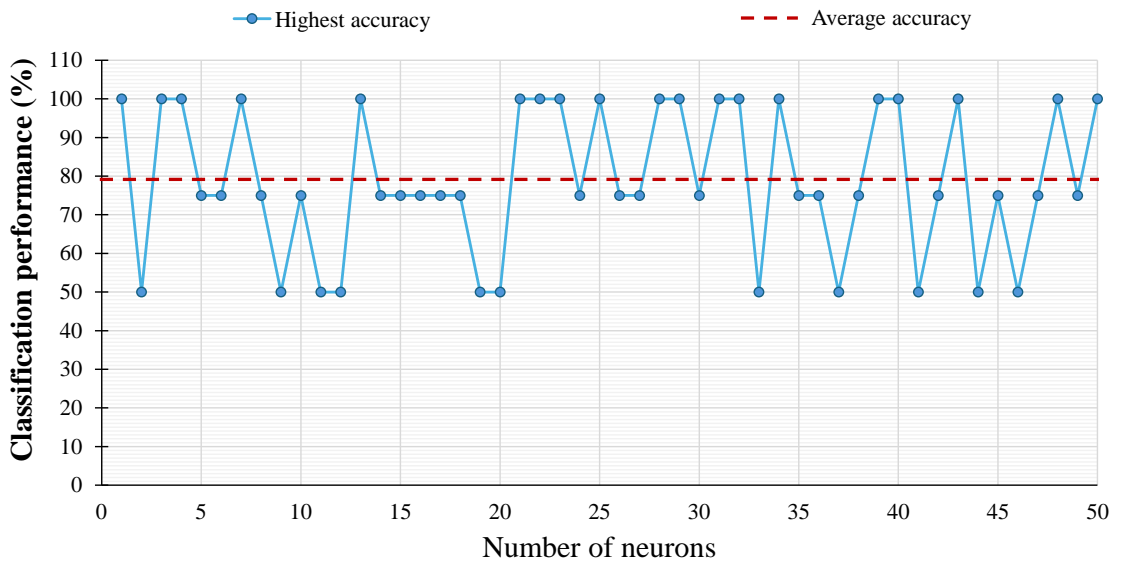


Figure 8.15: Classification performance of EEG-BCI prototype using ASPS using five-part frequency domain generated SCFs.

As in Figure 8.15, the chart highlights the maximum performance achieved over 50 runs, with the dotted line marking the average performance. Here, 50% is frequently observed, but 75% appears most often, indicating a strong bias towards higher classification values. 100% values are notably present in various instances, indicating significant consistency or accuracy in those cases. When comparing the two, the four-part FFT-generated SCF output displays a wider range of results, with values as low as 0% and many clustering between 50% and 75%. On the other hand, the five-part FFT-generated SCF output tends to yield higher classification values, with several instances of 100%, pointing to a more consistent or superior performance compared to the four-part setup.

The results and discussion demonstrate the efficacy of the newly developed EEG-BCI prototype. The integration of this hardware prototype with its associated software enables the recognition of two distinct mental imagery states, thus facilitating communication outputs. However, the current system's signal acquisition process is occasionally compromised by motion artefacts and/or environmental noise. The GUI-based application fulfils the basic requirements for fundamental communication tasks, but there are several avenues for potential enhancement. These include the reduction of noise and artefacts, the inclusion of additional mental tasks, an increase in the sampling rate, and improvements in the signal processing model. Further research should focus on optimising the placement of brain electrodes and refining ANN models and their architectures. Additionally, upgrading the front-end application to support both training and testing with real-time data from diverse subjects would significantly enhance its functionality.

## **8.8 Summary**

This chapter presents a novel EEG-BCI product developed to meet the objectives of this research. It underscores the importance of integrating cost-effective hardware with bespoke software designed for specific BCI applications. The chapter encompasses the design, development, and implementation of both the initial and upgraded EEG-BCI prototypes. Emphasis is placed on the reliable performance of low-cost hardware, which provides adequate channels and sampling rates, alongside advanced GUI-based software for data analysis and interpretation. This integration is crucial for achieving effective outcomes in BCI applications. The system ensures accurate capture and processing of brain signals, delivering reliable and meaningful data for its intended purpose. The model is trained offline using a customised approach, while the GUI application supports real-time testing with

subject data, enabling practical evaluation of the prototype. Additionally, this chapter identifies potential areas for future work aimed at advancing the prototype's capabilities.

The following chapter provides a comprehensive summary of the thesis, outlining the achievement of the research objectives, the key findings, and the contributions made to the field. It also presents recommendations for future research.

# **Chapter 9: Discussion and Conclusion**

## **9.1 Introduction**

The development of BCIs holds the potential for transformative impacts, particularly in enhancing communication and well-being for individuals with physical disabilities. This thesis outlines the research undertaken to develop an innovative BCI using EEG and AI to decode thought messages. The research methodically addresses the objectives set forth in Chapter 1. Each objective is pursued with meticulous care, skill, and thorough review, advancing step by step towards the overarching aim. Chapters 2 through 8 detail each phase of the research. Chapter 2 provides a comprehensive literature review of the relevant areas of this study. Chapter 3 explains the methodology employed. In Chapter 4 the bespoke analysis results of imaginations recognition are presented. Chapter 5 covers the group-based analysis results of imaginations recognition, and in Chapter 6 the results of imaginations recognition using image processing technique are explored. Chapter 7 reports on all the experimental performances of optimised sensors, and in Chapter 8 the design and development of a novel EEG-BCI prototype for thought message identification is discussed. This chapter synthesises the research outcomes, addressing the research questions and achieving the objectives, highlighting key findings and contributions to the field. It concludes with a discussion of the research's limitations and suggests directions for future work.

## **9.2 Addressing Research Questions and Accomplishing Objectives**

In order to achieve the goal of developing an innovative communication approach employing EEG and AI for discerning thought messages, this study addresses the research questions and fulfils the objectives outlined in Chapter 1, as detailed below.

**Objective 1:** To conduct a comprehensive literature review on fundamental neuroscience concepts, brain imaging systems, signal processing methods, classification algorithms, and relevant commercial products.

**Outcome:** An extensive literature review on the relevant areas of this research topic was conducted. As the research aims to design and develop a methodology for implementing BCI applications, Chapter 2 explores the state of the art in fundamental neuroscience concepts and their role in MND, brain imaging systems, signal processing methods, classification

algorithms, and relevant commercial products. The review of fundamental neuroscience concepts provides essential understanding of the neurobiological structure of the brain, its functional processes, and cognitive aspects. The brain imaging systems study helps to understand the capture process of cognitive functions and determine the requirement of the data collection arrangement. The review of signal processing methods provides insights into diverse methods, their strengths, and weaknesses. The analysis of classification algorithms highlights potential classifiers and current trends. Finally, the literature review also highlights on relevant commercial products in the field of BCIs. Overall, this literature review has enriched the research with critical insights and a deeper understanding of the topic.

Objective 2: To develop a brain signal processing algorithm and analyse brain signals using the algorithm, validating the results with appropriate ANNs.

Outcome: Considering the limitations of traditional signal processing methods, novel ASPS approach was adopted to investigate the capability of extraction and selection of features from brain signals. This approach incorporates both frequency domain and time-frequency domain analysis. To maintain simplicity and manage dimensionality, an elementary model was first designed and developed for examination through bespoke analysis. Prior brain signal data were used in this development. A comprehensive study and series of experiments were conducted, exploring various methods such as FFT, WT as well as different statistical functions. These methods were investigated individually and across several cohort sizes of subjects. This study successfully identified the optimal ASPS approach by integrating traditional signal processing techniques, configuring individual techniques, and selecting statistical functions. Chapter 4 and 5 discuss how the methodology has been developed step by step. This methodology has been applied to both bespoke and three group-based analyses, demonstrating its effectiveness.

Objective 3: To conduct experiments to collect brain signals using a commercial EEG device.

Outcome: EEG signal acquisition was conducted to ensure the development and evaluation of the proposed brain communication system. Data were collected from 10 participants, each performing five trials of predefined mental tasks, ensuring sufficient variability for robust analysis. Additionally, a single subject underwent 12 trials to assess intra-subject consistency and comparative performance across different trial numbers. This systematic data collection approach facilitated the evaluation of inter-subject variability and the reliability of the developed methodology. Practical challenges, including signal noise, artefact removal, and

experimental setup, were addressed to enhance data integrity. Chapter 6 discusses these experiments in detail, providing insights into sensor optimisation and methodological validation.

Objective 4: To optimise a neural network model and identify the most suitable ANN for this research.

Outcome: Following feature extraction, multiple ANN architectures were evaluated to determine the most effective classification model for recognising imagined tasks. LVQ and FFNN models with varying layer configurations were systematically tested, including architectures with single and dual hidden layers. Five different FFNN models were implemented and executed certain number of times to assess performance consistency. Comparative analyses of accuracy, computational efficiency, and dataset requirements indicated that a single-layer FFNN provided the optimal balance between accuracy and complexity. Additionally, CNN was explored for imagery classification, particularly in three-group analysis scenarios. Chapters 4 to 7 present detailed performance evaluations, leading to the selection of the most suitable ANN for this study.

Objective 5: To design and develop an EEG-BCI prototype for recording EEG signals and a software interface and evaluate its effectiveness in creating a communication system.

Outcome: A fully functional EEG-BCI prototype was developed, integrating hardware and software components to enable brain signal acquisition, processing, and classification. The hardware system was designed using EEG Click boards, a microcontroller, and optimised sensor placement, ensuring reliable signal acquisition. The prototype accommodates three EEG sensors, offering flexible positioning via electrode pads or a hairband mechanism for improved usability. A GUI was developed using MATLAB to facilitate data visualisation, signal processing, and real-time classification. The system supports automated signal acquisition, feature extraction, and classification using the trained FFNN model. This comprehensive BCI system represents a novel, low-cost approach to thought-based communication, demonstrating significant potential for assistive technology applications. Chapter 8 details the prototype's development, implementation, and performance evaluation.

### **9.3 Contribution to The Knowledge**

In this research, the key contributions to the knowledge are presented below:

- i. A novel implementation of the ASPS approach for brain signal processing.

- ii. A distinct combination of SCFs that demonstrates uniqueness in recognising specific imaginations and highlights the resemblance between subjects.
- iii. The optimised number of sensors required and their scalp locations to identify the thought messages via brain signals.
- iv. A method for recognising specific imaginations using the ASPS approach for feature extraction, combined with LVQ and FFNN for signal classification.
- v. A method for imaginations recognition using the ASPS approach, integrated with image processing techniques such as CNN for classification.
- vi. Identification of the most suitable ANN model and layer architecture for different sets of imagination recognition in terms of bespoke and broader populations.
- vii. A novel communication product named the EEG-BCI prototype for identifying thought messages.
- viii. A method for imagination recognition using the novel EEG-BCI prototype communication product.

#### **9.4 Key Findings**

This research conducts bespoke, group-based, combined analysis in order to recognise the imaginations for two phases of recorded data. According to the developed methodology, the key findings are organised chapter-by-chapter and presented here.

In Chapter 4, imaginations recognition through bespoke design analysis involves the development and verification of an elementary signal processing model. The findings are as follows:

- The ASPS approach successfully extracts the SCFs from raw signal data in the time domain and uses two-part FFT for frequency domain characteristics.
- Four statistical functions are applied within ASPS method, resulting in a total of 12 SCFs, which are sufficient for imagination recognition.
- Both subjects individually achieved 100% accuracy in recognising three and four imaginations using LVQ and single-layered FFNN model.
- Four imaginations were classified with 100% accuracy when both training and testing were performed by the same subject.
- Subjects 1 and 2 achieved 80% and 100% accuracy, respectively, in recognising five imaginations, indicating the influence of the quality of each individual's thoughts on the bespoke experiment.

- The single-layered FFNN is the most suitable model in terms of accuracy, architectural complexity, and computational time.
- The LVQ model performs well for smaller input datasets but requires longer training times compared to the FFNN models.
- When the model is trained by either subject and tested by both, only three imaginations are recognised with 100% accuracy.
- The best average classification accuracy for both training and testing by subject 2 is 67.4%, 77%, and 100% for recognising five, four, and three imaginations, respectively.

Chapter 5 discusses the development and verification of an advanced proposed model for signal processing through group-based analysis. The findings are:

- The ASPS approach, including FFT and DWT features, is capable of recognising five imaginations.
- Four statistical functions are applied within the ASPS method, producing a total of 32 SCFs, from which 12 SCFs are selected. These 12 SCFs are sufficient for recognising imaginations.
- The group-wise analysis consists of three groups based on the resemblance of imagination characteristics between subjects and an increasing number of subjects.
- The best classification accuracy for Group 1 (four subjects) is 100% for recognising two, three, and five imaginations.
- The SCFs for two imaginations are selected from three detailed components generated using DWT. The SCFs of three imaginations are extracted from four-part FFT, with three-part  $\Delta$  SCFs selected as the most significant.
- Group 1 achieves 100% as the highest accuracy in recognising three imaginations using any ANN model architecture, and in recognising two imaginations using most of the FFNN models.
- In five imaginations recognition, Group 2 (nine subjects) and Group 3 (nineteen subjects) achieve a maximum of 86.67% and 78.95% accuracy, respectively.
- Group 1 performs with an average classification accuracy of 100% for recognising three imaginations.
- In recognising three imaginations, Group 2 and Group 3 achieve average classification accuracies of 100% and 95%, respectively.

- Among the two ANN models (LVQ and FFNN), the single hidden layer-based FFNN is found to be the most suitable model for group-based analysis in terms of accuracy, architectural complexity, and computational time.

Chapter 6 employs image processing technique using CNNs for imaginations recognition through group-based analysis. The findings are:

- The ASPS approach, including CNN, can recognise different sets of imaginations.
- The ASPS approach using only FFT can recognise up to five imaginations through image processing.
- Employing EEG signals from 19 sensors is capable of recognising imaginations, with FFT involving ten-part analyses in feature extraction.
- The ASM produced in ASPS signal processing can be processed as heatmap images, which can be fed to CNN for classifying imaginations.
- Fifteen statistical functions are applied within the ASPS method, producing a total of 150 SCFs, from which 60 SCFs are selected.
- Group 1 achieves 100% accuracy in recognising three and four imaginations.
- Group 2 achieves the highest accuracy of 100% and an average accuracy of 92.47% in recognising three imaginations.
- Group 3 achieves up to 94.73% accuracy in recognising three imaginations.
- In group-based experiments, CNN is generally faster than LVQ and FFNN.

Chapter 7 includes the analysis of sensor optimisation based on the second phase of recorded data. The selected optimised sensors are verified through bespoke, group and combined subjects' data. The key findings are as follows:

- Brain signal acquisition involves a total of 57 trials from 10 subjects, which enables a more comprehensive analysis of both bespoke and various group performances. The dataset overcomes the limitations of the trial shortages encountered in previous chapters.
- Sensor optimisation report (summarised rating point table) provides a clear understanding of each sensor performance in recognising two, three, four, and five imaginations.
- The cross-tabulation analysis shows the performance of selected sensors for individuals in terms of different sets of imaginations recognition.

- The group analysis consists of three groups based on resemblance of sensor performance, with each group having different subjects.
- Verification for bespoke analysis, group analysis and combined data analysis is thoroughly conducted using the methodologies in Chapters 4 and 5.
- Comparative analyses among Chapters 4, 5, and 7 are presented.
- The methodology of feature extraction and selection, followed by the advanced proposed model in Chapter 5, produced the best performance for bespoke, groups, and combined data.
- Bespoke results achieve up to 100% accuracy and an average accuracy of more than 82% in recognising any number of imaginations.
- Different groups show performance variability, with Group G1 (six subjects) achieving up to 81.5% accuracy in recognising five imaginations, 98.1% in recognising four imaginations, and 100% in recognising two and three imaginations.
- Combined performance (Group G3: ten subjects) shows accuracies of 78.1%, 95.2%, 86.9%, and 100% in recognising five, four, three, and two imaginations, respectively.
- The overall analysis highlights a positive correlation between reducing the number of imagination tasks and improving performance.

Chapter 8 discusses the design and development of a novel EEG-BCI prototype. The key findings of this chapter are as follows:

- The implementation of an innovative EEG-BCI prototype integrates both hardware and software design and development.
- The prototype can record brain signals simultaneously from three different head positions using three sensors.
- Brain signals are processed and analysed using the ASPS approach, which includes FFT-based SCFs to recognise two imaginations.
- The developed GUI is a user-friendly application, error-free, and does not require a high computational system. It operates on Windows OS with MATLAB programming language and includes a signal processing toolbox package.
- The prototype has been tested by bespoke real-time data.
- The highest accuracies reached 100% when employing both 4-part and 5-part FFT generated  $\Delta$  SCFs.

- The average accuracies achieved are up to 55.5% and 79% with the use of 4-part and 5-part FFT generated  $\Delta$  SCFs, respectively.
- Signal acquisition should be carefully conducted, considering environmental factors, the subject's physical stability, and basic health and safety.
- The prototype is affordable, portable, and easy to install.

## 9.5 Limitations and Future Work

In Chapter 4, the bespoke experiments included only two subjects, which may affect the generalisability of the results. Varying the subjects or increasing the number of participants could yield different performance accuracies. Additionally, the data analysed consists of only two trials, often with the ANN model being trained on one trial and tested on another.

In Chapter 5, the advanced proposed model for signal processing was only applied in the group-based analysis. A comparison between the bespoke analysis using the advanced proposed model and the elementary model could have provided additional insights. While the number of imaginations was verified for two, three, and five imaginations, investigating four imaginations could have maintained performance consistency for observation and comparison purposes. Given that the dataset contained only two trials, the train-test split was performed on a 50%-50% basis.

Chapter 6 includes deep learning model where sometimes hardware requires computational specification. The proposed CNN model cannot run more than 60 iterations due to the high computational demands of image processing. Consequently, the validation in this chapter did not match the total number of runs in previous analyses. Bespoke design incorporating image processing could not be conducted due to having only two trials of data. Additionally, this analysis could not include data from the same three sensors used in Chapters 4 and 5, making it difficult to compare the performance deviations between ANNs and CNN algorithms. The shortage of trials persisted, as in the previous analyses.

The analysis in Chapter 7 is limited to evaluating group performance based solely on optimised sensor data and does not include comparative assessments with data from other sensors. This chapter partially compares group results with those in Chapter 5, although the group formation concepts differ. The average classification accuracy was calculated from 25 model runs due to time constraints.

In Chapter 8, the EEG-BCI prototype requires further refinement. Nearby electronic devices, lights, slight cable movements, or the subject's muscle movements can introduce noise. The internal ANN model currently classifies only two imaginations and is subject-dependent.

Based on the current limitations of the study, the potential future work could include:

Extending the research to evaluate the developed systems for individuals with disabilities, particularly patients with specific medical conditions such as locked-in syndrome or severe speech impairments, aims to enhance their ability to communicate effectively. Developing the EEG-BCI prototype with real-time data training and testing capabilities to create a subject-independent system. Further exploration of thought messages to enhance communication outputs and functionalities for specific applications.

## **9.6 Summary**

BCI applications have significantly advanced the potential for enhancing communication by converting brain signals into speech, text, and other actionable outputs, particularly benefiting individuals with disabilities. This research investigates the development of signal processing methods for feature extraction and selection to create viable BCI systems. Despite the inherent challenges in this field, this study offers substantial contributions to the understanding and utilisation of brain signal characteristics.

A novel implementation of the ASPS approach has been successfully evaluated, demonstrating its adequacy as a brain signal processing technique. This study validates the effectiveness of identifying up to five thought messages using the proposed methodologies, both for bespoke and broader population analyses. The research underscores the compatibility of ANNs and CNN with the proposed methodologies, identifying the most suitable ANN model architecture for recognising thought messages. Sufficient brain signal data were collected enabling the effectiveness of sensor optimisation, signal feature extraction, selection, and classification based on the proposed methodology. Additionally, the study introduces a novel EEG-BCI prototype that records EEG data and classifies two thought messages using the proposed methodology. Both the hardware and software interfaces were designed and developed to meet the research objectives.

This chapter provides a comprehensive explanation of how each research objective was examined in detail, offering insights into the adopted methodologies, obtained results, and the contributions made to the field. It also discusses the limitations encountered during the

study phases, some of which were addressed in Chapter 7. Finally, the chapter suggests directions for future research, taking into account the latest advancements in BCI technology and potential areas for further exploration. Overall, this study significantly advances BCI technology, setting the stage for future innovations in translating brain signals into functional communication modalities.

## References

- Abbas, J., Al-Habaibeh, A. and Su, D. (2011) *The Effect of Tool Fixturing Quality on the Design of Condition Monitoring Systems for Detecting Tool Conditions*, *Jordan Journal of Mechanical and Industrial Engineering*.
- Abed, Ahmed M, Al-Ani, M., Abed, Ahmed Mohammed and Shaban Al-Ani, M. (2018) 'Analysis and classification of brain signals using DWT and SVM', *Article in Journal of Theoretical and Applied Information Technology*, 31(10). Available at: [www.jatit.org](http://www.jatit.org).
- Abhang, P.A., Gawali, B.W. and Mehrotra, S.C. (2016) 'Technological Basics of EEG Recording and Operation of Apparatus', in *Introduction to EEG- and Speech-Based Emotion Recognition*. Elsevier, pp. 19–50. Available at: <https://doi.org/10.1016/b978-0-12-804490-2.00002-6>.
- Abiodun, O.I., Jantan, A., Omolara, A.E., Dada, K.V., Mohamed, N.A. and Arshad, H. (2018) 'State-of-the-art in artificial neural network applications: A survey', *Heliyon*, 4(11), p. e00938. Available at: <https://doi.org/10.1016/j.heliyon.2018.e00938>.
- Acharya, U.R., Oh, S.L., Hagiwara, Y., Tan, J.H. and Adeli, H. (2018) 'Deep convolutional neural network for the automated detection and diagnosis of seizure using EEG signals', *Computers in Biology and Medicine*, 100, pp. 270–278. Available at: <https://doi.org/10.1016/j.combiomed.2017.09.017>.
- Agarwal, S.K., Shah, S. and Kumar, R. (2015) 'Classification of mental tasks from EEG data using backtracking search optimization based neural classifier', *Neurocomputing*, 166, pp. 397–403. Available at: <https://doi.org/10.1016/j.neucom.2015.03.041>.
- Aggarwal, S. and Chugh, N. (2019) 'Signal processing techniques for motor imagery brain computer interface: A review', *Array*, 1–2. Available at: <https://doi.org/10.1016/j.array.2019.100003>.
- Agnihotri, P., Fazel-Rezai, R. and Kaabouch, N. (2010) 'Comparative analysis of various brain imaging techniques', in *2010 Annual International Conference of the IEEE Engineering in Medicine and Biology Society, EMBC'10*, pp. 3029–3032. Available at: <https://doi.org/10.1109/IEMBS.2010.5626144>.

Ahn, S. and Jun, S.C. (2017) ‘Multi-modal integration of EEG-fNIRS for brain-computer interfaces – Current limitations and future directions’, *Frontiers in Human Neuroscience*. Frontiers Media S.A. Available at: <https://doi.org/10.3389/fnhum.2017.00503>.

Akbari, H., Khalighinejad, B., Herrero, J.L., Mehta, A.D. and Mesgarani, N. (2019) ‘Towards reconstructing intelligible speech from the human auditory cortex’, *Scientific Reports*, 9(1). Available at: <https://doi.org/10.1038/s41598-018-37359-z>.

Akin, M. (2002) *Comparison of Wavelet Transform and FFT Methods in the Analysis of EEG Signals*, *Journal of Medical Systems*.

Akrami, A., Solhjoo, S., Motie-Nasrabadi, A. and Hashemi-Golpayegani, M.R. (2005) ‘EEG-based mental task classification: Linear and nonlinear classification of movement imagery’, in *Annual International Conference of the IEEE Engineering in Medicine and Biology - Proceedings*. Institute of Electrical and Electronics Engineers Inc., pp. 4626–4629. Available at: <https://doi.org/10.1109/iembs.2005.1615501>.

Al-Azmi, A., Al-Habaibeh, A. and Abbas, J. (2023) ‘Sensor fusion and the application of artificial intelligence to identify tool wear in turning operations’, *The International Journal of Advanced Manufacturing Technology*, 126(1–2), pp. 429–442. Available at: <https://doi.org/10.1007/s00170-023-11113-w>.

Albuquerque, V.H.C. de, Pinheiro, P.R., Papa, J.P., Tavares, J.M.R.S., Menezes, R.P. de and Oliveira, C.A.S. (2016) ‘Recent Advances in Brain Signal Analysis: Methods and Applications’, *Computational Intelligence and Neuroscience*, 2016, pp. 1–2. Available at: <https://doi.org/10.1155/2016/2742943>.

Al-Fahoum, A.S. and Al-Fraihat, A.A. (2014) ‘Methods of EEG Signal Features Extraction Using Linear Analysis in Frequency and Time-Frequency Domains’, *ISRN Neuroscience*, 2014, pp. 1–7. Available at: <https://doi.org/10.1155/2014/730218>.

Al-Habaibeh, A. (2000) *Rapid design of condition monitoring systems for machining operations*. Edited by M. and M.E. and M. University of Nottingham. Theses. Mechanical.

Al-Habaibeh, A. and Gindy, N. (2000) ‘A new approach for systematic design of condition monitoring systems for milling processes’, *Journal of Materials Processing Technology*, 107, pp. 243–251.

Al-Habaibeh, A. and Gindy, N. (2000) 'A new approach for systematic design of condition monitoring systems for milling processes', *Journal of Materials Processing Technology*, 107(1–3), pp. 243–251. Available at: [https://doi.org/10.1016/S0924-0136\(00\)00718-4](https://doi.org/10.1016/S0924-0136(00)00718-4).

Al-Habaibeh, A., Zorriassatine, F. and Gindy, N. (2002) 'Comprehensive experimental evaluation of a systematic approach for cost effective and rapid design of condition monitoring systems using Taguchi's method', *Journal of Materials Processing Technology*, pp. 372–383.

Alkhadafe, H. (2015) *Computational Intelligence for Fault Diagnosis in Gearbox Systems*.

Alkhadafe, H., Al-Habaibeh, A. and Lotfi, A. (2016) 'Condition monitoring of helical gears using automated selection of features and sensors', *Measurement: Journal of the International Measurement Confederation*, 93, pp. 164–177. Available at: <https://doi.org/10.1016/j.measurement.2016.07.011>.

Almajidy, R.K., Mottaghi, S., Ajwad, A.A., Boudria, Y., Mankodiya, K., Besio, W. and Hofmann, U.G. (2023) 'A case for hybrid BCIs: combining optical and electrical modalities improves accuracy', *Frontiers in Human Neuroscience*, 17. Available at: <https://doi.org/10.3389/fnhum.2023.1162712>.

An, X., Kuang, D., Guo, X., Zhao, Y. and He, L. (2014) 'A Deep Learning Method for Classification of EEG Data Based on Motor Imagery', in *LNBI*, pp. 203–210. Available at: [https://doi.org/10.1007/978-3-319-09330-7\\_25](https://doi.org/10.1007/978-3-319-09330-7_25).

al-Qerem, A., Kharbat, F., Nashwan, S., Ashraf, S. and blaou, khairi (2020) 'General model for best feature extraction of EEG using discrete wavelet transform wavelet family and differential evolution', *International Journal of Distributed Sensor Networks*, 16(3), p. 155014772091100. Available at: <https://doi.org/10.1177/1550147720911009>.

Atangana, R., Tchiotsop, D., Kenne, G. and DjoufackNkengfac k, L.C. (2020) 'EEG Signal Classification using LDA and MLP Classifier', *Health Informatics - An International Journal*, 9(1), pp. 14–32. Available at: <https://doi.org/10.5121/hij.2020.9102>.

El Bahy, M.M., Hosny, M., Mohamed, W.A. and Ibrahim, S. (2017) 'EEG signal classification using neural network and support vector machine in brain computer

interface’, in *Advances in Intelligent Systems and Computing*. Springer Verlag, pp. 246–256. Available at: [https://doi.org/10.1007/978-3-319-48308-5\\_24](https://doi.org/10.1007/978-3-319-48308-5_24).

Bajaj, N. (2021) ‘Wavelets for EEG Analysis’, in *Wavelet Theory*. IntechOpen. Available at: <https://doi.org/10.5772/intechopen.94398>.

Bansal, D. and Mahajan, R. (2019) ‘EEG Based BCI—Control Applications’, in *EEG-Based Brain-Computer Interfaces*. Elsevier, pp. 167–193. Available at: <https://doi.org/10.1016/B978-0-12-814687-3.00006-5>.

Barna, G. and Kaski, K. (1990) ‘Stochastic vs. deterministic neural networks for pattern recognition’, *Physica Scripta*, 1990(T33), pp. 110–115. Available at: <https://doi.org/10.1088/0031-8949/1990/T33/019>.

Bashashati, A., Fatourechi, M., Ward, R.K. and Birch, G.E. (2007) ‘A survey of signal processing algorithms in brain-computer interfaces based on electrical brain signals’, *Journal of Neural Engineering*. Available at: <https://doi.org/10.1088/1741-2560/4/2/R03>.

Bhardwaj, A. (2012) *Detection of Gallbladder Stone Using Learning Vector Quantization Neural Network*. Available at: <https://www.researchgate.net/publication/227854959>.

Bharti, M., Bharti, P., Kumar, M. and Kumar, P. (2021) ‘Diffuse scattering model for human brain wave (Alpha) propagation prediction during meditation inside a temple, through ray tracing, a hypothetical study’, *International Multidisciplinary Research Journal*, pp. 25–29. Available at: <https://doi.org/10.25081/imrj.2021.v11.7275>.

Bhuvaneshwari, M., Kanaga, E.G.M., Anitha, J., Raimond, K. and George, S.T. (2021) ‘A comprehensive review on deep learning techniques for a BCI-based communication system’, in *Demystifying Big Data, Machine Learning, and Deep Learning for Healthcare Analytics*. Elsevier, pp. 131–157. Available at: <https://doi.org/10.1016/B978-0-12-821633-0.00013-1>.

Bilucaglia, M., Duma, G.M., Mento, G., Semenzato, L. and Tressoldi, P.E. (2020) ‘Applying machine learning EEG signal classification to emotion-related brain anticipatory activity’, *F1000Research*, 9, p. 173. Available at: <https://doi.org/10.12688/f1000research.22202.1>.

- Birbaumer, N., Ghanayim, N., Hinterberger, T., Iversen, I., Kotchoubey, B., Kübler, A., Perelmouter, J., Taub, E. and Flor, H. (1999) 'A spelling device for the paralysed', *Nature*, 398(6725), pp. 297–298. Available at: <https://doi.org/10.1038/18581>.
- Blinowska, K. and Durka, P. (2006) 'Electroencephalography (EEG)', in *Wiley Encyclopedia of Biomedical Engineering*. Hoboken, NJ, USA: John Wiley & Sons, Inc. Available at: <https://doi.org/10.1002/9780471740360.ebs0418>.
- Buccino, A.P., Keles, H.O. and Omurtag, A. (2016) 'Hybrid EEG-fNIRS Asynchronous Brain-Computer Interface for Multiple Motor Tasks', *PLOS ONE*. Edited by B. He, 11(1), p. e0146610. Available at: <https://doi.org/10.1371/journal.pone.0146610>.
- Carter, R., Aldridge, S., Page, M. and Parker, S. (2019) *THE HUMAN BRAIN BOOK*. Updated new edition. Edited by M. Page. New York, NY: DK Publishing.
- Chaudhary, U., Xia, B., Silvoni, S., Cohen, L.G. and Birbaumer, N. (2017) 'Brain–Computer Interface–Based Communication in the Completely Locked-In State', *PLOS Biology*. Edited by N.F. Ramsey, 15(1), p. e1002593. Available at: <https://doi.org/10.1371/journal.pbio.1002593>.
- Chén, O.Y. (2019) 'The roles of statistics in human neuroscience', *Brain Sciences*, 9(8). Available at: <https://doi.org/10.3390/brainsci9080194>.
- Craik, A., He, Y. and Contreras-Vidal, J.L. (2019) 'Deep learning for electroencephalogram (EEG) classification tasks: a review', *Journal of Neural Engineering*, 16(3), p. 031001. Available at: <https://doi.org/10.1088/1741-2552/ab0ab5>.
- Cvetkovic, D., Übeyli, E.D. and Cosic, I. (2008) 'Wavelet transform feature extraction from human PPG, ECG, and EEG signal responses to ELF PEMF exposures: A pilot study', *Digital Signal Processing: A Review Journal*, 18(5), pp. 861–874. Available at: <https://doi.org/10.1016/j.dsp.2007.05.009>.
- Dadebayev, D., Goh, W.W. and Tan, E.X. (2022) 'EEG-based emotion recognition: Review of commercial EEG devices and machine learning techniques', *Journal of King Saud University - Computer and Information Sciences*. King Saud bin Abdulaziz University, pp. 4385–4401. Available at: <https://doi.org/10.1016/j.jksuci.2021.03.009>.

- Datta, S. and Boulgouris, N. V. (2021) ‘Recognition of grammatical class of imagined words from EEG signals using convolutional neural network’, *Neurocomputing*, 465, pp. 301–309. Available at: <https://doi.org/10.1016/j.neucom.2021.08.035>.
- Delimayanti, M.K., Purnama, B., Nguyen, N.G., Faisal, M.R., Mahmudah, K.R., Indriani, F., Kubo, M. and Satou, K. (2020) ‘Classification of brainwaves for sleep stages by high-dimensional FFT features from EEG signals’, *Applied Sciences (Switzerland)*, 10(5). Available at: <https://doi.org/10.3390/app10051797>.
- DeSesso, J.M. (2009) ‘Functional Anatomy of the Brain’, in D.W. McCandless (ed.) *Metabolic Encephalopathy*. New York, NY: Springer New York, pp. 1–14. Available at: [https://doi.org/10.1007/978-0-387-79112-8\\_1](https://doi.org/10.1007/978-0-387-79112-8_1).
- Fabietti, M., Mahmud, M. and Lotfi, A. (2021) ‘On-Chip Machine Learning for Portable Systems: Application to Electroencephalography-based Brain-Computer Interfaces’, in *Proceedings of the International Joint Conference on Neural Networks*. Institute of Electrical and Electronics Engineers Inc. Available at: <https://doi.org/10.1109/IJCNN52387.2021.9533413>.
- Farwell, L.A. and Donchin, E. (1988) ‘Talking off the top of your head: toward a mental prosthesis utilizing event-related brain potentials’, *Electroencephalography and Clinical Neurophysiology*, 70(6), pp. 510–523. Available at: [https://doi.org/10.1016/0013-4694\(88\)90149-6](https://doi.org/10.1016/0013-4694(88)90149-6).
- Gallegos-Ayala, G., Furdea, A., Takano, K., Ruf, C.A., Flor, H. and Birbaumer, N. (2014) ‘Brain communication in a completely locked-in patient using bedside near-infrared spectroscopy’, *Neurology*, 82(21), pp. 1930–1932. Available at: <https://doi.org/10.1212/WNL.0000000000000449>.
- Garcés, M.A. and Orosco, L.L. (2008) ‘EEG signal processing in brain–computer interface’, in *Smart Wheelchairs and Brain-Computer Interfaces*. Elsevier, pp. 95–110. Available at: <https://doi.org/10.1016/B978-0-12-812892-3.00005-4>.
- García, L., Ron-Angevin, R., Loubière, B., Renault, L., Le Masson, G., Lespinet-Najib, V. and André, J.M. (2017) ‘A Comparison of a Brain-Computer Interface and an Eye Tracker: Is There a More Appropriate Technology for Controlling a Virtual Keyboard in an ALS Patient?’, in pp. 464–473. Available at: [https://doi.org/10.1007/978-3-319-59147-6\\_40](https://doi.org/10.1007/978-3-319-59147-6_40).

- Gevins, A., Smith, M.E., McEvoy, L.K., Leong, H. and Le, J. (1999) 'Electroencephalographic imaging of higher brain function', *Philosophical Transactions of the Royal Society of London. Series B: Biological Sciences*. Edited by A. Howseman and S. Zeki, 354(1387), pp. 1125–1134. Available at: <https://doi.org/10.1098/rstb.1999.0468>.
- Gholamy, A., Kreinovich, V. and Kosheleva, O. (2018) *A Pedagogical Explanation A Pedagogical Explanation Part of the Computer Sciences Commons*. Available at: [https://scholarworks.utep.edu/cgi/viewcontent.cgi?article=2202&context=cs\\_techrep](https://scholarworks.utep.edu/cgi/viewcontent.cgi?article=2202&context=cs_techrep) (Accessed: 19 August 2024).
- Glassman, E.L. (2005) 'A wavelet-like filter based on neuron action potentials for analysis of human scalp electroencephalographs', *IEEE Transactions on Biomedical Engineering*, 52(11), pp. 1851–1862. Available at: <https://doi.org/10.1109/TBME.2005.856277>.
- Glover, G.H. (2011) 'Overview of Functional Magnetic Resonance Imaging', *Neurosurgery Clinics of North America*, 22(2), pp. 133–139. Available at: <https://doi.org/10.1016/j.nec.2010.11.001>.
- Graimann, B., Huggins, J.E., Levine, S.P. and Pfurtscheller, G. (2004) 'Toward a direct brain interface based on human subdural recordings and wavelet-packet analysis', *IEEE Transactions on Biomedical Engineering*, 51(6), pp. 954–962. Available at: <https://doi.org/10.1109/TBME.2004.826671>.
- Grover, V.P.B., Tognarelli, J.M., Crossey, M.M.E., Cox, I.J., Taylor-Robinson, S.D. and McPhail, M.J.W. (2015) 'Magnetic Resonance Imaging: Principles and Techniques: Lessons for Clinicians', *Journal of Clinical and Experimental Hepatology*. Elsevier B.V., pp. 246–255. Available at: <https://doi.org/10.1016/j.jceh.2015.08.001>.
- Gupta, A., Agrawal, R.K., Kirar, J.S., Kaur, B., Ding, W., Lin, C.T., Andreu-Perez, J. and Prasad, M. (2020) 'A hierarchical meta-model for multi-class mental task based brain-computer interfaces', *Neurocomputing*, 389, pp. 207–217. Available at: <https://doi.org/10.1016/j.neucom.2018.07.094>.
- Gupta, S. Sen, Soman, S., Raj, P.G. and Prakash, R. (2014) 'Improved classification of motor imagery datasets for BCI by using approximate entropy and WOSF features', in *2014 International Conference on Signal Processing and Integrated Networks, SPIN 2014*. IEEE Computer Society, pp. 90–94. Available at: <https://doi.org/10.1109/spin.2014.6776928>.

- Hadjiyannakis, K., Ogilvie, R.D., Alloway, C.E.D. and Shapiro, C. (1997) 'FFT analysis of EEG during stage 2-to-REM transitions in narcoleptic patients and normal sleepers', *Electroencephalography and Clinical Neurophysiology*, 103(5), pp. 543–553. Available at: [https://doi.org/10.1016/S0013-4694\(97\)00064-3](https://doi.org/10.1016/S0013-4694(97)00064-3).
- Halford, J.J., Sabau, D., Drislane, F.W., Tsuchida, T.N. and Sinha, S.R. (2016) 'American Clinical Neurophysiology Society Guideline 4: Recording Clinical EEG on Digital Media', *Journal of Clinical Neurophysiology*, 33(4), pp. 317–319. Available at: <https://doi.org/10.1097/WNP.0000000000000318>.
- Hamzah, H.A. and Abdalla, K.K. (2024) 'EEG-based emotion recognition systems; comprehensive study', *Heliyon*. Elsevier Ltd. Available at: <https://doi.org/10.1016/j.heliyon.2024.e31485>.
- Hartshorne, M.F. (1995) 'Positron Emission Tomography', in W.W. Orrison, J.D. Lewine, J.A. Sanders, and M.F. Hartshorne (eds) *Functional Brain Imaging*. Elsevier, pp. 187–212. Available at: <https://doi.org/10.1016/B978-0-8151-6509-5.50009-6>.
- Hebert, R., Lehmann, D., Tan, G., Travis, F. and Arenander, A. (2005) 'Enhanced EEG alpha time-domain phase synchrony during Transcendental Meditation: Implications for cortical integration theory', *Signal Processing*, 85(11), pp. 2213–2232. Available at: <https://doi.org/10.1016/J.SIGPRO.2005.07.009>.
- Heraz, A. and Frasson, C. (2011) 'Towards a Brain-Sensitive Intelligent Tutoring System: Detecting Emotions from Brainwaves', *Advances in Artificial Intelligence*, 2011, pp. 1–13. Available at: <https://doi.org/10.1155/2011/384169>.
- Herff, C., Heger, D., de Pestors, A., Telaar, D., Brunner, P., Schalk, G. and Schultz, T. (2015) 'Brain-to-text: decoding spoken phrases from phone representations in the brain', *Frontiers in Neuroscience*, 9, p. 217. Available at: <https://doi.org/10.3389/fnins.2015.00217>.
- Hinterberger, T., Schmidt, S., Neumann, N., Mellinger, J., Blankertz, B., Curio, G. and Birbaumer, N. (2004) 'Brain-computer communication and slow cortical potentials', *IEEE Transactions on Biomedical Engineering*, 51(6), pp. 1011–1018. Available at: <https://doi.org/10.1109/TBME.2004.827067>.

Hoshi, Y. (2009) 'Near-Infrared Spectroscopy for Studying Higher Cognition', in, pp. 83–93. Available at: [https://doi.org/10.1007/978-3-540-68044-4\\_6](https://doi.org/10.1007/978-3-540-68044-4_6).

Hramov, A.E., Maksimenko, V.A., Pchelintseva, S. V., Runnova, A.E., Grubov, V. V., Musatov, V.Yu., Zhuravlev, M.O., Koronovskii, A.A. and Pisarchik, A.N. (2017) 'Classifying the Perceptual Interpretations of a Bistable Image Using EEG and Artificial Neural Networks', *Frontiers in Neuroscience*, 11(DEC). Available at: <https://doi.org/10.3389/fnins.2017.00674>.

Huang, Z. and Wang, M. (2021) 'A review of electroencephalogram signal processing methods for brain-controlled robots', *Cognitive Robotics*, 1, pp. 111–124. Available at: <https://doi.org/10.1016/j.cogr.2021.07.001>.

Huisheng Lu, Mingshi Wang and Hongqiang Yu (2005) 'EEG Model and Location in Brain when Enjoying Music', in *2005 IEEE Engineering in Medicine and Biology 27th Annual Conference*. IEEE, pp. 2695–2698. Available at: <https://doi.org/10.1109/IEMBS.2005.1617026>.

Di Ieva, A. (2011) *BRAIN ANATOMY FROM A CLINICAL AND NEUROSURGICAL PERSPECTIVE A clinically oriented manual of neuroanatomy*.

Imran, A., Chaudhary, H., Tariq, M., Ali, Z., Ahad, A., Naqvi, H., Coelho, P.J. and Pires, I.M. (2024) 'Brain-Controlled Computer Tasks for Paralyzed Persons: Framework Overview', *Procedia Computer Science*, 237, pp. 28–35. Available at: <https://doi.org/10.1016/j.procs.2024.05.076>.

Ishino, K. and Hagiwara, M. (2003) 'A feeling estimation system using a simple electroencephalograph', in *SMC'03 Conference Proceedings. 2003 IEEE International Conference on Systems, Man and Cybernetics. Conference Theme - System Security and Assurance (Cat. No.03CH37483)*. IEEE, pp. 4204–4209. Available at: <https://doi.org/10.1109/ICSMC.2003.1245645>.

Jacob, J.E., Chandrasekharan, S., Nair, G.K., Cherian, A. and Iype, T. (2021) 'Effect of combining features generated through non-linear analysis and wavelet transform of EEG signals for the diagnosis of encephalopathy', *Neuroscience Letters*, 765. Available at: <https://doi.org/10.1016/j.neulet.2021.136269>.

- Jaswal, R. (2016) 'Brain Wave Classification and Feature Extraction of EEG Signal by Using FFT on Lab View', *International Research Journal of Engineering and Technology* [Preprint]. Available at: [www.irjet.net](http://www.irjet.net).
- Ji, N., Ma, L., Dong, H. and Zhang, X. (2019) 'EEG signals feature extraction based on DWT and EMD combined with approximate entropy', *Brain Sciences*, 9(8). Available at: <https://doi.org/10.3390/brainsci9080201>.
- Jirayucharoensak, S., Pan-Ngum, S. and Israsena, P. (2014) 'EEG-Based Emotion Recognition Using Deep Learning Network with Principal Component Based Covariate Shift Adaptation', *Scientific World Journal*, 2014. Available at: <https://doi.org/10.1155/2014/627892>.
- Kit, N.K., Amin, H.U., Ng, K.H., Price, J. and Subhani, A.R. (2023) 'EEG Feature Extraction based on Fast Fourier Transform and Wavelet Analysis for Classification of Mental Stress Levels using Machine Learning', *Advances in Science, Technology and Engineering Systems Journal*, 8(6), pp. 46–56. Available at: <https://doi.org/10.25046/aj080606>.
- Klem, G.H., Lüders, H., Jasper, H.H. and Elger, C.E. (1999) 'The ten-twenty electrode system of the International Federation. The International Federation of Clinical Neurophysiology.', *Electroencephalography and clinical neurophysiology. Supplement*, 52, pp. 3–6. Available at: <https://api.semanticscholar.org/CorpusID:27778550>.
- Kotsiopoulos, T., Sarigiannidis, P., Ioannidis, D. and Tzovaras, D. (2021) 'Machine Learning and Deep Learning in smart manufacturing: The Smart Grid paradigm', *Computer Science Review*. Elsevier Ireland Ltd. Available at: <https://doi.org/10.1016/j.cosrev.2020.100341>.
- Kousarrizi, M.R.N., Ghanbari, A.A., Teshnehlab, M., Aliyari, M. and Gharaviri, A. (2009) 'Feature extraction and classification of EEG signals using wavelet transform, SVM and artificial neural networks for brain computer interfaces', in *Proceedings - 2009 International Joint Conference on Bioinformatics, Systems Biology and Intelligent Computing, IJCBS 2009*, pp. 352–355. Available at: <https://doi.org/10.1109/IJCBS.2009.100>.

- Kumar, J.S. and Bhuvaneshwari, P. (2012) ‘Analysis of electroencephalography (EEG) signals and its categorization - A study’, in *Procedia Engineering*. Elsevier Ltd, pp. 2525–2536. Available at: <https://doi.org/10.1016/j.proeng.2012.06.298>.
- Lakshmi, M.R., Prasad, T. V and Chandra Prakash, V. (2014) *Survey on EEG Signal Processing Methods, International Journal of Advanced Research in Computer Science and Software Engineering*. Available at: <https://www.researchgate.net/publication/328419840>.
- Långkvist, M., Karlsson, L. and Loutfi, A. (2012) ‘Sleep Stage Classification Using Unsupervised Feature Learning’, *Advances in Artificial Neural Systems*, 2012, pp. 1–9. Available at: <https://doi.org/10.1155/2012/107046>.
- Lazarou, I., Nikolopoulos, S., Petrantonakis, P.C., Kompatsiaris, I. and Tsolaki, M. (2018) ‘EEG-based brain–computer interfaces for communication and rehabilitation of people with motor impairment: A novel approach of the 21st century’, *Frontiers in Human Neuroscience*. Frontiers Media S. A. Available at: <https://doi.org/10.3389/fnhum.2018.00014>.
- Ledwidge, P., Foust, J. and Ramsey, A. (2018) ‘Recommendations for Developing an EEG Laboratory at a Primarily Undergraduate Institution’, *The Journal of Undergraduate Neuroscience Education* [Preprint]. Available at: [www.funjournal.org](http://www.funjournal.org).
- Lewine, J.D. (1995) ‘Introduction to Functional Neuroimaging: Functional Neuroanatomy’, in W.W. Orrison, J.D. Lewine, J.A. Sanders, and M.F. Hartshorne (eds) *Functional Brain Imaging*. Elsevier, pp. 13–95. Available at: <https://doi.org/10.1016/B978-0-8151-6509-5.50006-0>.
- Li, G., Lee, C.H., Jung, J.J., Youn, Y.C. and Camacho, D. (2020) ‘Deep learning for EEG data analytics: A survey’, in *Concurrency and Computation: Practice and Experience*. John Wiley and Sons Ltd. Available at: <https://doi.org/10.1002/cpe.5199>.
- Li, M. and Chen, W. (2021) ‘FFT-based deep feature learning method for EEG classification’, *Biomedical Signal Processing and Control*, 66, p. 102492. Available at: <https://doi.org/10.1016/j.bspc.2021.102492>.

- Li, R., Yang, D., Fang, F., Hong, K.S., Reiss, A.L. and Zhang, Y. (2022) ‘Concurrent fNIRS and EEG for Brain Function Investigation: A Systematic, Methodology-Focused Review’, *Sensors*. MDPI. Available at: <https://doi.org/10.3390/s22155865>.
- Li, T.M., Chao, H.C. and Zhang, J. (2019) ‘Emotion classification based on brain wave: a survey’, *Human-centric Computing and Information Sciences*. Springer. Available at: <https://doi.org/10.1186/s13673-019-0201-x>.
- Lin, C.J. and Hsieh, M.H. (2009) ‘Classification of mental task from EEG data using neural networks based on particle swarm optimization’, *Neurocomputing*, 72(4–6), pp. 1121–1130. Available at: <https://doi.org/10.1016/j.neucom.2008.02.017>.
- Llorella, F.R., Iáñez, E., Azorín, J.M. and Patow, G. (2021) ‘Classification of imagined geometric shapes using EEG signals and convolutional neural networks’, *Neuroscience Informatics*, 1(4), p. 100029. Available at: <https://doi.org/10.1016/j.neuri.2021.100029>.
- Lopes da Silva, F. (2013) ‘EEG and MEG: Relevance to Neuroscience’, *Neuron*, 80(5), pp. 1112–1128. Available at: <https://doi.org/10.1016/J.NEURON.2013.10.017>.
- Lotte, F. (2012) *A new feature and associated optimal spatial filter for EEG signal classification: Waveform Length*. Available at: <http://www.bbc.de/competition/>.
- Lystad, R.P. and Pollard, H. (2009) ‘Functional neuroimaging: a brief overview and feasibility for use in chiropractic research.’, *The Journal of the Canadian Chiropractic Association*, 53(1), pp. 59–72. Available at: <http://www.ncbi.nlm.nih.gov/pubmed/19421353>.
- MacDonald, D.B. (2015) ‘Electroencephalography: Basic Principles and Applications’, in *International Encyclopedia of the Social & Behavioral Sciences: Second Edition*. Elsevier Inc., pp. 353–363. Available at: <https://doi.org/10.1016/B978-0-08-097086-8.55017-X>.
- Maiorana, E. (2020) ‘Deep learning for EEG-based biometric recognition’, *Neurocomputing*, 410, pp. 374–386. Available at: <https://doi.org/10.1016/j.neucom.2020.06.009>.
- Majoros, T., Oniga, S. and Xie, Y. (2021) ‘Motor imagery eeg classification using feedforward neural network’, *Annales Mathematicae et Informaticae*, 53, pp. 235–244. Available at: <https://doi.org/10.33039/ami.2021.04.007>.

- Marcuse, L. V, Fields, M.C. and Yoo, J. (Jenna) (2016) ‘Origin and technical aspects of the EEG’, in L. V Marcuse, M.C. Fields, and J. (Jenna) Yoo (eds) *Rowan’s Primer of EEG*. Second Edition. London: Elsevier, pp. 1–37. Available at: <https://doi.org/10.1016/B978-0-323-35387-8.00001-9>.
- McFarland, D.J., Krusienski, D.J., Sarnacki, W.A. and Wolpaw, J.R. (2008) ‘Emulation of computer mouse control with a noninvasive brain-computer interface’, *Journal of Neural Engineering*, 5(2), pp. 101–110. Available at: <https://doi.org/10.1088/1741-2560/5/2/001>.
- Michel, C.M., Murray, M.M., Lantz, G., Gonzalez, S., Spinelli, L. and Grave De Peralta, R. (2004) ‘EEG source imaging’, *Clinical Neurophysiology*, pp. 2195–2222. Available at: <https://doi.org/10.1016/j.clinph.2004.06.001>.
- Mishra, L., Behera, R., Pattanaik, S. and Singh, N.R. (2022) ‘Role of CT scan in medical and dental imaging’, in *Biomedical Imaging Instrumentation*. Elsevier, pp. 13–32. Available at: <https://doi.org/10.1016/B978-0-323-85650-8.00006-1>.
- Mizuno, Y., Mabuchi, H., Chakraborty, G. and Matsuhara, M. (2010) ‘Clustering of EEG data using maximum entropy method and LVQ’, in *Proceedings of the 10th WSEAS International Conference on Systems Theory and Scientific Computation*. Stevens Point, Wisconsin, USA: World Scientific and Engineering Academy and Society (WSEAS) (ISTASC’10), pp. 71–76.
- Montesinos López Osva Antonio and Montesinos López, A. and C.J. (2022) ‘Fundamentals of Artificial Neural Networks and Deep Learning’, in *Multivariate Statistical Machine Learning Methods for Genomic Prediction*. Cham: Springer International Publishing, pp. 379–425. Available at: [https://doi.org/10.1007/978-3-030-89010-0\\_10](https://doi.org/10.1007/978-3-030-89010-0_10).
- Murugappan, M. and Murugappan, S. (2013) ‘Human emotion recognition through short time Electroencephalogram (EEG) signals using Fast Fourier Transform (FFT)’, in *Proceedings - 2013 IEEE 9th International Colloquium on Signal Processing and its Applications, CSPA 2013*, pp. 289–294. Available at: <https://doi.org/10.1109/CSPA.2013.6530058>.
- Murugappan, M., Ramachandran, N. and Sazali, Y. (2010) ‘Classification of human emotion from EEG using discrete wavelet transform’, *Journal of Biomedical Science and Engineering*, 03(04), pp. 390–396. Available at: <https://doi.org/10.4236/jbise.2010.34054>.

- Murugappan, M., Rizon, M., Nagarajan, R. and Yaacob, S. (2008) 'EEG feature extraction for classifying emotions using FCM and FKM', *INTERNATIONAL JOURNAL OF COMPUTERS AND COMMUNICATIONS Issue*, 1(2), pp. 299–304.
- Narayan, Y. (2021) *Motor-Imagery based EEG Signals Classification using MLP and KNN Classifiers*, *Turkish Journal of Computer and Mathematics Education*.
- Naseer, N. and Hong, K.S. (2015) 'fNIRS-based brain-computer interfaces: A review', *Frontiers in Human Neuroscience*. Frontiers Media S. A. Available at: <https://doi.org/10.3389/fnhum.2015.00003>.
- Neuroimaging Market - Share, Size and Industry Analysis* (2023). Available at: <https://www.coherentmarketinsights.com/industry-reports/neuroimaging-market> (Accessed: 21 August 2024).
- Nguyen, T., Khosravi, A., Creighton, D. and Nahavandi, S. (2015) 'EEG signal classification for BCI applications by wavelets and interval type-2 fuzzy logic systems', *Expert Systems with Applications*, 42(9), pp. 4370–4380. Available at: <https://doi.org/10.1016/j.eswa.2015.01.036>.
- Nicolas-Alonso, L.F. and Gomez-Gil, J. (2012) 'Brain Computer Interfaces, a Review', *Sensors*, 12(2), pp. 1211–1279. Available at: <https://doi.org/10.3390/s120201211>.
- Niedermeyer, E., Schomer, D.L. and Lopes da Silva, F. H. (2017) *Niedermeyer's Electroencephalography*. Edited by D.L. Schomer and Fernando H. Lopes da Silva. Oxford University Press. Available at: <https://doi.org/10.1093/med/9780190228484.001.0001>.
- Niha, K. and Banu, W.A. (2016) 'Brain signal processing: Technologies, analysis and application', in *2016 IEEE International Conference on Computational Intelligence and Computing Research (ICIC)*. IEEE, pp. 1–6. Available at: <https://doi.org/10.1109/ICIC.2016.7919569>.
- Pandarathan, G., Mishra, S., Nedumaran, A.M., Padmanabhan, P. and Gulyás, B. (2018) 'The potential of cognitive neuroimaging: A way forward to the mind-machine interface', *Journal of Imaging*. MDPI Multidisciplinary Digital Publishing Institute. Available at: <https://doi.org/10.3390/jimaging4050070>.

- Pfurtscheller, G. and Pregenzer, M. (1999) 'LVQ and single trial EEG classification', in *Kohonen Maps*. Elsevier, pp. 317–327. Available at: <https://doi.org/10.1016/B978-044450270-4/50025-5>.
- Pinti, P., Tachtsidis, I., Burgess, P.W. and Hamilton, A.F. de C. (2023) 'Non-invasive optical imaging of brain function with fNIRS: Current status and way forward', in *Reference Module in Neuroscience and Biobehavioral Psychology*. Elsevier. Available at: <https://doi.org/10.1016/B978-0-12-820480-1.00028-0>.
- Pohlmeier, R., Buchner, H., Knoll, G., Rienacker, A., Beckmann, R. and Pesch, J. (1997) 'The influence of skull-conductivity misspecification on inverse source localization in realistically shaped finite element head models', *Brain Topography*, 9(3), pp. 157–162. Available at: <https://doi.org/10.1007/BF01190384>.
- Polat, K. and Güneş, S. (2008) 'Artificial immune recognition system with fuzzy resource allocation mechanism classifier, principal component analysis and FFT method based new hybrid automated identification system for classification of EEG signals', *Expert Systems with Applications*, 34(3), pp. 2039–2048. Available at: <https://doi.org/10.1016/j.eswa.2007.02.009>.
- Powell, M.J. (1977) 'Restart procedures for the conjugate gradient method', *Math. Program.*, 12(1), pp. 241–254. Available at: <https://doi.org/10.1007/BF01593790>.
- Power, S.P., Moloney, F., Twomey, M., James, K., O'Connor, O.J. and Maher, M.M. (2016) 'Computed tomography and patient risk: Facts, perceptions and uncertainties', *World Journal of Radiology*, 8(12), p. 902. Available at: <https://doi.org/10.4329/wjr.v8.i12.902>.
- Rácz, A., Bajusz, D. and Héberger, K. (2021) 'Effect of dataset size and train/test split ratios in qsar/qspr multiclass classification', *Molecules*, 26(4). Available at: <https://doi.org/10.3390/molecules26041111>.
- Rajashekhar, U., Neelappa, D. and Rajesh, L. (2022) 'Electroencephalogram (EEG) signal classification for brain–computer interface using discrete wavelet transform (DWT)', *International Journal of Intelligent Unmanned Systems*, 10(1), pp. 86–97. Available at: <https://doi.org/10.1108/IJIUS-09-2020-0057>.

- Ramadan, R.A. and Vasilakos, A. V. (2017) 'Brain computer interface: control signals review', *Neurocomputing*, 223, pp. 26–44. Available at: <https://doi.org/10.1016/j.neucom.2016.10.024>.
- Rehana, K., Tabish, S.A., Gojwari, T., Ahmad, R. and Abdul, H. (2013) 'Unit cost of CT scan and MRI at a large tertiary care teaching hospital in North India', *Health*, 05(12), pp. 2059–2063. Available at: <https://doi.org/10.4236/health.2013.512279>.
- Rihana, S., Damien, P. and Moujaess, T. (2012) 'Efficient eye blink detection system using RBF classifier', in *2012 IEEE Biomedical Circuits and Systems Conference: Intelligent Biomedical Electronics and Systems for Better Life and Better Environment, BioCAS 2012 - Conference Publications*, pp. 360–363. Available at: <https://doi.org/10.1109/BioCAS.2012.6418422>.
- Rögnvaldsson, T. (1992) 'Pattern Recognition with Artificial Neural Networks - a Benchmark Study of Scaling Behaviour', *Artificial Neural Networks*, pp. 1201–1205. Available at: <https://doi.org/10.1016/b978-0-444-89488-5.50080-4>.
- Saboo, K. V., Varatharajah, Y., Berry, B.M., Kremen, V., Sperling, M.R., Davis, K.A., Jobst, B.C., Gross, R.E., Lega, B., Sheth, S.A., Worrell, G.A., Iyer, R.K. and Kucewicz, M.T. (2019) 'Unsupervised machine-learning classification of electrophysiologically active electrodes during human cognitive task performance', *Scientific Reports*, 9(1). Available at: <https://doi.org/10.1038/s41598-019-53925-5>.
- Sainath, T.N., Kingsbury, B., Saon, G., Soltau, H., Mohamed, A., Dahl, G. and Ramabhadran, B. (2015) 'Deep Convolutional Neural Networks for Large-scale Speech Tasks', *Neural Networks*, 64, pp. 39–48. Available at: <https://doi.org/10.1016/j.neunet.2014.08.005>.
- Sairamya, N.J., Subathra, M.S.P. and Thomas George, S. (2022) 'Automatic identification of schizophrenia using EEG signals based on discrete wavelet transform and RLNDiP technique with ANN', *Expert Systems with Applications*, 192. Available at: <https://doi.org/10.1016/j.eswa.2021.116230>.
- Sakhavi, S. and Guan, C. (2017) 'Convolutional neural network-based transfer learning and knowledge distillation using multi-subject data in motor imagery BCI', in *2017 8th International IEEE/EMBS Conference on Neural Engineering (NER)*. IEEE, pp. 588–591. Available at: <https://doi.org/10.1109/NER.2017.8008420>.

- Saławun, W. (2014) 'Processing and spectral analysis of the raw EEG signal from the MindWave', *Przegląd Elektrotechniczny*, 90(2), pp. 169–173. Available at: <https://doi.org/10.12915/pe.2014.02.44>.
- Samar, V.J., Bopardikar, A., Rao, R. and Swartz, K. (1999) *Wavelet Analysis of Neuroelectric Waveforms: A Conceptual Tutorial, Brain and Language*. Available at: <http://www.idealibrary.comon>.
- Sankar, M., Narendra Babu, J., Halunde, S.S. and Mulik, M.B. (2019) 'Brain signal processing: Analysis, technologies and application', *Journal of Advanced Research in Dynamical and Control Systems*, 11(12), pp. 69–74. Available at: <https://doi.org/10.5373/JARDCS/V11I12/20193213>.
- Sarić, R., Jokić, D., Beganović, N., Pokvić, L.G. and Badnjević, A. (2020) 'FPGA-based real-time epileptic seizure classification using Artificial Neural Network', *Biomedical Signal Processing and Control*, 62. Available at: <https://doi.org/10.1016/j.bspc.2020.102106>.
- Sarracanie, M., Lapierre, C.D., Salameh, N., Waddington, D.E.J., Witzel, T. and Rosen, M.S. (2015) 'Low-Cost High-Performance MRI', *Scientific Reports*, 5, pp. 1–9. Available at: <https://doi.org/10.1038/srep15177>.
- Shaker, M.M. (2007) 'EEG Waves Classifier using Wavelet Transform and Fourier Transform', *World Academy of Science, Engineering and Technology, International Journal of Medical, Health, Biomedical, Bioengineering and Pharmaceutical Engineering*, 1, pp. 169–174. Available at: <https://api.semanticscholar.org/CorpusID:18959300>.
- Shakmak, B.H. (2016) *Condition Monitoring of Water Leakage Detection in Buried Pipes Using Sensor Fusion Systems*.
- Sharma, R., Kim, M. and Gupta, A. (2022) 'Motor imagery classification in brain-machine interface with machine learning algorithms: Classical approach to multi-layer perceptron model', *Biomedical Signal Processing and Control*, 71(PA), p. 103101. Available at: <https://doi.org/10.1016/j.bspc.2021.103101>.
- Shriram, R., Sundhararajan, Mahalingam, Sundhararajan, M and Daimiwal, N. (2012) 'EEG Based Cognitive Workload Assessment for Maximum Efficiency', *IOSR Journal of*

*Electronics and Communication Engineering (IOSR-JECE*, pp. 34–38. Available at: [www.iosrjournals.org](http://www.iosrjournals.org).

Singh, S.P. (2014) ‘Magnetoencephalography: Basic principles’, *Annals of Indian Academy of Neurology*, 17(SUPPL. 1). Available at: <https://doi.org/10.4103/0972-2327.128676>.

Smythies, J.R. (1995) ‘How do Brains Work? Papers of a Comparative Neurophysiologist. By T. H. Bullock. (Pp. 665.) Birkhauser: Boston, Mass.1993.’, *Psychological Medicine*. 2009/07/09, 25(6), pp. 1299–1300. Available at: <https://doi.org/10.1017/S0033291700033274>.

Soofi, A.A. and Awan, A. (2017) ‘Classification Techniques in Machine Learning: Applications and Issues’, *Journal of Basic & Applied Sciences*, 13, pp. 459–465. Available at: <https://doi.org/10.6000/1927-5129.2017.13.76>.

Stancin, I., Cifrek, M. and Jovic, A. (2021) ‘A Review of EEG Signal Features and Their Application in Driver Drowsiness Detection Systems’, *Sensors*, 21(11), p. 3786. Available at: <https://doi.org/10.3390/s21113786>.

Su, W.C., Dashtestani, H., Miguel, H.O., Condy, E., Buckley, A., Park, S., Perreault, J.B., Nguyen, T., Zeytinoglu, S., Millerhagen, J., Fox, N. and Gandjbakhche, A. (2023) ‘Simultaneous multimodal fNIRS-EEG recordings reveal new insights in neural activity during motor execution, observation, and imagery’, *Scientific Reports*, 13(1). Available at: <https://doi.org/10.1038/s41598-023-31609-5>.

Subasi, A. and Gursoy, M.I. (2010) ‘EEG signal classification using PCA, ICA, LDA and support vector machines’, *Expert Systems with Applications*, 37(12), pp. 8659–8666. Available at: <https://doi.org/10.1016/J.ESWA.2010.06.065>.

Subasi, A., Kiyimik, M.K., Alkan, A. and Koklukaya, E. (2005) ‘Neural network classification of EEG signals by using AR with MLE preprocessing for epileptic seizure detection’, *Mathematical and Computational Applications*, 10(1), pp. 57–70. Available at: <https://doi.org/10.3390/mca10010057>.

Subha, D.P., Joseph, P.K., Acharya U, R. and Lim, C.M. (2010) ‘EEG Signal Analysis: A Survey’, *Journal of Medical Systems*, 34(2), pp. 195–212. Available at: <https://doi.org/10.1007/s10916-008-9231-z>.

Tacke, M., Janson, K., Vill, K., Heinen, F., Gerstl, L., Reiter, K. and Borggraefe, I. (2022) 'Effects of a reduction of the number of electrodes in the EEG montage on the number of identified seizure patterns', *Scientific Reports*, 12(1). Available at: <https://doi.org/10.1038/s41598-022-08628-9>.

Talbot, K. (2002) 'Motor neurone disease', *Postgraduate Medical Journal*, 78(923), pp. 513–519. Available at: <https://doi.org/10.1136/pmj.78.923.513>.

Tan, D. and Nijholt, A. (2010) 'Brain-Computer Interfaces and Human-Computer Interaction', in, pp. 3–19. Available at: [https://doi.org/10.1007/978-1-84996-272-8\\_1](https://doi.org/10.1007/978-1-84996-272-8_1).

Tian, X. and Huber, D.E. (2008) 'Measures of spatial similarity and response magnitude in MEG and scalp EEG', *Brain Topography*, 20(3), pp. 131–141. Available at: <https://doi.org/10.1007/s10548-007-0040-3>.

*Top 5 Vendors in the Global Brain Monitoring Devices Market From 2017 to 2021: Technavio | Business Wire* (2017). Available at: <https://www.businesswire.com/news/home/20170703005538/en/Top-5-Vendors-in-the-Global-Brain-Monitoring-Devices-Market-From-2017-to-2021-Technavio> (Accessed: 21 August 2024).

*Top 10 Diagnostic Imaging Device Manufacturers & Leading Way* (2012). Available at: <https://www.hospitalmanagement.net/features/featuremedical-imaging-technology-diagnostic-device-manufacturers/?cf-view> (Accessed: 21 August 2024).

Trammel, T., Khodayari, N., Luck, S.J., Traxler, M.J. and Swaab, T.Y. (2023) 'Decoding semantic relatedness and prediction from EEG: A classification method comparison', *NeuroImage*, 277. Available at: <https://doi.org/10.1016/j.neuroimage.2023.120268>.

Treder, M.S. and Blankertz, B. (2010) '(C)overt attention and visual speller design in an ERP-based brain-computer interface', *Behavioral and Brain Functions*, 6(1), p. 28. Available at: <https://doi.org/10.1186/1744-9081-6-28>.

Tsinalis, O., Matthews, P.M., Guo, Y. and Zafeiriou, S. (2016) 'Automatic Sleep Stage Scoring with Single-Channel EEG Using Convolutional Neural Networks', *ArXiv*, abs/1610.01683. Available at: <https://api.semanticscholar.org/CorpusID:11607380>.

Uchida, S., Feinberg, I., March, J.D., Atsumi, Y. and Maloney, T. (1999) 'A Comparison of Period Amplitude Analysis and FFT Power Spectral Analysis of All-Night Human Sleep

EEG’, *Physiology & Behavior*, 67(1), pp. 121–131. Available at: [https://doi.org/10.1016/S0031-9384\(99\)00049-9](https://doi.org/10.1016/S0031-9384(99)00049-9).

Udina, C., Avtzi, S., Durduran, T., Holtzer, R., Rosso, A.L., Castellano-Tejedor, C., Perez, L.M., Soto-Bagaria, L. and Inzitari, M. (2020) ‘Functional Near-Infrared Spectroscopy to Study Cerebral Hemodynamics in Older Adults During Cognitive and Motor Tasks: A Review’, *Frontiers in Aging Neuroscience*. Frontiers Media S.A. Available at: <https://doi.org/10.3389/fnagi.2019.00367>.

Ullah, S. and Halim, Z. (2021) ‘Imagined character recognition through EEG signals using deep convolutional neural network’, *Medical and Biological Engineering and Computing*, 59(5), pp. 1167–1183. Available at: <https://doi.org/10.1007/s11517-021-02368-0>.

Usha Kumari, C., Kora, P., Meenakshi, K., Swaraja, K., Padma, T., Panigrahy, A.K. and Arun Vignesh, N. (2020) ‘Feature Extraction and Detection of Obstructive Sleep Apnea from Raw EEG Signal’, in *Advances in Intelligent Systems and Computing*. Springer, pp. 425–433. Available at: [https://doi.org/10.1007/978-981-15-1286-5\\_36](https://doi.org/10.1007/978-981-15-1286-5_36).

Vaid, S., Singh, P. and Kaur, C. (2015) ‘EEG signal analysis for BCI interface: A review’, in *International Conference on Advanced Computing and Communication Technologies, ACCT*. Institute of Electrical and Electronics Engineers Inc., pp. 143–147. Available at: <https://doi.org/10.1109/ACCT.2015.72>.

Vaquero, J.J. and Kinahan, P. (2015) ‘Positron Emission Tomography: Current Challenges and Opportunities for Technological Advances in Clinical and Preclinical Imaging Systems’, *Annual Review of Biomedical Engineering*, 17(1), pp. 385–414. Available at: <https://doi.org/10.1146/annurev-bioeng-071114-040723>.

Wahlund, L.O. (2020) ‘Structural brain imaging as a diagnostic tool in dementia, why and how?’, *Psychiatry Research - Neuroimaging*, 306. Available at: <https://doi.org/10.1016/j.psychresns.2020.111183>.

Wan Ismail, W.O.A.S., Hanif, M., Mohamed, S.B., Hamzah, N. and Rizman, Z.I. (2016) ‘Human emotion detection via brain waves study by using electroencephalogram (EEG)’, *International Journal on Advanced Science, Engineering and Information Technology*, 6(6), pp. 1005–1011. Available at: <https://doi.org/10.18517/ijaseit.6.6.1072>.

Wang, K., Zhao, Y., Xiong, Q., Fan, M., Sun, G., Ma, L. and Liu, T. (2016) 'Research on Healthy Anomaly Detection Model Based on Deep Learning from Multiple Time-Series Physiological Signals', *Scientific Programming*, 2016. Available at: <https://doi.org/10.1155/2016/5642856>.

Wei, J., Chen, T., Li, C., Liu, G., Qiu, J. and Wei, D. (2018) 'Eyes-open and eyes-closed resting states with opposite brain activity in sensorimotor and occipital regions: Multidimensional evidences from machine learning perspective', *Frontiers in Human Neuroscience*, 12. Available at: <https://doi.org/10.3389/fnhum.2018.00422>.

Wijeratne, U. and Perera, U. (2012) 'Intelligent Emotion Recognition System Using Electroencephalography and Active Shape Models', in *IEEE EMBS International Conference on Biomedical Engineering and Sciences*. IEEE. Available at: <https://ieeexplore.ieee.org/stamp/stamp.jsp?tp=&arnumber=6498051> (Accessed: 31 May 2023).

Williamson, S.J., Lϻ, Z.-L., Karron, D. and Kaufman, L. (1991) 'Advantages and limitations of magnetic source imaging', *Brain Topography*, 4(2), pp. 169–180. Available at: <https://doi.org/10.1007/BF01132773>.

Xu, H. and Xu, X. (2019) 'Lightweight EEG classification model based on EEG-sensor with few channels', in *Proceedings - 2019 International Conference on Cyber-Enabled Distributed Computing and Knowledge Discovery, CyberC 2019*. Institute of Electrical and Electronics Engineers Inc., pp. 464–473. Available at: <https://doi.org/10.1109/CyberC.2019.00086>.

XUE, G., CHEN, C., LU, Z.-L. and DONG, Q. (2010) 'Brain Imaging Techniques and Their Applications in Decision-Making Research', *Acta Psychologica Sinica*, 42(1), pp. 120–137. Available at: <https://doi.org/10.3724/SP.J.1041.2010.00120>.

Yang, J., Awais, M., Hossain, A., Lip Yee, P., Haowei, M., Mehedi, I.M. and Iskanderani, A.I.M. (2023) 'Thoughts of brain EEG signal-to-text conversion using weighted feature fusion-based Multiscale Dilated Adaptive DenseNet with Attention Mechanism', *Biomedical Signal Processing and Control*, 86. Available at: <https://doi.org/10.1016/j.bspc.2023.105120>.

Yu, J.H. and Sim, K.B. (2016) 'Classification of color imagination using Emotiv EPOC and event-related potential in electroencephalogram', *Optik*, 127(20), pp. 9711–9718. Available at: <https://doi.org/10.1016/j.ijleo.2016.07.074>.

Yuen, C.T., San, W.S., Seong, T.C. and Rizon, M. (2009) 'Classification of Human Emotions from EEG Signals using Statistical Features and Neural Network', *International Journal of Integrated Engineering*, 1. Available at: <https://api.semanticscholar.org/CorpusID:271540744>.

## Appendix

Table A1: Group 1 (4 Subjects) performances for 2 imaginations

<b>Group 1 (4 Subjects) performances for 2 imaginations</b>					
Layer Architecture index	Model	Hidden layer	Size	Best average performance	Highest accuracy
1	LVQ	1	3	61.25%	75.00%
2	FFNN	1	26	71.25%	100.00%
3	FFNN	2	36, 36	56.25%	100.00%
4	FFNN	2	36, 72	56.00%	100.00%
5	FFNN	2	72, 72	53.50%	100.00%
6	FFNN	2	72, 36	53.75%	87.50%

Table A2: Group 2 (9 Subjects) performances for 2 imaginations

<b>Group 2 (9 Subjects) performances for 2 imaginations</b>					
Layer Architecture index	Model	Hidden layer	Size	Best average performance	Highest accuracy
1	LVQ	1	3	53.33%	66.67%
2	FFNN	1	37	59.44%	88.89%
3	FFNN	2	36, 36	55.25%	87.50%
4	FFNN	2	36, 72	48.33%	77.78%
5	FFNN	2	72, 72	57.50%	87.50%
6	FFNN	2	72, 36	57.50%	87.50%

Table A3: Group 3 (19 Subjects) performances for 2 imaginations

<b>Group 3 (19 Subjects) performances for 2 imaginations</b>					
Layer Architecture index	Model	Hidden layer	Size	Best average performance	Highest accuracy
1	LVQ	1	5	50.52%	60.52%
2	FFNN	1	45	55.52%	73.68%
3	FFNN	2	36, 36	51.34%	68.42%
4	FFNN	2	36, 72	51.26%	68.42%
5	FFNN	2	72, 72	50.11%	65.79%
6	FFNN	2	72, 36	50.13%	65.79%

Table A4: Group 1 (4 Subjects) performances for 3 imaginations

<b>Group 1 (4 Subjects) performances for 3 imaginations</b>					
Layer Architecture index	Model	Hidden layer	Size	Best average performance	Highest accuracy
1	LVQ	1	3	98.30%	100%
2	FFNN	1	4	100%	100%
3	FFNN	2	36, 36	99.50%	100%
4	FFNN	2	36, 72	100%	100%
5	FFNN	2	72, 72	100%	100%
6	FFNN	2	72, 36	99.17%	100%

Table A5: Group 2 (9 Subjects) performances for 3 imaginations

<b>Group 2 (9 Subjects) performances for 3 imaginations</b>					
Layer Architecture index	Model	Hidden layer	Size	Best average performance	Highest accuracy
1	LVQ	1	3	97.04%	100%
2	FFNN	1	69	97.04%	100%
3	FFNN	2	36, 36	94.81%	100%
4	FFNN	2	36, 72	94.59%	100%
5	FFNN	2	72, 72	95.41%	100%
6	FFNN	2	72, 36	95.11%	100%

Table A6: Group 3 (19 Subjects) performances for 3 imaginations

<b>Group 3 (19 Subjects) performances for 3 imaginations</b>					
Layer Architecture index	Model	Hidden layer	Size	Best average performance	Highest accuracy
1	LVQ	1	87	84.03%	91.22%
2	FFNN	1	23	88.60%	94.74%
3	FFNN	2	48, 48	84.56%	91.23%
4	FFNN	2	48, 96	85.72%	94.74%
5	FFNN	2	96, 96	84.70%	94.74%
6	FFNN	2	96, 48	85.19%	91.23%

Table A7: Group 1 (4 Subjects) performances for 5 imaginations

<b>Group 1 (4 Subjects) performances for 5 imaginations</b>					
Layer Architecture index	Model	Hidden layer	Size	Best average performance	Highest accuracy
1	LVQ	1	7	79.75%	95.00%
2	FFNN	1	14	74.20%	95.00%
3	FFNN	2	36, 36	69.25%	90.00%
4	FFNN	2	36, 72	73.45%	100.00%
5	FFNN	2	72, 72	71.00%	95.00%
6	FFNN	2	72, 36	72.20%	95.00%

Table A8: Group 2 (9 Subjects) performances for 5 imaginations

<b>Group 2 (9 Subjects) performances for 5 imaginations</b>					
Layer Architecture index	Model	Hidden layer	Size	Best average performance	Highest accuracy
1	LVQ	1	8	72.06%	77.78%
2	FFNN	1	60	69.13%	86.67%
3	FFNN	2	36, 36	66.00%	80.00%
4	FFNN	2	36, 72	66.76%	77.78%
5	FFNN	2	72, 72	66.33%	77.78%
6	FFNN	2	72, 36	66.96%	80.00%

Table A9: Group 3 (19 Subjects) performances for 5 imaginations

<b>Group 3 (19 Subjects) performances for 5 imaginations</b>					
Layer Architecture index	Model	Hidden layer	Size	Best average performance	Highest accuracy
1	LVQ	1	87	64.83%	78.95%
2	FFNN	1	78	63.02%	70.53%
3	FFNN	2	36, 36	63.76%	78.95%
4	FFNN	2	36, 72	63.43%	71.58%
5	FFNN	2	72, 72	63.21%	77.90%
6	FFNN	2	72, 36	63.31%	73.68%

